

Evasion of T cell immunity by Epstein-Barr virus

Daniëlle Horst

The research described in this thesis was financially supported by:
The Dutch Cancer Society

Printing of this thesis was financially supported by:
The Dutch Cancer Society
The Netherlands Society of Medical Microbiology (NVMM) and the Netherlands
Society for Microbiology (NVvM)
The Infection and Immunity Center Utrecht
The University Medical Center Utrecht

Printed on FSC certified paper

ISBN: 978-94-6108-218-3

No part of this publication may be reproduced or transmitted without prior
permission of the author.

Evasion of T cell immunity by Epstein-Barr virus

Ontwijking van T cel immuniteit door Epstein-Barr virus

(met een samenvatting in het Nederlands)

Proefschrift

ter verkrijging van de graad van doctor aan de Universiteit Utrecht op gezag van de rector magnificus, prof.dr. G.J. van der Zwaan, ingevolge het besluit van het college voor promoties in het openbaar te verdedigen op vrijdag 14 oktober 2011 des ochtends te 10.30 uur

door

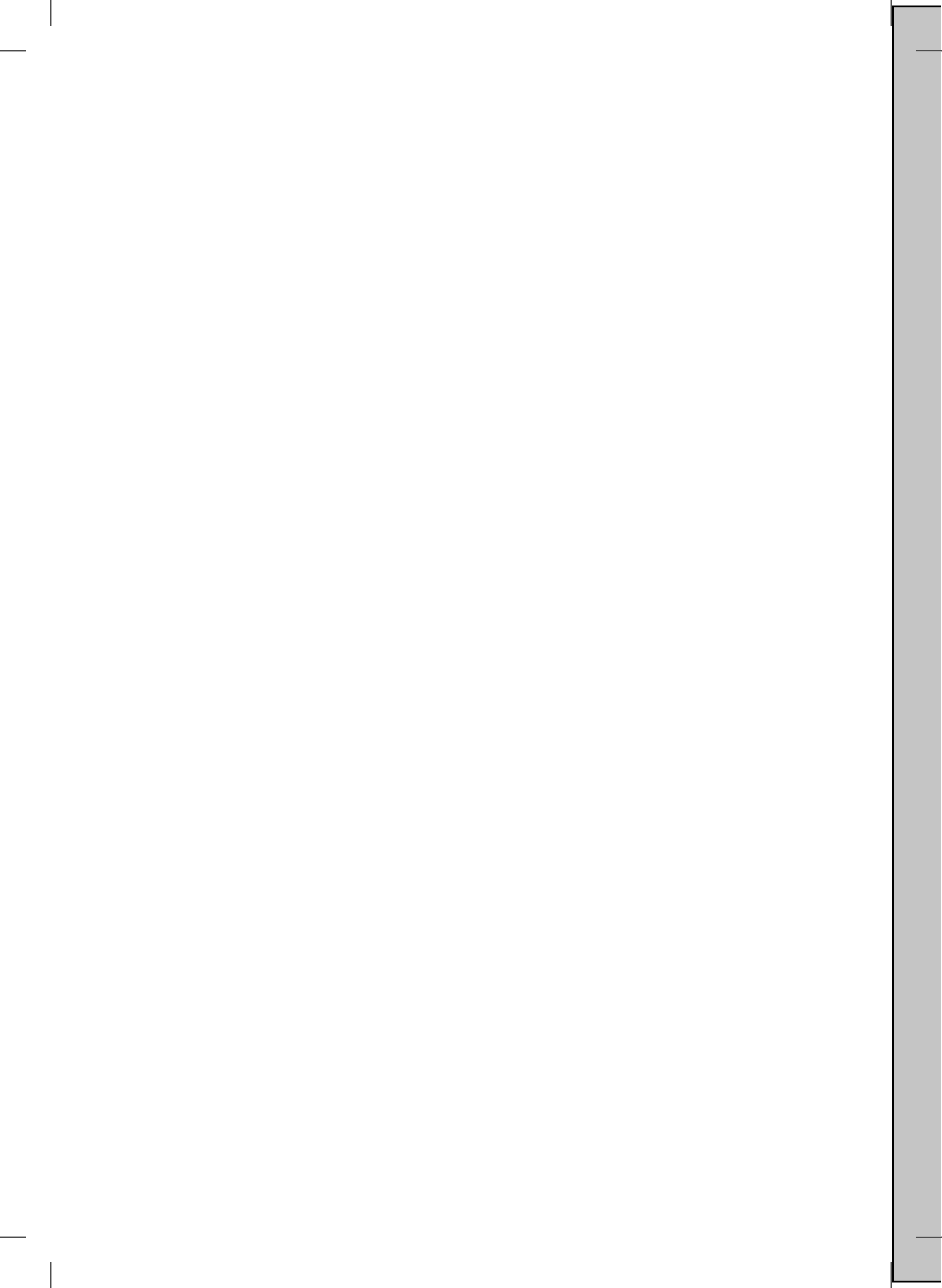
Daniëlle Horst

geboren op 14 juli 1982 te Zaanstad

Promotor: Prof.dr. E.J.H.J. Wiertz
Co-promotor: Dr. M.E. Ressing

Contents

Chapter 1	General introduction	7
Chapter 2	A CD8 ⁺ T cell immune evasion protein specific to Epstein-Barr virus and its close relatives in Old World primates	25
Chapter 3	Specific targeting of the EBV lytic phase protein BNLF2a to the transporter associated with antigen processing results in impairment of HLA class I-restricted antigen presentation	41
Chapter 4	EBV protein BNLF2a exploits host tail-anchored protein integration machinery to inhibit TAP	59
Chapter 5	Epstein-Barr virus isolates retain their capacity to evade T cell immunity through BNLF2a despite extensive sequence variation	79
Chapter 6	Stage-specific inhibition of MHC class I presentation by the Epstein-Barr virus BNLF2a protein during virus lytic cycle	91
Chapter 7	Residues required for host shutoff activity are located in the “bridge” of Epstein-Barr virus BGLF5	107
Chapter 8	General discussion	127
	Nederlandse samenvatting	146
	List of publications	148
	Curriculum Vitae	151



Chapter 1

General introduction

Partly published in:

Epstein-Barr virus evasion of CD8⁺ and CD4⁺ T cell immunity via concerted actions of multiple gene products

M.E. Ressing*, D. Horst*, B.D. Griffin*, J. Tellam, J. Zuo, R. Khanna, M. Rowe and E.J.H.J. Wiertz.

Seminars in Cancer Biology 2008

Viral evasion of T cell immunity: ancient mechanisms offering new applications

D. Horst*, M.C. Verweij*, A.J. Davison, M.E. Ressing and E.J.H.J. Wiertz.

Current Opinion in Immunology 2011

Exploiting human herpesvirus immune evasion for therapeutic gain: potential and pitfalls

D. Horst, M.E. Ressing and E.J.H.J. Wiertz.

Immunology and Cell Biology 2011

Viral inhibition of TAP: a striking example of convergent evolution

M.C. Verweij*, D. Horst*, B.D. Griffin, A.J. Davison, M.E. Ressing and E.J.H.J. Wiertz.

In preparation

* These authors contributed equally to this manuscript

General introduction – Part I

Herpesviruses

Viruses are experts at taking over host cells and converting them into virus-producing factories, a process that is essential for their existence. Following infection, a major factor determining the virus' success is adaptation to anti-viral measures taken by the host, notably those exerted by the immune system. An effective means to modulate or evade from virus-specific immune responses involves the use of dedicated immune evasion proteins, a strategy that is mastered by herpesviruses.

Herpesviruses are large, enveloped DNA viruses that infect a wide range of species including human beings, with almost every adult persistently carrying one or more. Yet, herpesviruses display a high degree of species specificity. Thus far, eight herpesviruses infecting humans have been identified, belonging to three herpesvirus subfamilies: the α -herpesviruses herpes simplexvirus types 1 and 2 (HSV-1 and HSV-2) and varicella-zoster virus (VZV), the β -herpesviruses human cytomegalovirus (HCMV) and human herpesvirus types 6 and 7 (HHV-6 and HHV-7), and the γ -herpesviruses Epstein-Barr virus (EBV) and Kaposi's sarcoma-associated herpesvirus (KSHV) (1). Herpesvirus infections usually cause only mild symptoms, but serious complications can arise, particularly in immunocompromised individuals. In addition, HCMV is the most common viral cause of congenital defects, and EBV and KSHV are associated with the development of several malignancies (2).

The characteristic lifelong persistence of herpesviruses reflects the delicate balance these viruses establish with the host's immune system. Following primary infection, abundant virus-specific T cell responses are induced that control viral replication and reduce virus-related pathology. Nevertheless, the virus persists, mostly in a latent state with limited viral gene expression. As a consequence, the virus-derived pool of potential antigens is minimized, thus hindering recognition and elimination of infected cells by the immune system. In addition, several latency-associated proteins have been found actively to impede detection of virus-infected cells by the host immune system (3-5). However, productive infection is required to yield viral offspring for dissemination to other hosts. During this replicative phase, an extensive repertoire of herpesvirus-encoded genes is expressed in a kinetically regulated fashion. Depending on the virus in question, this results in the synthesis of about 70 to over 200 viral proteins. Consequently, many viral antigens are potentially available. At this stage, immune evasion strategies exerted by the virus can prolong the period of virus production, thereby promoting spread within the host population.

Evasion occurs at multiple levels, targeting both

innate and adaptive branches of the immune response. Herpesviruses have been found to affect antiviral host responses by interfering with cytokine and chemokine signaling (6), by impairing the complement cascade (7), by preventing natural killer cell-mediated recognition and elimination of infected cells (8), and by inhibiting innate immune signaling by pattern-recognition receptors, such as Toll-like receptors and RIG-I-like receptors (9). Furthermore, the past decades have witnessed the elucidation of diverse strategies by which herpesviruses manipulate the host adaptive immune response (10, 11). These include utilizing herpesvirus-encoded Fc receptors to inhibit antibody-mediated effector mechanisms (12) and subverting the MHC class II (MHC II) (13) and, particularly, the MHC class I (MHC I) antigen processing and presentation pathways.

Antigen processing for presentation by MHC I molecules

At the cell surface, MHC I molecules present antigenic peptides to cytotoxic T lymphocytes (CTLs). In general, these peptides result from proteasomal degradation of cytosolic proteins, either of viral or cellular origin (Figure 1). These peptides are translocated into the ER lumen via the Transporter associated with Antigen Processing (TAP). TAP is a heterodimer composed of two subunits, TAP1 and TAP2, and forms part of the MHC I peptide-loading complex (PLC). In addition to TAP, this complex encompasses MHC I heavy chain / β 2-microglobulin (β 2m) heterodimers, calreticulin, tapasin, ERp57 and protein disulfide isomerase (PDI). Calreticulin is a chaperone that assists in proper folding of MHC I molecules. Within the PLC, tapasin exerts multiple functions; it stabilizes TAP protein expression and bridges TAP to MHC I molecules (14, 15). Furthermore, tapasin binds to the thiol oxidoreductase ERp57. This tapasin-ERp57 heterodimer stabilizes the PLC and has a peptide-editing function (16-19). PDI stabilizes a peptide-receptive conformation of the MHC I heavy chain / β 2m heterodimer (20). Overall, the composition of the PLC ensures optimal peptide loading of MHC I molecules. Proper assembly of peptide-loaded MHC I molecules allows them to travel to the cell surface.

MHC I-restricted antigen presentation to CTLs is an important process in the recognition of virus-infected cells by the immune system. Most peptides presented by MHC I molecules are derived from endogenously synthesized proteins, including, in case of a virus-infected cell, virus-encoded proteins. In addition, dendritic cells can present antigens of exogenous origin in the context of MHC I molecules, a process known as cross-presentation. This process is essential for the priming of T cell responses to many viruses (reviewed in (21)).

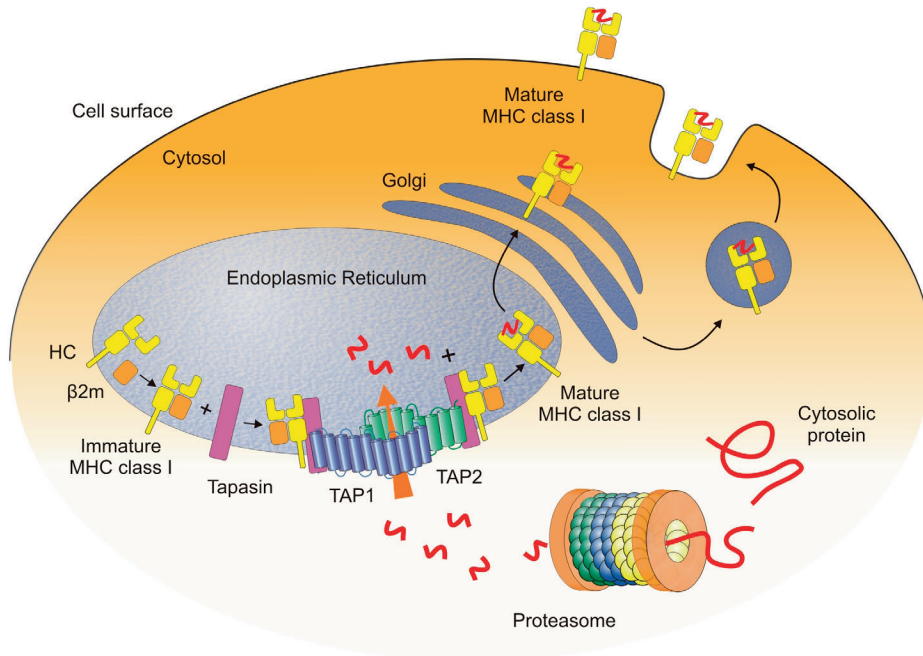


Figure 1. The MHC I peptide presentation pathway

The proteasome rapidly degrades viral proteins and fragments thereof into peptides. After assembly with $\beta 2m$, newly synthesized MHC I heavy chains (HC) are recruited to the peptide-loading complex. Constituents of this complex guide the folding of the MHC I complexes and control the loading of peptides that enter the ER via TAP. Tapasin links MHC I molecules to TAP and orchestrates the loading of peptides onto MHC I complexes. Properly loaded or mature MHC I complexes are transported to the cell surface, where they present their peptides to passing CTLs.

TAP-mediated peptide transport

TAP is a heterodimeric protein complex composed of two subunits, TAP1 and TAP2. Both subunits are multimembrane-spanning proteins with a C-terminal nucleotide binding domain (NBD) exposed in the cytosol. Hydrolysis of ATP at the NBDs of TAP1 and TAP2 is required to energize peptide transport (22). Elements of the cytosolic C-terminal domain and the cytosolic loop between the two C-terminal transmembrane (TM) domains are involved in peptide binding to TAP (23). Truncated forms of both TAP1 and TAP2 – composed of the six C-terminal TM domains together with the NBD – are sufficient for TAP-mediated peptide transport and form the so-called ‘6 + 6 TM’ TAP core complex (24). The first N-terminal TM domains of TAP1 and TAP2 are not essential for peptide transport, but are involved in binding tapasin. Though many studies have aimed to resolve completely the mechanism of TAP-mediated peptide transport, the precise details of how peptides are translocated are still unknown. Peptide transport has been proposed to occur in sequential steps, starting with peptide binding to TAP. This binding induces structural rearrangements, which allows ADP/ATP

exchange at TAP2, and dimerization of the two NBDs. Subsequently, peptide is released from its binding domain and is translocated into the ER lumen. ATP hydrolysis at TAP1 and TAP2 causes dissociation of the dimerized NBD, thereby resetting the transport cycle (25-29). In this way, conformational changes driven by ADP/ATP exchange and ATP hydrolysis at the TAP subunits lead to the transport of peptides into the ER.

Cells that naturally or experimentally lack expression of functional TAP complexes show a dramatic reduction in MHC I levels at their surface and a substantial decline in CTL sensitivity (30-35). Herpesviruses appear to have taken advantage of this extensive dependency of MHC I expression on TAP function by encoding viral proteins that specifically impair TAP-mediated peptide transport.

MHC I evasion by herpesviruses

Herpesviruses encode a plethora of proteins that interfere with MHC I-restricted antigen presentation (Figure 2). Firstly, the biosynthesis of MHC I molecules is blocked in cells infected both by alpha-,

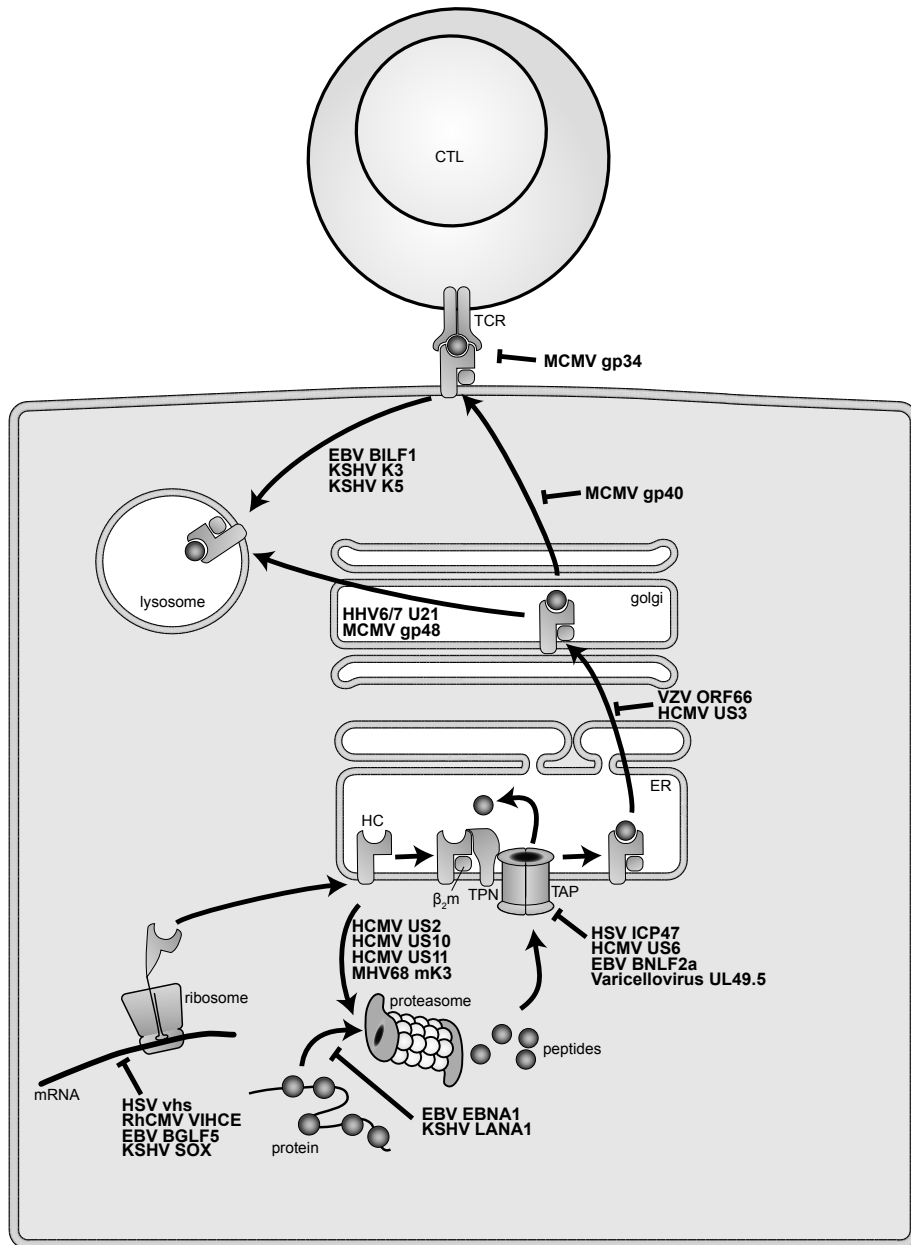


Figure 2. Herpesvirus interference with MHC I-restricted antigen presentation

HSV vhs, EBV BGLF5 and KSHV SOX induce degradation of mRNAs, among which those encoding for MHC I heavy chains. RhCMV VIHCE inhibits MHC I heavy chain synthesis in a signal peptide-dependent fashion. HCMV US2, US10 and US11 and MHV68 mK3 dislocate newly synthesized MHC I molecules back into the cytosol and enhance their proteasomal degradation. HHV-6 and 7-encoded U21 and MCMV gp48 redirect newly synthesized MHC I molecules to lysosomal compartments. EBV BILF1 and KSHV K3 and K5 induce the endocytosis and lysosomal degradation of cell surface MHC I molecules. VZV ORF66, HCMV US3 and MCMV gp40 interfere with MHC I trafficking. EBV EBNA1 and KSHV LANA1 inhibit their own proteasomal degradation, thereby impairing the generation of viral peptides. HSV ICP47, HCMV US6, EBV BNLF2a and the UL49.5 proteins of a number of varicelloviruses block TAP-mediated peptide transport into the ER. MCMV gp34 interferes with CTL recognition of peptide-loaded MHC I molecules at the cell surface. Abbreviations not mentioned in the text are: HC, heavy chain; TPN, tapasin.

beta- and gammaherpesviruses. Host shutoff proteins expressed by alpha- and gammaherpesviruses cause mRNA degradation, thereby inhibiting protein synthesis. A role for these viral proteins in immune evasion was demonstrated by the observation that the HSV-encoded virion host shutoff (vhs) protein reduces MHC I expression and hampers elimination of virus-infected cells by CTLs (36). Likewise, CTL recognition is diminished upon expression of BGLF5 and SOX (37), host shutoff proteins encoded by EBV (38) and KSHV (39), respectively. The Viral Inhibitor of Heavy Chain Expression (VIHCE) protein of the betaherpesvirus rhesus CMV (RhCMV) specifically inhibits the synthesis of MHC I heavy chains in a signal peptide-dependent fashion through a yet enigmatic mechanism (40).

Secondly, degradation of MHC I molecules is enhanced by several herpesviruses. The HCMV-encoded proteins US2 and US11 dislocate newly synthesized MHC I molecules from the ER into the cytosol, thereby accelerating their proteasomal degradation (41, 42). Recently, HCMV was found to encode an additional protein, US10, that induces proteasomal degradation of a subset of MHC I molecules (43). Expression of murine gammaherpesvirus 68 (MHV68) mK3 results in ubiquitination of MHC I molecules and their subsequent proteasomal degradation (44). HHV-6 and HHV-7 express the U21 protein that redirects newly synthesized MHC I molecules to lysosomal compartments (45, 46). Similarly, the mouse cytomegalovirus (MCMV) glycoprotein (gp) 48 induces lysosomal degradation of MHC I molecules (47). EBV BILF1 (48) and KSHV K3 and K5 (49, 50) enhance endocytosis of MHC I molecules from the cell surface, resulting in their lysosomal degradation. Thirdly, transport of MHC I molecules along the biosynthetic pathway is hampered by several herpesviruses. For instance, expression of VZV ORF66 delays transport of MHC I molecules through Golgi compartments and, consequently, reduces MHC I surface display (51, 52). Also cytomegaloviruses interfere with MHC I trafficking. The HCMV-encoded protein US3 induces degradation of PDI (20) and retains MHC I molecules in the ER in a tapasin-dependent manner (53-55). Alternatively, MCMV gp40 arrests MHC I in the ER-Golgi intermediate compartment and *cis*-Golgi (56).

Fourthly, herpesviruses reduce the availability of antigenic peptides for loading onto empty MHC I molecules. The latent EBV protein EBNA1 contains a Gly-Ala repeat that interferes with translation and proteasomal degradation *in cis* (57-59). Similarly, KSHV LANA1 inhibits its own degradation due to the presence of an acidic repeat region (60). Thereby, these two proteins impair the generation of antigenic peptides. In addition, several viral proteins prevent import of antigenic peptides into the ER lumen by blocking TAP function, each using a different strategy. Whereas HSV ICP47 competes with peptide

binding to the TAP complex (61-65), HCMV US6 interferes with binding of ATP to the transporter (66-70). Both of these mechanisms are combined by the EBV-encoded TAP inhibitor BNLF2a (71), despite the fact that this protein demonstrates no structural similarity to either the HSV- or HCMV-encoded TAP inhibitor. TAP-mediated peptide transport is also inhibited by several varicelloviruses. The UL49.5 proteins of all TAP-inhibiting varicelloviruses interfere with conformational transitions required for translocation of peptides over the ER membrane. Furthermore, UL49.5 of bovine herpesvirus 1 and related ruminant varicelloviruses target TAP for proteasomal degradation and the UL49.5 proteins of equid herpesvirus 1 and 4 affect the association of ATP with the nucleotide binding domains of TAP (72-74). Finally, herpesviruses obstruct the direct interaction of CTLs with MHC I molecules. At the cell surface, MCMV gp34 interferes with recognition of peptide-loaded MHC I complexes by CTLs (75). Overall, herpesviruses appear to interfere at each step of the MHC I-restricted antigen presentation pathway, thereby preventing elimination of virus-infected cells by the immune system.

General introduction – Part II

Epstein-Barr virus

EBV is a common virus, carried by over 90% of the adult human population worldwide. Whereas primary EBV infection of young children is usually unnoticed, primary infection of adolescents frequently results in the development of infectious mononucleosis (IM). IM is a self-limiting lymphoproliferative disease characterized by large numbers of atypical lymphocytes in the blood, mainly of CD8⁺ T cell origin. After resolution of IM, EBV infection is usually asymptomatic. However, EBV is associated with a number of malignancies like Burkitt's lymphoma, Hodgkin's lymphoma and nasopharyngeal carcinoma. In addition, EBV can cause post-transplantation lymphoproliferate diseases in immunocompromised patients (76).

B cells latently infected with EBV express a limited subset of up to 11 viral genes with concomitant cell proliferation (76). The pathogenicity of EBV-transformed B cells *in vivo* is counteracted by potent T cell responses directed towards several latent antigens (77). Indeed, such EBV-specific T cells can be used to successfully treat EBV-associated lymphomas that arise in immunosuppressed patients (78, 79). During latency, downregulated expression of EBV antigens by the infected cell is a major mechanism contributing to effective avoidance of elimination by T cells (76, 80, 81). In addition, some of the EBV latent gene products have been found to employ highly effective strategies to prevent recognition by CD8⁺ T cells *in cis*. EBNA1 is a typical example of this, as it inhibits its own processing into antigenic peptides through post-transcriptional and post-translational mechanisms. Other latent gene products, such as the Epstein-Barr virus-encoded small RNAs (EBERs), have a more general anti-inflammatory effect. These noncoding double-stranded RNA-like molecules, existing abundantly in EBV-infected cells, have recently been found to induce the anti-inflammatory cytokine IL-10 (82).

Transmission of EBV to another host requires production of infectious virus as occurs in the lytic phase. The chances for successful viral spread increase with the amount of progeny released and this depends on the lifespan of the EBV-producing cell. In general, lytically infected cells remain viable for at least 5 days (83). During this period, more than 80 EBV-encoded proteins are synthesized, creating a wide variety of targets for detection and destruction by the immune system. Abundant memory T cells are generated following primary infection (77) and these will respond within a few hours after reactivation to eliminate cells harboring replicating virus, unless counteracted by EBV-encoded immune evasion proteins.

Immune evasion by Epstein-Barr virus

Modulation of T cell recognition is of crucial importance for EBV, as this herpesvirus resides intracellularly for most of its life cycle and, following primary infection, abundant virus-specific memory T cells are induced that will immediately respond to viral reactivation. Interference with antiviral immunity during productive EBV infection has long remained underexplored due to the absence of an *in vitro* model to study EBV-producing cells. The development of an *in vitro* system for productive EBV infection (83) has permitted investigations into the strategies employed by EBV to counteract host immunity and has facilitated the identification of a number of specific EBV-encoded immune evasion molecules. Gradually, a more complete picture of EBV immune evasion strategies is emerging, revealing a plethora of mechanisms acting together.

During the latent phase, EBNA1, but also LMP1 (4), and the EBERs (82) contribute to immune evasion. A novel class of molecules that may promote survival of cells harboring EBV infection is formed by virus-encoded micro-RNAs (miRs) (84-86). Recent studies indicate that miRs encoded within the EBV BHRF1 region possess immunomodulatory capacities (87), whereas a miR encoded within the BALF region exerts anti-apoptotic activity (88). Also during the lytic phase of EBV infection, multiple evasion strategies are operational that function in a concerted action. Immediately after initiation of the lytic cycle, BNLF2a is produced. This gene product shuts down TAP-mediated import of antigenic peptides into the ER, thereby preventing peptide-loading of MHC I molecules (71). This will not only affect newly synthesized MHC I molecules, but also the large pool of pre-existing MHC I complexes present within the ER, thus serving as a first line of defense in the ER. Shortly after that, BGLF5 comes into play. Inhibition of cellular protein synthesis by BGLF5 ensures a block in supply of new MHC I molecules (38), thereby acting synergistically with BNLF2a. An EBV-encoded IL-10 homolog further compromises antigen presentation via the class I pathway by blocking the synthesis of TAP1 and the immunoproteasome subunit b1i/LMP2 (89). MHC I complexes that have reached the cell surface are down-modulated by BILF1 (48). EBV also affects antiviral activity of the host immune system through more general mechanisms, including interference with the action of the important antiviral cytokine IFN- γ (90). Thus, various steps in the MHC I antigen presentation pathway appear targeted by viral gene products, ensuring effective interference with the presentation of virus-encoded antigens by MHC I molecules at the cell surface. CD4⁺ T cell activation is subverted by EBV through the obstruction of MHC II/peptide-T cell receptor (TCR) interactions via the BZLF2 product gp42 (91). Host shutoff by BGLF5 and vIL-10 also affects MHC II expression. At the

surface of EBV⁺ B cells in lytic cycle, levels of MHC II molecules are downregulated through additional, yet unknown mechanism(s).

In conclusion, multiple EBV gene products act in concert to block antigen presentation via MHC I and MHC II molecules, thereby preventing the detection of cells harboring latent and replicating EBV by CD8⁺ and CD4⁺ T lymphocytes. These immune-evasive maneuvers are combined with other mechanisms preventing the induction of programmed cell death. Thus, the survival of latently and lytically EBV-infected cells involves a synergistic interplay of multiple viral gene products that is of great complexity. A profound understanding of these processes is essential for successful development of drugs and vaccines against EBV.

EBNA1, master of disguise

Expression of the Epstein-Barr virus nuclear protein EBNA1 is widespread in all forms of EBV infection, accentuating its central role in the maintenance of the viral DNA episome (92, 93), a process essential for viral persistence and associated oncogenic potential. EBNA1 achieves this by initiating DNA replication from the latent origin of replication (OriP), promoting stable segregation of latent EBV genomes during cell division and through transcriptional trans-activation of other EBV latent genes (94-96).

A wide range of studies have demonstrated that EBV latently infected B cells are able to escape immune recognition, due in part to an internal glycine-alanine repeat (GAR) domain within EBNA1, which prevents/limits MHC I-restricted presentation of EBNA1 epitopes linked *in cis* (57-59, 97-100). Removal of this repeat sequence restores normal recognition of EBV-infected B cells and their subsequent destruction by virus-specific T cells. In order to avoid immune surveillance, EBNA1 expression must remain at low but sustainable levels to avoid immune detection but still at levels sufficient to maintain a presence within the infected cell.

Several groups examining the molecular basis by which the GAR suppresses immune recognition have proposed that the presence of the GAR domain within the EBNA1 protein may inhibit its proteasomal processing resulting in suppression of presentation of EBNA1-derived antigenic peptides through the MHC I pathway (57). Indeed, this hypothesis was confirmed by subsequent studies demonstrating that the GAR domain can directly interfere with the proteasomal degradation of EBNA1 and other reporter proteins to which it is fused (58, 101-105). Although a recent study has cast some doubt on the participation of the GAR in the proteasomal degradation of native EBNA1 (106), the balance of experimental data at present favors the involvement of the GAR in such a role. Caution is required when assessing conflicting

reports of EBNA1 stability, as it has been reported that EBNA1 expression and function may be influenced by the nature of the epithelial cell background (107). Jones and colleagues demonstrated that EBNA1 is toxic in specific epithelial cell environments and that this effect involves EBNA1 degradation, cell growth inhibition, induction of apoptosis and processing of EBNA1 for MHC I presentation (107). Further support for inhibition of proteasomal processing as an important EBNA1 immune evasion strategy, has been provided by the recent identification of a functionally related homologue of EBNA1, LANA1, from KSHV, which was also shown to block proteasomal degradation and inhibit presentation of linked epitopes through the MHC I pathway (60). It should be noted that the LANA1 repeat does not share sequence similarity with EBNA1, but rather contains a long and strongly acidic domain. Interestingly, an engineered 40.7 kDa acidic protein, pGZr, encoded by a nested open reading frame of EBNA1 mRNA and displaying 65% amino acid sequence identity to the acidic repeat of LANA1, also inhibited presentation of a linked antigen, prompting Ossevoort and colleagues to propose a potential 'immuno-stealth' role of GZr in gene therapy (108, 109).

In addition to the GAR's putative role in inhibiting proteolysis, a study carried out by Yin *et al.* has reported that the GAR domain also inhibits EBNA1 self-synthesis and that this effect can be distinguished from its effect on proteasomal degradation (59). The Khanna group (110) confirmed that the GAR does indeed inhibit EBNA1 protein synthesis and as a consequence, MHC I-restricted presentation on the cell surface. Recent investigations have focused on elucidating the molecular basis for this inhibitory effect on EBNA1 synthesis. Tellam *et al.* have reported the discovery of an unexpected mechanism involving viral mRNAs and their role in enabling EBNA1 to escape the normally very efficient immune surveillance system (110). Examination of the EBNA1 mRNA sequence demonstrated biased codon usage encoding the GAR sequence (an extreme purine bias at odds with "normal" mammalian codon usage for glycine and alanine), suggesting a novel immune evasion strategy (110, 111). Predicted mRNA secondary structure analysis (MFOLD) showed that substitution of the codon bias of purines with pyrimidines dramatically altered EBNA1 mRNA stability. *In vitro* and *in vivo* translation assays using EBNA1 constructs expressing codon-modified sequences, while maintaining the same encoded protein sequence, demonstrated a significantly increased efficiency and amount of EBNA1 synthesis as the purine bias of the GAR was reduced. This resulted in a notable enhancement of MHC-peptide complexes detected on the surface of EBNA1 expressing cells, suggesting that the GAR mRNA sequence plays a major role in limiting the amount of EBNA1 antigen produced by virus-infected cells, via inhibition of the rate of translation

of the EBNA1 mRNA (110). The data suggest that this effect is most likely at the level of inhibition of elongation rate, due to the unique secondary structure likely to result from the purine biased RNA sequence. However, further research is required to elucidate the specific molecular lesion(s) caused by the purine-rich content of the GAR resulting in reduced translation of the EBNA1 mRNA and whether this occurs primarily at the level of initiation, elongation or termination of EBNA1 synthesis. Another piece of the EBV immune evasion puzzle comes from recent studies carried out by the Sample group (112) who propose autorepression of EBNA1 expression through the inhibition of pre-mRNA processing. Yoshioka *et al.* demonstrated that EBNA1 acts post- or co-transcriptionally to block processing of primary transcripts and that this autoregulation is likely to contribute to immune evasion by preventing unnecessary new synthesis, which in turn would limit the generation of EBNA1 antigenic epitopes derived from defective ribosomal products (DRiPs) believed to be the primary source of EBNA1 peptides presented through the MHC I pathway.

Avoidance of immune surveillance for EBV-infected cells is critical to latent infection by the virus. It is clear that EBV has evolved an effective mechanism to allow persistent latent infection by the addition of a unique “masking” glycine–alanine repeat sequence to the EBNA1 protein. The GAR effect on antigenic epitope generation may well represent a more general immune-evasive mechanism as hundreds of eukaryotic viral mRNAs have evolved with a purine bias (111). This sequence seems to act at both the protein and mRNA levels to ensure that only an “invisible” low level of EBNA1 antigenic peptides are present in each infected cell and presented to the immune system. Elucidation of the detailed molecular basis by which EBNA1 subverts the normal protein synthesis and antigen presentation processes of the host cell will suggest novel strategies to overcome latent EBV infections. Such future therapies may well include approaches based on specific “antisense” vaccines aimed at the purine-rich GAR RNA sequence, thus increasing the amount of EBNA1 protein in latently infected cells and facilitating immune recognition and subsequent targeting by the immune system.

vIL10, a multifunctional cytokine

Cytokine-mediated intercellular communication represents a fundamental component of the host immune response through which antiviral immunity can be coordinated. Viruses can subvert this part of the immune response at several levels, interfering with the intracellular signaling pathways responsible for inducing cytokine expression, producing soluble decoy receptors to bind host cytokines, and secreting cytokine homologs, or “virokines” to mimic the

immunosuppressive action of certain host proteins. As an example of the latter strategy, EBV encodes an IL-10 homolog (vIL-10), the product of the lytic phase BCRF-1 gene (113). Human IL-10 is a pleiotropic cytokine, which appears to exert both immunostimulatory and immunosuppressive actions depending on the target cell and local cytokine microenvironment at a given stage of the immune response (114). Despite a high degree of conservation, with 84% identity at the amino acid level, vIL-10 displays only a subset of the effects of the human cytokine, showing a substantially reduced ability to enhance mouse thymocyte and mast cell proliferation, while retaining certain immunosuppressive functions (115). The molecular basis for the retention of the immunosuppressive, but not immunostimulatory, functions of hIL-10 by the EBV homolog lies in a single amino acid difference at position 87 of the human protein (116). Altering the isoleucine at this position to an alanine, as possessed by vIL-10, markedly reduces the ability of the cytokine to stimulate thymocyte and mast cell proliferation, without modifying its immunosuppressive activities. Conversely, replacing the corresponding alanine from vIL-10 with an isoleucine provides the recombinant with immunostimulatory properties. vIL-10 binds to the IL-10 receptor complex with approximately 1000-fold less affinity than hIL-10, though this does not necessarily correlate with the specific activity of the protein. Thus, it appears that amino acid position 87 is involved in a key interaction with the IL-10 receptor complex, with the identity of that amino acid dictating the nature of the downstream biological responses.

Treatment of primary B lymphocytes with recombinant vIL-10 has been shown to cause a decrease in TAP1 mRNA and protein levels (89). Furthermore, vIL-10 causes a reduction in mRNA levels of b1i/LMP2, a subunit of the immunoproteasome that shares a bidirectional promoter with the TAP1 gene. This deficit in levels of antigen processing pathway components leads to a reduction in the capacity of B cells to translocate peptides into the ER and a downregulation of MHC I surface expression. EBV can also infect and replicate in monocytes and macrophages (117, 118). vIL-10 can inhibit the activation of antigen-specific CD4⁺ T cells when antigens are presented by monocytes (119). This arises partly from the ability of vIL-10 to inhibit both basal levels and IFN- γ -induced upregulation of MHC II molecule expression on monocytes (120). Such a function is shared by human IL-10, which prevents newly synthesized mature MHC II molecules from traveling to the cell surface, and also impedes their recycling after internalization (121). vIL-10 can further reduce the capacity of monocytes to stimulate T cells by inhibiting basal and IFN- γ -induced expression of intercellular adhesion molecule-1 (ICAM-1) and the co-stimulatory molecules CD80 and CD86, which are required to induce T cell IL-2 production and proliferation (120).

Inhibition of IFN- γ -induced MHC I expression can also be achieved if monocytes are treated with vIL-10 prior to IFN- γ , suggesting that the virokinine can inhibit monocyte/macrophage-directed CD8⁺ T cell activation. Aside from inhibiting the ability of monocytes to induce T cell activation, vIL-10 can also attenuate monocyte/macrophage production of pro-inflammatory cytokines such as IL-1 α , IL-1 β , TNF α , and IL-6 (122). In this way, it can hinder the ability of uninfected monocytes/macrophages to contribute to the inflammatory response during the productive phase of EBV infection.

BNLF2a, a powerful inhibitor of TAP-mediated peptide transport

Initiation of the lytic cycle of EBV is accompanied by a marked reduction of MHC I and MHC II expression at the cell surface (83, 123). One of the EBV-encoded proteins contributing to downregulation of MHC I at the cell surface is BNLF2a. This protein is expressed during the lytic phase of EBV infection and blocks TAP-mediated peptide transport, resulting in a diminished peptide supply into the ER lumen (71). Identification of the EBV-encoded TAP inhibitor was hampered by the lack of homology to other viral TAP inhibitors identified to date. As most viral immune evasion molecules are virus-specific proteins, γ 1 herpesvirus-specific gene products were screened for their ability to interfere with CTL cytotoxicity. This resulted in the identification of BNLF2a as an EBV-encoded protein preventing CTL-mediated cell lysis. Subsequent experiments demonstrated that cells stably expressing BNLF2a have reduced levels of MHC I at their surface and an almost complete block of TAP-mediated peptide transport into the ER lumen (71). Inhibition of TAP-mediated peptide transport is observed for several other members of the herpesvirus family. Although the TAP-inhibiting proteins encoded by these viruses have a similar function, there is no significant homology in structure and mechanism among these proteins (Figure 3). BNLF2a is a small membrane associated protein that lacks an obvious signal sequence, but carries a hydrophobic C terminus that serves as a membrane anchor. BNLF2a interferes with both ATP and peptide binding to TAP (71). In contrast, the human cytomegalovirus-encoded TAP inhibitor, US6, is a type I membrane protein that interferes with ATP binding to TAP, without affecting the binding of peptides to TAP. This blockage of ATP binding is caused by an indirect effect of US6, as the ER luminal domain of US6 is necessary and sufficient for interference with ATP binding to the cytosolic domain of TAP (66-69). This apparent discrepancy can be explained by the ability of US6 to alter the conformation of the TAP complex, thereby precluding ATP binding and hydrolysis (124). Another herpesvirus-encoded TAP inhibitor disrupting ATP

binding to TAP is expressed by equid herpesvirus 1 and 4, namely UL49.5 (73). Functional homologues of UL49.5 are found among others in bovine herpesvirus 1, pseudorabies virus and feline herpesvirus 1 (72-74). However, while all TAP-inhibiting UL49.5 proteins arrest TAP in a translocation-incompetent state, interference with ATP binding is only observed for the equid herpesvirus 1- and 4-encoded TAP inhibitors (73, 74). In contrast, UL49.5 of bovine herpesvirus 1 and related ruminant varicelloviruses targets TAP1 and TAP2 for degradation (72, 74). Another strategy to prevent TAP-mediated peptide transport is used by HSV-1 and -2. These viruses encode a cytosolic protein, ICP47, that competes with peptides for the cytosolic peptide binding site of TAP (61-64). Although BNLF2a shares its ability to interfere with ATP binding with US6 and the equid herpesvirus 1- and 4-encoded UL49.5 proteins, and its ability to prevent peptide binding to TAP with ICP47, these proteins have a completely different sequence and structure.

One feature these different viral TAP inhibitors have in common is their expression during the viral life cycle. BNLF2a (125, 126), US6 (67), UL49.5 (127), and ICP47 (65) are expressed (immediate) early in lytic infection. Early expression of the viral TAP inhibitors will aid in their function to prevent CTL recognition of viral peptides presented by MHC I molecules. As soon as the virus reactivates, antigenic viral peptides will be generated by the destruction of newly synthesized viral proteins by proteasomes (124). Early blockage of TAP-mediated peptide transport into the ER lumen will prevent loading of viral peptides, derived from early and late proteins, onto MHC I molecules and their subsequent display at the cell surface.

Homologues of BNLF2a are found in Old World primate γ 1 herpesviruses. These BNLF2a proteins demonstrate between 53 and 63% overall identity with their counterpart in EBV (71). Like EBV-encoded BNLF2a, the homologues encoded by rhesus, chimpanzee, orang-utan, and gorilla γ 1 herpesviruses downregulate MHC I expression at the cell surface, which is indicative of TAP-inhibition (71). Interestingly, the New World primate γ 1 herpesviruses sequenced so far lack a BNLF2a homologue, which suggests that this viral TAP inhibitor was acquired after branching of the Old World and New World primates during evolution (128).

In conclusion, EBV and related Old World γ 1 herpesviruses encode an immune evasion molecule, BNLF2a, that specifically blocks TAP-mediated peptide transport. The resulting downregulation of MHC I-peptide complexes at the cell surface protects cells harboring replicating EBV against recognition and lysis by EBV-specific CTLs.

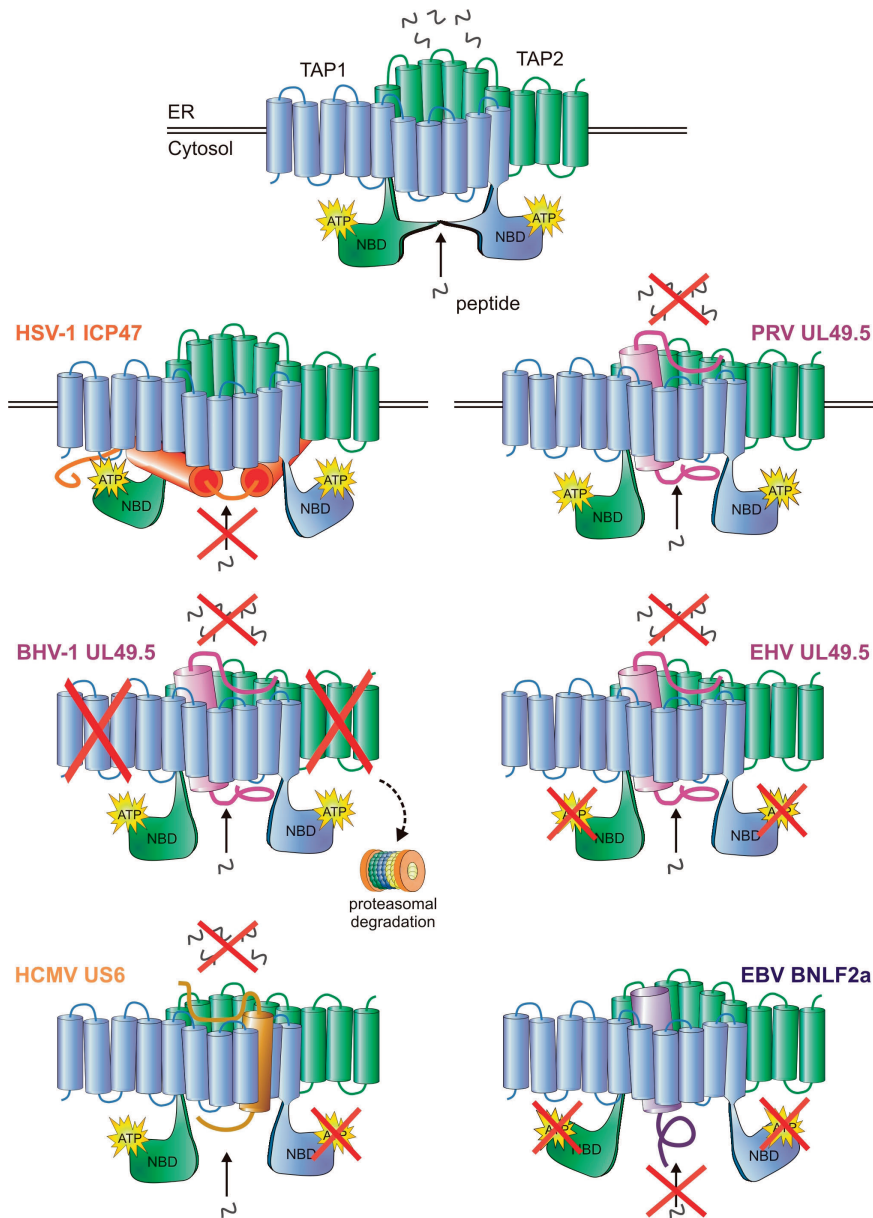


Figure 3. The interactions between herpesvirus-encoded TAP-inhibitors and their target

Upper cartoon: A model of the TAP transporter, which is comprised by the two subunits TAP1 and TAP2. Each subunit comprises a hydrophobic core (encompassing 10 and 9 transmembrane domains for TAP1 and TAP2, respectively), a nuclear binding domain (NBD) where ATP binds, and a region for peptide binding. The latter two regions face the cytosol. Lower cartoons: Schematic representations of the interaction between the viral proteins and TAP transport. The sites where TAP is affected are depicted. HSV-1 ICP47 prevents peptide transport by physically obstructing the peptide-binding site. Pseudorabies virus (PRV), equid herpesvirus (EHV) 1 and 4 and bovine herpesvirus 1 (BoHV-1) UL49.5 leave the transporter in conformational arrest, thereby preventing the structural changes that are needed to transport peptides. In addition, EHV UL49.5 prevents ATP binding to TAP, and BoHV-1 UL49.5 induces the degradation of both subunits. BoHV-1 UL49.5 is also known to interact with a region within the '6+6 TM' core domain of TAP, comprising the C-terminal 6 TM domains of both TAP1 and TAP2. HCMV US6 blocks TAP by inducing conformational changes that result in diminished ATP-binding. The protein interacts with TM domains 7-10 of TAP 1 and 1-4 of TAP2. EBV BNLF2a inhibits peptide transport by interfering with both peptide and ATP binding.

BILF1, a novel EBV immune evasion molecule

Most recently, the BILF1 gene product was shown to downregulate cell surface expression of MHC I and abrogate recognition of endogenous antigen by EBV-specific CD8⁺ T cells (48, 129). BILF1 interferes with cell surface expression of both pre-existing and newly synthesized MHC I molecules. Pre-existing MHC I molecules are more rapidly internalized from the cell surface and are degraded in lysosomes, whereas newly synthesized MHC I molecules are redirected during traveling on the exocytic pathway. Both of these mechanisms contribute to BILF1-mediated immune evasion (48, 129).

BILF1 is a seven transmembrane segment G-protein coupled receptor (GPCR) which, like many vGPCRs encoded by herpesviruses, shares structural and functional characteristics with chemokine receptors (130-132). The role of vGPCRs is thought to be to contribute to efficient lytic replication by reprogramming the host cell through multiple signaling pathways, often in a ligand-independent manner (132). One of the first demonstrations that vGPCRs might modulate immune-recognition processes was reported by Bodaghi and colleagues who showed that the HCMV US28 vGPCR can modify the chemokine environment of infected cells by binding and internalizing MCP-1 (monocyte chemoattractant protein) and RANTES (regulated on activation, normal T cell expressed and secreted) to efficiently sequester these chemokines (133). Numerous other examples of the immune-modulating potential of vGPCRs have since been reported, but BILF1 is the first vGPCR shown to specifically target MHC molecules for degradation. This property of BILF1 is, however, shared by its homologue encoded by the Rhesus γ 1-herpesvirus (CeHV15), which has 80% amino acid identity with EBV BILF1 (48). In contrast, the ORF74 protein of KSHV, which has 15% amino acid sequence identity with EBV BILF1 and is the most closely related human herpesvirus vGPCR, does not affect MHC I (48).

It is noteworthy that a cellular chemokine receptor, CXCR4, has also been shown to cause downregulation of expression of MHC I at the cell surface (134). Mechanistically, this process involves physical association of CXCR4 with the β 2m component of mature MHC I complexes, ubiquitination of the MHC I heavy chain, and endocytosis of MHC complexes into a late endosomal/lysosomal compartment where degradation presumably occurs. Superficially, this process is similar to the effect of BILF1 on MHC I. However, while the effect of CXCR4 is triggered by binding of its ligand (134), BILF1 signaling functions are ligand independent (130, 131). Furthermore, a K122A mutation of BILF1 that abolishes its signaling retains the ability to downregulate MHC I at the cell surface (48). In addition, CXCR4 was shown to complex with MHC I through binding to the β 2m

subunit (134) whereas BILF1 is unable to bind β 2m itself (48). Finally, activation of CXCR4 was shown to initiate ubiquitination of MHC I heavy chain molecules (134), whereas there is no evidence that BILF1 acts through ubiquitination of MHC I (48). Nevertheless, it is interesting that when co-expressed in the same cell, BILF1 and CXCR4 show almost complete co-localization and are both predominantly located in the plasma-membrane, whereas the KSHV ORF74 and HCMV US28 vGPCRs exhibit mainly intracellular localization (131).

While there remain unanswered questions about the precise mechanisms used by BILF1 to target MHC I complexes for degradation, the evidence to date clearly points to a role for this viral protein in protecting lytically infected cells from CD8⁺ T cell responses (129). It is interesting that the immune-evasive properties of BILF1 are genetically separable from its previously identified signaling function (48, 129). Taken together with the exonuclease and immune evasion-related host shut-off functions of BGLF5 (37), this raises the question of whether EBV has evolved a strategy of utilizing multifunctional proteins to evade immune responses.

BGLF5: the viral DNase, carries a host-shutoff function

The BGLF5 gene product was originally identified as an alkaline exonuclease (DNase) enzyme (135), which is highly conserved amongst all herpesviruses (38, 136, 137). Subsequently, it was shown, first for KSHV SOX (39, 138) and then for EBV BGLF5 (37, 38), that the exonuclease proteins of γ -herpesviruses possess an additional function which inhibits cellular protein synthesis. The inhibition of *de novo* protein synthesis by BGLF5 (and KSHV SOX) leads to a loss of MHC I molecules from the cell surface (38), and a marked impairment of recognition of endogenously processed antigen by EBV-specific CD8⁺ T cells (37). Mutational analysis of BGLF5 showed that the impairment of immune recognition correlated with host-shutoff function and not with alkaline exonuclease function (37, 38). A similar loss of MHC II from the cell surface is also observed following expression of BGLF5, and it is likely that immune recognition by CD4⁺ T cells is similarly impaired.

In α -herpesviruses, the virion host shutoff function is mediated by a separate gene, UL41 (139, 140) which can also interfere with recognition by CD8⁺ T cells (36). UL41 mediates protein synthesis shutoff by initiating degradation of RNA transcripts (139, 141, 142). Inhibition of protein synthesis by BGLF5 is likewise achieved by an overall increase of mRNA turnover (38), similarly to KSHV SOX (39, 143). Recently, it was demonstrated that BGLF5 and SOX have intrinsic RNase activity (144, 145). However, the precise mechanism of the supposed host specific

shutoff by EBV still remains to be determined. It is possible that BGLF5 is actually not host-mRNA specific, but that the burst of synthesis of new viral mRNAs during lytic cycle is simply substantially higher than the steady-state synthesis of cellular mRNAs. In addition, the EB2 protein encoded by EBV BMLF1 might work in concert with BGLF5 to selectively promote the cytosolic accumulation of intronless viral mRNAs and inhibit the expression of cellular intron-containing mRNAs (146-148).

BGLF5 protein is expressed with early antigen kinetics, being first detected at around 3–6 hours after lytic cycle induction, and independently of phosphonoacetic acid treatment (37). Both BNLF2a and BGLF5 transcripts peak at around 8–24 hours after induction of lytic cycle and decline thereafter (125). This late decline in BNLF2a and BGLF5 transcripts might be due to expression of BGLF5 itself since the shutoff function appears to affect its own mRNA as well as other viral and cellular RNAs (37). It is likely that an equilibrium is established between BGLF5 protein turnover and mRNA synthesis so that a constant low level of BGLF5 protein is established that does not completely inhibit viral mRNA expression. In this way, BGLF5 can contribute to immune evasion through late lytic cycle.

Outline of the thesis

This thesis describes the identification and characterization of the EBV TAP inhibitor BNLF2a (chapter 2). Chapter 3 and 4 report on structural and functional properties of BNLF2a that allow this viral protein to efficiently impair TAP-mediated peptide transport. Sequencing of EBV isolates revealed the existence of polymorphisms in the BNLF2a protein. In chapter 5, these BNLF2a variants were tested for MHC I downregulation. Using a recombinant EBV strain deleted for BNLF2a, it was demonstrated that BNLF2a contributes to CTL evasion during lytic infection (chapter 6). Furthermore, the mechanism of BGLF5-mediated host shutoff was investigated (chapter 7). These studies shed new light on the mechanisms that allow EBV and related lymphocryptoviruses to establish a life long infection in immunocompetent hosts.

References

1. Davison, A. J., R. Eberle, B. Ehlers, G. S. Hayward, D. J. McGeoch, A. C. Minson, P. E. Pellett, B. Roizman, M. J. Studdert, and E. Thiry. 2009. The order Herpesvirales. *Arch. Virol.* 154:171-177.
2. Rensing, M. E. and E. J. Wiertz. 2008. Manipulation of the immune response by Epstein-Barr virus and Kaposi's sarcoma-

associated herpesvirus: consequences for tumor development. *Semin. Cancer Biol.* 18:379-380.

3. Liang, C., J. S. Lee, and J. U. Jung. 2008. Immune evasion in Kaposi's sarcoma-associated herpes virus associated oncogenesis. *Semin. Cancer Biol.* 18:423-436.
4. Middeldorp, J. M. and D. M. Pegtel. 2008. Multiple roles of LMP1 in Epstein-Barr virus induced immune escape. *Semin. Cancer Biol.* 18:388-396.
5. Rensing, M. E., D. Horst, B. D. Griffin, J. Tellam, J. Zuo, R. Khanna, M. Rowe, and E. J. Wiertz. 2008. Epstein-Barr virus evasion of CD8(+) and CD4(+) T cell immunity via concerted actions of multiple gene products. *Semin. Cancer Biol.* 18:397-408.
6. Alcami, A. 2003. Viral mimicry of cytokines, chemokines and their receptors. *Nat. Rev. Immunol.* 3:36-50.
7. Lambris, J. D., D. Ricklin, and B. V. Geisbrecht. 2008. Complement evasion by human pathogens. *Nat. Rev. Microbiol.* 6:132-142.
8. Lanier, L. L. 2008. Evolutionary struggles between NK cells and viruses. *Nat. Rev. Immunol.* 8:259-268.
9. Bowie, A. G. and L. Unterholzner. 2008. Viral evasion and subversion of pattern-recognition receptor signalling. *Nat. Rev. Immunol.* 8:911-922.
10. Griffin, B. D., M. C. Verweij, and E. J. Wiertz. 2010. Herpesviruses and immunity: the art of evasion. *Vet. Microbiol.* 143:89-100.
11. Hansen, T. H. and M. Bouvier. 2009. MHC class I antigen presentation: learning from viral evasion strategies. *Nat. Rev. Immunol.* 9:503-513.
12. Lubinski, J., T. Nagashunmugam, and H. M. Friedman. 1998. Viral interference with antibody and complement. *Semin. Cell Dev. Biol.* 9:329-337.
13. Wiertz, E. J., R. Devlin, H. L. Collins, and M. E. Rensing. 2007. Herpesvirus interference with major histocompatibility complex class II-restricted T-cell activation. *J. Virol.* 81:4389-4396.
14. Lehner, P. J., M. J. Surman, and P. Cresswell. 1998. Soluble tapasin restores MHC class I expression and function in the tapasin-negative cell line .220. *Immunity.* 8:221-231.
15. Sadasivan, B., P. J. Lehner, B. Ortman, T. Spies, and P. Cresswell. 1996. Roles for calreticulin and a novel glycoprotein, tapasin, in the interaction of MHC class I molecules with TAP. *Immunity.* 5:103-114.
16. Dick, T. P., N. Bangia, D. R. Peaper, and P. Cresswell. 2002. Disulfide bond isomerization and the assembly of MHC class I-peptide complexes. *Immunity.* 16:87-98.
17. Dong, G., P. A. Wearsch, D. R. Peaper, P.

- Cresswell, and K. M. Reinisch. 2009. Insights into MHC class I peptide loading from the structure of the tapasin-ERp57 thiol oxidoreductase heterodimer. *Immunity*. 30:21-32.
18. Peaper, D. R. and P. Cresswell. 2008. The redox activity of ERp57 is not essential for its functions in MHC class I peptide loading. *Proc. Natl. Acad. Sci. U. S. A* 105:10477-10482.
 19. Wearsch, P. A. and P. Cresswell. 2007. Selective loading of high-affinity peptides onto major histocompatibility complex class I molecules by the tapasin-ERp57 heterodimer. *Nat. Immunol.* 8:873-881.
 20. Park, B., S. Lee, E. Kim, K. Cho, S. R. Riddell, S. Cho, and K. Ahn. 2006. Redox regulation facilitates optimal peptide selection by MHC class I during antigen processing. *Cell* 127:369-382.
 21. Kurts, C., B. W. Robinson, and P. A. Knolle. 2010. Cross-priming in health and disease. *Nat. Rev. Immunol.* 10:403-414.
 22. Neeffjes, J. J., F. Momburg, and G. J. Hammerling. 1993. Selective and ATP-dependent translocation of peptides by the MHC-encoded transporter. *Science* 261:769-771.
 23. Nijenhuis, M. and G. J. Hammerling. 1996. Multiple regions of the transporter associated with antigen processing (TAP) contribute to its peptide binding site. *J. Immunol.* 157:5467-5477.
 24. Koch, J., R. Guntrum, S. Heintke, C. Kyritsis, and R. Tampe. 2004. Functional dissection of the transmembrane domains of the transporter associated with antigen processing (TAP). *J. Biol. Chem.* 279:10142-10147.
 25. Chen, M., R. Abele, and R. Tampe. 2003. Peptides induce ATP hydrolysis at both subunits of the transporter associated with antigen processing. *J. Biol. Chem.* 278:29686-29692.
 26. Karttunen, J. T., P. J. Lehner, S. S. Gupta, E. W. Hewitt, and P. Cresswell. 2001. Distinct functions and cooperative interaction of the subunits of the transporter associated with antigen processing (TAP). *Proc. Natl. Acad. Sci. U. S. A* 98:7431-7436.
 27. Neumann, L. and R. Tampe. 1999. Kinetic analysis of peptide binding to the TAP transport complex: evidence for structural rearrangements induced by substrate binding. *J. Mol. Biol.* 294:1203-1213.
 28. Bouabe, H. and M. R. Knittler. 2003. The distinct nucleotide binding states of the transporter associated with antigen processing (TAP) are regulated by the nonhomologous C-terminal tails of TAP1 and TAP2. *Eur. J. Biochem.* 270:4531-4546.
 29. Procko, E., M. L. O'Mara, W. F. Bennett, D. P. Tieleman, and R. Gaudet. 2009. The mechanism of ABC transporters: general lessons from structural and functional studies of an antigenic peptide transporter. *FASEB J.* 23:1287-1302.
 30. Spies, T. and R. DeMars. 1991. Restored expression of major histocompatibility class I molecules by gene transfer of a putative peptide transporter. *Nature* 351:323-324.
 31. Spies, T., V. Cerundolo, M. Colonna, P. Cresswell, A. Townsend, and R. DeMars. 1992. Presentation of viral antigen by MHC class I molecules is dependent on a putative peptide transporter heterodimer. *Nature* 355:644-646.
 32. de la Salle H., D. Hanau, D. Fricker, A. Urlacher, A. Kelly, J. Salameró, S. H. Powis, L. Donato, H. Bausinger, M. Laforet, and . 1994. Homozygous human TAP peptide transporter mutation in HLA class I deficiency. *Science* 265:237-241.
 33. de la Salle H., J. Zimmer, D. Fricker, C. Angenieux, J. P. Cazenave, M. Okubo, H. Maeda, A. Plebani, M. M. Tongio, A. Dormoy, and D. Hanau. 1999. HLA class I deficiencies due to mutations in subunit 1 of the peptide transporter TAP1. *J. Clin. Invest* 103:R9-R13.
 34. de la Salle H., X. Saulquin, I. Mansour, S. Klayme, D. Fricker, J. Zimmer, J. P. Cazenave, D. Hanau, M. Bonneville, E. Houssaint, G. Lefranc, and R. Naman. 2002. Asymptomatic deficiency in the peptide transporter associated to antigen processing (TAP). *Clin. Exp. Immunol.* 128:525-531.
 35. Moins-Teisserenc, H. T., S. D. Gadola, M. Cella, P. R. Dunbar, A. Exley, N. Blake, C. Baykal, J. Lambert, P. Bigliardi, M. Willemsen, M. Jones, S. Buechner, M. Colonna, W. L. Gross, and V. Cerundolo. 1999. Association of a syndrome resembling Wegener's granulomatosis with low surface expression of HLA class-I molecules. *Lancet* 354:1598-1603.
 36. Tigges, M. A., S. Leng, D. C. Johnson, and R. L. Burke. 1996. Human herpes simplex virus (HSV)-specific CD8⁺ CTL clones recognize HSV-2-infected fibroblasts after treatment with IFN-gamma or when virion host shutoff functions are disabled. *J. Immunol.* 156:3901-3910.
 37. Zuo, J., W. Thomas, D. van Leeuwen, J. M. Middeldorp, E. J. Wiertz, M. E. Rensing, and M. Rowe. 2008. The DNase of gammaherpesviruses impairs recognition by virus-specific CD8⁺ T cells through an additional host shutoff function. *J. Virol.* 82:2385-2393.
 38. Rowe, M., B. Glaunsinger, D. van Leeuwen, J. Zuo, D. Sweetman, D. Ganem, J. Middeldorp, E. J. Wiertz, and M. E. Rensing. 2007. Host shutoff during productive Epstein-Barr virus infection is mediated by BGLF5 and may contribute to immune evasion. *Proc. Natl. Acad. Sci. U. S. A* 104:3366-3371.
 39. Glaunsinger, B. and D. Ganem. 2004. Lytic KSHV infection inhibits host gene expression by

- accelerating global mRNA turnover. *Mol. Cell* 13:713-723.
40. Powers, C. J. and K. Fruh. 2008. Signal peptide-dependent inhibition of MHC class I heavy chain translation by rhesus cytomegalovirus. *PLoS Pathog.* 4:e1000150.
 41. Wiertz, E. J., T. R. Jones, L. Sun, M. Bogyo, H. J. Geuze, and H. L. Ploegh. 1996. The human cytomegalovirus US11 gene product dislocates MHC class I heavy chains from the endoplasmic reticulum to the cytosol. *Cell* 84:769-779.
 42. Wiertz, E. J. H. J., D. Tortorella, M. Bogyo, J. Yu, W. Mothes, T. R. Jones, T. A. Rapoport, and H. L. Ploegh. 1996. Sec61-mediated transfer of a membrane protein from the endoplasmic reticulum to the proteasome for destruction. *Nature* 384:432-438.
 43. Park, B., E. Spooner, B. L. Houser, J. L. Strominger, and H. L. Ploegh. 2010. The HCMV membrane glycoprotein US10 selectively targets HLA-G for degradation. *J. Exp. Med.* 207:2033-2041.
 44. Boname, J. M. and P. G. Stevenson. 2001. MHC class I ubiquitination by a viral PHD/LAP finger protein. *Immunity*. 15:627-636.
 45. Glosson, N. L. and A. W. Hudson. 2007. Human herpesvirus-6A and -6B encode viral immunoevasins that downregulate class I MHC molecules. *Virology* 365:125-135.
 46. Hudson, A. W., P. M. Howley, and H. L. Ploegh. 2001. A human herpesvirus 7 glycoprotein, U21, diverts major histocompatibility complex class I molecules to lysosomes. *J. Virol.* 75:12347-12358.
 47. Reusch, U., W. Muranyi, P. Lucin, H. G. Burgert, H. Hengel, and U. H. Koszinowski. 1999. A cytomegalovirus glycoprotein re-routes MHC class I complexes to lysosomes for degradation. *EMBO J.* 18:1081-1091.
 48. Zuo, J., A. Currin, B. D. Griffin, C. Shannon-Lowe, W. A. Thomas, M. E. Rensing, E. J. Wiertz, and M. Rowe. 2009. The Epstein-Barr virus G-protein-coupled receptor contributes to immune evasion by targeting MHC class I molecules for degradation. *PLoS Pathog.* 5:e1000255.
 49. Coscoy, L. and D. Ganem. 2000. Kaposi's sarcoma-associated herpesvirus encodes two proteins that block cell surface display of MHC class I chains by enhancing their endocytosis. *Proc. Natl. Acad. Sci. U. S. A* 97:8051-8056.
 50. Ishido, S., C. Wang, B. S. Lee, G. B. Cohen, and J. U. Jung. 2000. Downregulation of major histocompatibility complex class I molecules by Kaposi's sarcoma-associated herpesvirus K3 and K5 proteins. *J. Virol.* 74:5300-5309.
 51. Abendroth, A., I. Lin, B. Slobedman, H. Ploegh, and A. M. Arvin. 2001. Varicella-zoster virus retains major histocompatibility complex class I proteins in the Golgi compartment of infected cells. *J. Virol.* 75:4878-4888.
 52. Eisfeld, A. J., M. B. Yee, A. Erazo, A. Abendroth, and P. R. Kinchington. 2007. Downregulation of class I major histocompatibility complex surface expression by varicella-zoster virus involves open reading frame 66 protein kinase-dependent and -independent mechanisms. *J. Virol.* 81:9034-9049.
 53. Ahn, K., A. Angulo, P. Ghazal, P. A. Peterson, Y. Yang, and K. Fruh. 1996. Human cytomegalovirus inhibits antigen presentation by a sequential multistep process. *Proc. Natl. Acad. Sci. U. S. A* 93:10990-10995.
 54. Jones, T. R., E. J. Wiertz, L. Sun, K. N. Fish, J. A. Nelson, and H. L. Ploegh. 1996. Human cytomegalovirus US3 impairs transport and maturation of major histocompatibility complex class I heavy chains. *Proc. Natl. Acad. Sci. U. S. A* 93:11327-11333.
 55. Park, B., Y. Kim, J. Shin, S. Lee, K. Cho, K. Fruh, S. Lee, and K. Ahn. 2004. Human cytomegalovirus inhibits tapasin-dependent peptide loading and optimization of the MHC class I peptide cargo for immune evasion. *Immunity*. 20:71-85.
 56. Ziegler, H., R. Thale, P. Lucin, W. Muranyi, T. Flohr, H. Hengel, H. Farrell, W. Rawlinson, and U. H. Koszinowski. 1997. A mouse cytomegalovirus glycoprotein retains MHC class I complexes in the ERGIC/cis-Golgi compartments. *Immunity*. 6:57-66.
 57. Levitskaya, J., M. Coram, V. Levitsky, S. Imreh, P. M. Steigerwald-Mullen, G. Klein, M. G. Kurilla, and M. G. Masucci. 1995. Inhibition of antigen processing by the internal repeat region of the Epstein-Barr virus nuclear antigen-1. *Nature* 375:685-688.
 58. Levitskaya, J., A. Sharipo, A. Leonchiks, A. Ciechanover, and M. G. Masucci. 1997. Inhibition of ubiquitin/proteasome-dependent protein degradation by the Gly-Ala repeat domain of the Epstein-Barr virus nuclear antigen 1. *Proc Natl Acad Sci USA* 94:12616-12621.
 59. Yin, Y., B. Manoury, and R. Fahraeus. 2003. Self-inhibition of synthesis and antigen presentation by Epstein-Barr virus-encoded EBNA1. *Science* 301:1371-1374.
 60. Zaldumbide, A., M. Ossevoort, E. J. Wiertz, and R. C. Hoeben. 2007. *In cis* inhibition of antigen processing by the latency-associated nuclear antigen 1 of Kaposi sarcoma herpes virus. *Mol. Immunol.* 44:1352-1360.
 61. Ahn, K., T. H. Meyer, S. Uebel, P. Sempe, H. Djaballah, Y. Yang, P. A. Peterson, K. Fruh, and R. Tampe. 1996. Molecular mechanism and species specificity of TAP inhibition by herpes simplex virus ICP47. *EMBO J* 15:3247-3255.
 62. Fruh, K., K. Ahn, H. Djaballah, P. Sempe, P.

- M. van Endert, R. Tampe, P. A. Peterson, and Y. Yang. 1995. A viral inhibitor of peptide transporters for antigen presentation. *Nature* 375:415-418.
63. Hill, A., P. Jugovic, I. York, G. Russ, J. Bennink, J. Yewdell, H. Ploegh, and D. Johnson. 1995. Herpes simplex virus turns off the TAP to evade host immunity. *Nature* 375:411-415.
64. Tomazin, R., A. B. Hill, P. Jugovic, I. York, P. van Endert, H. L. Ploegh, D. W. Andrews, and D. C. Johnson. 1996. Stable binding of the herpes simplex virus ICP47 protein to the peptide binding site of TAP. *EMBO J.* 15:3256-3266.
65. York, I. A., C. Roop, D. W. Andrews, S. R. Riddell, F. L. Graham, and D. C. Johnson. 1994. A cytosolic herpes simplex virus protein inhibits antigen presentation to CD8⁺ T lymphocytes. *Cell* 77:525-535.
66. Ahn, K., A. Gruhler, B. Galocha, T. R. Jones, E. J. Wiertz, H. L. Ploegh, P. A. Peterson, Y. Yang, and K. Fruh. 1997. The ER-luminal domain of the HCMV glycoprotein US6 inhibits peptide translocation by TAP. *Immunity* 6:613-621.
67. Hengel, H., J. O. Koopmann, T. Flohr, W. Muranyi, E. Goulmy, G. J. Hammerling, U. H. Koszinowski, and F. Momburg. 1997. A viral ER-resident glycoprotein inactivates the MHC-encoded peptide transporter. *Immunity* 6:623-632.
68. Hewitt, E. W., S. S. Gupta, and P. J. Lehner. 2001. The human cytomegalovirus gene product US6 inhibits ATP binding by TAP. *EMBO J.* 20:387-396.
69. Kyritsis, C., S. Gorbulev, S. Hutschenreiter, K. Pawlitschko, R. Abele, and R. Tampe. 2001. Molecular mechanism and structural aspects of transporter associated with antigen processing inhibition by the cytomegalovirus protein US6. *J. Biol. Chem.* 276:48031-48039.
70. Lehner, P. J., J. T. Karttunen, G. W. Wilkinson, and P. Cresswell. 1997. The human cytomegalovirus US6 glycoprotein inhibits transporter associated with antigen processing-dependent peptide translocation. *Proc Natl Acad Sci USA* 94:6904-6909.
71. Hislop, A. D., M. E. Rensing, D. van Leeuwen, V. A. Pudney, D. Horst, D. Koppers-Lalic, N. P. Croft, J. J. Neefjes, A. B. Rickinson, and E. J. Wiertz. 2007. A CD8⁺ T cell immune evasion protein specific to Epstein-Barr virus and its close relatives in Old World primates. *J. Exp. Med.* 204:1863-1873.
72. Koppers-Lalic, D., E. A. Reits, M. E. Rensing, A. D. Lipinska, R. Abele, J. Koch, R. M. Marcondes, P. Admiraal, D. van Leeuwen, K. Bienkowska-Szewczyk, T. C. Mettenleiter, F. A. Rijsewijk, R. Tampe, J. Neefjes, and E. J. Wiertz. 2005. Varicelloviruses avoid T cell recognition by UL49.5-mediated inactivation of the transporter associated with antigen processing. *Proc. Natl. Acad. Sci. U. S. A* 102:5144-5149.
73. Koppers-Lalic, D., M. C. Verweij, A. D. Lipinska, Y. Wang, E. Quinten, E. A. Reits, J. Koch, S. Loch, M. M. Rezende, F. Daus, K. Bienkowska-Szewczyk, N. Osterrieder, T. C. Mettenleiter, M. H. Heemskerk, R. Tampe, J. J. Neefjes, S. I. Chowdhury, M. E. Rensing, F. A. Rijsewijk, and E. J. Wiertz. 2008. Varicellovirus UL 49.5 proteins differentially affect the function of the transporter associated with antigen processing, TAP. *PLoS Pathog.* 4:e1000080.
74. Verweij, M. C., A. D. Lipinska, D. Koppers-Lalic, W. F. van Leeuwen, J. I. Cohen, P. R. Kinchington, I. Messaoudi, K. Bienkowska-Szewczyk, M. E. Rensing, F. A. Rijsewijk, and E. J. Wiertz. 2011. The Capacity of UL49.5 Proteins To Inhibit TAP Is Widely Distributed among Members of the Genus Varicellovirus. *J. Virol.* 85:2351-2363.
75. Doom, C. M. and A. B. Hill. 2008. MHC class I immune evasion in MCMV infection. *Med. Microbiol. Immunol.* 197:191-204.
76. Rickinson, A. B. and E. Kieff. 2007. Epstein-Barr Virus, p. 2655-2700. In D. M. Knipe and P. M. Howley (eds.), *Field's virology*, vol. 2. Lippincott Williams & Wilkins, a Wolters Kluwer Business, Philadelphia.
77. Rickinson, A. B. and D. J. Moss. 1997. Human cytotoxic T lymphocyte responses to Epstein-Barr virus infection. *Annu. Rev. Immunol.* 15:405-431.
78. Heslop, H. E., M. K. Brenner, and C. M. Rooney. 1994. Donor T cells to treat EBV-associated lymphoma. *N. Engl. J. Med.* 331:679-680.
79. Heslop, H. E. and C. M. Rooney. 1997. Adoptive cellular immunotherapy for EBV lymphoproliferative disease. *Immunol. Rev.* 157:217-222.
80. Hochberg, D., J. M. Middeldorp, M. Catalina, J. L. Sullivan, K. Luzuriaga, and D. A. Thorley-Lawson. 2004. Demonstration of the Burkitt's lymphoma Epstein-Barr virus phenotype in dividing latently infected memory cells *in vivo*. *Proc. Natl. Acad. Sci. U. S. A* 101:239-244.
81. Rowe, D. T., M. Rowe, G. I. Evan, L. E. Wallace, P. J. Farrell, and A. B. Rickinson. 1986. Restricted expression of EBV latent genes and T-lymphocyte-detected membrane antigen in Burkitt's lymphoma cells. *EMBO J.* 5:2599-2607.
82. Samanta, M., D. Iwakiri, and K. Takada. 2008. Epstein-Barr virus-encoded small RNA induces IL-10 through RIG-I-mediated IRF-3 signaling. *Oncogene* 27:4150-4160.
83. Rensing, M. E., S. E. Keating, D. van Leeuwen, D. Koppers-Lalic, I. Y. Pappworth, E. J. Wiertz, and M. Rowe. 2005. Impaired transporter associated with antigen processing-dependent

- peptide transport during productive EBV infection. *J. Immunol.* 174:6829-6838.
84. Cai, X., A. Schafer, S. Lu, J. P. Bilello, R. C. Desrosiers, R. Edwards, N. Raab-Traub, and B. R. Cullen. 2006. Epstein-Barr virus microRNAs are evolutionarily conserved and differentially expressed. *PLoS Pathog.* 2:e23.
 85. Grundhoff, A., C. S. Sullivan, and D. Ganem. 2006. A combined computational and microarray-based approach identifies novel microRNAs encoded by human gamma-herpesviruses. *RNA.* 12:733-750.
 86. Pfeffer, S., M. Zavolan, F. A. Grasser, M. Chien, J. J. Russo, J. Ju, B. John, A. J. Enright, D. Marks, C. Sander, and T. Tuschl. 2004. Identification of virus-encoded microRNAs. *Science* 304:734-736.
 87. Xia, T., A. O'Hara, I. Araujo, J. Barreto, E. Carvalho, J. B. Sapucaia, J. C. Ramos, E. Luz, C. Pedroso, M. Manrique, N. L. Toomey, C. Brites, D. P. Dittmer, and W. J. Harrington, Jr. 2008. EBV microRNAs in primary lymphomas and targeting of CXCL-11 by ebv-mir-BHRF1-3. *Cancer Res.* 68:1436-1442.
 88. Choy, E. Y., K. L. Siu, K. H. Kok, R. W. Lung, C. M. Tsang, K. F. To, D. L. Kwong, S. W. Tsao, and D. Y. Jin. 2008. An Epstein-Barr virus-encoded microRNA targets PUMA to promote host cell survival. *J. Exp. Med.*
 89. Zeidler, R., G. Eissner, P. Meissner, S. Uebel, R. Tampe, S. Lazis, and W. Hammerschmidt. 1997. Downregulation of TAP1 in B lymphocytes by cellular and Epstein-Barr virus-encoded interleukin-10. *Blood* 90:2390-2397.
 90. Morrison, T. E., A. Mauser, A. Wong, J. P. Ting, and S. C. Kenney. 2001. Inhibition of IFN-gamma signaling by an Epstein-Barr virus immediate-early protein. *Immunity.* 15:787-799.
 91. Rensing, M. E., D. van Leeuwen, F. A. Verreck, R. Gomez, B. Heemskerk, M. Toebe, M. M. Mullen, T. S. Jardetzky, R. Longnecker, M. W. Schilham, T. H. Ottenhoff, J. Neefjes, T. N. Schumacher, L. M. Hutt-Fletcher, and E. J. Wiertz. 2003. Interference with T cell receptor-HLA-DR interactions by Epstein-Barr virus gp42 results in reduced T helper cell recognition. *Proc. Natl. Acad. Sci. U. S. A* 100:11583-11588.
 92. Frappier, L. 2003. The biology of plasmids. ASM Press, Washington, D.C.
 93. Kieff, E. and A. B. Rickinson. 2007. Epstein-Barr Virus and Its Replication, p. 2603-2654. In D. M. Knipe and P. M. Howley (eds.), *Field's virology*, vol. 2. Lippincott Williams & Wilkins, a Wolters Kluwer Business, Philadelphia.
 94. Adams, A. 1987. Replication of latent Epstein-Barr virus genomes in Raji cells. *J. Virol.* 61:1743-1746.
 95. Lupton, S. and A. J. Levine. 1985. Mapping genetic elements of Epstein-Barr virus that facilitate extrachromosomal persistence of Epstein-Barr virus-derived plasmids in human cells. *Mol. Cell Biol.* 5:2533-2542.
 96. Yates, J. L., N. Warren, and B. Sugden. 1985. Stable replication of plasmids derived from Epstein-Barr virus in various mammalian cells. *Nature* 313:812-815.
 97. Lee, S. P., J. M. Brooks, H. Al Jarrah, W. A. Thomas, T. A. Haigh, G. S. Taylor, S. Humme, A. Schepers, W. Hammerschmidt, J. L. Yates, A. B. Rickinson, and N. W. Blake. 2004. CD8 T cell recognition of endogenously expressed Epstein-Barr virus nuclear antigen 1. *J. Exp. Med.* 199:1409-1420.
 98. Tellam, J., G. Connolly, K. J. Green, J. J. Miles, D. J. Moss, S. R. Burrows, and R. Khanna. 2004. Endogenous presentation of CD8⁺ T cell epitopes from Epstein-Barr virus-encoded nuclear antigen 1. *J. Exp. Med.* 199:1421-1431.
 99. Tellam, J., M. H. Fogg, M. Rist, G. Connolly, D. Tschärke, N. Webb, L. Heslop, F. Wang, and R. Khanna. 2007. Influence of translation efficiency of homologous viral proteins on the endogenous presentation of CD8⁺ T cell epitopes. *J. Exp. Med.* 204:525-532.
 100. Voo, K. S., T. Fu, H. Y. Wang, J. Tellam, H. E. Heslop, M. K. Brenner, C. M. Rooney, and R. F. Wang. 2004. Evidence for the presentation of major histocompatibility complex class I-restricted Epstein-Barr virus nuclear antigen 1 peptides to CD8⁺ T lymphocytes. *J. Exp. Med.* 199:459-470.
 101. Heessen, S., A. Leonchiks, N. Issaeva, A. Sharipo, G. Selivanova, M. G. Masucci, and N. P. Dantuma. 2002. Functional p53 chimeras containing the Epstein-Barr virus Gly-Ala repeat are protected from Mdm2- and HPV-E6-induced proteolysis. *Proc. Natl. Acad. Sci. U. S. A* 99:1532-1537.
 102. Heessen, S., N. P. Dantuma, P. Tessarz, M. Jellne, and M. G. Masucci. 2003. Inhibition of ubiquitin/proteasome-dependent proteolysis in *Saccharomyces cerevisiae* by a Gly-Ala repeat. *FEBS Lett.* 555:397-404.
 103. Hoyt, M. A., J. Zich, J. Takeuchi, M. Zhang, C. Govaerts, and P. Coffino. 2006. Glycine-alanine repeats impair proper substrate unfolding by the proteasome. *EMBO J.* 25:1720-1729.
 104. Sharipo, A., M. Imreh, A. Leonchiks, S. Imreh, and M. G. Masucci. 1998. A minimal glycine-alanine repeat prevents the interaction of ubiquitinated I kappaB alpha with the proteasome: a new mechanism for selective inhibition of proteolysis. *Nat. Med.* 4:939-944.
 105. Zhang, M. and P. Coffino. 2004. Repeat sequence of Epstein-Barr virus-encoded nuclear antigen 1 protein interrupts proteasome substrate processing. *J. Biol. Chem.* 279:8635-8641.
 106. Daskalogianni, C., S. Apcher, M. M. Candeias,

- N. Naski, F. Calvo, and R. Fahraeus. 2008. GLY-ALA repeats induce position and substrate specific regulation of 26S proteasome-dependent partial processing. *J. Biol. Chem.*
107. Jones, R. J., L. J. Smith, C. W. Dawson, T. Haigh, N. W. Blake, and L. S. Young. 2003. Epstein-Barr virus nuclear antigen 1 (EBNA1) induced cytotoxicity in epithelial cells is associated with EBNA1 degradation and processing. *Virology* 313:663-676.
 108. Ossevoort, M., A. Zaldumbide, S. J. Cramer, E. I. van der Voort, R. E. Toes, and R. C. Hoeben. 2006. Characterization of an immuno 'stealth' derivative of the herpes simplex virus thymidine-kinase gene. *Cancer Gene Ther.* 13:584-591.
 109. Ossevoort, M., A. Zaldumbide, A. J. te Velthuis, M. Melchers, M. E. Rensing, E. J. Wiertz, and R. C. Hoeben. 2007. The nested open reading frame in the Epstein-Barr virus nuclear antigen-1 mRNA encodes a protein capable of inhibiting antigen presentation *in cis*. *Mol. Immunol.* 44:3588-3596.
 110. Tellam, J., C. Smith, M. Rist, N. Webb, L. Cooper, T. Vuocolo, G. Connolly, D. C. Tschärke, M. P. Devoy, and R. Khanna. 2008. Regulation of protein translation through mRNA structure influences MHC class I loading and T cell recognition. *Proc. Natl. Acad. Sci. U. S. A* 105:9319-9324.
 111. Cristillo, A. D., J. R. Mortimer, I. H. Barrette, T. P. Lillierap, and D. R. Forsdyke. 2001. Double-stranded RNA as a not-self alarm signal: to evade, most viruses purine-load their RNAs, but some (HTLV-1, Epstein-Barr) pyrimidine-load. *J. Theor. Biol.* 208:475-491.
 112. Yoshioka, M., M. M. Crum, and J. T. Sample. 2008. Autorepression of Epstein-Barr virus nuclear antigen 1 expression by inhibition of pre-mRNA processing. *J. Virol.* 82:1679-1687.
 113. Moore, K. W., P. Vieira, D. F. Fiorentino, M. L. Trounstine, T. A. Khan, and T. R. Mosmann. 1990. Homology of cytokine synthesis inhibitory factor (IL-10) to the Epstein-Barr virus gene BCRF1. *Science* 248:1230-1234.
 114. Mocellin, S., M. C. Panelli, E. Wang, D. Nagorsen, and F. M. Marincola. 2003. The dual role of IL-10. *Trends Immunol.* 24:36-43.
 115. Moore, K. W., M. R. de Waal, R. L. Coffman, and A. O'Garra. 2001. Interleukin-10 and the interleukin-10 receptor. *Annu. Rev. Immunol.* 19:683-765.
 116. Ding, Y., L. Qin, S. V. Kotenko, S. Pestka, and J. S. Bromberg. 2000. A single amino acid determines the immunostimulatory activity of interleukin 10. *J. Exp. Med.* 191:213-224.
 117. Savard, M., C. Belanger, M. Tardif, P. Gourde, L. Flamand, and J. Gosselin. 2000. Infection of primary human monocytes by Epstein-Barr virus. *J. Virol.* 74:2612-2619.
 118. Shimakage, M., M. Kimura, S. Yanoma, M. Ibe, S. Yokota, G. Tsujino, T. Kozuka, T. Dezawa, S. Tamura, A. Ohshima, M. Yutsudo, and A. Hakura. 1999. Expression of latent and replicative-infection genes of Epstein-Barr virus in macrophage. *Arch. Virol.* 144:157-166.
 119. de Waal, M. R., J. Haanen, H. Spits, M. G. Roncarolo, V. A. te, C. Figdor, K. Johnson, R. Kastelein, H. Yssel, and J. E. De Vries. 1991. Interleukin 10 (IL-10) and viral IL-10 strongly reduce antigen-specific human T cell proliferation by diminishing the antigen-presenting capacity of monocytes via downregulation of class II major histocompatibility complex expression. *J. Exp. Med.* 174:915-924.
 120. Salek-Ardakani, S., J. R. Arrand, and M. Mackett. 2002. Epstein-Barr virus encoded interleukin-10 inhibits HLA-class I, ICAM-1, and B7 expression on human monocytes: implications for immune evasion by EBV. *Virology* 304:342-351.
 121. Koppelman, B., J. J. Neeffjes, J. E. De Vries, and M. R. de Waal. 1997. Interleukin-10 down-regulates MHC class II alpha beta peptide complexes at the plasma membrane of monocytes by affecting arrival and recycling. *Immunity.* 7:861-871.
 122. Vieira, P., R. Waal-Malefyt, M. N. Dang, K. E. Johnson, R. Kastelein, D. F. Fiorentino, J. E. deVries, M. G. Roncarolo, T. R. Mosmann, and K. W. Moore. 1991. Isolation and expression of human cytokine synthesis inhibitory factor cDNA clones: homology to Epstein-Barr virus open reading frame BCRF1. *Proc. Natl. Acad. Sci. U. S. A* 88:1172-1176.
 123. Keating, S., S. Prince, M. Jones, and M. Rowe. 2002. The lytic cycle of Epstein-Barr virus is associated with decreased expression of cell surface major histocompatibility complex class I and class II molecules. *J. Virol.* 76:8179-8188.
 124. Reits, E. A., J. C. Vos, M. Gromme, and J. Neeffjes. 2000. The major substrates for TAP *in vivo* are derived from newly synthesized proteins. *Nature* 404:774-778.
 125. Yuan, J., E. Cahir-McFarland, B. Zhao, and E. Kieff. 2006. Virus and cell RNAs expressed during Epstein-Barr virus replication. *J. Virol.* 80:2548-2565.
 126. Croft, N. P., C. Shannon-Lowe, A. I. Bell, D. Horst, E. Kremmer, M. E. Rensing, E. J. Wiertz, J. M. Middeldorp, M. Rowe, A. B. Rickinson, and A. D. Hislop. 2009. Stage-specific inhibition of MHC class I presentation by the Epstein-Barr virus BNLF2a protein during virus lytic cycle. *PLoS Pathog.* 5:e1000490.
 127. Lipinska, A. D., D. Koppers-Lalic, M. Rychlowski, P. Admiraal, F. A. Rijsewijk, K. Bienkowska-Szewczyk, and E. J. Wiertz. 2006. Bovine herpesvirus 1 UL49.5 protein inhibits the transporter associated with antigen processing

- despite complex formation with glycoprotein M. *J. Virol.* 80:5822-5832.
128. Rivaille, P., Y. G. Cho, and F. Wang. 2002. Complete genomic sequence of an Epstein-Barr virus-related herpesvirus naturally infecting a new world primate: a defining point in the evolution of oncogenic lymphocryptoviruses. *J. Virol.* 76:12055-12068.
 129. Zuo, J., L. L. Quinn, J. Tamblin, W. A. Thomas, R. Feederle, H. J. Delecluse, A. D. Hislop, and M. Rowe. 2011. The Epstein-Barr virus-encoded BILF1 protein modulates immune recognition of endogenously processed antigen by targeting major histocompatibility complex class I molecules trafficking on both the exocytic and endocytic pathways. *J. Virol.* 85:1604-1614.
 130. Beisser, P. S., D. Verzijl, Y. K. Gruijthuisen, E. Beuken, M. J. Smit, R. Leurs, C. A. Bruggeman, and C. Vink. 2005. The Epstein-Barr virus BILF1 gene encodes a G protein-coupled receptor that inhibits phosphorylation of RNA-dependent protein kinase. *J. Virol.* 79:441-449.
 131. Paulsen, S. J., M. M. Rosenkilde, J. Eugen-Olsen, and T. N. Kledal. 2005. Epstein-Barr virus-encoded BILF1 is a constitutively active G protein-coupled receptor. *J. Virol.* 79:536-546.
 132. Rosenkilde, M. M., M. J. Smit, and M. Waldhoer. 2008. Structure, function and physiological consequences of virally encoded chemokine seven transmembrane receptors. *Br. J. Pharmacol.* 153 Suppl 1:S154-S166.
 133. Bodaghi, B., T. R. Jones, D. Zipeto, C. Vita, L. Sun, L. Laurent, F. Arenzana-Seisdedos, J. L. Virelizier, and S. Michelson. 1998. Chemokine sequestration by viral chemoreceptors as a novel viral escape strategy: withdrawal of chemokines from the environment of cytomegalovirus-infected cells. *J. Exp. Med.* 188:855-866.
 134. Wang, Z., L. Zhang, A. Qiao, K. Watson, J. Zhang, and G. H. Fan. 2008. Activation of CXCR4 triggers ubiquitination and down-regulation of major histocompatibility complex class I (MHC-I) on epithelioid carcinoma HeLa cells. *J. Biol. Chem.* 283:3951-3959.
 135. Baylis, S. A., D. J. Purifoy, and E. Littler. 1989. The characterization of the EBV alkaline deoxyribonuclease cloned and expressed in *E. coli*. *Nucleic Acids Res.* 17:7609-7622.
 136. Knopf, C. W. and K. Weisshart. 1990. Comparison of exonucleolytic activities of herpes simplex virus type-1 DNA polymerase and DNase. *Eur. J. Biochem.* 191:263-273.
 137. Sheaffer, A. K., S. P. Weinheimer, and D. J. Tenney. 1997. The human cytomegalovirus UL98 gene encodes the conserved herpesvirus alkaline nuclease. *J. Gen. Virol.* 78 (Pt 11):2953-2961.
 138. Glaunsinger, B., L. Chavez, and D. Ganem. 2005. The exonuclease and host shutoff functions of the SOX protein of Kaposi's sarcoma-associated herpesvirus are genetically separable. *J. Virol.* 79:7396-7401.
 139. Everly, D. N., Jr., P. Feng, I. S. Mian, and G. S. Read. 2002. mRNA degradation by the virion host shutoff (Vhs) protein of herpes simplex virus: genetic and biochemical evidence that Vhs is a nuclease. *J. Virol.* 76:8560-8571.
 140. Koppers-Lalic, D., F. A. Rijsewijk, S. B. Verschuren, van Gaans-Van den Brink JA, A. Neisig, M. E. Rensing, J. Neeffjes, and E. J. Wiertz. 2001. The UL41-encoded virion host shutoff (vhs) protein and vhs-independent mechanisms are responsible for down-regulation of MHC class I molecules by bovine herpesvirus 1. *J. Gen. Virol.* 82:2071-2081.
 141. Elgadi, M. M., C. E. Hayes, and J. R. Smiley. 1999. The herpes simplex virus vhs protein induces endoribonucleolytic cleavage of target RNAs in cell extracts. *J. Virol.* 73:7153-7164.
 142. Glaunsinger, B. A. and D. E. Ganem. 2006. Messenger RNA turnover and its regulation in herpesviral infection. *Adv. Virus Res.* 66:337-394.
 143. Glaunsinger, B. and D. Ganem. 2004. Highly selective escape from KSHV-mediated host mRNA shutoff and its implications for viral pathogenesis. *J. Exp. Med.* 200:391-398.
 144. Buisson, M., T. Geoui, D. Flot, N. Tarbouriech, M. E. Rensing, E. J. Wiertz, and W. P. Burmeister. 2009. A bridge crosses the active-site canyon of the Epstein-Barr virus nuclease with DNase and RNase activities. *J. Mol. Biol.* 391:717-728.
 145. Bagneris, C., L. C. Briggs, R. Savva, B. Ebrahimi, and T. E. Barrett. 2011. Crystal structure of a KSHV-SOX-DNA complex: insights into the molecular mechanisms underlying DNase activity and host shutoff. *Nucleic Acids Res.*
 146. Gruffat, H., J. Batisse, D. Pich, B. Neuhierl, E. Manet, W. Hammerschmidt, and A. Sergeant. 2002. Epstein-Barr virus mRNA export factor EB2 is essential for production of infectious virus. *J. Virol.* 76:9635-9644.
 147. Ruvolo, V., E. Wang, S. Boyle, and S. Swaminathan. 1998. The Epstein-Barr virus nuclear protein SM is both a post-transcriptional inhibitor and activator of gene expression. *Proc. Natl. Acad. Sci. U. S. A* 95:8852-8857.
 148. Ruvolo, V., L. Sun, K. Howard, S. Sung, H. J. Delecluse, W. Hammerschmidt, and S. Swaminathan. 2004. Functional analysis of Epstein-Barr virus SM protein: identification of amino acids essential for structure, transactivation, splicing inhibition, and virion production. *J. Virol.* 78:340-352.

Chapter 2

A CD8⁺ T cell immune evasion protein specific to Epstein-Barr virus and its close relatives in Old World primates

A.D. Hislop*, M.E. Ressing*, D. van Leeuwen, V.A. Pudney, D. Horst, D. Koppers-Lalic, N.P. Croft, J.J. Neefjes, A.B. Rickinson and E.J.H.J. Wiertz.

The Journal of Experimental Medicine 2007

* These authors contributed equally to this manuscript

Abstract

γ 1-Herpesviruses such as Epstein-Barr virus (EBV) have a unique ability to amplify virus loads *in vivo* through latent growth-transforming infection. Whether they, like α - and β -herpesviruses, have been driven to actively evade immune detection of replicative (lytic) infection remains a moot point. We were prompted to readdress this question by recent work (Pudney, V.A., A.M. Leese, A.B. Rickinson, and A.D. Hislop. 2005. *J. Exp. Med.* 201:349–360; Rensing, M.E., S.E. Keating, D. van Leeuwen, D. Koppers-Lalic, I.Y. Pappworth, E.J.H.J. Wiertz, and M. Rowe. 2005. *J. Immunol.* 174:6829–6838) showing that, as EBV-infected cells move through the lytic cycle, their susceptibility to EBV-specific CD8⁺ T cell recognition falls dramatically, concomitant with reductions in transporter associated with antigen processing (TAP) function and surface human histocompatibility leukocyte antigen (HLA) class I expression. Screening of genes that are unique to EBV and closely related γ 1-herpesviruses of Old World primates identified an early EBV lytic cycle gene, BNLF2a, which efficiently blocks antigen-specific CD8⁺ T cell recognition through HLA-A-, HLA-B-, and HLA-C-restricting alleles when expressed in target cells *in vitro*. The small (60-amino acid) BNLF2a protein mediated its effects through interacting with the TAP complex and inhibiting both its peptide- and ATP-binding functions. Furthermore, this targeting of the major histocompatibility complex class I pathway appears to be conserved among the BNLF2a homologues of Old World primate γ 1-herpesviruses. Thus, even the acquisition of latent cycle genes endowing unique growth-transforming ability has not liberated these agents from evolutionary pressure to evade CD8⁺ T cell control over virus replicative foci.

Introduction

Herpesviruses are an ancient virus family whose members have long histories of coevolution with their host species (1). A hallmark of herpesvirus biology is the ability to colonize a naive host through the productive (lytic) infection of permissive cells, usually at a mucosal site of virus transmission, and thereafter to persist within that host as a nonproductive (latent) infection of a different specialized cell type. Persistence within the now-immune host is achieved through the down-regulation of all viral antigen expression in latently infected cells. Subsequently, occasional reactivations from latency can serve to reestablish the foci of virus replication at mucosal sites, providing a source of infectious virions for transmission to other individuals.

In the best studied system, HSV, a member of the α -herpesvirus subfamily establishing latency in neurons, the possibilities of successful reactivation are increased if the virus initially establishes a high latent virus genome load (2, 3); this in turn is reliant on the level of virus replication initially achieved during primary infection of the naive host (3, 4). Because the host CD8⁺ T cell response is the principle means of controlling this initial replication, any factor restricting the efficiency of that control would be to the advantage of the virus. Indeed, HSV was the first herpesvirus in which a CD8⁺ T cell evasion mechanism was recognized. This involves an immediate early protein of the HSV lytic cycle, ICP47, which inhibits the peptide transporter associated with antigen processing (TAP) by acting as a pseudosubstrate preventing peptide binding and transport. Consequently, TAP cannot pump potentially antigenic peptides from proteasomal digestion in the cytoplasm into the endoplasmic reticulum for loading onto MHC class I molecules (5, 6). Other herpesviruses heavily dependent on virus replication to establish a latent viral load, such as the β -subfamily human and mouse cytomegaloviruses, have likewise been found to possess several CD8⁺ T cell evasion mechanisms targeting either TAP or MHC class I assembly (7, 8).

The situation has been less clear for lymphocryptoviruses (LCVs), the most recently evolved (γ 1) herpesvirus genus, whose members are found only in Old World and some New World primate species and whose prototype is the EBV of humans. These viruses are orally transmitted, replicate in oropharyngeal epithelial sites and establish latency in B lymphocytes (for review see reference 9). When first colonizing the B cell system, LCVs use their unique growth-transforming ability to directly drive the expansion of latently infected B cells and only later down-regulate latent antigen expression to establish an immunologically silent infection of the memory B cell pool (10). This ability to expand the latently infected cell reservoir independent of lytic virus replication has raised debate as to whether LCVs might be under less

intense immunological pressure to evade T cell control over the lytic cycle (11).

We were prompted to return to this question by two recent findings in the EBV system, both suggestive of an active immune evasion strategy in the lytic cycle. First, cells productively infected with EBV *in vitro* showed HLA class I down-regulation and reduced TAP function (12). Second, *in vitro* assays on lytically infected target cells using CD8⁺ T cell clones specific for immediate early-, early-, or late-expressed EBV antigens indicated much poorer presentation as the lytic cycle progressed (13). In this paper, we show that EBV and other Old World LCVs have indeed acquired an evasion strategy that specifically targets the peptide transporter TAP, thus limiting the supply of antigenic fragments to MHC class I molecules and, ultimately, their presentation to CD8⁺ T cells.

Results

Screening of γ 1-herpesvirus-specific lytic cycle genes for inhibition of CD8⁺ T cell recognition

We reasoned that any specific immune evasion function associated with EBV replication would most likely map to a lytic cycle gene restricted to the γ 1-herpesvirus (LCV) genus. Genomic sequences of HSV, CMV, and Kaposi's sarcoma-associated herpesvirus, the prototypic α , β , and γ 2 human herpesviruses, were aligned alongside those of two Old World γ 1 viruses, EBV and rhesus LCV, and with the recently discovered New World γ 1 virus of marmosets. This identified 11 LCV-specific genes that were present in the Old World viruses, some of which were also found in the New World virus. 4 out of these 11 genes are centrally positioned in the EBV genome; 2 of the 4, BLLF1 and BZLF2, encode viral envelope glycoproteins known to be involved in B cell entry, whereas the other 2, BLLF2 and BHLF1, were of particular interest because their functions are unknown. The other seven LCV-specific genes all lie within a 35-kb region at the right-hand end of the EBV genome and are identified as open blocks in the genome maps shown in Fig. 1. Two of these, BARF1 and BALF1, have homologies to the cellular CSF-1 receptor and bcl2 genes, respectively, implying functions other than the interception of antigen processing pathways, whereas a third gene, LF3, is deleted in the B95.8 virus strain that displays HLA class I down-regulation in the lytic cycle. The remaining unique genes in this region, BNLF2a, BNLF2b, BILF1, and BILF2, were selected for further study alongside BLLF2 and BHLF1.

All six genes were separately cloned into recombinant vaccinia virus vectors, as was the immune evasion gene from HSV, ICP47, as a positive control. These recombinants were then tested for their ability to inhibit CD8⁺ T cell killing when introduced into target cells along with a second vaccinia vector encoding an indicator target antigen. Such experiments were

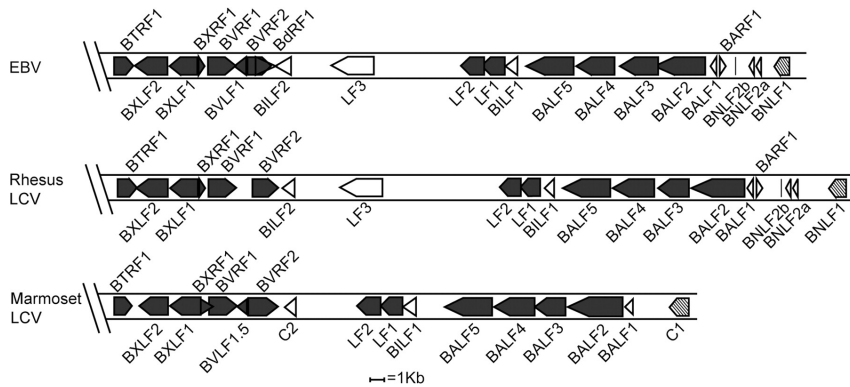


Figure 1. Diagrammatic alignment of the right-hand ends of the sequenced γ 1-herpesviruses

ORFs of EBV, the rhesus LCV, and marmoset LCV are shown as boxes; closed symbols represent ORFs with homologues in other herpesviruses; open symbols represent genes found only in γ 1-herpesviruses; and hatched symbols represent latent genes.

performed in the two cell types that EBV naturally infects *in vivo*, epithelial cells and B lymphocytes. Fig. 2 A (top) presents the results from a representative assay in the HLA-B*0801-positive epithelial cell line SVK using EBV nuclear antigen (EBNA) 3A as the target antigen and a CD8⁺ T cell clone specific for an HLA-B*0801-restricted EBNA3A epitope as the effector. Expression of one of the six EBV genes in question, BNLF2a, reduced the level of CD8⁺ T cell killing almost to background levels, as did the positive control ICP47. None of the other EBV genes tested (including BILF2, BLLF2, and BHLF1; not depicted) ever gave such an effect. Fig. 2 A (bottom) presents data from an essentially similar assay conducted in an EBV-transformed B lymphoblastoid cell line (LCL). In this case, the cells were infected with a vaccinia virus encoding, as an indicator antigen, an invariant chain-tagged form of the EBNA3C protein that is processed by the HLA class I and class II pathways, thereby allowing both CD8⁺ and CD4⁺ T cell recognition to be assayed simultaneously on the same target cells. As shown in Fig. 2 A (middle), expression of BNLF2a (and of ICP47) reduced target cell killing by an HLA-B*2705-restricted EBNA3C-specific CD8⁺ T cell clone to the background level seen on unmanipulated LCL targets. This background level represents recognition of preexisting epitopes derived from EBNA3C expressed from the resident EBV genome. In contrast, neither vaccinia BNLF2a nor any of the other proteins tested had any effect on the presentation of invariant chain-tagged EBNA3C to a DQ5-restricted EBNA3C-specific CD4⁺ T cell clone (Fig. 2 A, bottom).

Fig. 2 B shows the results of subsequent experiments conducted using EBV-transformed B cell lines with different HLA alleles to assess any allele-specific effects of BNLF2a on CD8⁺ T cell recognition. These assays used several different EBV latent (EBNA2 and EBNA3B) and lytic (BMLF1, BMRF1, BZLF1, and BGLF4) target antigens encoding epitopes recognized in the context of HLA-A (A*0201 and A*2402),

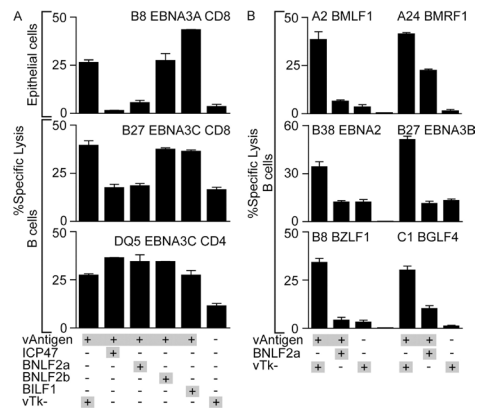


Figure 2. Representative cytotoxicity assays testing recognition of target cells coexpressing EBV-unique genes and target proteins

(A) Epithelial cells (top) were infected with vaccinia viruses expressing EBNA3A (vAntigen) and combinations of the indicated viruses expressing genes unique to EBV or a control vaccinia virus lacking an inserted gene (vTk-), before being incubated with HLA-B*0801-restricted CD8⁺ T cell clones specific for EBNA3A. EBV-transformed B cells (middle and bottom) were coinfecting with modified vaccinia Ankara expressing invariant chain-targeted EBNA3C (vAntigen) and the indicated combinations of vaccinia viruses. In parallel assays, the infected B cells were incubated with either HLA-B*2705-restricted CD8⁺ T cell clones specific for EBNA3C (middle) or CD4⁺ T cell clones restricted by HLA DQ5 specific for EBNA3C (bottom). (B) EBV-transformed B cells were infected with vaccinia viruses expressing BNLF2a, and the different EBV antigens indicated (vAntigen) encoding epitopes presented through a range of HLA types. Infected cells were incubated with cognate CD8⁺ T cells specific for an HLA-A*0201 epitope encoded by BMLF1, an HLA-A*2402 epitope encoded by BMRF1, an HLA-B*38 epitope encoded by EBNA2, an HLA-B*2705 epitope encoded by EBNA3B, an HLA-B*0801 epitope encoded by BZLF1, or an HLA-C*0101 epitope encoded by BGLF4. Error bars represent means \pm SD.

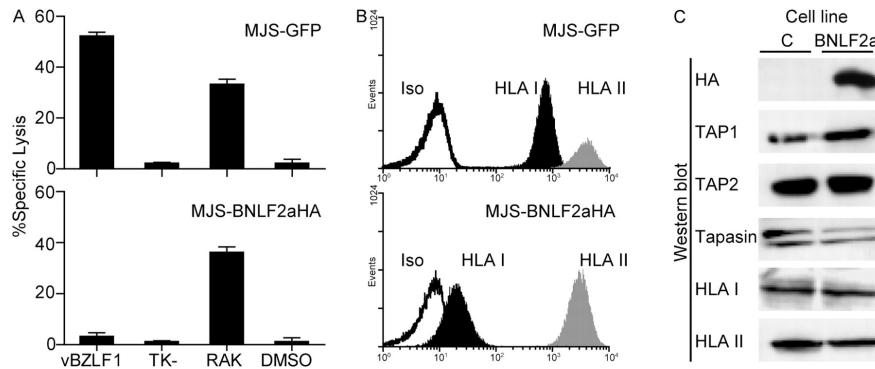


Figure 3. Expression of BNL2a prevents CD8⁺ T cell recognition by disrupting antigen presentation

(A) MJS cells were retrovirally transduced to express BNL2aHA (bottom) or control GFP (top). These cells were either infected with vaccinia viruses expressing BZLF1 or a control TK- virus, or sensitized with RAKFKQLL peptide or DMSO as a control before being incubated with CD8⁺ T cells specific for the BZLF1-encoded RAKFKQLL epitope in 5-h cytotoxicity assays. Error bars represent means \pm SD. (B) Flow cytometry histograms of the same cell lines show surface staining for HLA class I (B9.12.1) and HLA class II (L243), or staining with an isotype control. (C) Lysates of the two cell lines were separated by SDS-PAGE and analyzed by immunoblotting with antibodies specific for the HA tag (12CA5), TAP1 (148.3), TAP2 (435.4), tapasin (7F6), HLA class I heavy chains (HC10), and HLA class II DR α chains (DA6-147).

HLA-B (B*0801, B*2705, and B*3801), and HLA-C (C*0101) molecules. We observed marked inhibition of target cell killing by BNL2a throughout such experiments (Fig. 2 B).

EBV BNL2a causes cell-surface HLA class I down-regulation

To determine the mechanism of BNL2a-mediated inhibition of CD8⁺ T cell recognition, BNL2a containing a hemagglutinin (HA) epitope tag (BNL2aHA) was expressed in the melanoma cell line MelJuSo (MJS) through retroviral transduction. Initially, we performed cytotoxicity assays on the transduced cells to confirm that retrovirus-mediated expression of BNL2aHA in MJS cells recapitulates the BNL2a-induced phenotype described in the previous section. Fig. 3 A shows the results of a cytotoxicity assay using the HLA-B*0801-positive MJS cells expressing either BNL2aHA or GFP as targets. Infection of MJS cells with recombinant vaccinia virus expressing the EBV BZLF1 antigen resulted in recognition by BZLF1-specific CD8⁺ T cells (Fig. 3 A, top), but this was abrogated in BNL2aHA-expressing MJS cells (Fig. 3 A, bottom). However, when the target cells were sensitized with the relevant synthetic epitope peptide from BZLF1 (RAKFKQLL), the cells were lysed equally well whether or not BNL2a was present (Fig. 3 A). These data indicate that BNL2a blocks presentation of antigens that require endogenous processing before being presented to HLA class I-restricted T cells.

Because HLA class I levels have been found to be markedly reduced during productive EBV infection (12), we next examined whether expression of BNL2a affected the display of HLA molecules (Fig. 3 B). At the surface of transduced MJS cells,

levels of HLA class I were substantially reduced on BNL2aHA-expressing cells compared with control cells. This was a specific effect, because expression of HLA class II (Fig. 3 B) and transferrin receptor (not depicted) were unaffected.

Down-regulation of surface HLA class I molecules can result from viral interference at specific stages of the class I antigen presentation pathway and may involve the degradation of HLA class I molecules and other components of the HLA class I peptide-loading complex (7, 8). To investigate whether BNL2a affects levels of the components of the HLA class I peptide-loading complex, lysates of BNL2aHA or control transduced MJS cells were subjected to Western blot analysis for TAP1, TAP2, tapasin, and HLA class I. No marked differences were observed in the steady-state levels of these proteins (Fig. 3 C). Thus, despite reduced surface HLA class I levels, cells expressing BNL2aHA contained similar levels of the major components of the HLA class I peptide-loading complex.

EBV BNL2a blocks peptide transport by TAP

Surface HLA class I down-regulation can also result from the reduced supply of peptides to nascent HLA class I molecules in the endoplasmic reticulum. This in turn relies on the efficient generation of peptides by the proteasome and other peptidases and the transport of these peptides into the endoplasmic reticulum by the TAP complex. In EBV-infected B cells that have entered the virus lytic cycle, surface HLA class I down-regulation coincides with reduced peptide transport by TAP (12). To evaluate whether the inhibition of HLA class I expression by BNL2a involves interference with TAP function, we used an *in vitro* peptide translocation assay to examine TAP

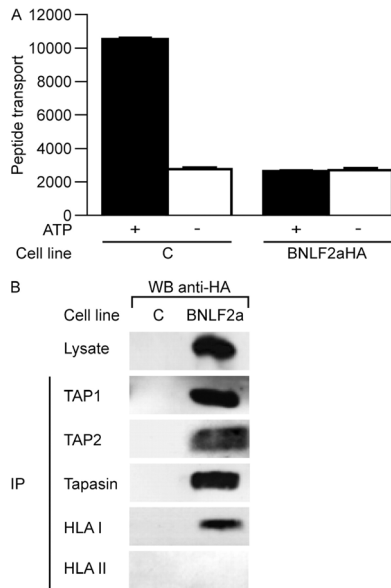


Figure 4. EBV BNLF2a blocks peptide transport by TAP
 (A) TAP-dependent peptide transport in BNLF2aHA-expressing and control MJS cells was assessed by permeabilizing the cells with streptolysin O and incubating them with a fluoresceinated peptide in the presence or absence of ATP. Translocated peptides that had become glycosylated in the endoplasmic reticulum were recovered by adsorption to concanavalin A–sepharose beads. After elution, the recovered peptide was quantitated by fluorometry in arbitrary units. Error bars represent the SEM of triplicates in a representative experiment. (B) Digitonin lysates of BNLF2aHA-expressing and control MJS-GFP cells were subjected to immunoprecipitation (IP) with antibodies specific for TAP1 (148.3), TAP2 (435.4), tapasin (R.gp46C), HLA class I heavy chains (HC10), and HLA class II DR α chains (DA6-147). Cell lysates and immune complexes were separated by SDS-PAGE, followed by Western blot analysis and staining with anti-HA antibody (12CA5) to detect HA-tagged BNLF2a.

activity in BNLF2aHA-expressing and control MJS cells. In control cells, fluorescent model peptides were efficiently transported across the endoplasmic reticulum membrane in an ATP-dependent manner. In contrast, peptide translocation was strongly impaired in BNLF2aHA-expressing cells (Fig. 4 A).

We next investigated whether BNLF2a was associated with the peptide-loading complex by performing coimmunoprecipitation experiments. BNLF2aHA-expressing or control cells were lysed using the mild detergent digitonin to preserve protein–protein interactions. TAP1, TAP2, tapasin, and HLA class I molecules were immunoprecipitated from the lysates, and all precipitates were probed with an HA-specific mAb to detect BNLF2aHA. Fig. 4 B shows that BNLF2a coprecipitates with TAP1, TAP2, tapasin, and HLA class I molecules, but not with HLA class II and the transferrin receptor (used as controls; TfR data not depicted).

EBV BNLF2a blocks TAP function by preventing the binding of peptides and ATP

TAP-mediated translocation of peptides into the endoplasmic reticulum is initiated by the interaction of peptides with the cytosolic peptide binding domains of TAP, followed by the binding and hydrolysis of ATP, which facilitates the opening of the transmembrane pore and peptide translocation (14, 15). We therefore evaluated the effect of BNLF2aHA on these steps in peptide transfer. The ability of peptides to bind to TAP in the presence of BNLF2a was examined by incubating radiolabeled peptides containing a photoactivatable cross-linker with microsomes derived from BNLF2aHA-expressing or control MJS cells. Peptides were covalently linked to their binding partners by UV irradiation and then separated by PAGE. In control MJS cells, radiolabeled peptides covalently linked to TAP were observed (Fig. 5 A; expressed as 100% in the quantitation depicted in Fig. 5 B), whereas such peptides failed to bind TAP in microsomes from BNLF2aHA-expressing cells (Fig. 5, A and B). As a specificity control, microsomes were incubated with both the radiolabeled reporter peptide and an unlabeled peptide derived from the HSV-1 ICP47 protein that is known to prevent peptide binding to TAP (16, 17). No binding of the radiolabeled peptide to TAP was observed in the presence of the ICP47 peptide (Fig. 5, A and B).

We next asked whether BNLF2a might also affect the binding of ATP to TAP. Lysates of BNLF2aHA-transduced or control cells were made using either the detergents digitonin, which preserves protein interactions within the peptide-loading complex, or 1% NP-40, which releases HLA class I, tapasin, and BNLF2a from TAP (see later in this section). Proteins capable of binding ATP were purified from the lysates by incubation with ATP-agarose beads and pelleting; these fractions, as well as the nonbinding supernatant (free) fractions, were subjected to Western blot analysis for the presence of TAP1, TAP2, tapasin, HLA class I, or BNLF2aHA. In control cells, ATP binds to the TAP subunits solubilized either in digitonin or NP-40 (Fig. 5 C, lanes 1 and 3), whereas tapasin and HLA class I molecules were coisolated only with ATP-bound TAP recovered from digitonin lysates (Fig. 5 C, compare lane 1 with lane 3). In contrast, the ATP-bound fraction from digitonin lysates of BNLF2aHA-expressing cells contained little of the four components of the peptide-loading complex (Fig. 5 C, lane 2), indicating that the EBV protein inhibits the interaction of ATP with the TAP proteins. Accordingly, BNLF2aHA was not detected in the ATP-agarose pellet fraction (lane 2) but was present in the supernatant fraction of BNLF2a-transduced MJS cells (lane 6). Interestingly, BNLF2a was released from TAP in NP-40 lysates, which restored the ATP-binding capacity of the TAP subunits, implying a low-affinity interaction of BNLF2a with TAP that prevents binding to ATP-agarose beads (lane 4).

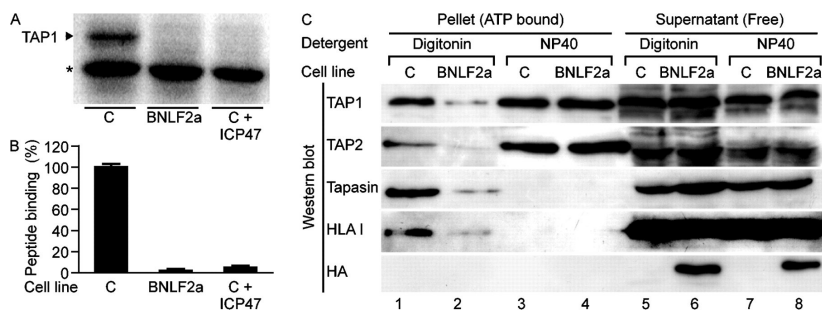


Figure 5. EBV BNLF2a inhibits peptide and ATP binding to TAP

(A) Microsomes prepared from BNLF2aHA-expressing and control MJS cells were incubated with a radiolabeled model peptide; where indicated, an excess of ICP47 competitor peptide was included in this incubation. After UV cross-linking, microsomes were lysed, and the proteins were separated by SDS-PAGE and exposed to a phosphorimaging screen. The position where TAP1 migrated in parallel immunoprecipitation experiments is shown by the arrowhead. The asterisk denotes a nonspecific background band. (B) Quantification of triplicate bands representing TAP-bound peptide. Results are shown as the percentage of peptide binding relative to peptide binding in control MJS cells (set as 100%). Error bars represent means \pm SD. (C) Digitonin and NP-40 lysates of MJS-BNLF2aHA and control MJS-GFP cells were incubated with ATP-agarose beads. ATP-agarose-bound (pellet) and unbound (supernatant) protein fractions were separated by SDS-PAGE and immunoblotted. Membranes were probed with antibodies specific for TAP1 (148.3), TAP2 (435.4), tapasin (7F6), HLA class I heavy chain (HC10), and the HA tag (12CA5).

BNLF2a homologues are encoded by other Old World γ 1 primate herpesviruses and down-regulate HLA class I expression

Because earlier genomic alignments had shown that a BNLF2a homologous gene was present in the Rhesus LCV genome, we went on to sequence the equivalent region from the LCV genomes of baboons (papio herpesvirus), chimpanzees (pan herpesvirus),

orangutans (orangutan herpesvirus), and gorillas (gorilla herpesvirus). Each virus genome contained an equivalent BNLF2a open reading frame (ORF). Fig. 6 A shows the predicted amino acid sequence of these homologous proteins alongside those of EBV and the rhesus macaque LCV. These proteins show between 53 and 63% overall identity and share similar features; they are small 59–60-amino acid proteins, and each

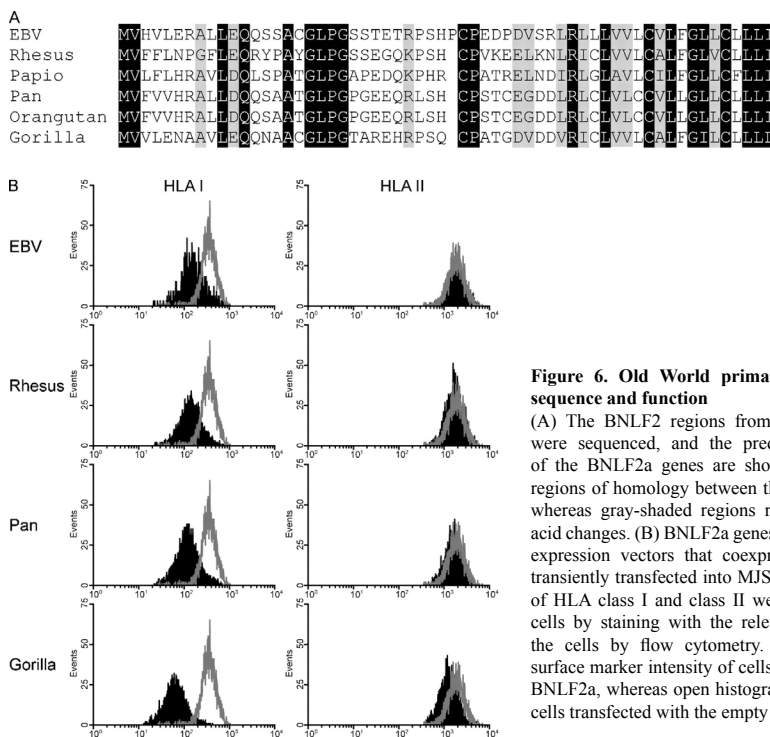


Figure 6. Old World primate γ 1-herpesvirus BNLF2a sequence and function

(A) The BNLF2 regions from the indicated herpesviruses were sequenced, and the predicted amino acid sequence of the BNLF2a genes are shown. Black regions represent regions of homology between the different BNLF2a species, whereas gray-shaded regions represent conservative amino acid changes. (B) BNLF2a genes were subcloned into plasmid expression vectors that coexpressed GFP, and these were transiently transfected into MJS cells. At 48 h, surface levels of HLA class I and class II were assessed on GFP-positive cells by staining with the relevant antibody and analyzing the cells by flow cytometry. Black histograms represent surface marker intensity of cells transfected with the relevant BNLF2a, whereas open histograms represent the intensity of cells transfected with the empty vector plasmid.

has a hydrophobic C terminus and several sites in the nonhydrophobic region where the sequence is conserved. Homology or alignment searches using programs such as the basic local alignment search tool reveal no obvious matches with any other protein in the database (unpublished data).

To test whether the BNL2a homologues within the nonhuman LCVs had retained BNL2a-like function, the relevant coding sequences were introduced into plasmid expression vectors under the control of the CMV immediate early promoter and transiently transfected into the human MJS cell line. Plasmid constructs were engineered to coexpress GFP using an internal ribosome entry site (IRES) element allowing identification of transfected cells. Fig. 6 B shows the flow cytometric analysis of MJS cells that had been transfected with the BNL2a genes derived from EBV, the rhesus LCV, pan herpesvirus (note that the pan and orangutan BNL2a genes had identical sequences), or gorilla herpesvirus. Cells were stained for surface HLA class I or surface HLA class II as a control. In each case, expression of BNL2a derived from the different viruses reproducibly caused down-regulation of surface HLA class I to different degrees depending on the species from which the gene was derived, whereas HLA class II levels were unaffected. We subsequently extended these studies by transfecting other available Old World primate cell lines with the different BNL2a genes and measuring the surface MHC class I levels of the transfected cells as before. Fig. S1 shows histograms of MHC class I staining of transfected LLC-MK2 cells (Rhesus macaque), orangutan B cells transformed with the endogenous orangutan herpesvirus (orangutan LCL), and Cos cells (African green monkey). All BNL2a expression constructs showed down-regulation of surface MHC class I in LLC-MK2 cells and Cos cells, with a more subtle down-regulation observed in transformed orangutan LCLs. The inhibitory effects of the various LCV BNL2a proteins therefore appear to be conserved and operate in various cells of Old World primate origin.

Discussion

This study was prompted by recent work (13) looking into target cell recognition by CD8⁺ T cell clones specific for EBV-lytic cycle antigens. This had shown that recognition was most efficient using clones against immediate early antigens, less so for clones against early antigens, and much less so for late antigen-specific effectors, despite the fact that the latter had the highest avidity in epitope peptide titration assays (13). Therefore, antigen processing function appeared to be progressively impaired as cells moved through the lytic cycle. Two observations argued against this being a secondary effect of general cytopathology associated with virus replication. Thus, in B LCLs *in*

vitro where a small percentage of cells enter the lytic cycle, cells in the late phase of virus replication appear to remain viable for several days. More importantly, surface HLA class I levels on lytically infected cells begin to fall in the early phase of the cycle before other surface proteins, including HLA class II, are affected (12). This implied that EBV was actively impeding lytic cycle antigen presentation to CD8⁺ T cells.

Noting that immune evasion strategies within the herpesvirus family tend to be virus subfamily or genus specific, we focused on the six lytic cycle genes that were unique to the γ 1 genus and of unknown function. This identified one such gene, BNL2a, as encoding a CD8 immune evasion protein. When expressed from a vaccinia vector in target cells, the BNL2a protein reproducibly inhibited recognition of various indicator antigens (EBV latent and lytic cycle proteins) by CD8⁺ T cell clones restricted through several HLA-A, -B, and -C alleles. In contrast, class II antigen presentation in BNL2a-expressing cells remained intact, and only presentation by the HLA class I pathway was impeded. The BNL2a protein was found to function by blocking both peptide and ATP binding to the TAP complex, thereby impairing peptide loading of HLA class I molecules and their expression at the cell surface.

It is notable that BNL2a transcripts initially appear in the early phase of the lytic cycle, peaking 8–12 h after lytic cycle induction in a B cell line (18). The majority of EBV lytic cycle transcripts are expressed in the late phase after BNL2a expression, at a time when the protein's effects are likely to be well established. This would explain why the late proteins are poorly processed and presented by lytically infected cells. In contrast, the two immediate early proteins, BZLF1 and BRLF1, expressed in the first wave of viral gene expression before BNL2a are efficiently recognized by their cognate T cells (13). The less efficient presentation of the four early antigens tested in our previous study (13) likely reflects the fact that they are expressed before BNL2a's inhibitory effects are optimal. These antigens are known to be BZLF1/BRLF1 induced and, therefore, appear very soon after the immediate early-to-early transition, probably just before BNL2a expression (19–23).

It is also interesting to note how the actions of BNL2a might explain the highly skewed composition of the lytic antigen-induced CD8⁺ T cell response to EBV infection, whereby antigens expressed before or at the latest coincident with BNL2a during the course of the lytic cycle constitute by far the most dominant targets. Thus when we derived CD8⁺ T cell clones from the expanded CD8⁺ population of IM patients in an unbiased manner, we often identified strong CD8 reactivities specific for the two immediate early proteins and for a small subset of early proteins, but only rarely to other early proteins or to any of the late proteins analyzed (11, 13). Similarly, when T cells were cloned from the joints of rheumatoid arthritis

patients and tested against an EBV-cDNA expression library, only T cells specific for immediate early or a small number of early proteins were detected (24, 25). Thus, very few responses to late proteins have been described and, when they occur, these responses are weak (26). Yet, in principle, all lytic cycle proteins should be available as exogenous antigens for cross-presentation by dendritic cells during the priming of the CD8⁺ T cell response. We infer that, after priming, the subsequent numerical dominance of immediate early and early antigen-specific responses reflects the importance of direct contact between primed CD8⁺ T cells and lytically infected target cells in selectively amplifying responses to epitopes that are well presented on those target cells.

BNLF2a is one of a set of genes, including two others with immunomodulatory function, BCRF1 (viral IL-10 homologue) and BARF1 (viral GCSF-receptor), that have been acquired by the γ 1 viruses of Old World primates but are absent from the New World γ 1 virus analyzed thus far (27, 28). This implies acquisition, in the last 50 million years or so, after the Old World/New World fork in primate evolution. The Old World primate viruses have also acquired a more complex set of latent growth-transforming genes over this same period. Thus, it may be the combination of these more sophisticated immune-evasion and growth-transforming strategies that underlies the apparently greater prevalence that the Old World viruses achieve in their host population compared with their New World counterpart (29).

BNLF2a is the first TAP-specific inhibitor identified in γ 1-herpesviruses, and like the other three herpesvirus TAP inhibitors identified so far, BNLF2a has its own unique structure and mechanism of action. Simplexviruses and varicelloviruses, both members of the α subfamily, use different strategies to inactivate TAP. The simplexviruses HSV1 and 2 encode a small cytosolic protein, ICP47, which acts as a high affinity competitor for peptide binding to TAP yet does not affect ATP binding to the transporter complex (5, 6, 17, 30, 31). In contrast, the varicellovirus bovine herpesvirus 1 and several of its relatives encode the UL49.5 gene product, which renders TAP translocation incompetent without affecting its ability to bind peptide or ATP (32, 33). Ultimately, bovine herpesvirus 1 UL49.5 targets TAP1 and TAP2 for degradation by proteasomes (32, 33). In the case of β -herpesviruses, the prototypic virus of this subfamily, human CMV, inhibits TAP function via the endoplasmic reticulum luminal domain of the transmembrane protein US6. This protein reduces association of ATP to TAP1 and promotes binding to TAP2 but does not interfere with peptide binding, nor does it influence the stability of the transporter complex (34–38). In the case of the γ 2-herpesvirus, mouse γ -herpesvirus 68, TAP is targeted secondarily for slow degradation by the virus-encoded ubiquitin ligase mK3, whose primary function is to rapidly target MHC class I heavy chains

for proteasomal degradation (39–46).

In contrast to the described TAP inhibitors in the other herpesviruses, BNLF2a disables TAP function by blocking both the association of peptides with the peptide binding site and the interaction of ATP with the nucleotide binding domains of the transporter. How this small 60-amino acid protein, which consists of a hydrophilic N-terminal domain of 42 residues and a hydrophobic domain of 18 residues, achieves both of these functions is currently unclear. Despite the absence of an obvious N-terminal signal sequence, preliminary data suggest that BNLF2a is membrane-associated (unpublished data). This may be a consequence of binding to TAP or may result from posttranslational insertion of the hydrophobic C terminus into the endoplasmic reticulum membrane, as has been reported for other proteins (47). The small size of BNLF2a and the relative distance between the peptide and ATP binding sites of TAP may preclude BNLF2a from acting directly on both of these sites. The expected exposure of BNLF2a's N terminus in the cytosol would, however, suggest that this part interacts with cytosolic domains of the TAP complex. BNLF2a may then interfere directly with peptide or ATP binding while simultaneously disrupting subsequent steps of the translocation cycle through an indirect mechanism, e.g., by inhibiting conformational transitions required for proper function of the TAP complex.

The ability of an infected cell to escape CD8⁺ T cell recognition is likely to be most efficient when multiple points of the antigen processing pathway are targeted by viral immune evasion proteins. In the case of HSV2-infected cells, two viral proteins, the TAP inhibitor ICP47 and the host shutoff protein encoded by UL-41, have been shown to act synergistically to prevent CD8⁺ T cell lysis (48). In such an infection model, the long-lived TAP complexes are unlikely to be affected in the short term by the virus host shutoff function. Thus, cells infected with mutant HSV viruses lacking either of these two genes show partial inhibition of CD8⁺ T cell function, whereas cells infected with viruses expressing both genes show a dramatic reduction in their ability to be lysed by CD8⁺ T cells. Interesting in this context is the recent identification of the EBV-encoded gene BGLF5, which is at least one gene responsible for host protein synthesis shutoff (49). Expression of BGLF5 is sufficient to inhibit synthesis of host proteins, including HLA class I molecules, causing a decrease in surface class I levels. Coexpression of BNLF2a and BGLF5 by EBV could then represent an effective strategy for inhibiting the HLA class I antigen processing pathway (12).

In summary, the prototype γ 1-herpesvirus, EBV, evades CD8⁺ T cell detection in the lytic cycle through a strategy that is unique in its molecular detail yet targets antigen presentation at the same point, TAP-mediated peptide transport, that is targeted by several other herpesviruses. The fact that the TAP inhibitors encoded by the different herpesvirus genera share

no obvious homology presents a striking example of convergent evolution. Their existence testifies to the strength of the evolutionary pressure exerted on many herpesviruses by CD8⁺ T cell responses against virus replicative infections. The present work indicates that, despite their ability to amplify viral loads *in vivo* through nonreplicative latent infection, EBV and Old World γ 1-herpesvirus relatives have indeed been subjected to the same immune pressure.

Materials and Methods

CD8⁺ T cell clones, vaccinia viruses, and cytotoxicity assays

EBV-specific CD8⁺ T cell clones were generated from PBMCs of infectious mononucleosis patients by limiting dilution cloning, as previously described (11). CD8⁺ T cell clones used in this study were specific for the following epitopes derived from the respective EBV gene products: RAKFKQLL from BZLF1 and QAKWRLQTL from EBNA3A (both presented by HLA-B*0801 [50, 51]), GLCTLVAML from BMLF1 (presented by HLA-A*0201 [11]), CYDHAQTHL from BMRF1 (presented by HLA A*2402 [13]), YHLIVDTSLS from EBNA2 (presented by HLA-B*38 [52]), HRCQAIRKK from EBNA3B (presented by HLA-B*2705 [53]), and an undefined epitope derived from BGLF4 (presented by HLA-C*0101 [13]). CD4⁺ T cell clones specific for the HLA DQ5-presented epitope SDDELPIYIDPNMEP from EBNA 3C were produced by the stimulation of PBMCs from healthy donors, with their autologous EBV-transformed B cell line and limiting dilution cloning these cells, as previously described (54). All experiments were approved by the South Birmingham Health Authority Local Research Ethics Committee. Recombinant vaccinia viruses were used to express individual EBV B95.8 strain genes, as previously described, and a vaccinia virus lacking an insert (ν Tk⁻) used for control infections (13, 54). Target cells infected with the vaccinia viruses for cytotoxicity assays were either SV40-transformed keratinocytes, HLA-matched EBV-transformed B LCLs, or the melanoma cell line MJS (HLA-A*01, -B*08, and -Cw*07) (55). Target cells were infected with vaccinia viruses at a multiplicity of infection of 10, incubated for 16 h, and used as targets in standard 5-h chromium release assays. Where indicated in the figures, target cells were sensitized with synthetic CTL epitope peptide (Alta Biosciences) at a concentration of 5 μ M for 90 min before use in cytotoxicity assays.

Antibodies

The antibodies used in this study have been described elsewhere (32, 55). Mouse mAbs used to detect human cellular proteins were as follows: W6/32 or B9.12.1, which recognizes β 2-microglobulin-associated HLA class I complexes (Immunotech); HC10 (provided

by H. Ploegh, Whitehead Institute for Biomedical Research, Cambridge, MA), specific for HLA class I heavy chains; anti-HLA-DR mAb L243 (American Type Culture Collection); DA6-147, specific for HLA-DR α chains (provided by P. Cresswell, Howard Hughes Medical Institute, Yale University School of Medicine, New Haven, CT); and 148.3 directed to TAP1 and 435.4 directed to TAP2 (provided by R. Tampe, Johann Wolfgang Goethe-University, Frankfurt, Germany and by P. van Ender, Hopital Necker, Paris, France, respectively). Anti-tapsin antibodies used were a rabbit serum, R.gp46C, against the C-terminal region (provided by P. Cresswell) and a rat mAb, 7F6 (provided by R. Tampe). To detect HA-tagged BNLF2a, the influenza-specific mAb 12CA5 was used (Roche Diagnostics).

Retroviral transduction of cell lines

Retroviral constructs were engineered by cloning the BNLF2a gene into the pLZRS retroviral vector. Immediately downstream from this gene was an IRES, which allowed co expression of a marker gene, truncated nerve growth factor. The BNLF2a sequence was modified at the C terminus to encode four methionines and the influenza HA epitope to allow detection (denoted as BNLF2aHA). Virus was produced using the Phoenix packaging cell line and used to transduce MJS cells, as previously described (55). As a control, MJS cells were transduced with an IRES-GFP-expressing retrovirus.

Flow cytometry analysis of surface HLA class I and II

Surface levels of HLA class I and II molecules were measured by flow cytometric analysis after staining with the antibodies W6/32 or B9.12.1 for class I molecules or L243 for class II molecules. In all cases, aliquots of cells were stained with the appropriate isotype controls, and bound antibodies were detected using a goat anti-mouse phycoerythrin antibody. Stained cells were analyzed on a flow cytometer (Epics; Beckman Coulter), and data was processed using Win MDI software (Scripps Research Institute).

Peptide transport assay

TAP-mediated peptide transport assays were conducted by permeabilizing aliquots of 3×10^6 MJS cells with 2.5 IU/ml of streptolysin O (Murex Diagnostics) and incubating these cells with 200 nmol of the fluoresceinated peptide CVNKTERAY (provided by W. Benckhuijsen and J.W. Drijfhout, Leiden University Medical Center, Leiden, Netherlands) in the presence or absence of 10 mM ATP at 37°C for 10 min. Translocation was terminated by lysing cells with ice-cold lysis buffer (1% Triton X-100, 500 mM NaCl, 2 mM MgCl₂, 50 mM Tris HCl, pH 8), and the nuclei were removed by centrifugation. Peptides that had been glycosylated in the endoplasmic reticulum were isolated from lysates by incubation with

concanavalin A–sepharose beads (GE Healthcare). These peptides were eluted from the beads with 500 mM mannopyranoside, 10 mM EDTA, 50 mM Tris HCl, pH 8, and fluorescence was detected using a fluorescence plate reader (Cyto fluor; PerSeptive Biosystems).

Western blot analysis and immunoprecipitations

SDS-PAGE and immunoblotting were performed as previously reported (32, 56). MJS cells transfected with retroviruses expressing either BNL2aHA or GFP were lysed using either 1% NP-40 or 1% digitonin made in 50 mM Tris HCl, pH 7.5, 5 mM MgCl₂, 150 mM NaCl, 1 mM leupeptin, and 1 mM 4-(2-aminoethyl) benzenesulfonyl fluoride. Lysates of solubilized proteins, equivalent to 2×10^5 cells, were separated by SDS-PAGE and transferred to polyvinylidene difluoride membranes (GE Healthcare). Proteins of interest were detected by incubating the membranes with specific antibodies followed by horseradish peroxidase (HRP)–conjugated secondary antispecies antibodies (Jackson ImmunoResearch Laboratories). Bound HRP-labeled antibodies were visualized using ECL Plus (GE Healthcare).

For immunoprecipitation experiments, cell lysates prepared with 1% digitonin solution were incubated with the different specific antibodies for at least 2 h at 4°C. Protein G–sepharose beads (GE Healthcare) were used to isolate immune complexes, which were washed with 0.1% digitonin and subjected to Western blot analysis. Antibodies that bound the blotted proteins were detected using ExactaCruz (Santa Cruz Biotechnology, Inc.), according to the manufacturer's instructions.

Peptide binding assay

TAP-containing microsomal membranes were prepared from MJS cells transduced with BNL2aHA or GFP by homogenization of the cells with a cell cracker (EMBL) and removal of the nuclei by centrifugation. The ability of peptides to bind to TAP complexes in the microsomes was assessed by incubation with an ¹²⁵I-labeled peptide 5PS2 (ERYDKSE-[BPA]-L [57]) containing a photoactivatable cross-linker in the absence or presence of 2.5 μM of unlabeled HSV-1 ICP47 competitor peptide (16). After incubation for 15 min on ice, microsomes were washed with PBS, and peptide–protein interactions were covalently linked by UV exposure for 10 min on ice at a distance of 2 cm using a UVP lamp (B-100A; Blak-Ray) with a mercury lamp (Par 38; Sylvania). Samples were analyzed by SDS-PAGE, and bound peptide was quantitated by phosphoimaging. Migration of peptide-bound TAP1 was confirmed by immunoprecipitation.

ATP-agarose binding assay

MJS cells transduced with BNL2aHA or GFP were lysed with 1% digitonin or 1% NP-40, as described in Western blot analysis and immunoprecipitations.

Nuclei were removed, and lysates were incubated with hydrated C-8 ATP-agarose beads (13-μM; final concentration; Sigma-Aldrich) at 4°C for 2 h. The beads were centrifuged to provide a supernatant fraction and a pellet fraction. Proteins bound to the ATP-agarose pellet fraction were eluted with 500 mM EDTA, and these as well as the supernatant fraction were analyzed by Western blot.

Cloning and transient expression of BNL2a genes

BNL2a homologues were cloned from the following LCVs: papio herpesvirus, rhesus herpesvirus, pan herpesvirus, orangutan herpesvirus, and gorilla herpesvirus. PCR primers were designed to hybridize to a sequence flanking the BNL2 region, which was conserved between EBV and the rhesus herpesvirus. PCR products were amplified from either a genomic DNA fragment of rhesus herpesvirus (provided by F. Wang, Harvard Medical School, Boston, MA) or from DNA extracted from B cell lines spontaneously transformed with the endogenous LCV of each host species. This amplified BNL2 region of each virus was cloned into the plasmid pCR2.1TOPO (Invitrogen), and inserts were sequenced using standard techniques. Sequences are available from GenBank/EMBL/DBJ under accession nos. EF207711 (papio herpesvirus), EF207712 (pan herpesvirus), EF207713 (orangutan herpesvirus), and EF207714 (gorilla herpesvirus).

For functional studies, the BNL2a genes were subcloned into a modified pCDNA3 vector (provided by E. Reits) and expressed under the control of the CMV immediate early promoter. Immediately downstream from BNL2a was an IRES element followed by the GFP gene, allowing co expression of this marker. Plasmids were transfected into either MJS cells, the Rhesus macaque kidney cell line LLC-MK2, or the African green monkey kidney fibroblast like cell line Cos using Lipofectamine 2000 (Invitrogen), or transfected by electroporation into orangutan B cells transformed with their endogenous LCV. Transfected cells were cultured for 48 h before staining for surface marker expression and flow cytometric analysis, as described in Flow cytometry analysis of surface HLA class I and II.

Acknowledgements

We thank Paul Lehner for helpful advice and the provision of reagents.

This work was supported by a program grant from the Medical Research Council UK, grant UL 2005-3259 from the Dutch Cancer Society (to D. Horst), the M.W. Beijerinck Virology Fund of the Royal Academy of Arts and Sciences (M.E. Rensing), grant Vidi 917.76.330 from the Netherlands Organisation for Scientific Research (to M.E. Rensing), the Dutch Diabetes Research Foundation (D. Koppers-Lalic), and National Institutes of Health grant AI26296.

The authors have no conflicting financial interests.

References

1. McGeoch, D.J., F.J. Rixon, and A.J. Davison. 2006. Topics in herpesvirus genomics and evolution. *Virus Res.* 117:90–104.
2. Sawtell, N.M. 1998. The probability of *in vivo* reactivation of herpes simplex virus type 1 increases with the number of latently infected neurons in the ganglia. *J. Virol.* 72:6888–6892.
3. Sawtell, N.M., R.L. Thompson, L.R. Stanberry, and D.I. Bernstein. 2001. Early intervention with high-dose acyclovir treatment during primary herpes simplex virus infection reduces latency and subsequent reactivation in the nervous system *in vivo*. *J. Infect. Dis.* 184:964–971.
4. Sawtell, N. 1997. Comprehensive quantification of herpes simplex virus latency at the single-cell level. *J. Virol.* 71:5423–5431.
5. Hill, A., P. Jugovic, I. York, G. Russ, J. Bennink, J. Yewdell, H. Ploegh, and D. Johnson. 1995. Herpes simplex virus turns off the TAP to evade host immunity. *Nature.* 375:411–415.
6. Fruh, K., K. Ahn, H. Djaballah, P. Sempe, P.M. van Endert, R. Tampe, P.A. Peterson, and Y. Yang. 1995. A viral inhibitor of peptide transporters for antigen presentation. *Nature.* 375:415–418.
7. Vossen, M.T., E.M. Westerhout, C. Soderberg-Naucler, and E.J. Wiertz. 2002. Viral immune evasion: a masterpiece of evolution. *Immunogenetics.* 54:527–542.
8. Lilley, B.N., and H.L. Ploegh. 2005. Viral modulation of antigen presentation: manipulation of cellular targets in the ER and beyond. *Immunol. Rev.* 207:126–144.
9. Rickinson, A.B., and E. Kieff. 2006. Epstein-Barr Virus. In *Fields Virology*. Fifth edition. D.M. Knipe, P.M. Howley, D.E. Griffin, R.A. Lamb, M.A. Martin, B. Roizman, and S.E. Strauss, editors. Lippincott Williams & Wilkins, Philadelphia. 2655–2700.
10. Kuppers, R. 2003. B cells under influence: transformation of B cells by Epstein-Barr virus. *Nat. Rev. Immunol.* 3:801–812.
11. Steven, N.M., N. Annels, A. Kumar, A. Leese, M.G. Kurilla, and A.B. Rickinson. 1997. Immediate early and early lytic cycle proteins are frequent targets of the Epstein-Barr virus-induced cytotoxic T cell response. *J. Exp. Med.* 185:1605–1617.
12. Rensing, M.E., S.E. Keating, D. van Leeuwen, D. Koppers-Lalic, I.Y. Pappworth, E.J.H.J. Wiertz, and M. Rowe. 2005. Impaired transporter associated with antigen processing-dependent peptide transport during productive EBV infection. *J. Immunol.* 174:6829–6838.
13. Pudney, V.A., A.M. Leese, A.B. Rickinson, and A.D. Hislop. 2005. CD8⁺ immunodominance among Epstein-Barr virus lytic cycle antigens directly reflects the efficiency of antigen presentation in lytically infected cells. *J. Exp. Med.* 201:349–360.
14. Reits, E.A., A.C. Griekspoor, and J. Neeffjes. 2000. How does TAP pump peptides? Insights from DNA repair and traffic ATPases. *Immunol. Today.* 21:598–600.
15. van Endert, P.M., L. Saveanu, E.W. Hewitt, and P.J. Lehner. 2002. Powering the peptide pump: TAP crosstalk with energetic nucleotides. *Trends Biochem. Sci.* 27:454–461.
16. Galocha, B., A. Hill, B.C. Barnett, A. Dolan, A. Raimondi, R.F. Cook, J. Brunner, D.J. McGeoch, and H.L. Ploegh. 1997. The active site of ICP47, a herpes simplex virus-encoded inhibitor of the major histocompatibility complex (MHC)-encoded peptide transporter associated with antigen processing (TAP), maps to the NH₂-terminal 35 residues. *J. Exp. Med.* 185:1565–1572.
17. Neumann, L., W. Kraas, S. Uebel, G. Jung, and R. Tampe. 1997. The active domain of the herpes simplex virus protein ICP47: a potent inhibitor of the transporter associated with antigen processing (TAP). *J. Mol. Biol.* 272:484–492.
18. Yuan, J., E. Cahir-McFarland, B. Zhao, and E. Kieff. 2006. Virus and cell RNAs expressed during Epstein-Barr virus replication. *J. Virol.* 80:2548–2565.
19. Rooney, C.M., D.T. Rowe, T. Ragot, and P.J. Farrell. 1989. The spliced BZLF1 gene of Epstein-Barr virus (EBV) transactivates an early EBV promoter and induces the virus productive cycle. *J. Virol.* 63:3109–3116.
20. Kenney, S., E. Holley-Guthrie, E.-C. Mar, and M. Smith. 1989. The Epstein-Barr virus BMLF1 promoter contains an enhancer element that is responsive to the BZLF1 and BRLF1 transactivators. *J. Virol.* 63:3878–3883.
21. Holley-Guthrie, E.A., E.B. Quinlivan, E.-C. Mar, and S. Kenney. 1990. The Epstein-Barr virus (EBV) BMRF1 promoter for early antigen (EA-D) is regulated by the EBV transactivators, BRLF1 and BZLF1, in a cell-specific manner. *J. Virol.* 64:3753–3759.
22. Ragozy, T., and G. Miller. 1999. Role of the Epstein-Barr virus Rta protein in activation of distinct classes of viral lytic cycle genes. *J. Virol.* 73:9858–9866.
23. Liu, C., N. Sista, and J. Pagano. 1996. Activation of the Epstein-Barr virus DNA polymerase promoter by the BRLF1 immediate-early protein is mediated through USF and E2F. *J. Virol.* 70:2545–2555.
24. Scotet, E., J. David-Ameline, M.-A. Peyrat, A. Moreau-Aubry, D. Pinczon, A. Lim, J. Even, G. Semana, J.M. Berthelot, R. Breathnach, *et*

- al.* 1996. T cell response to Epstein-Barr virus transactivators in chronic rheumatoid arthritis. *J. Exp. Med.* 184:1791–1800.
25. Scotet, E., M.A. Peyrat, X. Saulquin, C. Retiere, C. Couedel, F. Davodeau, N. Dulphy, A. Toubert, J.D. Bignon, A. Lim, *et al.* 1999. Frequent enrichment for CD8⁺ T cells reactive against common herpesviruses in chronic inflammatory lesions: towards a reassessment of the physiopathological significance of T cell clonal expansions found in autoimmune inflammatory processes. *Eur. J. Immunol.* 29:973–985.
 26. Bharadwaj, M., S.R. Burrows, J.M. Burrows, D.J. Moss, M. Catalina, and R. Khanna. 2001. Longitudinal dynamics of antigen-specific CD8⁺ cytotoxic T lymphocytes following primary Epstein-Barr virus infection. *Blood.* 98:2588–2589.
 27. Cho, Y., J. Ramer, P. Rivaille, C. Quink, R.L. Garber, D. Beier, and F. Wang. 2001. An Epstein-Barr-related herpesvirus from marmoset lymphomas. *Proc. Natl. Acad. Sci. USA.* 98:1224–1229.
 28. Rivaille, P., Y.-G. Cho, and F. Wang. 2002. Complete genomic sequence of an Epstein-Barr virus-related herpesvirus naturally infecting a New World Primate: a defining point in the evolution of oncogenic lymphocryptoviruses. *J. Virol.* 76:12055–12068.
 29. Fogg, M.H., A. Carville, J. Cameron, C. Quink, and F. Wang. 2005. Reduced prevalence of Epstein-Barr virus-related lymphocryptovirus infection in sera from a New World primate. *J. Virol.* 79:10069–10072.
 30. Ahn, K., T.H. Meyer, S. Uebel, P. Sempe, H. Djaballah, Y. Yang, P.A. Peterson, K. Fruh, and R. Tampe. 1996. Molecular mechanism and species specificity of TAP inhibition by herpes simplex virus ICP47. *EMBO J.* 15:3247–3255.
 31. Tomazin, R., A.B. Hill, P. Jugovic, I. York, P. van Endert, H.L. Ploegh, D.W. Andrews, and D.C. Johnson. 1996. Stable binding of the herpes simplex virus ICP47 protein to the peptide binding site of TAP. *EMBO J.* 15:3256–3266.
 32. Koppers-Lalic, D., E.A.J. Reits, M.E. Rensing, A.D. Lipinska, R. Abele, J. Koch, M.M. Rezende, P. Admiraal, D. van Leeuwen, K. Bienkowska-Szewczyk, *et al.* 2005. Varicelloviruses avoid T cell recognition by UL49.5-mediated inactivation of the transporter associated with antigen processing. *Proc. Natl. Acad. Sci. USA.* 102:5144–5149.
 33. Lipinska, A.D., D. Koppers-Lalic, M. Rychlowski, P. Admiraal, F.A.M. Rijsewijk, K. Bienkowska-Szewczyk, and E.J.H.J. Wiertz. 2006. Bovine herpesvirus 1 UL49.5 protein inhibits the transporter associated with antigen processing despite complex formation with glycoprotein M. *J. Virol.* 80:5822–5832.
 34. Ahn, K., A. Gruhler, B. Galocha, T.R. Jones, E.J.H.J. Wiertz, H.L. Ploegh, P.A. Peterson, Y. Yang, and K. Fruh. 1997. The ER-luminal domain of the HCMV glycoprotein US6 inhibits peptide translocation by TAP. *Immunity.* 6:613–621.
 35. Hengel, H., J.-O. Koopmann, T. Flohr, W. Muranyi, E. Goulmy, G.J. Hammerling, U.H. Koszinowski, and F. Momburg. 1997. A viral ER-resident glycoprotein inactivates the MHC-encoded peptide transporter. *Immunity.* 6:623–632.
 36. Lehner, P.J., J.T. Karttunen, G.W.G. Wilkinson, and P. Cresswell. 1997. The human cytomegalovirus US6 glycoprotein inhibits transporter associated with antigen processing-dependent peptide translocation. *Proc. Natl. Acad. Sci. USA.* 94:6904–6909.
 37. Kyritsis, C., S. Gorbulev, S. Hutschenreiter, K. Pawlitschko, R. Abele, and R. Tampe. 2001. Molecular mechanism and structural aspects of transporter associated with antigen processing inhibition by the cytomegalovirus protein US6. *J. Biol. Chem.* 276:48031–48039.
 38. Hewitt, E.W., S.S. Gupta, and P.J. Lehner. 2001. The human cytomegalovirus gene product US6 inhibits ATP binding by TAP. *EMBO J.* 20:387–396.
 39. Boname, J.M., J.S. May, and P.G. Stevenson. 2005. The murine gamma-herpesvirus-68 MK3 protein causes TAP degradation independent of MHC class I heavy chain degradation. *Eur. J. Immunol.* 35:171–179.
 40. Boname, J.M., and P.G. Stevenson. 2001. MHC class I ubiquitination by a viral PHD/LAP finger protein. *Immunity.* 15:627–636.
 41. Boname, J.M., B.D. de Lima, P.J. Lehner, and P.G. Stevenson. 2004. Viral degradation of the MHC class I peptide loading complex. *Immunity.* 20:305–317.
 42. Lybarger, L., X. Wang, M.R. Harris, I. Virgin, W. Herbert, and T.H. Hansen. 2003. Virus subversion of the MHC class I peptide-loading complex. *Immunity.* 18:121–130.
 43. Wang, X., L. Lybarger, R. Connors, M.R. Harris, and T.H. Hansen. 2004. Model for the interaction of gammaherpesvirus 68 RING-CH finger protein mK3 with major histocompatibility complex class I and the peptide-loading complex. *J. Virol.* 78:8673–8686.
 44. Yu, Y.Y.L., M.R. Harris, L. Lybarger, L.A. Kimpler, N.B. Myers, H.W. Virgin IV, and T.H. Hansen. 2002. Physical association of the K3 protein of gamma-2 herpesvirus 68 with major histocompatibility complex class I molecules with impaired peptide and beta(2)-microglobulin assembly. *J. Virol.* 76:2796–2803.
 45. Wang, X., Y. Ye, W. Lencer, and T.H. Hansen. 2006. The viral E3 ubiquitin ligase mK3 uses the

- Derlin/p97 endoplasmic reticulum-associated degradation pathway to mediate down-regulation of major histocompatibility complex class I proteins. *J. Biol. Chem.* 281:8636–8644.
46. Wang, X., R. Connors, M.R. Harris, T.H. Hansen, and L. Lybarger. 2005. Requirements for the selective degradation of endoplasmic reticulum-resident major histocompatibility complex class I proteins by the viral immune evasion molecule mK3. *J. Virol.* 79:4099–4108.
 47. Borgese, N., S. Brambillasca, P. Soffientini, M. Yabal, and M. Makarow. 2003. Biogenesis of tail-anchored proteins. *Biochem. Soc. Trans.* 31:1238–1242.
 48. Tigges, M.A., S. Leng, D.C. Johnson, and R.L. Burke. 1996. Human herpes simplex virus (HSV)-specific CD8⁺ CTL clones recognize HSV-2-infected fibroblasts after treatment with IFN-gamma or when virion host shutoff functions are disabled. *J. Immunol.* 156:3901–3910.
 49. Rowe, M., B. Glaunsinger, D. van Leeuwen, J. Zuo, D. Sweetman, D. Ganem, J. Middeldorp, E.J. Wiertz, and M.E. Rensing. 2007. Host shutoff during productive Epstein-Barr virus infection is mediated by BGLF5 and may contribute to immune evasion. *Proc. Natl. Acad. Sci. USA.* 104:3366–3371.
 50. Bogedain, C., H. Wolf, S. Modrow, G. Stuber, and W. Jilg. 1995. Specific cytotoxic T-lymphocytes recognize the immediate-early transactivator ZTA of Epstein-Barr virus. *J. Virol.* 69:4872–4879.
 51. Burrows, S.R., J. Gardner, R. Khanna, T. Steward, D.J. Moss, S. Rodda, and A. Suhrbier. 1994. Five new cytotoxic T-cell epitopes identified within Epstein-Barr virus nuclear antigen 3. *J. Gen. Virol.* 75:2489–2493.
 52. Chapman, A.L.N., A.B. Rickinson, W.A. Thomas, R.F. Jarrett, J. Crocker, and S.P. Lee. 2001. Epstein-Barr virus-specific cytotoxic T lymphocyte responses in the blood and tumour site of Hodgkin's disease patients: implications for a T cell-based therapy. *Cancer Res.* 61:6219–6226.
 53. Rickinson, A.B., and D.J. Moss. 1997. Human cytotoxic T lymphocyte responses to Epstein-Barr virus infection. *Annu. Rev. Immunol.* 15:405–431.
 54. Taylor, G.S., H.M. Long, T.A. Haigh, M. Larsen, J. Brooks, and A.B. Rickinson. 2006. A role for intercellular antigen transfer in the recognition of EBV-transformed B cell lines by EBV nuclear antigen-specific CD4⁺ T cells. *J. Immunol.* 177:3746–3756.
 55. Rensing, M.E., D. van Leeuwen, F.A.W. Verreck, R. Gomez, B. Heemskerk, M. Toebe, M.M. Mullen, T.S. Jardetzky, R. Longnecker, M.W. Schilham, *et al.* 2003. Interference with T cell receptor-HLA-DR interactions by Epstein-Barr virus gp42 results in reduced T helper cell recognition. *Proc. Natl. Acad. Sci. USA.* 100:11583–11588.
 56. Rensing, M.E., D. van Leeuwen, F.A.W. Verreck, S. Keating, R. Gomez, K.L.M.C. Franken, T.H.M. Ottenhoff, M. Spriggs, T.N. Schumacher, L.M. Hutt-Fletcher, *et al.* 2005. Epstein-Barr virus gp42 is posttranslationally modified to produce soluble gp42 that mediates HLA class II immune evasion. *J. Virol.* 79:841–852.
 57. Spee, P., J. Subject, and J. Neefjes. 1999. Identification of novel peptide binding proteins in the endoplasmic reticulum: ERp72, calnexin, and grp170. *Biochemistry.* 38:10559–10566.

Supplementary data

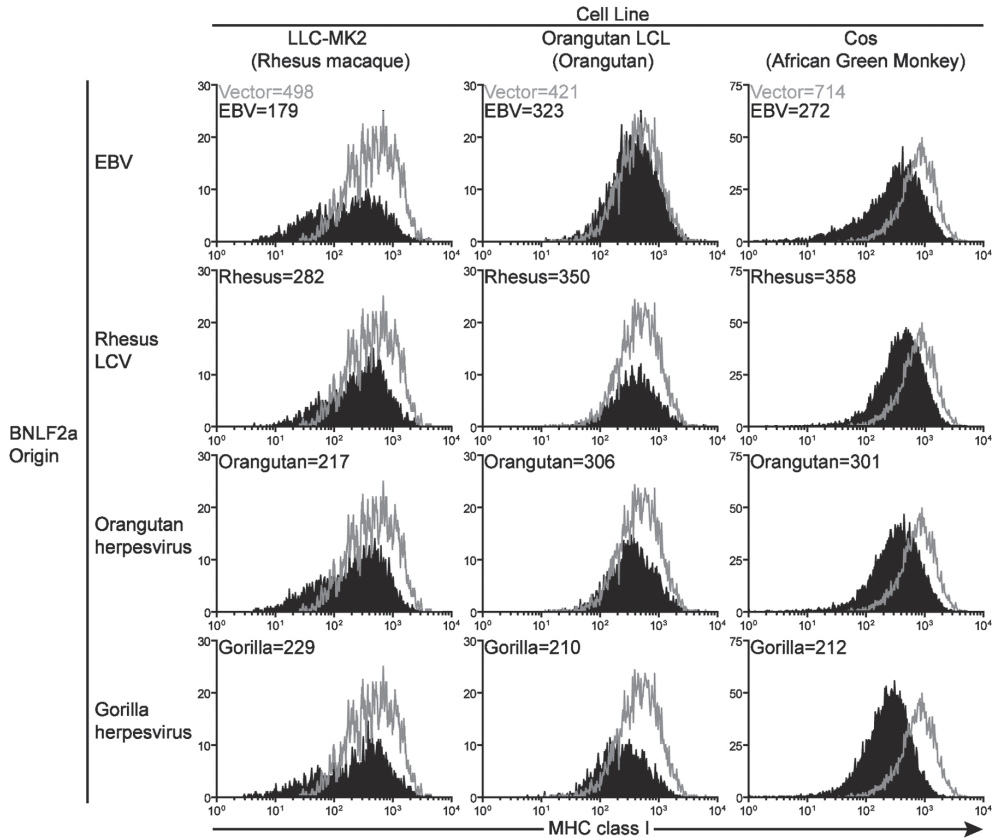


Figure S1. Expression of LCV BNL2a genes causes down-regulation of surface MHC class I in cell lines of primate origin LLC-MK2 cells (Rhesus macaque), orangutan B cells transformed with their endogenous LCV (orangutan herpesvirus), or Cos cells (African green monkey) were transfected with the plasmid vectors coexpressing BNL2a and GFP used in Fig. 6. Cell-surface levels of MHC class I molecules on GFP-positive cells were measured at 48 h after transfection by staining cells with the W6/32 mAb and analyzing by flow cytometry. Black histograms represent the surface marker intensity of cells transfected with the relevant BNL2a; open histograms represent the intensity of cells transfected with the empty vector plasmid. Geometric mean fluorescence values for MHC class I staining on the GFP-positive cells are shown in the top left of each histogram.

Chapter 3

Specific targeting of the EBV lytic phase protein BNLF2a to the transporter associated with antigen processing results in impairment of HLA class I-restricted antigen presentation

D. Horst, D. van Leeuwen, N.P. Croft, M.A. Garstka, A.D. Hislop, E. Kremmer, A.B. Rickinson, E.J.H.J. Wiertz and M.E. Rensing.

The Journal of Immunology 2009

Abstract

EBV persists for life in the human host while facing vigorous antiviral responses that are induced upon primary infection. This persistence supports the idea that herpesviruses have acquired dedicated functions to avoid immune elimination. The recently identified EBV gene product BNLF2a blocks TAP. As a result, reduced amounts of peptides are transported by TAP from the cytoplasm into the endoplasmic reticulum (ER) lumen for binding to newly synthesized HLA class I molecules. Thus, BNLF2a perturbs detection by cytotoxic T cells. The 60-aa-long BNLF2a protein prevents the binding of both peptides and ATP to TAP, yet further mechanistic insight is, to date, lacking. In this study, we report that EBV BNLF2a represents a membrane-associated protein that colocalizes with its target TAP in subcellular compartments, primarily the ER. In cells devoid of TAP, expression levels of BNLF2a protein are greatly diminished, while ER localization of the remaining BNLF2a is retained. For interactions of BNLF2a with the HLA class I peptide-loading complex, the presence of TAP2 is essential, whereas tapasin is dispensable. Importantly, we now show that in B cells supporting EBV lytic replication, the BNLF2a protein is expressed early in infection, colocalizing and associating with the peptide-loading complex. These results imply that, during productive EBV infection, BNLF2a contributes to TAP inhibition and surface HLA class I down-regulation. In this way, EBV BNLF2a-mediated evasion from HLA class I-restricted T cell immunity contributes to creating a window for undetected virus production.

Introduction

Cytotoxic T lymphocytes play an essential role in the control of many viral infections. Through their TCRs, CD8⁺ CTLs scrutinize body cells for the presence of intracellular foreign invaders reflected at the cell surface by virus-derived peptides bound to host MHC class I molecules (HLA in humans). In general, these peptides result from protein degradation by cytosolic proteasomes and are then transported into the endoplasmic reticulum (ER) lumen by the transporter associated with Ag processing, TAP. TAP is a heterodimer composed of two multimembrane-spanning subunits, TAP1 and TAP2, with cytosolic C-terminal domains for the binding of peptide substrates and ATP. To ensure efficient acquisition of optimal peptide cargo by nascent MHC class I complexes, TAP is part of the MHC class I peptide-loading complex (PLC). Besides TAP1 and TAP2, the PLC comprises MHC class I H chains, β 2-microglobulin (β 2m), tapasin, ERp57, and the chaperone calreticulin. Tapasin bridges TAP and MHC class I molecules and stabilizes TAP expression (1, 2). The complex of tapasin and the thiol oxidoreductase ERp57 exerts a peptide-editing function (3, 4). Once newly synthesized MHC class I H chain/ β 2m/peptide trimers are assembled, they are allowed to exit the ER and travel through the Golgi to the cell surface.

Even in the face of functional antiviral immune responses, herpesviruses are capable of establishing lifelong persistent infections in their hosts. This hallmark is shared by all members of the herpesvirus family, classified into α -, β -, and γ -subfamilies. The past decade has provided ample evidence that herpesviruses have acquired gene products that thwart host antiviral responses (5, 6, 7, 8). Prominent among these are viral proteins that interfere with MHC class I-restricted Ag presentation at various locations along the Ag processing route. For example, MHC class I molecules are retained intracellularly in cells infected with both human and murine CMV (HCMV and MCMV, respectively; both β -herpesviruses). To achieve this, the HCMV US3 protein prevents the exit of MHC class I molecules from the ER in a tapasin-dependent manner (9, 10), and MCMV m152/gp40 is responsible for the retention of MHC class I in the ER-Golgi intermediate compartment (11). An alternative strategy of MHC class I immune evasion adopted by several viruses is the acceleration of MHC class I turnover. In cells expressing the HCMV US2 or US11 proteins, MHC class I molecules are degraded rapidly upon synthesis and, interestingly, this occurs by proteasomes following the dislocation of MHC class I molecules into the cytosol (12, 13). Increased degradation of MHC class I molecules is also achieved by viral E3 ubiquitin ligases encoded by two members of the γ -herpesvirus subfamily. The murine γ -herpesvirus MHV68 encodes mK3, the expression of which leads to proteasomal degradation

of MHC class I as well as other components of the PLC (14, 15, 16, 17, 18). The human Kaposi sarcoma-associated herpesvirus expresses two proteins, K3 and K5, that target MHC class I molecules for proteolysis at a different location compared with mK3, i.e., in lysosomes following endocytosis (19, 20, 21). Enhanced lysosomal degradation is also effected by two β -herpesvirus gene products; the U21 protein of the human herpesvirus HHV-7 (22, 23) and m06/gp48 of MCMV (24) redirect newly synthesized MHC class I complexes to endolysosomal compartments.

Finally, TAP appears to be an attractive target for viral inhibition of Ag presentation to MHC class I-restricted CTLs, and TAP is blocked by a growing list of herpesvirus-encoded proteins. Within the α -herpesvirus subfamily, some members of the simplex viruses and the varicelloviruses encode TAP-inhibiting proteins. Infection with HSV type 1 or 2 leads to immediate early expression of ICP47, blocking peptide transport by TAP. ICP47 binds to the cytosolic domains of both TAP subunits, thereby outcompeting the binding of Ag-derived peptides (25, 26, 27, 28, 29, 30, 31, 32). The TAP inhibitor encoded by members of the varicelloviruses, UL49.5, lacks sequence homology to ICP47. UL49.5 codes for a transmembrane protein that binds to TAP, inducing a translocation-incompetent state of the peptide transporter (33). The mechanism of TAP inhibition shows variation among different varicelloviruses; bovine herpesvirus (BHV) type 1 (BHV-1) UL49.5 additionally targets TAP for proteasomal degradation, whereas equine herpesvirus type 1 and type 4 UL49.5 interferes with ATP binding to TAP (34). In the β -herpesvirus HCMV, yet another gene product is responsible for blocking TAP-mediated peptide transport; the membrane protein US6 inhibits TAP through its ER luminal domain by interfering with ATP binding to the cytosolic nucleotide-binding domains of TAP (35, 36, 37, 38, 39). Until recently, only the subfamily of γ -herpesviruses lacked a dedicated TAP-inhibiting protein.

Within the γ -herpesvirus subfamily, EBV is the prototype γ 1-herpesvirus infecting >90% of adult human beings worldwide. Although asymptomatic in the majority of infected individuals, EBV is the causative agent of infectious mononucleosis and a number of malignant tumors, such as Burkitt's lymphoma and nasopharyngeal carcinoma. The importance of T cells in controlling EBV infection is underscored by the development of EBV-transformed B cell lymphomas in immunocompromised patients that can be cured with adoptively transferred EBV-specific CTLs (40). Following primary infection, EBV resides in memory B cells, mostly as a latent infection. During latency, only a fraction (up to nine) of viral proteins are expressed, thereby reducing the target Ags to be recognized by the host immune system. EBV occasionally reactivates from latency, which leads to the expression of >80 viral proteins and the

production of viral particles that can amplify the latent pool or mediate viral transmission to another host. It is now becoming increasingly clear that EBV has also acquired dedicated immune evasion strategies that delay the elimination of virus-producing cells. Using a newly developed culture system for productive EBV infection, we have found that HLA class I expression is down-regulated at the surface of lytically EBV-infected B cells when compared with cells harboring a latent EBV infection, and this coincides with a block in TAP-mediated peptide transport (41). Subsequently, we identified BNLF2a as an EBV lytic cycle protein capable of blocking TAP function by interfering with binding of both peptides and of ATP to TAP (42). Functional homologues of EBV BNLF2a were found in Old World primate γ 1-herpesviruses. Thus, γ -herpesviruses also appear to encode immune evasion molecules specifically targeting peptide transport by TAP.

In this article, we report novel mechanistic aspects of the EBV-encoded BNLF2a protein, representing the first dedicated inhibitor of TAP in γ -herpesviruses, and we provide evidence for its role during natural EBV infection.

Results

EBV BNLF2a colocalizes with TAP

The EBV lytic cycle gene product BNLF2a hampers HLA class I Ag presentation by blocking TAP-mediated peptide transport (42). TAP is a

multimembrane-spanning protein complex localized to the ER. Strikingly, the predicted sequence of the 60-aa BNLF2a protein lacks an obvious signal sequence for cotranslational insertion into the ER membrane (Fig. 1A). To study the intracellular localization of BNLF2a, a mAb (clone 8E2) was raised against the N terminus of BNLF2a. For immunofluorescence assays, we used MJS/TAP1-GFP cells derived from the human melanoma cell line MelJuSo stably expressing the human TAP1 subunit tagged with GFP at its cytosolic C terminus (47). TAP1-GFP assembled into functional TAP1-TAP2 complexes and fluorescence microscopy revealed the TAP complexes to be primarily located in the ER and capable of reaching cis-Golgi compartments (57, 58) (Fig. 1B, upper row). Retroviral transduction of MJS/TAP1-GFP cells to introduce stable EBV BNLF2a expression resulted in inhibition of the peptide-transporting function of TAP by the viral immune evasion molecule (data not shown). In paraformaldehyde-fixed, detergent-permeabilized, BNLF2a-transduced cells probed with the anti-BNLF2a mAb 8E2, a typical perinuclear ER-like staining was observed, whereas control cells were negative (Fig. 1B, left column). This distribution of BNLF2a mostly coincided with the fluorescence pattern observed for TAP1-GFP (Fig. 1B, second column from left). Colocalization of BNLF2a was also found with the ER-resident chaperone calnexin (stained with mAb AF8; data not shown). These combined data demonstrate colocalization of BNLF2a with its target TAP.

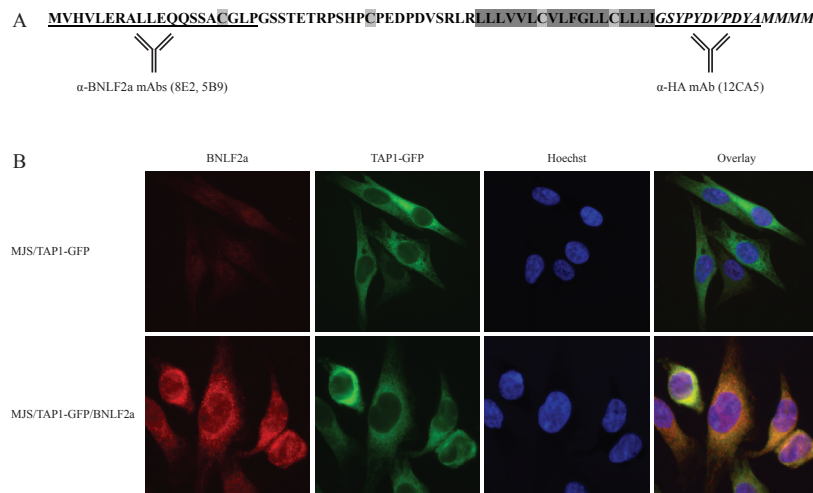


Figure 1. EBV BNLF2a colocalizes with TAP

A, Amino acid sequence of HA4M-tagged BNLF2a. The hydrophobic C terminus of BNLF2a is highlighted in dark gray, the cysteine residues are highlighted in light gray, and the HA4M tag is shown in italics. The epitopes recognized by the anti-BNLF2a (α -BNLF2a) and anti-HA (α -HA) mAbs are underlined. B, Immunofluorescence analysis of MJS/TAP1-GFP cells stably expressing BNLF2a and control MJS/TAP1-GFP cells. After fixing and permeabilizing the cells, intracellular localization of the BNLF2a protein was visualized using the BNLF2a-specific Ab 8E2. Nuclei were visualized using Hoechst stain (Sigma-Aldrich).

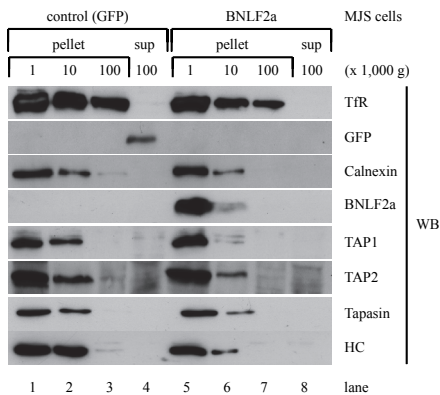


Figure 2. EBV BNLF2a is a membrane-associated protein
Subcellular fractionation of MJS/GFP and MJS/BNLF2a cells was performed by differential centrifugation, as described in the Materials and Methods. 1,000 × g, 10,000 × g, and 100,000 × g pellets and 100,000 × g supernatant (sup) fractions were separated by SDS-PAGE and analyzed by Western blotting (WB) for the presence of the control transmembrane protein transferrin receptor (TfR; H68.4 mAb), the control cytosolic protein GFP (anti-GFP rabbit sera), as well as calnexin (anti-calnexin rabbit sera), BNLF2a (5B9 mAb), TAP1 (148.3 mAb), TAP2 (435.4 mAb), tapasin (7F6 mAb), and HLA class I H chains (HC) (HC10 mAb).

EBV BNLF2a represents a membrane-associated protein

Immunofluorescence analysis suggested that BNLF2a was absent from the cytosol despite the fact that the protein lacks an N-terminal signal sequence. BNLF2a contains a hydrophobic domain at its C terminus that could serve as a tail anchor for membrane insertion (Fig. 1A). To investigate whether BNLF2a is a cytosolic or a membrane-associated protein, we performed subcellular fractionation experiments. Cell homogenates of control GFP-expressing cells and BNLF2a-expressing cells were sedimented by differential centrifugation to separate membranous organelles (1,000, 10,000, and 100,000 × g pellet fractions) from cytosol (100,000 × g supernatant fraction). As expected, the recycling membrane protein transferrin receptor is detected by Western blotting in all pellet fractions, whereas the cytosolic GFP is only present in the supernatant fraction of GFP-expressing control cells (Fig. 2, lane 4). Calnexin-staining in the 1,000 and 10,000 × g pellets suggests these to contain ER-derived microsomes (Fig. 2). The fact that the 100,000 × g supernatant was completely devoid of BNLF2a, combined with the detection of BNLF2a in the 1,000 and 10,000 × g pellets of MJS/BNLF2a cells (Fig. 2, lanes 5 and 6), indicates that BNLF2a is membrane associated rather than cytosolic. A similar distribution pattern was observed for components of the PLC, including TAP1, TAP2, tapasin, and HLA class I heavy chains (Fig. 2). Thus, BNLF2a occurs as a membrane-associated protein in subcellular

compartments, most likely ER, where it colocalizes with the PLC.

EBV BNLF2a does not drastically alter the composition of the PLC

Because BNLF2a colocalizes and coprecipitates with various components of the PLC, we next addressed the question whether binding of the viral TAP inhibitor would alter the composition of the PLC. By Western blotting, we investigated the proteins that coprecipitated with major constituents of the PLC from cells lysed in the presence of the mild detergent digitonin (Fig. 3). Substantial amounts of BNLF2a associated with TAP1, TAP2, and tapasin in BNLF2a-expressing MJS cells (Fig. 3A), in agreement with our previous data (42). TAP1, TAP2, tapasin, and HLA class I H chains were all detected in immune complexes precipitated with Abs specific for TAP1, TAP2, or tapasin. The amounts of coprecipitated proteins were similar for BNLF2a-expressing and control cells (Fig. 3A). From these experiments, we conclude that expression of BNLF2a does not expel individual components from the PLC, nor does it prevent the binding of HLA class I to the PLC. We additionally performed immunoprecipitations

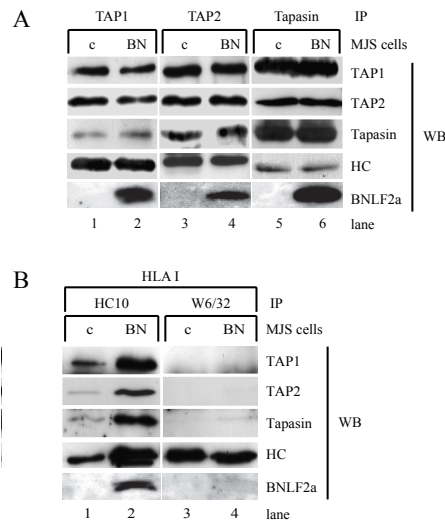


Figure 3. EBV BNLF2a interacts with intact HLA class I PLCs

Postnuclear digitonin lysates of MJS cells stably expressing BNLF2a (BN) and control MJS cells (c) were subjected to immunoprecipitations (IP) using Abs specific for TAP1 (148.3), TAP2 (435.4), and tapasin (R.gp48C) to assess association of BNLF2a with these PLC-components (A) or HC10 and W6/32, Abs recognizing immature and mature HLA class I molecules, respectively, to investigate the effect of BNLF2a expression on HLA class I maturation (B). Denatured immunoprecipitates were separated by SDS-PAGE and stained for TAP1 (148.3 mAb), TAP2 (435.4 mAb), tapasin (7F6 mAb), HLA class I H chains (HC10 mAb), and BNLF2a (5B9 mAb) in Western blot (WB) analysis.

with two Abs against HLA class I that, under native immunoprecipitation conditions, recognize different pools of class I molecules; mAb HC10 is directed against free, immature HLA class I H chains (59), whereas mAb W6/32 recognizes a conformational epitope on β 2m-associated, peptide-loaded, mature HLA class I molecules (43). Please note that under denaturing conditions, as in Western blots, probing with HC10 reveals the total pool of HLA class I. BNLF2a only coprecipitates with immature (HC10-reactive) HLA class I (Fig. 3B), substantial amounts of which reside in the PLC as visualized by the presence of TAP1, TAP2, and tapasin in these HC10-reactive immune complexes. Interestingly, BNLF2a expression appears to lead to increased amounts of HC10-reactive HLA class I (Fig. 3B), although the total amounts of HLA class I coprecipitated with TAP1, TAP2, or tapasin were not drastically altered (Fig. 3A). This paradox could indicate that the total amounts of HLA class I H chains within the PLC are similar but that their HC10-reactivity is increased, for instance as a consequence of reduced stability of the HLA class I H chain- β 2m complex. BNLF2a does not interact with mature, W6/32-reactive HLA class

I complexes that have probably left the PLC (Fig. 3B; no coprecipitation of TAP1, TAP2, or tapasin with mAb W6/32). In BNLF2a-expressing cells, the W6/32-reactive HLA class I complexes appear not fully matured, because they display a slightly faster mobility in SDS-PAGE compared with the HLA class I heavy chains from control cells, reminiscent of the compromised glycan modifications normally accompanying maturation.

In conclusion, the above results indicate that, although BNLF2a appears to retard the formation of stable HLA class I complexes, the overall composition of the PLC is not affected by the expression of BNLF2a.

Cysteine residues of BNLF2a are dispensable for TAP inhibition

The amino acid sequence of EBV BNLF2a contains four cysteine residues (Fig. 1A), three of which are conserved in BNLF2a homologues of Old World primate γ 1-herpesviruses (42). To investigate whether these cysteine residues are critical to BNLF2a function and, thereby, to HLA class I immune evasion, we created a mutant with all of the cysteines replaced by serines (BNLF2a Δ cys). Through retroviral transduction, MJS

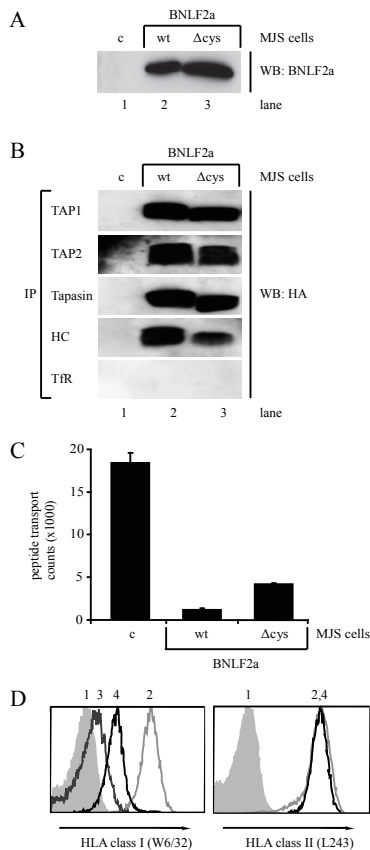


Figure 4. Cysteine residues within BNLF2a are not essential for TAP inhibition

A, BNLF2aHA4M (wt, wild type) and BNLF2aHA4M proteins in which the cysteine residues have been replaced by serines (Δ cys) are detectable in Western blots (WB) of total postnuclear Nonidet P-40 lysates of MJS cells stably expressing BNLF2a or BNLF2a Δ cys, but not in control MJS cells (c). Western blots were stained for BNLF2a using mAb 5B9. B, BNLF2a Δ cys interacts with components of the HLA class I PLC. Digitonin lysates of MJS cells stably expressing BNLF2a (wt) or BNLF2a Δ cys (Δ cys) and control MJS cells (c) were subjected to immunoprecipitations (IP) using Abs specific for TAP1 (148.3), TAP2 (435.4), tapasin (R.gp48C), HLA class I H chains (HC10), and transferrin receptor (TfR; H68.4). Precipitates were separated by SDS-PAGE and analyzed for BNLF2a expression using mAb 12CA5 specific for the HA tag added to the C terminus of the viral protein. C, BNLF2a Δ cys still inhibits TAP-dependent peptide transport. MJS cells stably expressing BNLF2a (wt) or BNLF2a Δ cys (Δ cys) and control MJS cells (c) were analyzed for their ability to transport peptides via TAP using a dedicated peptide transport assay. Cells were permeabilized with streptolysin O and incubated with fluoresceinated peptides in the presence or absence of ATP. Upon cell lysis, Con A-Sepharose beads were used to precipitate translocated peptides that were glycosylated in the ER. After elution from the beads, the amount of precipitated fluorescent peptide was quantified in arbitrary counts using a multilabel reader. Counts obtained for the samples incubated in the absence of ATP never exceeded 5% of the counts obtained for the control samples incubated in the presence of ATP (data not shown). D, HLA class I surface expression is down-regulated on MJS cells stably expressing either wild-type BNLF2a (line 3) or BNLF2a Δ cys (line 4) compared with MJS cells expressing GFP (line 2) as detected in flow cytometry using W6/32 as the primary Ab followed by allophycocyanin-conjugated anti-mouse secondary mAbs. Line 1 represents a negative control (no first Ab). HLA class II surface expression, as detected by the mAb L243, is unaffected by the expression of BNLF2a Δ cys.

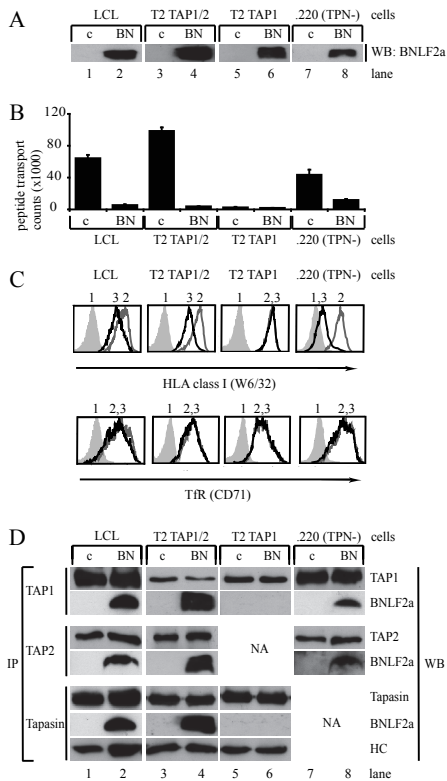


Figure 5. TAP2 is required for association of BNLF2a with the peptide-loading complex, whereas full-length tapasin is not

A, BNLF2a is expressed in EBV-transformed wild-type and PLC-mutant LCLs. Total postnuclear Nonidet P-40 lysates of wild-type LCLs, TAP1 and TAP2 reconstituted T2 cells (T2 TAP1 TAP2), TAP2-deficient B cells (T2 TAP1), and B cells with mutant tapasin (.220 (TPN-)) expressing BNLF2a (BN) or control GFP (c) were separated by SDS-PAGE and Western blots (WB) were analyzed for BNLF2a expression using BNLF2a-specific Abs. B, Effect of BNLF2a on TAP transport activity in PLC-mutant LCLs. LCL, T2 TAP1 TAP2, T2 TAP1, and .220 (TPN-) cells stably expressing BNLF2a (BN) or GFP (c) were analyzed for their ability to transport peptides via TAP using the peptide transport assay described in Fig. 4C. C, HLA class I expression at the surface of BNLF2a-expressing PLC-mutant LCLs. LCL, T2 TAP1 TAP2, T2 TAP1, and .220 (TPN-) cells stably expressing BNLF2a (line 3) or GFP (line 2) were stained for HLA class I (W6/32 mAb) or transferrin receptor (CD71 mAb) and analyzed by flow cytometry. Line 1 represents a negative control (no first Ab). D, Interactions of BNLF2a with components of the PLC in mutant LCLs. Digitonin lysates of LCL, T2 TAP1 TAP2, T2 TAP1, and .220 (TPN-) cells expressing BNLF2a (BN) or GFP (c) were subjected to immunoprecipitation (IP) using Abs specific for TAP1 (148.3), TAP2 (435.4), and tapasin (R.gp48C). Precipitates were separated by SDS-PAGE and stained for TAP1 (148.3), TAP2 (435.4), tapasin (7F6), BNLF2a (5B9), and HLA class I heavy chains (HC10) using Western blot (WB) analysis. NA, not applicable (target Ags detected by the TAP2- and tapasin-specific Abs were not expressed in T2 TAP1 and .220 (TPN-) cell lines, respectively).

cells were generated stably expressing the cysteine-less BNLF2a at levels comparable to those of wild-type HA4M-tagged BNLF2a, as detected in Western blotting (Fig. 4A).

First, the contribution of the cysteine residues to the association of BNLF2a with the PLC was evaluated. Postnuclear digitonin lysates of control, BNLF2a-, and BNLF2a Δ cys-expressing MJS cells were subjected to immunoprecipitations with mAbs specific for components of the PLC, and these immune complexes were analyzed for coprecipitation of BNLF2a by Western blotting (Fig. 4B). Both wild-type BNLF2a and the BNLF2a Δ cys mutant were found to associate with TAP1, TAP2, tapasin, and HC10-reactive HLA class I H chains (Fig. 4B), but not with control transferrin receptors. Thus, the cysteine residues of BNLF2a are dispensable for interactions of BNLF2a with the PLC.

Second, we compared TAP-inhibiting properties of wild-type and cysteine-less BNLF2a in an *in vitro* peptide translocation assay. In permeabilized control cells, fluorescent peptides were efficiently transported across the ER membrane in an ATP-dependent manner, whereas peptide translocation was significantly impaired both in wild-type and BNLF2a Δ cys-expressing cells (Fig. 4C). Therefore, the cysteine residues of BNLF2a do not appear critical to the inhibition of TAP function.

Third, flow cytometry was used to analyze cell surface HLA class I expression. On cells stably expressing the BNLF2a Δ cys mutant, a marked down-regulation of HLA class I was observed (Fig. 4D), although this down-regulation was slightly less pronounced than that seen for wild-type BNLF2a-expressing cells. Surface down-regulation was selective for HLA class I molecules, because levels of HLA class II and transferrin receptor remained unaffected (Figs. 4D and 5C) (42).

In summary, BNLF2a Δ cys interacts with the PLC, blocks TAP-mediated peptide transport, and down-regulates surface HLA class I levels, indicating that the cysteine residues within BNLF2a are not essential for immune evasion from HLA class I-restricted Ag presentation.

Interaction of EBV BNLF2a with the PLC requires the presence of TAP2 but not tapasin

To investigate the contribution of different members of the PLC to the inhibition of TAP function by BNLF2a, we made use of mutant B cell lines lacking individual components of the PLC. In comparison to the MJS cells used up to this point, B cells represent more professional APCs displaying, amongst others, elevated levels of TAP and HLA class I molecules. We therefore first verified that BNLF2a expression also yielded an HLA class I immune evasion phenotype in B cells. A wild-type B LCL, MoDo, was retrovirally transduced to stably express BNLF2a; for comparison, control cells were transduced with GFP-encoding

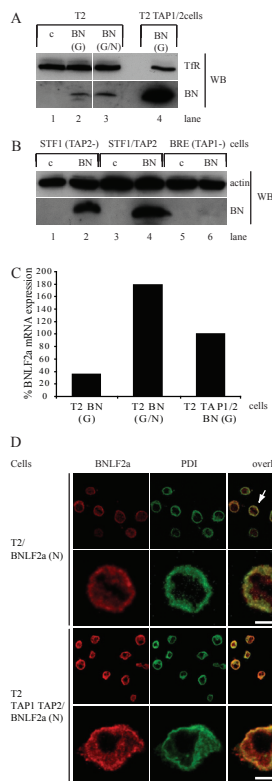


Figure 6. TAP stabilizes BNLf2a, but is not essential for its ER localization

A, BNLf2a protein expression is stabilized by the presence of the TAP complex. Postnuclear Nonidet P-40 lysates of T2 and T2 TAP1 TAP2 cells expressing BNLf2a (BN) or control GFP (c) were separated by SDS-PAGE and Western blots (WB) were stained with mAbs specific for the control protein transferrin receptor (TfR; H68.4) and BNLf2a (5B9). T2/BNLf2a (G) cells were additionally transduced with BNLf2a-IRES-NGFR retrovirus in an attempt to achieve detectable levels of BNLf2a protein expression, thereby generating the T2/BNLf2a (G/N) cell line. B, The TAP complex stabilizes the BNLf2a protein. Postnuclear Nonidet P-40 lysates of STf1, STf1/TAP2, and BRE cells expressing BNLf2a (BN) or corresponding control cells (c) were separated by SDS-PAGE and Western blots were analyzed for actin and BNLf2a expression using the mAbs AC-74 and 5B9, respectively. C, Quantification of BNLf2a mRNA levels in T2 cells in the presence or absence of TAP. RNA isolated from T2 and T2 TAP1 TAP2 cells expressing BNLf2a (BN) was used for the synthesis of cDNA. PCRs were performed in the presence of SYBR Green to allow real-time detection of actin mRNA as a control and BNLf2a mRNA. Cycle threshold (Ct) values were calculated and BNLf2a mRNA expression in the various cell lines was corrected for actin expression using the formula ($2^{-\Delta Ct}$). For comparison, relative BNLf2a mRNA levels were expressed as a percentage of the levels in T2 TAP1 TAP2/BNLf2a cells set at 100%. D, Localization of BNLf2a is similar in T2 and T2 TAP1 TAP2 cells. After fixing and permeabilizing T2/BNLf2a (N) and T2 TAP1 TAP2/BNLf2a (N) cells, intracellular localization of BNLf2a and the ER marker PDI was visualized by confocal microscopy using mAb 8E2 and anti-PDI rabbit serum, respectively. The arrows point to the cells that have been magnified in the pictures displayed in the panels shown below. Scale bar is 10 μ m.

retroviruses (Fig. 5A, lanes 1 and 2). As anticipated, BNLf2a-expressing B cells displayed impaired TAP-dependent peptide translocation (Fig. 5B, bars labeled "LCL"), surface HLA class I down-regulation (Fig. 5C, left panel), and association of BNLf2a with the PLC (Fig. 5D, lanes 1 and 2) like that previously found for MJS/BNLf2a cells. These results show that BNLf2a functions as an immune evasion protein in B cells, a natural host cell for EBV infection, and indicate that LCLs can be used to delineate the contributors to BNLf2a-induced TAP inhibition.

Mutagenesis and complement selection of LCL 721 resulted in several derivatives displaying low levels of HLA class I surface expression that were subsequently attributed to various genetic defects. Among these mutant LCLs are T2 cells (49) lacking expression of both TAP1 and TAP2 and .220 cells (50) lacking expression of full-length tapasin (TPN-). Additionally, T2-derived cell lines have been obtained with reconstituted expression of human TAP1 alone (T2 TAP1) or of both TAP1 and TAP2 (T2 TAP1 TAP2) (51). It was not possible to generate T2 cells expressing TAP2 only due to the instability of TAP2 when expressed in isolation (60). These mutant LCLs were transduced to express BNLf2a (Fig. 5A) and used to evaluate the contribution of TAP2 and tapasin to the viral inhibition of peptide transport.

First, the involvement of TAP was evaluated using the T2-derived cell lines. Immune evasion by BNLf2a was examined functionally using TAP-dependent peptide translocation assays (Fig. 5B) and flow cytometric analysis of HLA class I surface expression (Fig. 5C). In T2 cells with reconstituted TAP1 and TAP2, TAP was functional as reflected by the transport of fluoresceinated peptides (Fig. 5B) and high levels of surface HLA class I expression (Fig. 5C). Expression of BNLf2a caused a dramatic inhibition of peptide translocation in T2 TAP1 TAP2 cells and, consequently, a reduction in surface HLA class I (as in LCL cells; Fig. 5, B and C). Surface levels of a control protein, transferrin receptor (TfR), remained unaffected (Fig. 5C). In contrast to the restoration of both TAP subunits, the reconstitution of TAP1 alone was not sufficient to complement the Ag processing defect in T2 cells; accordingly, upon the introduction of BNLf2a into T2 TAP1 cells, no reduction in peptide translocation or surface HLA class I expression was apparent (Fig. 5, B and C). This observation indicates that the block of BNLf2a to HLA class I-restricted Ag presentation occurs entirely at the level of TAP function. Coimmunoprecipitation experiments were used to further delineate which TAP subunits are required for BNLf2a to interact with the PLC. In immune complexes precipitated from digitonin

lysates of BNLF2a-expressing T2 TAP1 TAP2 cells, BNLF2a is detected in association with TAP1, TAP2, and tapasin (Fig. 5D, lane 4), as for LCL cells (Fig. 5D, lane 2). In contrast, no coprecipitation of BNLF2a with TAP1 or tapasin was observed for T2 TAP1 cells (Fig. 5D, lane 6), whereas, as a control, the association of tapasin with HLA class I was detected under these conditions. Because T2 TAP1 TAP2 and T2 TAP1 cells only differ in the expression of the TAP2 subunit, these data demonstrate that the presence of TAP2 molecules is required for the interaction of BNLF2a with the PLC.

Second, we addressed the role of tapasin in BNLF2a-mediated TAP inhibition by exploiting the .220 cells. In these cells, a deletion in exon 2 results in an extensive truncation and severe instability of the tapasin protein (61). Despite the absence of full-length tapasin, BNLF2a induces the inhibition of TAP-mediated peptide transport and surface HLA class I down-regulation (Fig. 5B and C, sections marked .220 (TPN⁻) cells). In line with this, full-length tapasin does not need to be present for the association of BNLF2a with the PLC to occur, as shown by coprecipitations of BNLF2a with both TAP1 and TAP2 in .220 (TPN⁻) cells (Fig. 5D).

In summary, we conclude that expression of tapasin is not essential for the functionality of BNLF2a, whereas TAP2 is required for BNLF2a to associate with the PLC.

TAP is required for stable expression of the BNLF2a protein, but not for its ER localization

To address whether the TAP complex is essential for ER localization of BNLF2a, we expressed the viral protein in T2 cells that lack both TAP subunits (49). Surprisingly, Western blot analysis of Nonidet P-40 cell lysates revealed that the protein levels of BNLF2a were strongly diminished in the absence of TAP1 and TAP2 (Fig. 6A, compare lane 2 with lane 4). Additional transduction of T2/BNLF2a (Fig. 6A, lanes labeled "G") cells with a BNLF2a-IRES-NGFR retrovirus did not result in greatly increased BNLF2a protein expression (Fig. 6A, lane 3). For comparison, the control protein transferrin receptor (TfR) was expressed in BNLF2a⁺ T2 cells to levels that at least equalled those in T2 TAP1 TAP2 cells (Fig. 6A). These results were confirmed in other TAP-deficient cells, namely immortalized fibroblasts from individuals with TAP defects. BRE cells lack both expression of full-length TAP1 due to a deletion in the coding sequence (53) and that of TAP2, which is unstable in the absence of TAP1 (60). As controls, STF1 cells expressing TAP1 but lacking TAP2 due to a mutation in the TAP2 gene were analyzed in parallel, as well as STF1 cells reconstituted with the human TAP2 gene (STF1/TAP2 cells) (52). Upon transduction of these cell lines with BNLF2a-IRES-NGFR retroviruses, all cells became NGFR⁺ to a comparable degree (data not shown). Whereas abundant BNLF2a expression was achieved

in the TAP⁺ cell lines (Fig. 6B, lanes 2 and 4), virtually no BNLF2a protein was detected in lysates from TAP⁻ cells (Fig. 6B, lane 6), confirming that the absence of TAP precludes proper expression of this EBV protein. Next, we determined BNLF2a mRNA levels in the T2-derived cell lines. Using semiquantitative RT-PCR, no major differences in BNLF2a transcripts became apparent when comparing TAP⁻ and TAP⁺ cells (data not shown). To obtain quantitative information, quantitative PCR was performed on cDNA isolated from T2/BNLF2a (Fig. 6C, left bar marked "G") cells, additionally transduced T2/BNLF2a (middle bar marked "G/N") cells, and T2 TAP1 TAP2/BNLF2a cells (right bar marked "G"). Additional transduction of the TAP⁻ cells with BNLF2a retroviruses did yield enhanced BNLF2a mRNA expression to levels exceeding those in TAP-reconstituted T2 cells (Fig. 6C), but this was not accompanied by markedly higher BNLF2a protein levels (Fig. 6A). Thus, the combined results indicate that TAP is required for stable expression of BNLF2a at the protein level.

Despite the low levels of BNLF2a protein in TAP-deficient cells, immunofluorescence stainings were performed to determine the intracellular localization of BNLF2a in the absence of TAP. The signal obtained with the BNLF2a-specific mAb 8E2 was much weaker in T2 cells compared with T2 TAP1 TAP2 cells (Fig. 6D), which is in agreement with the Western blotting results. Yet, irrespective of coexpression of TAP, BNLF2a colocalized with the ER marker PDI (Fig. 6D). In conclusion, the EBV-encoded TAP inhibitor BNLF2a is unstable when expressed in cells lacking TAP complexes but still localizes to the ER, implying that ER localization of BNLF2a is not dependent on the interaction of BNLF2a with TAP.

During productive EBV infection, BNLF2a colocalizes and interacts with the HLA class I PLC

Up to this point, we have shown that the EBV lytic phase protein BNLF2a, when expressed in isolation, interacts with the PLC, inhibits peptide transport by TAP, and induces surface HLA class I down-regulation. As a result, BNLF2a prevents recognition by HLA class I-restricted T cells (above data and Ref. 42). Having observed this immune-evasive property of BNLF2a, we aimed at investigating whether BNLF2a fulfills a similar function in the context of natural EBV infection. To this end, we exploited a strategy to identify and isolate populations of productively EBV-infected Burkitt's lymphoma cells (AKBM cells) on the basis of expression of a reporter fusion protein, rat CD2-GFP, placed under the control of an early EBV promoter (41). This lytic cycle culture system, in combination with the newly generated mAbs specific for BNLF2a, permitted us now to examine BNLF2a during replicative EBV infection.

By Western blot analysis of cells stably transduced to express BNLF2a, the viral protein was detectable as a 7-kDa band that was absent from control cells (Figs.

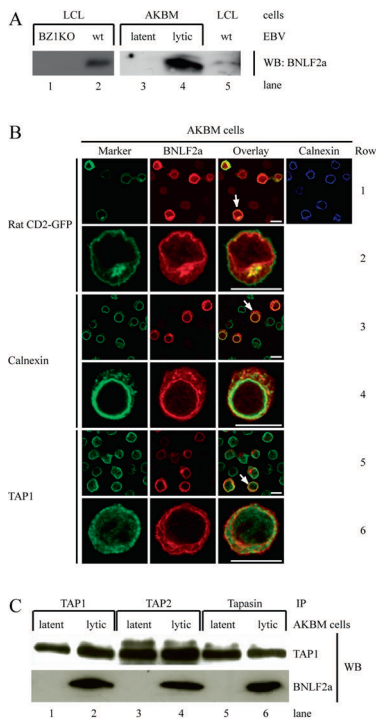


Figure 7. During productive EBV infection, BNLF2a colocalizes with TAP and interacts with the PLC

A, BNLF2a expression in EBV-transformed B cells and productively infected EBV⁺ Burkitt's lymphoma cells. BNLF2a expression in EBV-transformed B cells was examined using Western blot (WB) analysis (5B9 mAb) of postnuclear Nonidet P-40 lysates of B cells transformed with either wild-type (wt) EBV or BZLF1 KO (BZ1KO) virus. Deletion of BZLF1 from EBV precludes entry from latency into the lytic cycle for BZ1KO LCL, whereas 1–5% of wild-type EBV-transformed LCLs spontaneously enters the lytic cycle. EBV⁺ AKBM Burkitt's lymphoma cells were incubated with anti-IgG for 18 h to reactivate EBV and were subjected to magnetic cell sorting to obtain an almost pure population of lytically infected AKBM cells. Postnuclear Nonidet P-40 lysates of uninduced (latent) and lytic AKBM cells and control LCLs (MoDo) were separated by SDS-PAGE and analyzed by Western blotting using BNLF2a-specific rat mAbs. B, BNLF2a colocalizes with TAP1 and calnexin during lytic EBV infection. AKBM cells were incubated with anti-IgG for 6 h to induce productive EBV infection and, after fixing and permeabilizing the cells, the intracellular localization of BNLF2a, calnexin, and TAP1 was visualized by confocal microscopy using the Abs 8E2, AF8, and 148.3, respectively. Rat CD2-GFP was used as a marker for lytic phase induction. The arrows point to the cells that have been magnified in the pictures displayed in the panels shown below. Scale bar is 10 μ m. C, In the context of productive EBV infection, BNLF2a associates with the HLA class I PLC. Uninduced (latent) and sorted lytically infected AKBM cells (as in A) were lysed using 1% digitonin and subjected to immunoprecipitation (IP) using Abs specific for TAP1 (148.3), TAP2 (435.4), and tapasin (R.gp48C). Precipitates were separated by SDS-PAGE and analyzed for TAP1 and BNLF2a expression on Western blots (WB) probed with Abs specific to these proteins.

2–6). Postnuclear Nonidet P-40 lysates of EBV⁺ B cells (LCL and AKBM) were chosen as a source of naturally expressed BNLF2a. Approximately 1–5% of B cells latently infected with EBV spontaneously enters the lytic cycle. The EBV-encoded, immediately early transactivator BZLF1 is critical to viral reactivation, and cells transformed with an EBV mutant lacking the BZLF1 gene (BZ1KO) fail to enter the lytic cycle (55). Because a specific 7 kDa-protein band was detected only in wild-type EBV-transformed B cells and not in reactivation-deficient BZ1KO cells (Fig. 7A), BNLF2a appears expressed strictly during lytic infection. AKBM cells provide the opportunity to efficiently induce and synchronize EBV reactivation by crosslinking surface IgG. In lytic AKBM cells, isolated for 18 h postinduction, BNLF2a protein expression was observed, but not in latently infected cells (Fig. 7A). Compared with LCLs, BNLF2a expression levels appeared largely elevated in lytic AKBM cells, reflecting the amounts of cells in the lytic cycle ranging from $\leq 5\%$ of LCLs to $>90\%$ of induced and sorted AKBM cells (Fig. 7A).

Next, we examined the intracellular localization of BNLF2a in productively infected cells using fluorescence microscopy. At 6 h postinduction, ~30–40% of cells have entered the lytic phase of infection as marked by the expression of rat CD2-GFP (Fig. 7B, row 1). Interestingly, BNLF2a is expressed in some cells that are not (yet) GFP positive (Fig. 7B, row 1), implying that BNLF2a is expressed early in infection, likely before rat CD2-GFP is expressed from the early BMRF1 promoter. As expected, rat CD2-GFP is localized to the cell surface, whereas BNLF2a is expressed intracellularly (Fig. 7B, rows 1 and 2). In AKBM cells stained for BNLF2a expression, a typical perinuclear staining is observed that mostly coincides with the expression of calnexin and TAP1 (Fig. 7B, rows 3–6). This colocalization of BNLF2a with calnexin and TAP1 in lytically EBV-infected AKBM cells resembles the situation observed in MJS cells stably expressing BNLF2a (Fig. 1), suggesting that the intracellular localization of BNLF2a is not influenced by the coexpression of other viral proteins. From these experiments, we conclude that BNLF2a colocalizes with TAP in the ER compartment in the context of a lytic EBV infection.

Finally, we investigated whether BNLF2a interacts with components of the HLA class I PLC in the context of the full repertoire of lytic phase proteins. Sorted, productively EBV-infected AKBM cells (lytic) and control EBV⁺ cells in latency (latent) were lysed using 1% digitonin to preserve protein-protein interactions. Lysates were subjected to immunoprecipitation with Abs against TAP1, TAP2, and tapasin. Western blots of the immunoprecipitates were probed with TAP1- or BNLF2a-specific mAbs. In both latently and lytically EBV-infected cells, TAP1 was found to coprecipitate with TAP2 and tapasin (Fig. 7C), indicating PLCs were present. In lytically EBV-infected cells, BNLF2a

Virus	Inhibitor	Degradation of TAP1/2	Interference with peptide binding	Interference with ATP binding	Conformational alterations	References
HSV-1/2	ICP47	No	Yes	No	Yes	(25-32)
HCMV	US6	No	No	Yes	Yes	(35-39, 47)
BHV-1	UL49.5	Yes	No	No	Yes	(33)
EHV-1/4	UL49.5	No	No	Yes	Yes	(34)
PRV	UL49.5	No	No	No	Yes	(34)
EBV	BNLF2a	No	Yes	Yes	Not tested	(42)

Table I. Comparison of the mechanisms by which herpesvirus-encoded proteins specifically interfere with TAP-mediated peptide transport. ^a Equine herpesvirus 1 and 4, ^b Pseudorabies virus.

associated with TAP1, TAP2, and tapasin (Fig. 7C) as evidence of BNLF2a interacting with the PLC in productively EBV-infected cells.

In conclusion, these data demonstrate that in EBV⁺ B cells, BNLF2a is expressed during the lytic cycle, colocalizes with TAP, and occurs in association with the HLA class I PLC, thereby allowing interference with TAP function during the productive phase of EBV infection.

Discussion

In this study, we have acquired the following novel information on the EBV-encoded TAP inhibitor BNLF2a: it localizes to the ER membrane together with TAP; it does not drastically alter the composition of the PLC; and it inhibits TAP function even in the absence of tapasin. BNLF2a cannot interact with the PLC in cells devoid of TAP2, and the presence of TAP is required for BNLF2a protein stability. Importantly, BNLF2a expression results in HLA class I down-regulation at the surface of B cells, representing natural host cells for EBV. Finally, the lytic phase protein BNLF2a is abundantly present during EBV replication in B cells and interacts with PLC components, allowing blockade of TAP function. Despite the absence of apparent sequence homology, mechanistically, BNLF2a shares inhibition of peptide binding with the HSV-encoded ICP47 protein (25, 30) and obstruction of ATP binding with both the HCMV-encoded US6 protein (37, 38) and the equine herpesvirus-encoded UL49.5 protein (34). In the following, we discuss features of BNLF2a in comparison with other viral TAP inhibitors (Table I). The ER-resident MHC class I PLC forms a key target for viral immune evasion. When analyzing the subcellular distribution of BNLF2a, we observed strict membrane association and colocalization with TAP and the ER markers calnexin and PDI (Figs. 1, 2, 6D, and 7B), reminiscent of two other TAP inhibitors, HCMV US6 (35, 36) and BHV-1 UL49.5 (33). The latter two represent integral type I membrane proteins with cleavable signal sequences at their N termini for cotranslational membrane insertion, as well as transmembrane domains toward their C termini. In contrast, BNLF2a lacks an obvious N-terminal signal sequence (Fig. 1A). Still, the EBV-encoded TAP inhibitor is membrane associated and, even in

the absence of TAP, localizes to the ER (Fig. 6D). In this respect, BNLF2a differs from HSV ICP47, which also lacks a signal sequence but has been detected primarily as a cytosolic protein with small amounts associating with membranes (26, 31). ICP47 is unstructured in aqueous solutions but adopts an α -helical structure upon association with membranes (62, 63), thereby rendering the protein functionally active as a competitor for the binding of peptides at the cytosolic domains of TAP. No structural information is available for BNLF2a, but the amino acid composition of this EBV protein is remarkably hydrophobic at its C-terminal end. This hydrophobic domain creates the possibility of anchoring BNLF2a in the ER membrane while leaving the N terminus exposed in the cytosol. This way of membrane anchoring BNLF2a could contribute to the observed membrane localization.

In addition to colocalizing in the ER, BNLF2a also appears to associate with PLCs, as deduced from coimmunoprecipitation experiments (Figs. 3–5 and 7 and Ref. 42). Incorporation of BNLF2a did not drastically alter the overall composition of the PLC. Still, PLC-associated HLA class I H chains from BNLF2a-expressing cells displayed increased reactivity with mAb HC10 under native conditions (Fig. 3), indicating these H chains to be devoid of peptide and β 2m. Instability of HLA class I molecules might be caused by a block or delay in HLA class I maturation due to impaired peptide supply in the ER following BNLF2a-mediated TAP inhibition. This is in line with results showing retarded acquisition of endoglycosidase H-resistant glycans on HLA class I heavy chains in BNLF2a-expressing cells (data not shown). Taken together, BNLF2a interacts with intact PLCs and, by preventing TAP-mediated peptide transport, effects retardation of HLA class I maturation, ultimately leading to reduced HLA class I display at the cell surface.

Substitution of the four cysteines within BNLF2a did not abolish its interaction with PLC components and, accordingly, the cysteine-less BNLF2a mutant retained its TAP-inhibiting properties (Fig. 4). Two of four cysteines in BNLF2a are anticipated to be exposed in the cytosol, a reducing environment where disulfide bond formation is less likely; the other two cysteines are in the presumed membrane-spanning domain. The situation is different for US6; its eight cysteine residues reside ER lumenally and are likely to be involved in the formation of an intramolecular

and possibly also an intermolecular network of S=S bridges. This oligomer formation of US6 supposedly contributes to an aberrant conformation of the TAP transporter, thereby preventing acquisition of ATP for energizing peptide transport (64).

To delineate the role of individual PLC components for BNLf2a-induced TAP inhibition, mutant B cell lines were used. A critical role for TAP2 is implicated by the observation that BNLf2a no longer coprecipitates with the PLC in TAP2-deficient cells (T2 TAP1 cells; Fig. 5). At this stage, we cannot discriminate whether this is due to TAP2 being essential in the formation of proper transporter complexes to which BNLf2a binds, or whether TAP2 by itself represents the direct interaction partner targeted by BNLf2a. For comparison, assembly of TAP subunits into a preformed heterodimer is absolutely required for US6 (37, 64), whereas BHV-1 UL49.5 can interact weakly with single TAP subunits, albeit interactions with the TAP1-TAP2 complex are much stronger (54, 65). In BNLf2a-expressing T2 TAP1 cells, tapasin can still interact with HLA class I H chains (Fig. 5) despite the absence of TAP heterodimers. Because tapasin immunoprecipitates from T2 TAP1 cells do not contain detectable amounts of BNLf2a, direct interactions between tapasin and the EBV protein are unlikely. Accordingly, BNLf2a expression induced HLA class I down-regulation in tapasin-deficient 220 cells. In this respect, BNLf2a resembles US6, for which tapasin is not required to inhibit TAP function (36).

Coexpression of TAP is required for BNLf2a protein stability (Fig. 6). This unexpected observation is in line with TAP being the direct interaction partner for BNLf2a. Interestingly, the viral protein appears stable in cells in which only the TAP1 subunit is present (Fig. 5), suggesting that a (transient) association may occur between TAP1 and BNLf2a. It has not been possible to visualize such a direct interaction by coimmunoprecipitation experiments performed on lysates from T2 TAP1/BNLf2a cells (Fig. 5). To our knowledge, there is no precedent of a role for TAP in stabilizing protein expression for other known herpesvirus-encoded TAP inhibitors.

For T2 cells reconstituted with TAP1 and TAP2 (T2 TAP1 TAP2 cells), expression of EBV BNLf2a reduced HLA class I levels at the cell surface to those observed for T2 cells lacking a functional TAP transporter (Fig. 5). This observation implies that the only step in the Ag processing pathway affected by BNLf2a is the function of TAP. This, in turn, means that only the display of (viral) antigenic peptides critically depending on TAP transport for HLA class I presentation will be affected by the BNLf2a-imposed block.

Based on and further extrapolating the combined results obtained for BNLf2a expressed in isolation in various cell lines, we propose the following model for EBV-induced immune evasion through the inhibition of TAP-mediated peptide transport. Upon translation,

BNLf2a is inserted into the ER membrane, most likely through its C-terminal hydrophobic domain. BNLf2a then interacts with the HLA class I PLC, with TAP being the direct interaction partner and tapasin being dispensable. The interaction of BNLf2a with TAP stabilizes the viral protein. Exposure of the N-terminal domain of BNLf2a in the cytosol could then interfere with the binding of peptides and ATP to the cytosolic domains of TAP, either directly or through the induction of conformational changes of TAP. This culminates in a block of the peptide-transporting function of TAP, ultimately leading to reduced levels of HLA class I molecules at the cell surface and loss of cytotoxic T cell recognition.

In this study, we obtained for the first time information on the EBV-encoded TAP inhibitor in the context of natural viral infection. This was facilitated by the availability of an EBV lytic cycle culture system in B cells and the generation of BNLf2a-specific Abs allowing detection of untagged BNLf2a as it occurs in productively virus-infected cells. Using the *in vitro* culture system for EBV, a block in TAP-mediated peptide transport and down-regulation of HLA class I cell surface levels have been observed upon initiation of the EBV lytic cycle (41). We have now demonstrated that BNLf2a is expressed in productively EBV-infected cells in which it is found to colocalize with TAP and associate with the HLA class I PLC (Fig. 7). Interestingly, BNLf2a protein expression appeared early in infection, probably before rat CD2-GFP was expressed from the early BMRF1 promoter (Fig. 7B). Although this expression of BNLf2a was earlier than anticipated on the basis of mRNA expression analysis (66), (immediate) early expression of BNLf2a would make sense from an immune evasion point of view. Antigenic peptides are generated immediately upon the start of viral replication and simultaneous production of the BNLf2a TAP inhibitor would prevent transport of these viral peptides into the ER for presentation to CTLs. Similarly, other viral TAP inhibitors appear (immediate) early in infection, such as ICP47 (31), US6 (36), and UL49.5 (67).

These combined results strongly suggest that the BNLf2a gene product is responsible for TAP inhibition during the productive phase of EBV infection, thereby contributing to surface HLA class I down-regulation and escape from CTL destruction *in vivo*.

Materials and Methods

Antibodies

The following mouse mAbs have been used in this study: W6/32, which recognizes β 2m-associated HLA class I molecules (43); HC10, recognizing non- β 2m-associated class I H chains (provided by H. Ploegh, Whitehead Institute for Biomedical Research, Cambridge, MA); 148.3, directed against TAP1 (provided by R. Tampe, Johann Wolfgang Goethe

University, Frankfurt, Germany); 435.4, directed against TAP2 (provided by P. van Endert, Hospital Necker, Paris, France); OX34, specific for rat CD2 (provided by M. Rowe, University of Birmingham Medical School, Birmingham, U.K.); H68.4 and CD71, both recognizing the transferrin receptor (Roche Diagnostics and BD Biosciences Pharmingen, respectively); AC-74, recognizing actin (Sigma-Aldrich); L243, recognizing HLA-DR (American Type Culture Collection); 12CA5, detecting an influenza virus hemagglutinin (HA) epitope that is used as a protein tag (Roche Diagnostics); and AF8 (44), recognizing calnexin (provided by M. Brenner, Harvard Medical School, Boston, MA). Tapasin-specific rabbit serum, R.gp48C, was provided by P. Cresswell (Howard Hughes Medical Institute, Yale University School of Medicine, New Haven, CT). Specific rabbit sera were used to detect GFP (45), protein disulfide isomerase (PDI; provided by I. Majoul, Royal Holloway University of London, Egham, U.K.), and calnexin (provided by I. Braakman, Utrecht University, Utrecht, The Netherlands). mAbs against BNLF2a and tapasin were produced by immunizing Lou/C rats with keyhole limpet hemocyanin-coupled peptides corresponding to N-terminal amino acids of BNLF2a or tapasin. Fusion of the myeloma cell line P3X63-Ag8.653 with rat immune spleen cells was performed using standard protocols. The initial screening of the Abs was conducted by ELISA with the peptides coupled to OVA and using an irrelevant peptide as a control. MVH 8E2 (rat IgG₁) and MVH 5B9 (rat IgG_{2b}) recognizing BNLF2a, as well as TAP 7F6 (rat IgG₁) specific for tapasin, are used in this study.

Constructs and production of replication-deficient recombinant retroviruses

The gene encoding BNLF2a with a C-terminal HA tag and four methionine residues (BNLF2aHA4M) was cloned into the pLZRS retroviral vector as described (42). This pLZRS vector contains an internal ribosomal entry site (IRES) immediately downstream of the inserted gene of interest to allow coexpression of a marker gene, in our case either truncated nerve growth factor receptor (NGFR) or enhanced GFP. A mutant of BNLF2aHA4M in which all cysteine residues are replaced by serines (BNLF2aΔcys) was constructed using the following primers: 5'-CGG GCA GGC CGG AGG CAG-3' (ascys1), 5'-GTC CTC GGG GGA GGG GTG-3' (ascys2), 5'-GAG CAG GGA TAA AAG TCC AAA CAG GAC AGA GAG TAC-3' (ascys3-4), 5'-GTC CTC TGC CTC CGG CCT G-3' (scys1), 5'-CTA GCC ACC CCT CCC CCG-3' (scys2), 5'-GTA CTC TCT GTC CTG TTT GGA CTT TTA TCC CTG CTC-3' (scys3-4), 5'-TCT AGC ATT TAG GTG ACA TAG TAG-3' (sp6), 5'-TAA TAC GAG TCA CTA TAG GGA GA-3' (t7), 5'-GGG AAT TCA TGG TAC ACG TC-3' (sbn), and 5'-AGA TCT CGA GTT ACA TCA TCA TCA TGG CAT

AGT CGG GCA CAT C-3' (asbn). Four PCRs were performed using a BNLF2aHA4M-encoding plasmid as template. The primers used in these reactions were t7 and ascys1 (PCR1), scys1 and ascys2 (PCR2), scys2 and ascys3-4 (PCR3), and scys3-4 and sp6 (PCR4). The products of PCR1 and PCR2 were combined and used as template in a PCR with the primers t7 and ascys2 (PCR5). Likewise, the products of PCR3 and PCR4 were combined and, together with the primers scys2 and sp6, used in a PCR (PCR6). The products of PCR5 and PCR6 were combined and used as template in a PCR with the primers sbn and asbn (PCR7). The resulting BNLF2aΔcys product of PCR7 was cloned into the pLZRS IRES GFP vector.

Retroviral vectors were transfected into the Phoenix A packaging cell line to produce replication-deficient recombinant retroviruses, as described (42).

Cell lines and retroviral transduction

Cell lines were maintained in complete culture medium consisting of RPMI 1640 (Invitrogen) supplemented with 10% FCS, 2 mM glutamine, 100 U/ml penicillin, and 100 μg/ml streptomycin, with the exception of STF1-169, STF1-169/TAP2, and BRE-169 cells, which were maintained in complete culture medium consisting of DMEM (Invitrogen) supplemented with 10% FCS, 2 mM glutamine, 100 U/ml penicillin, and 100 μg/ml streptomycin.

Retroviral transductions were performed essentially as described (42). In brief, cells were transduced with BNLF2aHA4M-, BNLF2aΔcys-, or control IRES-GFP-expressing retroviruses. Transduced cells were sorted by FACS to achieve expression in all cells.

Mel JuSo (MJS) is a human melanoma cell line (46). Both MJS cells and MJS cells stably transfected with TAP1-GFP (MJS/TAP1-GFP) (47) were transduced with replication-deficient retroviruses encoding BNLF2aHA4M-IRES-NGFR to generate the cell lines MJS/BNLF2a and MJS/TAP1-GFP/BNLF2a, respectively. To generate MJS/BNLF2aΔcys cells, MJS cells were transduced with BNLF2aΔcys-IRES-GFP retroviruses.

MoDo (48), T2 (49), and .220 (50) cells are EBV-transformed B lymphoblastoid cell lines (LCLs). MoDo cells were obtained from E. Goulmy (Leiden University Medical Center, Leiden, The Netherlands). T2 cells stably transfected to express TAP1 only (T2 TAP1) or both TAP1 and TAP2 (T2 TAP1 TAP2) were obtained from P. Lehner (Cambridge Institute for Medical Research, Cambridge, U.K.) (51), and .220 cells were obtained from E. Reits (Academic Medical Center, Amsterdam, The Netherlands). MoDo LCL, T2, T2 TAP1, and T2 TAP1 TAP2 cells were retrovirally transduced to express BNLF2aHA4M (coexpressing GFP as a marker), thereby generating the following cell lines: LCL/BNLF2a, T2/BNLF2a, T2 TAP1/BNLF2a, and T2 TAP1 TAP2/BNLF2a, respectively. T2/BNLF2a cells were additionally transduced with a retrovirus encoding BNLF2aHA4M-

IRES-NGFR, resulting in the T2/BNLF2a (G/N) cell line. For immunofluorescence microscopy, T2 and T2 TAP1 TAP2 cells were transduced with retroviruses encoding BNLF2aHA4M-IRES-NGFR, resulting in the T2/BNLF2a (N) and T2 TAP1 TAP2/BNLF2a (N) cell lines. Transduction of .220 cells with a retrovirus encoding BNLF2aHA4M-IRES-NGFR resulted in the .220 (TPN-)/BNLF2a cell line. In parallel, cells were transduced with control IRES-GFP retroviruses.

STF1-169 (52), STF1-169/TAP2, and BRE-169 (53) cells are immortalized fibroblasts (provided by H. de la Salle, Institut National de la Santé et de la Recherche Médicale Unité, Strasbourg, France). Immortalization of these cells and complementation of the STF1-169 cells with the TAP2 gene has been described previously (54). STF1-169, STF1-169/TAP2, and BRE-169 cells were retrovirally transduced to express BNLF2aHA4M (coexpressing NGFR as a marker), thereby generating the cell lines STF1/BNLF2a, STF1/TAP2/BNLF2a, and BRE/BNLF2a, respectively.

The AKBM cell line is an EBV⁺ Burkitt's lymphoma B cell line (Akata) stably transfected with the pHEBO-BMRF1p-rCD2-GFP reporter plasmid (41). The BZLF1 knockout (KO) LCL was generated as described (55).

Immunofluorescence

T2 and AKBM cells were incubated with l-polylysine (Sigma-Aldrich) for 15 min at 37°C to facilitate binding to coverslips, whereas MJS cells were grown overnight on coverslips. Cells attached to coverslips were washed with PBS and fixed in 3–4% paraformaldehyde for 30 min. After washing with PBS and permeabilization with 0.1–0.2% Triton X-100 for 5 min and blocking with BSA in PBS for 60 min, cells were incubated with primary Abs for 60–90 min. After washing with PBS, cells were incubated with fluorescently labeled secondary Abs (Jackson ImmunoResearch Laboratories) and Hoechst to visualize nuclei (Sigma-Aldrich) for 30–45 min, washed again with PBS, and embedded on microscope slides with Mowiol (Sigma-Aldrich). All incubation steps were performed at room temperature. Cells were visualized with a fluorescence microscope (Zeiss Axioskop 2) or a confocal microscope (Leica TCS SP2).

Immunoprecipitation and Western blot analysis

Immunoprecipitation experiments, SDS-PAGE, and immunoblotting were performed as previously described (33, 42). In brief, cells were lysed using either 0.5% Nonidet P-40 buffer (0.5% Nonidet P-40, 50 mM Tris-HCl (pH 7.5), 5 mM MgCl₂, 10 μM leupeptin, and 1 mM 4-(2-aminoethyl)benzenesulfonyl fluoride (AEBSF)) or 1% digitonin buffer (1% digitonin, 50 mM Tris-HCl (pH 7.5), 5 mM MgCl₂, 150 mM NaCl, 10 μM leupeptin, and 1 mM AEBSF) for 45 min at 4°C and subsequently centrifuged at 16,000 × g for 15

min at 4°C to obtain postnuclear lysates.

For immunoprecipitation experiments, 1% digitonin cell lysates were incubated with specific Abs and protein A- and protein G-Sepharose beads (GE Healthcare) for at least 2 h at 4°C. Isolated immune complexes were washed with 0.1% digitonin buffer.

For Western blot analysis, immune complexes or cell lysates were denatured in sample buffer, separated by SDS-PAGE, and transferred to polyvinylidene difluoride membranes (GE Healthcare). Proteins of interest were detected by incubating the membranes with specific Abs followed by HRP-conjugated secondary Abs (Jackson ImmunoResearch Laboratories or DakoCytomation). Ab binding was visualized using ECL Plus (GE Healthcare).

Subcellular fractionation

Fractionation of cells was performed essentially as described (12). In brief, 10⁷ cells were washed and resuspended in 1 ml of homogenization buffer (0.25 M sucrose, 10 mM triethanolamine, 10 mM potassium acetate, and 1 mM EDTA (pH 7.6)). Cells were homogenized on ice using a Dounce homogenizer with a tight fitting pestle (70 strokes). The homogenate was spun at 1,000 × g for 10 min at 4°C. The 1,000 × g pellet was stored on ice and the supernatant was subsequently centrifuged at 10,000 × g for 30 min at 4°C. The subsequent 10,000 × g pellet was also stored on ice and the supernatant was now centrifuged at 100,000 × g for 60 min at 4°C using a TLA 120.2 fixed-angle rotor and a Beckman Optima TLX ultracentrifuge. The 100,000 × g supernatant was collected and all pellets (1,000 × g, 10,000 × g, and 100,000 × g pellets) were resuspended in 0.5% Nonidet P-40 lysis mix in the presence of 10 μM leupeptin and 1 mM AEBSF). After incubation for 40 min at 4°C, lysates were centrifuged at 16,000 × g for 15 min at 4°C. Sample buffer was added to all four supernatants and the samples were incubated for 5 min at 95°C. Protein expression was analyzed by Western blotting.

Peptide transport assay

Peptide transport assays were performed essentially as described (33). In brief, 2 × 10⁶ cells were permeabilized with 2 IU/ml streptolysin O (Murex Diagnostics) for 10 min at 37°C and subsequently incubated with 4.5 μM fluoresceinated peptide CVNKTERAY (provided by W. Benckhuijsen and J. W. Drijfhout, Leiden University Medical Center, Leiden, The Netherlands) in the presence of 10 mM ATP or 0.125 M EDTA for 10 min at 37°C. Peptide transport was blocked by the addition of 1 ml of cold lysis buffer (1% Triton X-100, 500 mM NaCl, 2 mM MgCl₂, and 50 mM Tris-HCl (pH 8.0)). After lysis for 30 min at 4°C, cells were centrifuged at 16,000 × g for 20 min at 4°C to obtain postnuclear lysates. Glycosylated peptides were isolated from these lysates by incubation with Con A-Sepharose beads

(GE Healthcare) for 2 h at 4°C. After washing of the beads with the first (three times) and the second (one time) wash buffer (0.1% Triton X-100, 500 mM NaCl, 2 mM MgCl₂, 50 mM Tris-HCl (pH 8.0) and 500 mM NaCl, 50 mM Tris-HCl (pH 8.0), respectively), glycosylated peptides were eluted from the beads with elution buffer (500 mM mannopyranoside, 10 mM EDTA, and 50 mM Tris-HCl (pH 8.0)) during a 1-h incubation step at room temperature. Fluorescence was measured using a Mithras LB 940 multilabel reader (Berthold Technologies).

Flow cytometry

Surface levels of HLA class I, HLA class II, and transferrin receptor were analyzed by flow cytometry. Cells were stained with mAbs W6/32, L243, and CD71, respectively, and, after washing, with secondary goat anti-mouse PE Abs (Jackson ImmunoResearch Laboratories) or goat anti-mouse allophycocyanin Abs (Leinco Technologies) at 4°C. Stained cells were analyzed on a FACSCalibur flow cytometer using CellQuest Pro software (BD Biosciences).

Quantitative PCR

Cellular RNA was isolated from cells using TRIzol (Invitrogen) according to the manufacturer's instructions. cDNA was synthesized using random nanomer primers and Moloney murine leukemia virus reverse transcriptase (Finnzymes). The absence of genomic DNA was verified by parallel reactions performed in the absence of reverse transcriptase.

To detect actin and BNLF2a cDNA, the following primers were used: 5'-GGC ATC CTC ACC CTG AAG TA-3' (sActin); 5'-GGG GTG TTG AAG GTC TCA AA-3' (asActin) (56); 5'-ACG GCT GCA GAC CAT GGT ACA CGT CCT GGA GC-3' (sBNphilic); and 5'-TAC CGC TCG AGT TAT CTT AGT CTG CTG ACG TCT G-3' (asBNphilic).

For quantitative real-time PCR, SYBR Green was added to the reactions. Amplifications were performed using an ICycler (Bio-Rad) and data were analyzed with the accompanying software.

Productive EBV infection

Synchronous reactivation of EBV and isolation of B cells in the lytic cycle was performed essentially as described (41). In brief, AKBM cells, harboring the latent EBV genome, were cultured in the presence of anti-human IgG Abs (Cappel) for the indicated times to reactivate the virus following crosslinking of surface Ig. Cells that have entered the lytic cycle of EBV infection express the rat CD2-GFP reporter protein (from the EBV early BMRF1 promoter). Almost pure populations of productively EBV-infected AKBM cells were isolated by MACS (Miltenyi Biotec) on the basis of specific staining with Abs directed against rat CD2 (clone OX34) and secondary anti-mouse Abs conjugated to magnetic beads.

Acknowledgements

We gratefully acknowledge Jan-Wouter Drijfhout and Willemien Benckhuijsen (Leiden University Medical Center, Leiden, The Netherlands), Hidde Ploegh (Whitehead Institute, Cambridge, MA), Jacques Neefjes (The Netherlands Cancer Institute, Amsterdam, The Netherlands), Henri de la Salle (Institut National de la Santé et de la Recherche Médicale Unité, Strasbourg, France), Paul Lehner (Cambridge Institute for Medical Research, Cambridge, United Kingdom), and Robert Tampé (Biocenter, Goethe University, Frankfurt/Main, Germany) for helpful discussions and for generously sharing reagents and constructs.

These studies have been financially supported by Dutch Cancer Foundation Grant RUL 2005-3259, Royal Dutch Academy of Sciences Beijerinck Premium 2005, and the Netherlands Scientific Organization (NWO) Vidi Grant 917.76.330.

The authors have no financial conflict of interest.

References

1. Lehner, P. J., M. J. Surman, P. Cresswell. 1998. Soluble tapasin restores MHC class I expression and function in the tapasin-negative cell line .220. *Immunity* 8: 221-231.
2. Sadasivan, B., P. J. Lehner, B. Ortman, T. Spies, P. Cresswell. 1996. Roles for calreticulin and a novel glycoprotein, tapasin, in the interaction of MHC class I molecules with TAP. *Immunity* 5: 103-114.
3. Kienast, A., M. Preuss, M. Winkler, T. P. Dick. 2007. Redox regulation of peptide receptivity of major histocompatibility complex class I molecules by ERp57 and tapasin. *Nat. Immunol.* 8: 864-872.
4. Wearsch, P. A., P. Cresswell. 2007. Selective loading of high-affinity peptides onto major histocompatibility complex class I molecules by the tapasin-ERp57 heterodimer. *Nat. Immunol.* 8: 873-881.
5. Vossen, M. T., E. M. Westerhout, C. Soderberg-Naucler, E. J. Wiertz. 2002. Viral immune evasion: a masterpiece of evolution. *Immunogenetics* 54: 527-542.
6. Wiertz, E. J., S. Mukherjee, H. L. Ploegh. 1997. Viruses use stealth technology to escape from the host immune system. *Mol. Med. Today* 3: 116-123.
7. Yewdell, J. W., A. B. Hill. 2002. Viral interference with antigen presentation. *Nat. Immunol.* 3: 1019-1025.
8. Lilley, B. N., H. L. Ploegh. 2005. Viral modulation of antigen presentation: manipulation of cellular targets in the ER and beyond. *Immunol. Rev.* 207: 126-144.
9. Gruhler, A., P. A. Peterson, K. Fruh. 2000. Human

- cytomegalovirus immediate early glycoprotein US3 retains MHC class I molecules by transient association. *Traffic* 1: 318-325.
10. Park, B., Y. Kim, J. Shin, S. Lee, K. Cho, K. Fruh, S. Lee, K. Ahn. 2004. Human cytomegalovirus inhibits tapasin-dependent peptide loading and optimization of the MHC class I peptide cargo for immune evasion. *Immunity* 20: 71-85.
 11. Ziegler, H., R. Thale, P. Lucin, W. Muranyi, T. Flohr, H. Hengel, H. Farrell, W. Rawlinson, U. H. Koszinowski. 1997. A mouse cytomegalovirus glycoprotein retains MHC class I complexes in the ERGIC/cis-Golgi compartments. *Immunity* 6: 57-66.
 12. Wiertz, E. J., T. R. Jones, L. Sun, M. Bogoy, H. J. Geuze, H. L. Ploegh. 1996. The human cytomegalovirus US11 gene product dislocates MHC class I heavy chains from the endoplasmic reticulum to the cytosol. *Cell* 84: 769-779.
 13. Wiertz, E. J. H. J., D. Tortorella, M. Bogoy, J. Yu, W. Mothes, T. R. Jones, T. A. Rapoport, H. L. Ploegh. 1996. Sec61-mediated transfer of a membrane protein from the endoplasmic reticulum to the proteasome for destruction. *Nature* 384: 432-438.
 14. Stevenson, P. G., S. Efstathiou, P. C. Doherty, P. J. Lehner. 2000. Inhibition of MHC class I-restricted antigen presentation by γ 2-herpesviruses. *Proc. Natl. Acad. Sci. USA* 97: 8455-8460.
 15. Boname, J. M., P. G. Stevenson. 2001. MHC class I ubiquitination by a viral PHD/LAP finger protein. *Immunity* 15: 627-636.
 16. Boname, J. M., B. D. de Lima, P. J. Lehner, P. G. Stevenson. 2004. Viral degradation of the MHC class I peptide loading complex. *Immunity* 20: 305-317.
 17. Yu, Y. Y., M. R. Harris, L. Lybarger, L. A. Kimpler, N. B. Myers, H. W. Virgin, T. H. Hansen. 2002. Physical association of the K3 protein of γ -2 herpesvirus 68 with major histocompatibility complex class I molecules with impaired peptide and β 2-microglobulin assembly. *J. Virol.* 76: 2796-2803.
 18. Lybarger, L., X. Wang, M. R. Harris, H. W. Virgin, T. H. Hansen. 2003. Virus subversion of the MHC class I peptide-loading complex. *Immunity* 18: 121-130.
 19. Coscoy, L., D. Ganem. 2000. Kaposi's sarcoma-associated herpesvirus encodes two proteins that block cell surface display of MHC class I chains by enhancing their endocytosis. *Proc. Natl. Acad. Sci. USA* 97: 8051-8056.
 20. Ishido, S., C. Wang, B. S. Lee, G. B. Cohen, J. U. Jung. 2000. Downregulation of major histocompatibility complex class I molecules by Kaposi's sarcoma-associated herpesvirus K3 and K5 proteins. *J. Virol.* 74: 5300-5309.
 21. Lehner, P. J., S. Hoer, R. Dodd, L. M. Duncan. 2005. Downregulation of cell surface receptors by the K3 family of viral and cellular ubiquitin E3 ligases. *Immunol. Rev.* 207: 112-125.
 22. Hudson, A. W., P. M. Howley, H. L. Ploegh. 2001. A human herpesvirus 7 glycoprotein, U21, diverts major histocompatibility complex class I molecules to lysosomes. *J. Virol.* 75: 12347-12358.
 23. Hudson, A. W., D. Blom, P. M. Howley, H. L. Ploegh. 2003. The ER-luminal domain of the HHV-7 immunoevasin U21 directs class I MHC molecules to lysosomes. *Traffic* 4: 824-837.
 24. Reusch, U., W. Muranyi, P. Lucin, H. G. Burgert, H. Hengel, U. H. Koszinowski. 1999. A cytomegalovirus glycoprotein re-routes MHC class I complexes to lysosomes for degradation. *EMBO J.* 18: 1081-1091.
 25. Ahn, K., T. H. Meyer, S. Uebel, P. Sempe, H. Djaballah, Y. Yang, P. A. Peterson, K. Fruh, R. Tampe. 1996. Molecular mechanism and species specificity of TAP inhibition by herpes simplex virus ICP47. *EMBO J.* 15: 3247-3255.
 26. Fruh, K., K. Ahn, H. Djaballah, P. Sempe, P. M. van Endert, R. Tampe, P. A. Peterson, Y. Yang. 1995. A viral inhibitor of peptide transporters for antigen presentation. *Nature* 375: 415-418.
 27. Galocha, B., A. Hill, B. C. Barnett, A. Dolan, A. Raimondi, R. F. Cook, J. Brunner, D. J. McGeoch, H. L. Ploegh. 1997. The active site of ICP47, a herpes simplex virus-encoded inhibitor of the major histocompatibility complex (MHC)-encoded peptide transporter associated with antigen processing (TAP), maps to the NH₂-terminal 35 residues. *J. Exp. Med.* 185: 1565-1572.
 28. Hill, A., P. Jugovic, I. York, G. Russ, J. Bennink, J. Yewdell, H. Ploegh, D. Johnson. 1995. Herpes simplex virus turns off the TAP to evade host immunity. *Nature* 375: 411-415.
 29. Neumann, L., W. Kraas, S. Uebel, G. Jung, R. Tampe. 1997. The active domain of the herpes simplex virus protein ICP47: a potent inhibitor of the transporter associated with antigen processing. *J. Mol. Biol.* 272: 484-492.
 30. Tomazin, R., A. B. Hill, P. Jugovic, I. York, P. van Endert, H. L. Ploegh, D. W. Andrews, D. C. Johnson. 1996. Stable binding of the herpes simplex virus ICP47 protein to the peptide binding site of TAP. *EMBO J.* 15: 3256-3266.
 31. York, I. A., C. Roop, D. W. Andrews, S. R. Riddell, F. L. Graham, D. C. Johnson. 1994. A cytosolic herpes simplex virus protein inhibits antigen presentation to CD8⁺ T lymphocytes. *Cell* 77: 525-535.
 32. Lacaille, V. G., M. J. Androlewicz. 1998. Herpes simplex virus inhibitor ICP47 destabilizes the transporter associated with antigen processing (TAP) heterodimer. *J. Biol. Chem.* 273: 17386-17390.

33. Koppers-Lalic, D., E. A. Reits, M. E. Rensing, A. D. Lipinska, R. Abele, J. Koch, R. M. Marcondes, P. Admiraal, D. van Leeuwen, K. Bienkowska-Szewczyk, et al 2005. Varicelloviruses avoid T cell recognition by UL49.5-mediated inactivation of the transporter associated with antigen processing. *Proc. Natl. Acad. Sci. USA* 102: 5144-5149.
34. Koppers-Lalic, D., M. C. Verweij, A. D. Lipinska, Y. Wang, E. Quinten, E. A. Reits, J. Koch, S. Loch, M. M. Rezende, F. Daus, et al 2008. Varicellovirus UL 49.5 proteins differentially affect the function of the transporter associated with antigen processing, TAP. *PLoS Pathog.* 4: e1000080
35. Ahn, K., A. Gruhler, B. Galocha, T. R. Jones, E. J. Wiertz, H. L. Ploegh, P. A. Peterson, Y. Yang, K. Fruh. 1997. The ER-luminal domain of the HCMV glycoprotein US6 inhibits peptide translocation by TAP. *Immunity* 6: 613-621.
36. Hengel, H., J. O. Koopmann, T. Flohr, W. Muranyi, E. Goulmy, G. J. Hammerling, U. H. Koszinowski, F. Momburg. 1997. A viral ER-resident glycoprotein inactivates the MHC-encoded peptide transporter. *Immunity* 6: 623-632.
37. Hewitt, E. W., S. S. Gupta, P. J. Lehner. 2001. The human cytomegalovirus gene product US6 inhibits ATP binding by TAP. *EMBO J.* 20: 387-396.
38. Kyritsis, C., S. Gorbulev, S. Hutschenreiter, K. Pawlitschko, R. Abele, R. Tampe. 2001. Molecular mechanism and structural aspects of transporter associated with antigen processing inhibition by the cytomegalovirus protein US6. *J. Biol. Chem.* 276: 48031-48039.
39. Lehner, P. J., J. T. Karttunen, G. W. Wilkinson, P. Cresswell. 1997. The human cytomegalovirus US6 glycoprotein inhibits transporter associated with antigen processing-dependent peptide translocation. *Proc. Natl. Acad. Sci. USA* 94: 6904-6909.
40. Gottschalk, S., H. E. Heslop, C. M. Roon. 2002. Treatment of Epstein-Barr virus-associated malignancies with specific T cells. *Adv. Cancer Res.* 84: 175-201.
41. Rensing, M. E., S. E. Keating, D. van Leeuwen, D. Koppers-Lalic, I. Y. Pappworth, E. J. Wiertz, M. Rowe. 2005. Impaired transporter associated with antigen processing-dependent peptide transport during productive EBV infection. *J. Immunol.* 174: 6829-6838.
42. Hislop, A. D., M. E. Rensing, D. van Leeuwen, V. A. Pudney, D. Horst, D. Koppers-Lalic, N. P. Croft, J. J. Neefjes, A. B. Rickinson, E. J. Wiertz. 2007. A CD8⁺ T cell immune evasion protein specific to Epstein-Barr virus and its close relatives in Old World primates. *J. Exp. Med.* 204: 1863-1873.
43. Barnstable, C. J., W. F. Bodmer, G. Brown, G. Galfre, C. Milstein, A. F. Williams, A. Ziegler. 1978. Production of monoclonal antibodies to group A erythrocytes, HLA and other human cell surface antigens-new tools for genetic analysis. *Cell* 14: 9-20.
44. Hochstenbach, F., V. David, S. Watkins, M. B. Brenner. 1992. Endoplasmic reticulum resident protein of 90 kilodaltons associates with the T- and B-cell antigen receptors and major histocompatibility complex antigens during their assembly. *Proc. Natl. Acad. Sci. USA* 89: 4734-4738.
45. van den Born, E., C. C. Posthuma, K. Knoops, E. J. Snijder. 2007. An infectious recombinant equine arteritis virus expressing green fluorescent protein from its replicase gene. *J. Gen. Virol.* 88: 1196-1205.
46. van Ham, S. M., E. P. Tjin, B. F. Lillemeier, U. Gruneberg, K. E. van Meijgaarden, L. Pastoors, D. Verwoerd, A. Tulp, B. Canas, D. Rahman, et al 1997. HLA-DO is a negative modulator of HLA-DM-mediated MHC class II peptide loading. *Curr. Biol.* 7: 950-957.
47. Reits, E. A., J. C. Vos, M. Gromme, J. Neefjes. 2000. The major substrates for TAP *in vivo* are derived from newly synthesized proteins. *Nature* 404: 774-778.
48. Oosten, L. E., D. Koppers-Lalic, E. Blokland, A. Mulder, M. E. Rensing, T. Mutis, A. G. van Halteren, E. J. Wiertz, E. Goulmy. 2007. TAP-inhibiting proteins US6, ICP47 and UL49.5 differentially affect minor and major histocompatibility antigen-specific recognition by cytotoxic T lymphocytes. *Int. Immunol.* 19: 1115-1122.
49. Salter, R. D., D. N. Howell, P. Cresswell. 1985. Genes regulating HLA class I antigen expression in T-B lymphoblast hybrids. *Immunogenetics* 21: 235-246.
50. Shimizu, Y., R. DeMars. 1989. Production of human cells expressing individual transferred HLA-A,-B,-C genes using an HLA-A,-B,-C null human cell line. *J. Immunol.* 142: 3320-3328.
51. Karttunen, J. T., P. J. Lehner, S. S. Gupta, E. W. Hewitt, P. Cresswell. 2001. Distinct functions and cooperative interaction of the subunits of the transporter associated with antigen processing (TAP). *Proc. Natl. Acad. Sci. USA* 98: 7431-7436.
52. de la Salle, H., D. Hanau, D. Fricker, A. Urlacher, A. Kelly, J. Salamero, S. H. Powis, L. Donato, H. Bausinger, M. Laforet, et al 1994. Homozygous human TAP peptide transporter mutation in HLA class I deficiency. *Science* 265: 237-241.
53. de la Salle, H., J. Zimmer, D. Fricker, C. Angenieux, J. P. Cazenave, M. Okubo, H. Maeda, A. Plebani, M. M. Tongio, A. Dormoy, D. Hanau. 1999. HLA class I deficiencies due to

- mutations in subunit 1 of the peptide transporter TAP1. *J. Clin. Invest* 103: R9-R13.
54. Verweij, M. C., D. Koppers-Lalic, S. Loch, F. Klauschies, H. de la Salle, E. Quinten, P. J. Lehner, A. Mulder, M. R. Knittler, R. Tampe, et al 2008. The varicellovirus UL49.5 protein blocks the transporter associated with antigen processing (TAP) by inhibiting essential conformational transitions in the 6+6 transmembrane TAP core complex. *J. Immunol.* 181: 4894-4907.
 55. Feederle, R., M. Kost, M. Baumann, A. Janz, E. Drouet, W. Hammerschmidt, H. J. Delecluse. 2000. The Epstein-Barr virus lytic program is controlled by the co-operative functions of two transactivators. *EMBO J.* 19: 3080-3089.
 56. Ovstebo, R., K. B. Haug, K. Lande, P. Kierulf. 2003. PCR-based calibration curves for studies of quantitative gene expression in human monocytes: development and evaluation. *Clin. Chem.* 49: 425-432.
 57. Kleijmeer, M. J., A. Kelly, H. J. Geuze, J. W. Slot, A. Townsend, J. Trowsdale. 1992. Location of MHC-encoded transporters in the endoplasmic reticulum and cis-Golgi. *Nature* 357: 342-344.
 58. Russ, G., F. Esquivel, J. W. Yewdell, P. Cresswell, T. Spies, J. R. Bennink. 1995. Assembly, intracellular localization, and nucleotide binding properties of the human peptide transporters TAP1 and TAP2 expressed by recombinant vaccinia viruses. *J. Biol. Chem.* 270: 21312-21318.
 59. Stam, N. J., H. Spits, H. L. Ploegh. 1986. Monoclonal antibodies raised against denatured HLA-B locus heavy chains permit biochemical characterization of certain HLA-C locus products. *J. Immunol.* 137: 2299-2306.
 60. Seliger, B., U. Ritz, R. Abele, M. Bock, R. Tampe, G. Sutter, I. Drexler, C. Huber, S. Ferrone. 2001. Immune escape of melanoma: first evidence of structural alterations in two distinct components of the MHC class I antigen processing pathway. *Cancer Res.* 61: 8647-8650.
 61. Copeman, J., N. Bangia, J. C. Cross, P. Cresswell. 1998. Elucidation of the genetic basis of the antigen presentation defects in the mutant cell line .220 reveals polymorphism and alternative splicing of the tapasin gene. *Eur. J. Immunol.* 28: 3783-3791.
 62. Beinert, D., L. Neumann, S. Uebel, R. Tampe. 1997. Structure of the viral TAP-inhibitor ICP47 induced by membrane association. *Biochemistry* 36: 4694-4700.
 63. Pfander, R., L. Neumann, M. Zweckstetter, C. Seger, T. A. Holak, R. Tampe. 1999. Structure of the active domain of the herpes simplex virus protein ICP47 in water/sodium dodecyl sulfate solution determined by nuclear magnetic resonance spectroscopy. *Biochemistry* 38: 13692-13698.
 64. Halenius, A., F. Momburg, H. Reinhard, D. Bauer, M. Lobigs, H. Hengel. 2006. Physical and functional interactions of the cytomegalovirus US6 glycoprotein with the transporter associated with antigen processing. *J. Biol. Chem.* 281: 5383-5390.
 65. Loch, S., F. Klauschies, C. Scholz, M. C. Verweij, E. J. Wiertz, J. Koch, R. Tampe. 2008. Signaling of a varicelloviral factor across the endoplasmic reticulum membrane induces destruction of the peptide-loading complex and immune evasion. *J. Biol. Chem.* 283: 13428-13436.
 66. Yuan, J., E. Cahir-McFarland, B. Zhao, E. Kieff. 2006. Virus and cell RNAs expressed during Epstein-Barr virus replication. *J. Virol.* 80: 2548-2565.
 67. Lipinska, A. D., D. Koppers-Lalic, M. Rychlowski, P. Admiraal, F. A. Rijsewijk, K. Bienkowska-Szewczyk, E. J. Wiertz. 2006. Bovine herpesvirus 1 UL49.5 protein inhibits the transporter associated with antigen processing despite complex formation with glycoprotein M. *J. Virol.* 80: 5822-5832.

Chapter 4

EBV protein BNLF2a exploits host tail-anchored protein integration machinery to inhibit TAP

D. Horst, V. Favalaro*, F. Vilardi*, H.C. van Leeuwen, M.A. Garstka, A.D. Hislop, C. Rabu, E. Kremmer, A.B. Rickinson, S. High, B. Dobberstein, M.E. Rensing** and E.J.H.J. Wiertz**.

The Journal of Immunology 2011

*** These authors contributed equally to this manuscript

Abstract

EBV, the prototypic human γ 1-herpesvirus, persists for life in infected individuals, despite the presence of vigorous antiviral immunity. CTLs play an important role in the protection against viral infections, which they detect through recognition of virus-encoded peptides presented in the context of HLA class I molecules at the cell surface. The viral peptides are generated in the cytosol and are transported into the endoplasmic reticulum (ER) by TAP. The EBV-encoded lytic-phase protein BNLF2a acts as a powerful inhibitor of TAP. Consequently, loading of antigenic peptides onto HLA class I molecules is hampered, and recognition of BNLF2a-expressing cells by cytotoxic T cells is avoided. In this study, we characterize BNLF2a as a tail-anchored (TA) protein and elucidate its mode of action. Its hydrophilic N-terminal domain is located in the cytosol, whereas its hydrophobic C-terminal domain is inserted into membranes posttranslationally. TAP has no role in membrane insertion of BNLF2a. Instead, Asna1 (also named TRC40), a cellular protein involved in posttranslational membrane insertion of TA proteins, is responsible for integration of BNLF2a into the ER membrane. Asna1 is thereby required for efficient BNLF2a-mediated HLA class I downregulation. To optimally accomplish immune evasion, BNLF2a is composed of two specialized domains: its C-terminal tail anchor ensures membrane integration and ER retention, whereas its cytosolic N terminus accomplishes inhibition of TAP function. These results illustrate how EBV exploits a cellular pathway for TA protein biogenesis to achieve immune evasion, and they highlight the exquisite adaptation of this virus to its host.

Introduction

The γ -herpesvirus EBV is carried by >90% of the adult human population. Whereas infection experienced early in childhood is mostly asymptomatic, primary infection of adolescents frequently results in the development of infectious mononucleosis. In addition, EBV is associated with a number of malignancies, among which are Burkitt's lymphoma, nasopharyngeal carcinoma, gastric carcinoma, Hodgkin's lymphoma, and posttransplant lymphoproliferative diseases (1). After primary infection, EBV persists by latently infecting memory B cells. The EBV genome is maintained as an episome and replicates during cell division. During latency, nine viral proteins are expressed at the most, which limits recognition of EBV-infected cells by the immune system. In contrast, during productive (lytic) infection, which is required for the generation of viral particles and infection of other hosts, >80 proteins are synthesized. This increase in viral protein expression results in the generation of many viral Ags that may be detected by the immune system (2). To prevent elimination of productively infected cells by the immune system, EBV has acquired specific immune evasion proteins (3). CTLs play an important role in protecting the host against intracellular pathogens such as viruses. The importance of CTLs in controlling EBV infection can be inferred from the fact that EBV-associated lymphomas frequently occur under conditions of compromised T cell function. The importance of CTLs is further illustrated by the successful treatment of EBV-related tumors by adoptive transfer of EBV-specific CTLs (4). The viral invader is detected by CTLs through recognition of virus-derived peptides presented in the context of HLA class I molecules at the surface of the infected cell. These peptides are generated by proteasomal degradation of proteins or fragments thereof and are transported from the cytosol into the endoplasmic reticulum (ER) by TAP. In the ER, these peptides bind to newly synthesized HLA class I molecules, which subsequently travel to the cell surface for inspection by CTLs (5–7). Peptide transport by TAP forms a bottleneck in the HLA class I Ag presentation pathway, as substantiated by the identification of TAP-inhibiting proteins in a number of viruses, including EBV. Although these proteins all block TAP-mediated peptide transport, there is no structural or functional homology among them. ICP47, encoded by HSV, is a cytosolic protein that competes for peptide binding to TAP (8–10). Human CMV-encoded US6 is a type I membrane protein blocking ATP binding to TAP (11–13). The UL49.5 proteins of a number of varicelloviruses have been found to block TAP as well (14). These type I membrane proteins cause a conformational arrest of TAP. The UL49.5 protein of bovine herpesvirus 1 additionally targets TAP for degradation. The recently

identified cowpox-encoded TAP inhibitor CPXV12 has been classified as a type II membrane protein (15, 16), interfering with peptide transport in an as-yet unresolved way. Finally, the EBV-encoded BNLF2a protein interferes with both peptide and ATP binding to TAP (17). BNLF2a is a small membrane-associated protein composed of only 60 aa residues and lacking a bona fide signal sequence.

At present, it is unclear whether BNLF2a is integrated into the ER membrane, and if so, how this might occur. Other important features, such as its mode of interaction with TAP and the mechanism of TAP inhibition, remain to be elucidated. In this study, we characterize the EBV-encoded TAP inhibitor BNLF2a as a tail-anchored (TA) protein and report on its structural and functional properties that allow this small viral protein to efficiently block T cell recognition.

Results

The C-terminal hydrophobic domain of BNLF2a serves as a membrane anchor

EBV BNLF2a has an N-terminal hydrophilic domain and a hydrophobic C-terminal domain with a predicted α -helical structure (Fig. 1). These features are reminiscent of TA proteins, a class of proteins that are inserted into membranes via their hydrophobic C termini, leaving their N termini exposed in the cytosol. To evaluate whether the topology of BNLF2a resembles that of TA proteins, two approaches were taken.

First, proteinase K digestions were performed on semipermeabilized cells. Cells stably expressing BNLF2a were either semipermeabilized with digitonin or lysed in RIPA buffer. In digitonin-permeabilized cells, proteinase K can only reach and degrade cytosolic protein domains, leaving luminal structures intact. Accordingly, an Ab directed against the cytoplasmic domain of TfR could no longer detect TfR when the cells were semipermeabilized and treated with proteinase K (Fig. 2A, compare lanes 1 and 2). Under these conditions, an Ab against the ER-luminal domain of calnexin detected a lower m.w. form of calnexin, representing a molecule from which the cytoplasmic domain had been removed by proteinase K (Fig. 2A, lane 2). After lysis in RIPA buffer, all membranous structures are dissolved, thereby allowing proteinase K to degrade both cytosolic and luminal proteins (Fig. 2A, lane 4).

To study whether and how BNLF2a is orientated in the membrane, an Ab that specifically recognizes the N-terminal domain of BNLF2a and an Ab specific for the HA-tag added to the C terminus of BNLF2a were used. Proteinase K treatment of digitonin-permeabilized cells resulted in a marked reduction in the amount of full-length BNLF2a as detected by the Ab directed against the N-terminal domain of the viral

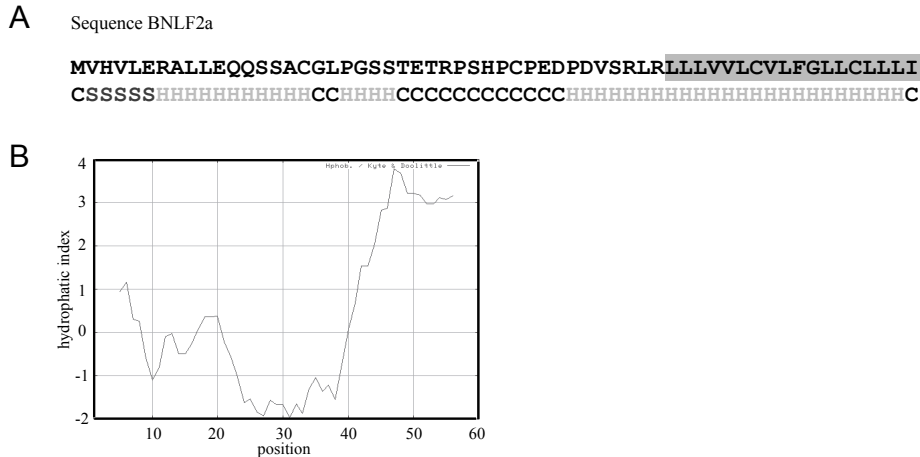


Figure 1. Protein structure of EBV-encoded BNLF2a

A, Amino acid sequence of BNLF2a with the hydrophobic C terminus highlighted. Secondary structure prediction of BNLF2a as determined by the I-TASSER server. Sheets are indicated with S and helices with H. B, Hydropathicity profile of BNLF2a as determined by the method of Kyte and Doolittle (39).

protein (Fig. 2A, lane 2). Staining with the anti-HA Ab revealed a lower m.w. form of BNLF2a in proteinase K-treated, digitonin-permeabilized cells (Fig. 2A, lane 2). This band was absent from untreated cells (Fig. 2A, lane 1). After lysis of the cells in RIPA buffer, no BNLF2a protein was detected using the BNLF2a-specific Ab (Fig. 2A, lane 4). Because a degradation product was observed using an Ab directed against the C-terminal HA-tag and not with the BNLF2a-specific Ab recognizing the N-terminal domain, these results suggest that the N terminus of BNLF2a is exposed in the cytosol, whereas the C terminus is orientated toward the ER lumen. A small amount of full-length BNLF2a was still detectable under conditions that were sufficient to completely digest the cytosolic domains of TrR and calnexin (Fig. 2A, lanes 1 and 2). This suggests that the N terminus of BNLF2a is not easily accessible to proteinase K, possibly because of association of BNLF2a with TAP. Proteinase K digestions performed on TAP-deficient cells indicated that this is indeed the case. BNLF2a was readily digested by proteinase K in TAP-deficient T2 cells, whereas reconstitution of TAP expression in these cells precluded its complete digestion (Supplemental Fig. 1). These data indicate that BNLF2a is protected from proteolytic degradation through its interaction with the TAP complex.

A second approach to address the topology of BNLF2a is based on the acquisition of N-linked glycans in the ER. For this purpose, an epitope-tag derived from rhodopsin containing an N-linked glycosylation consensus sequence (opsin-tag) was added to the C terminus of BNLF2a (BNo). The capacity of BNo to block TAP function was not affected by the addition of the opsin-tag, as reflected by effective and specific

downregulation of HLA class I surface expression (Fig. 2B).

Cell lysates of BNLF2a- and BNo-expressing cells were treated with EndoH to remove N-linked glycans from ER-resident proteins and subsequently subjected to Western blotting. Treatment of BNo with EndoH resulted in a protein band migrating at a lower m.w. (Fig. 2C, compare lanes 4 and 5), demonstrating that the opsin-tag was indeed glycosylated and thus present in the ER lumen. The glycosylated form of BNo can be coimmunoprecipitated with TAP1 (Fig. 2D, lane 4), indicating that this form of BNo is capable of interacting with TAP.

In conclusion, the hydrophobic C-terminal domain of BNLF2a is inserted into the ER membrane, whereas the N-terminal domain is exposed in the cytosol. Thereby, BNLF2a exhibits one of the hallmarks of TA proteins.

BNLF2a is inserted into membranes posttranslationally

Another characteristic of TA proteins is their posttranslational membrane insertion. Because of the localization of the hydrophobic domain at the C terminus, this domain is released from ribosomes only after completion of protein synthesis (40, 41). To explore whether BNLF2a is integrated into membranes posttranslationally, *in vitro* translation reactions were performed for BNo. As controls, RAMP4 and HLA-A2 were taken along; RAMP4 is a known TA protein that is inserted into membranes posttranslationally (27), whereas integration of the type I membrane protein HLA-A2 occurs strictly cotranslationally. As a source of ER, microsomal membranes were added either during the translation reaction or after protein

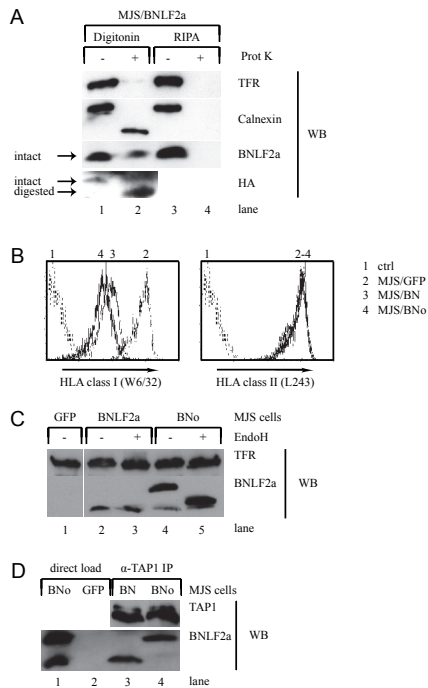


Figure 2. Hydrophobic domain of BNLf2a serves as a membrane anchor

A, MJS/BNLf2a cells, either lysed in RIPA buffer or permeabilized with digitonin, were incubated with or without 100 μ g/ml proteinase K. Protein samples were separated by SDS-PAGE and analyzed by Western blotting for the presence of the control transmembrane proteins Tfr (mAb H68.4) and calnexin (mAb AF8). BNLf2a was detected using a mAb specific for BNLf2a (5B9) and the HA-tag added to the C terminus of BNLf2a (L2CA5). B, MJS cells stably expressing GFP (lane 2), BNLf2a (lane 3), or BNo (lane 4) were stained for HLA class I (mAb W6/32) or HLA class II (mAb L243) and analyzed by flow cytometry. Lane 1 represents a negative control (secondary Ab only). C, Postnuclear lysates of MJS cells stably expressing GFP, BNLf2a, or BNo were incubated with EndoH. Protein samples were separated by SDS-PAGE and analyzed by Western blotting for the presence of Tfr (mAb H68.4) as a control and BNLf2a (mAb 5B9). D, Digitonin lysates of MJS cells stably expressing BNLf2a (BN) or BNo were subjected to immunoprecipitations using Abs specific for TAP1 (mAb 148.3). Immune complexes and control postnuclear lysates were separated by SDS-PAGE and analyzed by Western blotting for TAP1 (mAb 148.3) and BNLf2a (mAb 5B9) expression.

synthesis was blocked, allowing proteins to be inserted into the membranes both co- and posttranslationally, respectively. As expected, Ro was membrane-inserted irrespective of the moment of membrane addition (Fig. 3A, lanes 5 and 6), whereas membrane integration of HLA-A2 was entirely dependent on the presence of microsomes during translation (Fig. 3A, lanes 3 and 4).

BNo was integrated into microsomal membranes that were added after termination of translation (Fig. 3A, lane 2), indicating that BNLf2a can be inserted into membranes posttranslationally. The amounts of glycosylated proteins were higher when membranes were added at the start of translation, both for BNo and Ro (Fig. 3). This might be due to a difference in the time available for membrane insertion (90 min for membrane insertion during translation, compared with 30 min for membrane insertion after translation). Alternatively, the TA proteins might be unstable when they are not integrated into membranes.

In summary, these results demonstrate that BNLf2a can be integrated into membranes after termination of protein synthesis. Because BNLf2a thus exhibits the two most important features of TA proteins, namely their characteristic membrane topology and their ability to be inserted into membranes posttranslationally, BNLf2a can be classified as a TA protein.

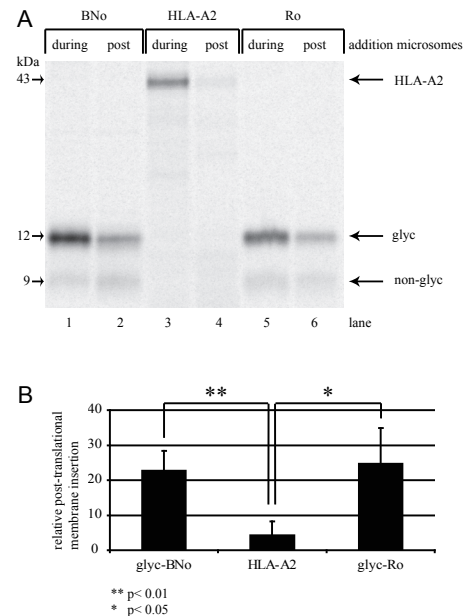


Figure 3. BNLf2a is posttranslationally inserted into membranes

A, *In vitro* translation reactions were performed in the presence of [35 S]methionine/cysteine using mRNA encoding BNo, HLA-A2, or Ro. Microsomes were added either at the start of translation or after termination of translation by cycloheximide. Microsomes were pelleted, denatured, and separated by SDS-PAGE. Translation products were visualized by phosphorimaging. B, Quantification of A. The amount of protein that was inserted into microsomes added posttranslationally was corrected for the amount of protein inserted into microsomes added at the start of translation. Data are represented as mean \pm SD. **p < 0.01, *p < 0.05 as determined by a t test.

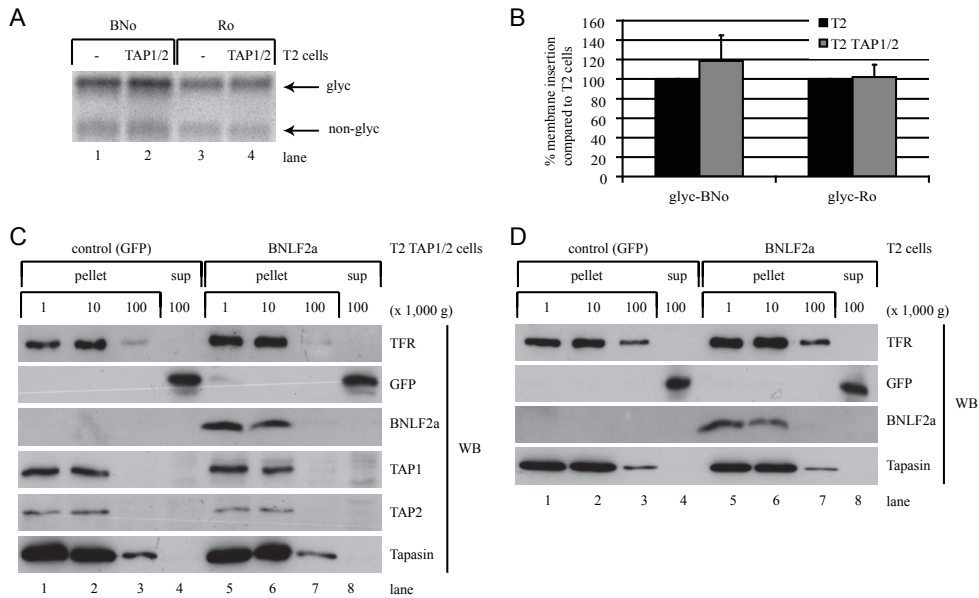


Figure 4. Membrane insertion and association of BNLf2a is independent of TAP expression

A, *In vitro* translation reactions were performed in the presence of [³⁵S]methionine/cysteine using mRNA encoding BNo or Ro. Semipermeabilized T2 or T2 TAP1/2 cells were added after termination of translation by cycloheximide. Total lysates of these cells were separated by SDS-PAGE. Translation products were visualized by phosphorimaging. B, Quantification of A. Samples were corrected for the amount of protein inserted into membranes of semipermeabilized T2 cells (set at 100%). Data are represented as mean ± SD. C, T2 TAP1/2 cells (reconstituted with TAP1 and TAP2) stably expressing GFP or BNLf2a were subjected to subcellular fractionation by differential centrifugation, as described in the Materials and Methods. The 1,000 × g, 10,000 × g, and 100,000 × g pellets and 100,000 × g supernatant (sup) were separated by SDS-PAGE and analyzed by Western blotting for the presence of TfR (mAb H68.4), cytosolic GFP (anti-GFP rabbit serum), BNLf2a (mAb 8E2/5B9), TAP1 (mAb 148.3), TAP2 (mAb 435.4), and tapasin (mAb 7F6). D, T2 cells (lacking TAP) stably expressing GFP or BNLf2a were fractionated and analyzed as described in C.

Membrane insertion of BNLf2a does not depend on TAP expression

Although a small group of TA proteins can insert into membranes spontaneously, most of them require cellular components for assistance (42, 43). Besides transporting peptides, TAP could potentially also translocate the transmembrane domain of the small BNLf2a protein into the ER membrane, resulting in stable expression of the viral protein in association with the TAP complex.

To determine the influence of TAP on membrane insertion of BNLf2a, *in vitro* translations were performed. TAP-deficient T2 cells (31) and T2 cells reconstituted with TAP1 and TAP2 (32) (TAP1/2 cells) were semipermeabilized using digitonin and added to *in vitro*-synthesized BNo and Ro. Prior to adding the semipermeable cells, translation was stopped by addition of cycloheximide to ascertain that protein insertion occurred posttranslationally. No differences were seen for the membrane insertion of the control protein Ro in cells that do or do not express TAP (Fig. 4A, 4B). In the presence of TAP, a small, statistically insignificant increase in the percentage of glycosylated, membrane-inserted BNo protein was observed when compared with TAP-deficient T2 cells

(Fig. 4A, 4B).

The influence of TAP on membrane association of BNLf2a was additionally investigated by subcellular fractionation experiments performed using T2 and T2 TAP1/2 cells. Cells expressing BNLf2a or the control protein GFP were homogenized and sedimented by differential centrifugation, thereby separating membranous organelles (pellet fractions) from cytosol (supernatant fraction). Protein content of the different fractions was analyzed by Western blotting. Whereas the membrane protein TfR was detected in the pellet fractions, cytosolic GFP was only detected in the supernatant fraction (Fig. 4C, 4D), showing separation of membrane and cytosolic proteins using this assay. TAP1, TAP2, and tapasin are detected in the pellet fractions (Fig. 4C, 4D). In TAP-expressing cells, BNLf2a was also associated with membranes as deduced from its presence in the 1,000 × g and 10,000 × g pellet fractions (Fig. 4C). This is consistent with previous results (22) and the proteinase K digestion experiments (Fig. 2A). A similar distribution was observed for BNLf2a in TAP-deficient cells (Fig. 4D). In conclusion, TAP is dispensable for membrane insertion of the BNLf2a protein.

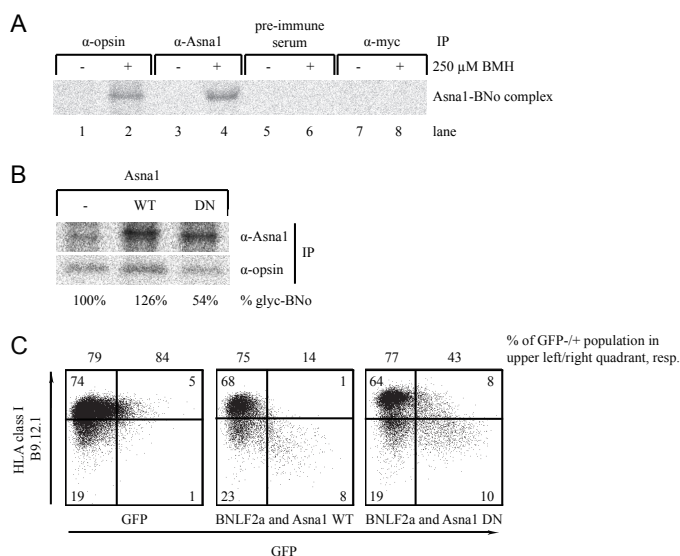


Figure 5. Asn1 is involved in the membrane insertion and functionality of BNLF2a

A, *In vitro* translation reactions were performed in the presence of [³⁵S]methionine/cysteine using mRNA encoding BNo. After cross-linking with 250 μM BMH, the reactions were subjected to immunoprecipitations under denaturing conditions using Abs specific for the opsin-tag (mAb R2-15) and Asn1 (anti-Asn1 rabbit serum), preimmune rabbit serum, and the control anti-c-Myc Ab (mAb 9E10). Immune complexes were separated by SDS-PAGE and visualized by phosphorimaging. B, HeLa cells were transiently transfected to express BNo and to coexpress the empty vector as a control, Asn1-myc wild-type (Asn1 WT), or the dominant negative Asn1-myc SW1 mutant (Asn1 DN) in a ratio of 3:1. After 42 h, cells were pulsed with [³⁵S]methionine/cysteine for 15 min. Postnuclear lysates were subjected to immunoprecipitations using Abs specific for Asn1 (anti-Asn1 rabbit serum) and the opsin-tag added to the C terminus of BNLF2a (mAb R2-15). Immune complexes were separated by SDS-PAGE and visualized by phosphorimaging. The amount of glycosylated BNo protein was quantified and compared with the amount of glycosylated BNo protein in empty vector-transfected control cells (set at 100%). C, MJS cells were transiently transfected to express BNLF2a and to coexpress either Asn1 wild-type (Asn1 WT) or the dominant negative Asn1 SW1 mutant (Asn1 DN) in a ratio of 1:3. The BNLF2a-expression vector contains an IRES immediately downstream of the BNLF2a gene to allow coexpression of the viral protein and GFP. As a control, cells were transfected to express GFP. After 48 h, cells were stained for cell surface expression of HLA class I (mAb B9.12.1) and analyzed by flow cytometry.

Asn1 facilitates membrane insertion of BNLF2a

The cellular protein Asn1 is involved in membrane insertion of TA proteins that have a highly hydrophobic tail (44). Because BNLF2a contains an extremely hydrophobic C terminus [predicted $\Delta G = -3.249$ (45)], we investigated whether this viral protein requires Asn1 for membrane insertion. To examine the interaction of Asn1 with BNLF2a, radioactively labeled BNo was synthesized *in vitro* and subsequently incubated with the cross-linker BMH. Proteins and cross-linked protein products were immunoprecipitated using Abs specific for the C-terminal opsin-tag and Asn1. In the presence of BMH, a band was observed at the position corresponding to the size of a BNo-Asn1 heterodimer, which was absent from the control samples incubated without cross-linker (Fig. 5A, lanes 2 and 4, 1 and 3, respectively). This band was also not detected when preimmune serum or a control anti-c-Myc Ab was used for precipitation (Fig. 5A, lanes 6 and 8), demonstrating specificity of the association between BNLF2a and Asn1. The results of these experiments

are comparable to those performed with Ro (Ref. 27 and data not shown). Thus, we conclude that the viral TAP inhibitor BNLF2a interacts with Asn1.

Next, living cells were used to investigate functional involvement of Asn1 in membrane insertion of BNLF2a using a dominant-negative (DN) mutant of Asn1 (SW1). This protein has the aspartic acid residue at position 74, located in the nucleotide binding site, replaced by an alanine residue (29). Cells were transiently transfected with BNo and no, wild-type, or DN Asn1. Western blot analysis of cell lysates confirmed similar transfection efficiencies in cells expressing wild-type or DN Asn1 (Supplemental Fig. 2). After pulse-labeling of the cells, Asn1 and BNo were precipitated using Abs against Asn1 and against the opsin-tag, respectively. Although some endogenous Asn1 was present in the cells, there was clear overexpression of the transfected Asn1 proteins (Fig. 5B). Upon expression of wild-type Asn1, an increase in the amount of glycosylated BNo was observed. In contrast, the amount of glycosylated BNo was decreased in cells expressing the DN form

of Asn1 (Fig. 5B). These data demonstrate that membrane insertion of BNL2a is aided by Asn1.

Finally, we investigated whether Asn1 contributes to the function of BNL2a as a TAP inhibitor. To this end, MJS cells were transiently transfected to express either wild-type or DN Asn1 in combination with BNL2a, the latter using a BNL2a-IRES-GFP vector, resulting in simultaneous expression of the viral protein and GFP. After 48 h, cell surface expression of HLA class I molecules was determined by flow cytometry. For GFP-expressing control cells, no alterations in HLA class I cell surface expression were observed as compared with untransfected, GFP-negative cells (Fig. 5C, left panel). Coexpression of BNL2a and wild-type Asn1 resulted in specific downregulation of cell surface HLA class I expression that correlated with GFP expression (Fig. 5C, middle panel, Supplemental Fig. 3). This BNL2a-mediated HLA class I downregulation was partially reversed upon coexpression of DN Asn1 (Fig. 5C, right panel). Quantification of these data revealed that high HLA class I levels were observed for only 14% of the GFP-positive BNL2a-expressing cells that coexpressed wild-type Asn1; of the GFP-positive BNL2a-expressing cells that coexpressed DN Asn1, 43% of the cells had high HLA class I levels. In the corresponding GFP-negative control cells, 75 and 77% of the cells had high HLA class I levels (Fig. 5C). These results demonstrate that expression of a DN mutant of Asn1 hampers BNL2a-mediated HLA class I downregulation. In contrast, the function of another viral TAP inhibitor, the type I membrane protein BHV-1 UL49.5, is unaffected by expression of DN Asn1 (Supplemental Fig. 3).

Taken together, these results show that membrane insertion of BNL2a is facilitated by Asn1 and that the ability of the EBV TAP inhibitor BNL2a to downregulate HLA class I at the cell surface is diminished in the absence of functional Asn1.

The tail anchor of BNL2a mediates ER retention

To dissect the functions of the hydrophilic and hydrophobic domains of BNL2a, mutants of the viral protein were generated. First, an attempt was made to express deletion mutants of BNL2a encompassing either the hydrophilic domain or the hydrophobic tail anchor. However, these mutant proteins were unstable (Supplemental Fig. 4). Therefore, chimeric constructs were generated containing either the N-terminal hydrophilic domain of BNL2a fused to the C-terminal hydrophobic tail anchor domain of RAMP4 (BN-Ro) or vice versa (R-BNo) (Fig. 6A). MJS cells were transduced to stably express BNo, the BNL2a chimeras, or GFP as a negative control. Cell lysates were analyzed by Western blotting to ensure proper expression of the constructs. Visualization using a BNL2a-specific Ab revealed multiple bands for BNo and BN-Ro, representing glycosylated and nonglycosylated proteins (Fig. 6B, middle panel).

R-BNo could only be detected using the opsin-specific Ab because this protein lacks the N-terminal BNL2a epitope recognized by the BNL2a-specific Ab (Fig. 6B, lane 4, lower panel). Both BN-Ro and R-BNo proteins appeared to be expressed at higher levels than BNo (Fig. 6B, lanes 3, 4, and 2, respectively). Interestingly, in addition to the two bands representing nonglycosylated and glycosylated protein, a third, broad, high m.w. band was detected for BN-Ro using both BNL2a- and opsin-specific Abs (Fig. 6B, lane 3). This might represent BN-Ro that has passed through the Golgi compartments where the glycans have been modified further to become EndoH-resistant.

To investigate the nature of the protein species observed, cell lysates were treated with EndoH or PNGaseF. Whereas EndoH can only remove immature glycans of ER-resident proteins, PNGaseF can additionally cleave modified, complex glycans of proteins that have traveled to the Golgi and beyond. For BNo, treatment with either EndoH or PNGaseF resulted in reduction of its m.w. to the size of the unglycosylated protein (Fig. 6C, upper left panel, lanes 2 and 3). The same pattern is observed for Ro and R-BNo (Fig. 6C, right panels), showing that BNo, Ro, and R-BNo are all retained in the ER. The situation is different for BN-Ro; the higher m.w. forms are EndoH resistant (Fig. 6C, lower left panel), implying that this pool of the BN-Ro population has left the ER and has traveled to the Golgi compartment.

These findings are supported by immunofluorescence stainings in which paraformaldehyde-fixed, detergent-permeabilized cells were probed with the anti-opsin Ab and an Ab against the ER marker PDI. A typical perinuclear ER-like staining is observed for PDI in all cell lines (Fig. 6D, middle panels). Most of the BNo, Ro, and R-BNo proteins colocalized with PDI (Fig. 6D, right panels). In contrast, a substantial proportion of the BN-Ro pool was present outside the ER compartment (Fig. 6D), indicative of migration to Golgi compartments and beyond.

From this, it can be deduced that the hydrophobic domain of BNL2a not only mediates membrane anchoring but also contributes to both stability and ER retention of the viral TAP inhibitor.

The hydrophilic domain of BNL2a is essential for immune evasion

To examine functionality of the BNL2a chimeras, cells stably expressing BNo or the chimeras were analyzed for HLA class I downregulation by flow cytometry. Whereas GFP-expressing control cells had high levels of HLA class I at their surface, virtually no HLA class I was detected on cells expressing BNo (Fig. 7A, upper left panel). Cells expressing BN-Ro also had a diminished surface expression of HLA class I molecules when compared with GFP-expressing cells, although this downregulation was not as strong as that observed for BNo-expressing cells (Fig. 7A, compare middle left and upper left panels). In contrast,

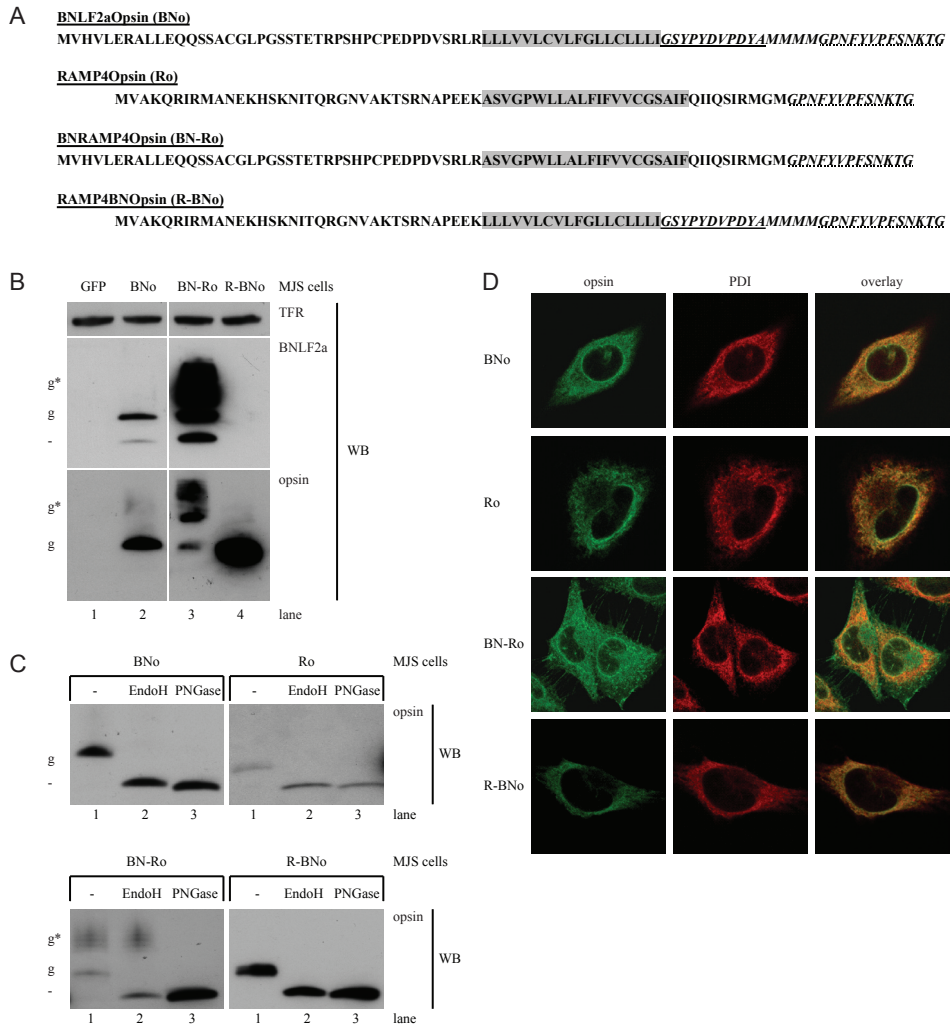


Figure 6. The tail anchor of BNLF2a is involved in ER retention

A, Amino acid sequence of BNo, Ro, and mutants thereof with the hydrophobic C-terminal domains highlighted and the HA4M and opsin-tag shown in italics. The epitope sequences recognized by the monoclonal anti-HA and anti-opsin Abs are underlined using a continuous and striped line, respectively. B, Postnuclear NP-40 lysates of MJS cells stably expressing GFP, BNo, BN-Ro, or R-BNo were separated by SDS-PAGE and analyzed by Western blotting for protein expression using Abs against the control protein TFR (mAb H86.4), the N terminus of BNLF2a (mAb 5B9), and the opsin-tag added to the C terminus of the proteins (mAb R2-15). (-, not glycosylated protein; g, glycosylated protein; g*, protein with modified glycans). C, Postnuclear lysates of MJS cells stably expressing BNo, Ro, BN-Ro, or R-BNo were incubated with EndoH or PNGaseF. Protein samples were separated by SDS-PAGE and analyzed by Western blotting using an Ab specific to the opsin-tag added to the C terminus of the proteins (mAb R2-15). (-, not glycosylated protein; g, glycosylated protein; g*, protein with modified glycans). D, MJS cells stably expressing BNo, Ro, BN-Ro, or R-BNo were analyzed by immunofluorescence. After fixing and permeabilizing the cells, subcellular localization of proteins was visualized by confocal microscopy using a mAb specific to the opsin-tag (R2-15) and anti-PDI rabbit serum. Scale bars, 10 μ m.

R-BNo had virtually no effect on HLA class I surface display. No alteration in HLA class II levels was seen for any of the cell lines (Fig. 7A, right panels). Functionality of the BNLF2a chimeras was further tested using an *in vitro* peptide translocation assay. In GFP-expressing control cells, peptides were efficiently

translocated across the ER membrane. BNo blocked TAP-mediated peptide transport almost completely, whereas BN-Ro had a weaker but still significant effect. No inhibition was seen upon expression of R-BNo (Fig. 7B). These results are in agreement with the extent of (mutant) BNLF2a-mediated HLA class I

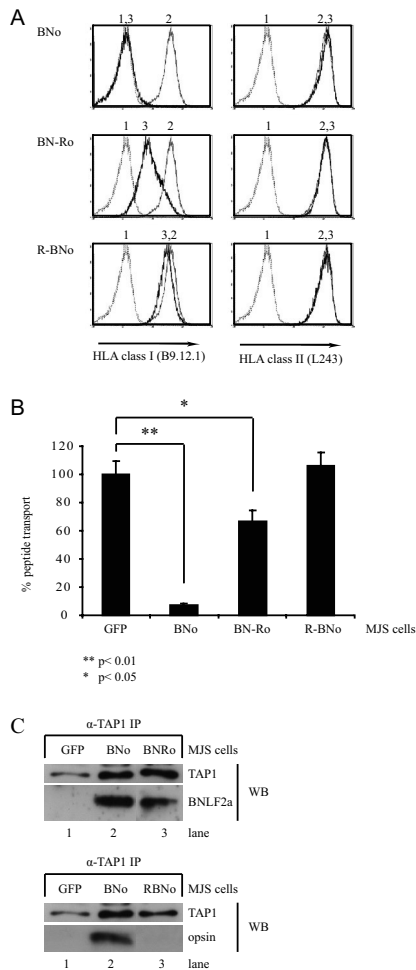


Figure 7. Cytosolic domain of BNLF2a is essential for TAP inhibition

A, MJS cells stably expressing GFP (lane 2) or BNo, BN-Ro, and R-BNo (lane 3) were stained for HLA class I (mAb B9.12.1) or HLA class II (mAb L243) and analyzed by flow cytometry. Lane 1 represents a negative control (secondary Ab only). B, MJS cells stably expressing GFP, BNo, BN-Ro, or R-BNo were analyzed for their ability to transport peptides via TAP. Permeabilized cells were incubated with fluorescent peptides containing an N-linked glycosylation consensus sequence. Con A-Sepharose beads were used to isolate those peptides that were glycosylated and thus transported into the ER. The amount of precipitated fluorescent peptide of GFP-expressing cells was set at 100%. Data are represented as mean \pm SD. **p < 0.01, *p < 0.05 as determined by a t test. C, Digitonin lysates of MJS cells stably expressing GFP, BNo, BN-Ro, or R-BNo were subjected to immunoprecipitations using Abs specific for TAP1 (mAb 148.3). Immune complexes were separated by SDS-PAGE and analyzed by Western blotting for protein expression using Abs specific for TAP1 (mAb 148.3), the N terminus of BNLF2a (mAb 5B9), and the opsin-tag added to the C terminus of the proteins (mAb R2-15).

downregulation observed by flow cytometry.

Interactions between the BNLF2a chimeras and the TAP complex were examined in coimmunoprecipitation experiments. BN-Ro coprecipitated with TAP, as did full-length BNo (Fig. 7C, upper panel, lanes 2 and 3), implying that the N-terminal domain of BNLF2a is sufficient to mediate association with TAP complex. No coprecipitation of R-BNo with TAP was observed (Fig. 7C, lower panel, lane 3), indicating that interactions with TAP do not occur in the absence of the N terminus of BNLF2a.

Taken together, these results indicate that the hydrophilic domain of BNLF2a is capable of binding to the TAP complex and inhibiting TAP function. The tail anchor of BNLF2a mediates insertion into the membrane and retains the viral protein in the ER.

Discussion

In this study, we have identified the EBV-encoded TAP inhibitor BNLF2a as a TA protein. TAP is not required for integration of BNLF2a into membranes. Instead, membrane insertion of BNLF2a is facilitated by Asn1. Accordingly, Asn1 is required for efficient HLA class I downregulation mediated by the viral protein. BNLF2a exerts its function as an immune evasion protein through the combined action of its two subdomains. The hydrophobic C terminus of BNLF2a is inserted into membranes and mediates ER retention, whereas the hydrophilic N-terminal domain of BNLF2a resides in the cytosol and blocks TAP function.

As a characteristic of TA proteins, BNLF2a is inserted into membranes posttranslationally. In the absence of membranes, the viral TAP inhibitor was found to associate with Asn1. This protein is part of a larger complex, the cytosolic transmembrane domain recognition complex, that facilitates insertion of TA proteins into membranes (27, 46). Expression of a DN mutant of Asn1 resulted in reduced insertion of BNLF2a into membranes and impaired BNLF2a-mediated HLA class I downregulation. These results indicate that the cellular Asn1 pathway for TA protein biogenesis has been adopted by EBV to elude the host immune system.

The effect of DN Asn1 appears not absolute: membrane insertion of BNLF2a is partially reduced and reversal of BNLF2a-mediated HLA class I downregulation is also incomplete. Recently, another immune evasion protein, the human herpesvirus 6-encoded protein U24, was found to rely on Asn1 for downregulation of CD3 ϵ and TfR. Also in those cases, no complete reversion of human herpesvirus 6 U24 function was observed for cells expressing DN Asn1 (47). In view of the important role of TA proteins in many cellular processes, it is likely that alternative pathways facilitating membrane insertion of TA proteins exist that may partially compensate for

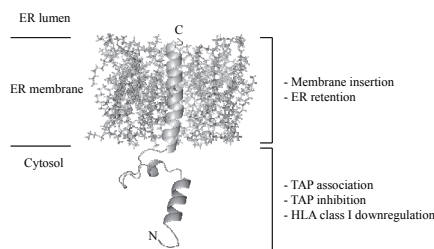


Figure 8. Model of BNLF2a protein structure

Predicted tertiary structure of BNLF2a (ribbon) with the C-terminal helix inserted in a lipid bilayer (sticks) as determined using the I-TASSER server.

Asn1 deficiency.

Using chimeras of the viral TAP inhibitor and another TA protein, RAMP4, dedicated functions could be assigned to different domains of BNLF2a. Although a RAMP4-BNLF2a fusion protein lost all immune evasive properties, the BNLF2a-RAMP4 chimera retained most of its TAP-inhibiting capacity. This indicates that the cytosolic hydrophilic N-terminal domain of BNLF2a is essential for TAP inhibition and HLA class I downregulation. The reduced activity of BNLF2a-RAMP4 compared with wild-type BNLF2a suggests that the tail anchor adds to the efficiency of TAP inhibition. The cytosolic domain and the tail anchor of BNLF2a are both required for stable protein expression. Unexpectedly, although BNLF2a and RAMP4 reside in the ER, the BNLF2a-RAMP4 fusion protein is expressed both at the ER membrane and in post-ER compartments. These findings indicate that the hydrophobic C terminus of BNLF2a plays a role in ER targeting and retention.

Previously, we have shown that the TAP complex is required for stable expression of the BNLF2a protein (22). We now demonstrate that TAP confers protection from proteolysis to the viral protein. This was inferred from experiments in TAP-deficient cells, where the hydrophilic domain of BNLF2a is freely exposed in the cytosol and readily accessible for degradation by the ubiquitin proteasome system and/or other proteases. Further evidence for a role of TAP in BNLF2a's association with or insertion into membranes was not found.

On the basis of these combined results, we propose the following model for the biogenesis and function of BNLF2a. After translation, the EBV-encoded TA protein interacts with Asn1, facilitating insertion of the hydrophobic C terminus of BNLF2a into the ER membrane and leaving the hydrophilic N-terminal domain exposed in the cytosol (Fig. 8). The hydrophobic C-terminal domain is required for retention of BNLF2a in the ER and increases the efficiency of TAP inhibition. The N-terminal domain interacts with the TAP complex. This arrangement ensures effective interference with the binding of both peptide and ATP to TAP, thereby blocking TAP-

mediated peptide transport.

In conclusion, this study reveals how an EBV-encoded protein uses a cellular pathway for TA protein biogenesis to inhibit TAP-mediated peptide transport, allowing the virus to effectively impair HLA class I-restricted Ag presentation and escape from CTL recognition. Homologs of EBV-encoded BNLF2a have been found in several related lymphocryptoviruses occurring in Old World primates. These BNLF2a proteins all impair HLA class I-restricted Ag presentation, most likely through a similar strategy as described for EBV BNLF2a in the current study. These findings highlight the importance of CTL immunity in protection against lymphocryptoviruses and illustrate how millions of years of coevolution have resulted in an excellent adaptation of EBV and related lymphocryptoviruses to their respective host species.

Materials and Methods

Abs

The following mouse mAbs have been used in this study: W6/32 (18) and B9.12.1 (19) (provided by A. Mulder, Leiden University Medical Center, Leiden, The Netherlands), which both recognize β 2-microglobulin-associated HLA class I molecules; 148.3, directed against TAP1 (provided by R. Tampé, Johann Wolfgang Goethe University, Frankfurt/Main, Germany); 435.4, directed against TAP2 (provided by P. van Ender, Hospital Necker, Paris, France); 12CA5, detecting an influenza virus hemagglutinin (HA) epitope that is used as a protein tag (Roche Diagnostics); H68.4, recognizing transferrin receptor (TfR; Roche Diagnostics); AF8 (20), recognizing calnexin (provided by M. Brenner, Harvard Medical School, Boston, MA); R2-15, recognizing a rhodopsin-derived epitope that is used as a protein tag (21); 9E10, recognizing a c-Myc-derived epitope that is used as a protein tag (Developmental Studies Hybridoma Bank, Iowa University); DM1A, recognizing tubulin (Sigma-Aldrich); and L243, recognizing HLA-DR (American Type Culture Collection). BNLF2a was detected using the rat mAbs 5B9 and 8E2 (22). The rat mAb 7F6 was used for detection of tapasin (Ref. 23; provided by R. Tampé). Specific rabbit sera were used to detect protein disulfide isomerase (PDI; provided by I. Majoul, Royal Holloway University of London, Egham, U.K.) and GFP (Santa Cruz Biotechnology and Ref. 24). Anti-Asn1 Abs were raised against four OVA-conjugated synthetic peptides (EAEEFEDAPDVEPL, FDQKFSKVPTKVKGYD, VSEQFKDPEQTT, and LEPYKPPSAQ) in rabbits (Peptide Specialty Laboratories, Heidelberg, Germany).

Constructs

The gene encoding BNLF2a with a C-terminal HA-tag and four methionines (BNLF2aHA4M/BNLF2a) was cloned into the pLZRS retroviral vector as described

previously (17). This pLZRS vector contains an internal ribosomal entry site (IRES) immediately downstream of the inserted gene-of-interest to allow coexpression of a marker gene, in this case, truncated nerve growth factor receptor. The *BNLF2aHA4M* and *bovine herpesvirus-1 UL49.5* genes were cloned into a pLV lentiviral vector (pLV-CMV-IRES-eGFP) (25). This vector contains an IRES downstream of the inserted gene-of-interest and *eGFP* (provided by R.C. Hoeben, Department of Molecular Cell Biology, Leiden University Medical Center).

The BNLf2a-philic and BNLf2a-phobic mutants were constructed using a BNLf2aHA4M-encoding plasmid as template for PCR. The following primers were used: 5'-ACG GCT GCA GAC CAT GGT ACA CGT CCT GGA GC-3' (sBNLF2a-philic), 5'-TAC CGC TCG AGT TAT CTT AGT CTG CTG ACG TCT G-3' (asBNLF2a-philic), 5'-ACG GCT GCA GAC CAT GCT ACT CCT GGT GGT ACT CTG-3' (sBNLF2a-phobic), and 5'-AGA TCT CGA GTT ACA TCA TCA TCA TG-3' (asBNLF2a-phobic). The resulting products were cloned into the pLV-IRES-eGFP vector.

BNLF2aOpsin (BNo) was constructed using a BNLf2aHA4M-encoding plasmid as a template for PCR. The following primers were used: sBNLF2a-philic and 5'-AGA TTC TAG ATT AGC CCG TCT TGT TGG AGA AAG GCA CGT AGA AGT TTG GGC CCA TCA TCA TCA TGG CAT AGT C-3' (asHA4MOpsin). The resulting product was cloned into the pcDNA3-IRES-nlsGFP (26) (provided by E. Reits, Academic Medical Center, Amsterdam, The Netherlands) and pLV-IRES-eGFP vectors.

The gene encoding RAMP4Opsin (Ro) was cloned into the pcDNA3-IRES-nlsGFP and pLV-IRES-eGFP vectors. The pGEM4Z-R4/glyc 3'-UTR plasmid (27) was used as a template for PCR. The following primers were used: 5'-ACG GCT GCA GAC CAT GGT CGC CAA GCA G-3' (sRAMP4) and 5'-AGA TTC TAG ATC AGC CCG TCT TGT TGG AG-3' (asOpsin).

BNLF2aRAMP4Opsin (BN-Ro) was constructed using a BNLf2aHA4M-encoding and Ro-encoded plasmid as a template for the generation of the hydrophilic domain of BNLf2a and the hydrophobic domain of Ro, respectively. The following primers were used: sBNLF2a-philic, 5'-AGA TCT CGA GAC GTC TGG GTC CTC GGG-3' (asBNLF2a-philic fusion), 5'-AGA TCT CGA GAC TAA GAG CGT CGG TAG GAC CCT GG-3' (sBNRAMP4), and asOpsin. Both PCR products were cloned into the pLV-IRES-eGFP vector; the hydrophilic domain of BNLf2a was cloned upstream of the hydrophobic domain of Ro.

RAMP4BNLF2aOpsin (R-BNo) was constructed using a BNo-encoding plasmid as a template for PCR. To generate the hydrophobic domain of BNo, the following primers were used: 5'-AGA TCT CGA GAA ATG CCC CCG AAG AAA AGC TAC TCC TGG TGG TAC TCT G-3' (sRAMP4BN) and asOpsin. The

obtained PCR product was cloned into the pLV-Ro-IRES-eGFP vector, thereby replacing the hydrophobic part of Ro with the hydrophobic part of BNo.

The construction of pcDNA3-HLA-A2.1 has been described by Kikkert *et al.* (28). The coding sequence for human Asn1 was amplified by PCR from pcDNA3-hAsn1 (a gift from B. Schwappach, Faculty of Life Sciences, University of Manchester, Manchester, U.K.) with the following primers: 5'-GAA TTC TCC ACC ATG GCG GCA GGG GTG-3' (Asn1-F) and 5'-CTA CTA CAA GTC CTC TTC AGA AAT GAG CTT TTG CTC CTG GGC ACT GGG GGG CTT G-3' (Asn1myc-R). The PCR product was cloned into the pcDNA3.1/V5-His-TOPO vector (Invitrogen), according to the manufacturer's instructions, giving the final plasmid pcDNA3.1-Asn1myc. Generation of the D74A mutant of Asn1 (SW1) has been described previously (29). The empty pcDNA3 vector was used as a negative control.

Cell lines

Mel JuSo (MJS) is a human melanoma cell line (30). T2 cells (31) are TAP-deficient EBV-transformed B lymphoblastoid cells. Reconstituted T2 cells stably expressing TAP1 and TAP2 (T2 TAP1/2) were obtained from P. Lehner (Cambridge Institute for Medical Research, Cambridge, U.K.) (32). HEK 293T cells were used for the production of replication-deficient retro- and lentiviruses. HeLa is a human cervical cancer cell line (ATCC CCL-2).

MJS, T2, and T2 TAP1/2 cells were maintained in complete culture medium consisting of RPMI 1640 (Invitrogen) supplemented with 10% FCS (PAA Laboratories), 2 mM glutamine, 100 U/ml penicillin, and 100 µg/ml streptomycin. The HEK 293T cells were maintained in complete culture medium consisting of DMEM (Invitrogen) supplemented with 10% FCS (Life Technologies), 2 mM glutamine, 100 U/ml penicillin, and 100 µg/ml streptomycin. HeLa cells were grown in DMEM containing 4.5 g/liter glucose, 10% FCS, and 2 mM L-glutamine.

The generation of the retrovirally transduced MJS/BNLF2a cell line has been described previously (17). MJS cells were lentivirally transduced to express eGFP, BNLf2a, BNo, Ro, BN-Ro, or R-BNo, thereby generating the following cell lines: MJS/GFP, MJS/BN, MJS/BNo, MJS/Ro, MJS/BN-Ro, and MJS/R-BNo, respectively. All lentivirus-transduced cells (co)express eGFP as a marker. The generation of the retrovirus-transduced cell lines T2/GFP, T2/BNLF2a, T2 TAP1/2/GFP, and T2 TAP1/2/BNLF2a has been described previously (22).

Production of and transduction with replication-deficient retro- and lentiviruses

pLZRS retroviral vectors were transfected into the Phoenix A packaging cell line to produce replication-deficient recombinant retroviruses, as described previously (17). For the production of replication-

deficient recombinant lentiviruses, HEK 293T cells were transfected with a pLV-CMV-IRES-eGFP lentiviral vector encoding the gene-of-interest, in addition to pCMV-VSVG, pMDLg-RRE, and pRSV-REV (provided by R. C. Hoeben) using calcium phosphate precipitation, as described previously (33). After 48 and 72 h, lentivirus-containing culture supernatants were collected and passaged through a 0.45- μ m filter.

Retroviral transductions were performed essentially as described previously (17). In brief, cells were infected with retroviruses and FACS sorted to achieve reporter expression in all cells. Lentiviral transductions were performed according to the same protocol used for retroviral transductions.

Transient transfection of MJS cells

Cells were transiently transfected using the Amaxa Nucleofector II, according to the manufacturers' instructions. For the transfection of MJS cells, program T-020 and solution L were used.

Immunofluorescence

MJS cells were grown overnight on coverslips and fixed in 4% paraformaldehyde for 30 min at 37°C. After permeabilization with 0.1% Triton X-100 for 5 min, cells were stained with primary Abs for 60 min. Subsequently, cells were stained with fluorescently labeled secondary Abs (Jackson ImmunoResearch Laboratories) for 30 min and embedded on microscope slides with Mowiol (Sigma-Aldrich). All incubation steps were performed at room temperature unless stated otherwise. Cells were visualized with a confocal microscope (Leica TCS SP2).

Immunoprecipitation and Western blot analysis

Immunoprecipitation experiments, SDS-PAGE, and immunoblotting were performed as described previously (22). Cells were lysed using either 0.5% Nonidet P-40 (NP-40) buffer or 1% digitonin buffer and subsequently centrifuged to obtain postnuclear lysates. For transiently transfected cells, total cell lysates were made by boiling the cells in sample buffer [0.05 M Tris (pH 8), 2% SDS, 10% glycerol, 5% 2-ME, and 0.025% bromophenol blue].

For coimmunoprecipitation experiments, 1% digitonin cell lysates were incubated with specific Abs and protein A- and protein G-Sepharose beads (GE Healthcare) at 4°C for at least 2 h.

For Western blot analysis, immune complexes or cell lysates were denatured in sample buffer, separated by SDS-PAGE, and transferred to polyvinylidene difluoride membranes (GE Healthcare). Proteins of interest were detected by incubating the membranes with specific Abs, followed by HRP-conjugated secondary Abs (Jackson ImmunoResearch Laboratories or DakoCytomation). Ab binding was visualized using ECL plus (GE Healthcare).

Endoglycosidase H and peptide-N-glycosidase F digestion

Postnuclear NP-40 lysates were denatured in sample buffer and treated with Endoglycosidase H₁ (EndoH; New England Biolabs) or peptide-N-glycosidase F (PNGaseF; Roche), according to the instructions of the manufacturer.

Proteinase K digestion

Cells were either lysed in radioimmunoprecipitation assay (RIPA) buffer (1% NP-40, 0.5% sodium deoxycholate, and 0.1% SDS in PBS) for 45 min and subsequently centrifuged at 16,000 \times g at 4°C for 20 min to obtain postnuclear lysates or resuspended in permeabilization buffer [0.04% digitonin, 25 mM HEPES (pH 7.2), 115 mM potassium acetate, 5 mM sodium acetate, 2.5 mM MgCl₂, and 0.5 mM EGTA] for protein digestions. Samples were incubated with proteinase K at 4°C for 20 min, followed by the addition of 2 mM PMSF to stop proteolysis. The postnuclear RIPA samples were denatured in sample buffer. The digitonin-permeabilized cells were first pelleted at 16,000 \times g at 4°C for 10 min and subsequently denatured in sample buffer.

Peptide transport assay

Peptide transport assays were performed as described previously (22). In brief, 2 \times 10⁶ cells were permeabilized with 2 IU/ml Streptolysin O (Murex Diagnostics) at 37°C for 10 min and subsequently incubated with 4.5 μ M of the fluoresceinated peptide CVNKTERAY (provided by W. Benckhuijsen and J. W. Drijfhout, Leiden University Medical Center) in the presence of 10 mM ATP or 0.125 M EDTA at 37°C for 10 min. Peptide transport was blocked by the addition of 1 ml cold lysis buffer [1% Triton X-100, 500 mM NaCl, 2 mM MgCl₂, and 50 mM Tris HCl (pH 8)]. Glycosylated peptides were isolated from postnuclear lysates by incubation with Con A-Sepharose beads (GE Healthcare) at 4°C for 2 h. After washing of the beads, glycosylated peptides were eluted from the beads with elution buffer [500 mM mannopyranoside, 10 mM EDTA, and 50 mM Tris HCl (pH 8)] at room temperature during a 1-h incubation step. Fluorescence was measured using a Mithras LB 940 multilabel reader (Berthold Technologies). Values obtained for the samples incubated in the presence of ATP were corrected for the background values obtained in the absence of ATP.

Flow cytometry

Surface levels of HLA class I and HLA class II were analyzed by flow cytometry. Cells were stained with specific primary Abs, washed, and stained with secondary goat anti-mouse PE Abs (Jackson ImmunoResearch Laboratories) or goat anti-mouse allophycocyanin Abs (Leinco Technologies) at 4°C. Cells were analyzed on a FACSCalibur flow cytometer using CellQuest Pro software (BD Biosciences).

Subcellular fractionation

Fractionation of cells was performed essentially as described previously (34). A total of 10^7 cells were washed and resuspended in 1 ml homogenization buffer [0.25 M sucrose, 10 mM triethanolamine, 10 mM potassiumacetate, and 1 mM EDTA (pH 7.6)]. Cells were homogenized on ice using a Dounce homogenizer with a tight fitting pestle (100–110 strokes). The homogenate was spun at $1000 \times g$ at $4^\circ C$ for 10 min. The $1,000 \times g$ pellet was stored on ice, and the supernatant was subsequently centrifuged at $10,000 \times g$ at $4^\circ C$ for 30 min. The $10,000 \times g$ pellet was also stored on ice, and the supernatant was now centrifuged at $100,000 \times g$ at $4^\circ C$ for 60 min using a TLA 120.2 fixed-angle rotor and a Beckman Optima TLX ultracentrifuge. The $100,000 \times g$ supernatant was collected, and all pellets ($1,000 \times g$, $10,000 \times g$, and $100,000 \times g$) were resuspended in 0.5% NP-40 buffer. After incubation at $4^\circ C$ for 30 min, lysates were centrifuged at $16,000 \times g$ at $4^\circ C$ for 15 min. Sample buffer was added to all four supernatants, and the samples were incubated at $95^\circ C$ for 5 min. Protein expression was analyzed by Western blotting.

RT-PCR

RNA was isolated from transiently transfected MJS cells using TRIzol (Invitrogen), according to the instructions of the manufacturer. cDNA was synthesized using Oligo(dT)₂₀ (Invitrogen) and Moloney murine leukemia virus reverse transcriptase (Finnzymes). To verify that no genomic DNA was present, parallel reactions were performed in the absence of reverse transcriptase.

To detect GAPDH, BNLF2a (full-length), BNLF2a-philic, and BNLF2a-phobic cDNA, the following primers were used: 5'-CAT CAC CAT CTT CCA GGA GC-3' (sGAPDH), 5'-GGA TGA TGT TCT GGA GAG CC-3' (asGAPDH), sBNLF2a-philic, asBNLF2a-philic, sBNLF2a-phobic, and asBNLF2a-phobic.

Generation of semipermeabilized cells

Semipermeabilized cells were generated essentially as described by Wilson *et al.* (35). 6×10^6 cells were washed, resuspended in KHM buffer [110 mM KOAc, 20 mM HEPES (pH 7.2), and 2 mM MgOAc] containing 5 $\mu g/ml$ digitonin and incubated on ice for 5 min. Subsequently, cells were washed with KHM buffer, resuspended in HEPES buffer [50 mM HEPES (pH 7.2) and 90 mM KOAc], and incubated on ice for 10 min. After centrifugation, cells were resuspended in KHM buffer and incubated with 1 mM CaCl₂ and micrococcal nuclease for 12 min at room temperature to remove endogenous mRNA. The nuclease was inhibited by the addition of 4 mM EGTA, and after centrifugation, cells were resuspended in KHM buffer and stored at $-80^\circ C$.

In vitro transcription and translation

pcDNA3(-IRES-nlsGFP)-derived vectors were linearized and used for *in vitro* transcription with T7 polymerase (Invitrogen). Transcripts were translated at $30^\circ C$ for 90 min in the presence of [³⁵S]methionine/cysteine (EasyTag EXPRESS³⁵S protein labeling mix; PerkinElmer) in rabbit reticulocyte lysate (Promega). To examine membrane insertion, canine pancreatic microsomal membranes (Promega) were added either at the start of translation or after termination of translation by the addition of 1 mM cycloheximide. Alternatively, semipermeabilized cells were added after termination of translation by cycloheximide. These posttranslation membrane insertion reactions were incubated at $30^\circ C$ for 30 min. Microsomal membranes or semipermeabilized cells were separated from the supernatant by centrifugation and denatured in sample buffer. Samples were separated by SDS-PAGE and visualized by phosphorimaging. Densitometric analysis was done with Quantity One.

Chemical cross-linking with bis(maleimido)hexane

Chemical cross-linking experiments were performed essentially as described previously (27). *In vitro* transcription and translation reactions were performed in the absence of microsomal membranes as described above. After translation, samples were filtered using micro bio-spin P-6 columns [Bio-Rad; equilibrated in 20 mM HEPES-KOH (pH 7.5), 80 mM KOAc, and 0.5 mM Mg(OAc)₂] and subsequently cross-linked with 250 μM bis(maleimido)hexane (BMH) (Pierce Biotechnology) at room temperature for 20 min. Reactions were quenched by the addition of 10 mM DTT and incubation on ice for 5 min and subsequently denatured in the presence of 1% SDS by incubation at $65^\circ C$ for 5 min. After addition of nondenaturing buffer [1% Triton X-100, 50 mM Tris (pH 7.4), 300 mM NaCl, 5 mM EDTA, 0.02% sodiumazide, 10 μM leupeptin, and 1 mM 4-(2-aminoethyl) benzenesulfonyl fluoride], samples were subjected to denaturing immunoprecipitations. Isolated immune complexes were washed with NET buffer [50 mM Tris (pH 7.5), 150 mM NaCl, 5 mM EDTA, 0.5% NP-40, and 0.1% SDS] and denatured in sample buffer. Samples were separated by SDS-PAGE and visualized by phosphorimaging.

Metabolic labeling of cells

HeLa cells were transfected using calcium phosphate transfection as described previously (36). After 42 h, cells were depleted of methionine and cysteine for 2 h and subsequently metabolically labeled by addition of 100 $\mu Ci/ml$ [³⁵S]methionine/cysteine (EasyTag EXPRESS³⁵S protein labeling mix (PerkinElmer) for 15 min. Cells were lysed using 1% Triton X-100 buffer [50 mM HEPES (pH 7.5), 150 mM NaCl, 1.5 mM MgCl₂, 10% glycerol, 1% Triton X-100, 1 mM EGTA, 1 mM PMSF, and protease inhibitor mixture complete EDTA free (Roche)] on ice for 10 min.

Nonsoluble material was pelleted by centrifugation at $16,000 \times g$ at 4°C for 10 min. The lysates were diluted with immunoprecipitation buffer [20 mM HEPES (pH 7.5), 150 mM NaCl, 10% glycerol, and 0.1% Triton X-100] and incubated with specific Abs and protein A-Sepharose beads (Amersham Biosciences) for 3 h. Isolated immune complexes were washed five times with immunoprecipitation buffer. Immune complexes were denatured in sample buffer, separated by SDS-PAGE and visualized by phosphorimaging. Densitometric analysis was done with ImageJ.

Tertiary structure model of BNLF2a

BNLF2a three-dimensional structural predictions were made using the I-TASSER server with National Center for Biotechnology Information Reference Sequence: YP_401721.1 without assigning additional restraints (37). The first model predicted by I-TASSER was used as input for the CHARMM-GUI Membrane Builder (38) using the following options: Orientation, Align the First Principle Axis Along Z; System Building Options, Replacement method; and other settings as default. The ribbon presentation was generated using the Pymol program.

Acknowledgments

We thank Rob Hoeben, Martijn Rabelink, Maikel Wouters, Jan-Wouter Drijfhout, Willemien Benckhuijsen (Leiden University Medical Center), Hidde Ploegh (Whitehead Institute, Cambridge, MA), Nathan Croft (University of Birmingham), Paul Lehner (Cambridge Institute for Medical Research), and Robert Tampé (Biocenter, Goethe University) for helpful discussions and for generously sharing reagents and constructs.

This work was supported by Dutch Cancer Foundation Grant RUL 2005-3259 (to D.H., M.E.R., and E.J.H.J.W.), the Royal Dutch Academy of Sciences Beijerinck Premium 2005 (to M.E.R.), Netherlands Scientific Organization Grant NWO Vidi 917.76.330 (to M.E.R.), Deutsche Forschungsgemeinschaft Grant SFB638-A2 (to B.D.), and the Biotechnology and Biological Sciences Research Council, United Kingdom (to C.R. and S.H.).

The authors have no financial conflicts of interest.

References

- Rickinson, A. B., and E. Kieff. 2001. Epstein-Barr Virus. In *Field's virology*, Vol. 2. D. M. Knipe and P. M. Howley, eds. Lippincott Williams & Wilkins, Philadelphia, pp. 2575.
- Kieff, E., and A. B. Rickinson. 2007. Epstein-Barr Virus and Its Replication. In *Field's virology*, Vol. 2. D. M. Knipe and P. M. Howley, eds. Lippincott Williams & Wilkins, a Wolters Kluwer Business, Philadelphia, pp. 2603.
- Ressing, M. E., D. Horst, B. D. Griffin, J. Tellam, J. Zuo, R. Khanna, M. Rowe, and E. J. Wiertz. 2008. Epstein-Barr virus evasion of CD8(+) and CD4(+) T cell immunity via concerted actions of multiple gene products. *Semin. Cancer Biol.* 18:397.
- Gottschalk, S., H. E. Heslop, and C. M. Roon. 2002. Treatment of Epstein-Barr virus-associated malignancies with specific T cells. *Adv. Cancer Res.* 84:175.
- Cresswell, P. 2000. Intracellular surveillance: controlling the assembly of MHC class I-peptide complexes. *Traffic.* 1:301.
- Wearsch, P. A., and P. Cresswell. 2008. The quality control of MHC class I peptide loading. *Curr. Opin. Cell Biol.* 20:624.
- Scholz, C., and R. Tampe. 2009. The peptide-loading complex--antigen translocation and MHC class I loading. *Biol. Chem.* 390:783.
- Fruh, K., K. Ahn, H. Djaballah, P. Sempe, P. M. van Endert, R. Tampe, P. A. Peterson, and Y. Yang. 1995. A viral inhibitor of peptide transporters for antigen presentation. *Nature* 375:415.
- Hill, A., P. Jugovic, I. York, G. Russ, J. Bennink, J. Yewdell, H. Ploegh, and D. Johnson. 1995. Herpes simplex virus turns off the TAP to evade host immunity. *Nature* 375:411.
- York, I. A., C. Roop, D. W. Andrews, S. R. Riddell, F. L. Graham, and D. C. Johnson. 1994. A cytosolic herpes simplex virus protein inhibits antigen presentation to CD8⁺ T lymphocytes. *Cell* 77:525.
- Ahn, K., A. Gruhler, B. Galocha, T. R. Jones, E. J. Wiertz, H. L. Ploegh, P. A. Peterson, Y. Yang, and K. Fruh. 1997. The ER-luminal domain of the HCMV glycoprotein US6 inhibits peptide translocation by TAP. *Immunity* 6:613.
- Hengel, H., J. O. Koopmann, T. Flohr, W. Muranyi, E. Goulmy, G. J. Hammerling, U. H. Koszinowski, and F. Momburg. 1997. A viral ER-resident glycoprotein inactivates the MHC-encoded peptide transporter. *Immunity* 6:623.
- Lehner, P. J., J. T. Karttunen, G. W. Wilkinson, and P. Cresswell. 1997. The human cytomegalovirus US6 glycoprotein inhibits transporter associated with antigen processing-dependent peptide translocation. *Proc Natl Acad Sci USA* 94:6904.
- Koppers-Lalic, D., E. A. Reits, M. E. Ressing, A. D. Lipinska, R. Abele, J. Koch, R. M. Marcondes, P. Admiraal, D. van Leeuwen, K. Bienkowska-Szewczyk, T. C. Mettenleiter, F. A. Rijsewijk, R. Tampe, J. Neeffjes, and E. J. Wiertz. 2005. Varicelloviruses avoid T cell recognition by UL49.5-mediated inactivation of the transporter associated with antigen processing. *Proc. Natl. Acad. Sci. U. S. A* 102:5144.
- Alzhanova, D., D. M. Edwards, E. Hammarlund,

- I. G. Scholz, D. Horst, M. J. Wagner, C. Upton, E. J. Wiertz, M. K. Slifka, and K. Fruh. 2009. Cowpox virus inhibits the transporter associated with antigen processing to evade T cell recognition. *Cell Host. Microbe* 6:433.
16. Byun, M., M. C. Verweij, D. J. Pickup, E. J. Wiertz, T. H. Hansen, and W. M. Yokoyama. 2009. Two mechanistically distinct immune evasion proteins of cowpox virus combine to avoid antiviral CD8 T cells. *Cell Host. Microbe* 6:422.
 17. Hislop, A. D., M. E. Rensing, D. van Leeuwen, V. A. Pudney, D. Horst, D. Koppers-Lalic, N. P. Croft, J. J. Neefjes, A. B. Rickinson, and E. J. Wiertz. 2007. A CD8⁺ T cell immune evasion protein specific to Epstein-Barr virus and its close relatives in Old World primates. *J. Exp. Med.* 204:1863.
 18. Barnstable, C. J., W. F. Bodmer, G. Brown, G. Galfre, C. Milstein, A. F. Williams, and A. Ziegler. 1978. Production of monoclonal antibodies to group A erythrocytes, HLA and other human cell surface antigens—new tools for genetic analysis. *Cell* 14:9.
 19. Malissen, B., N. Rebai, A. Liabeuf, and C. Mawas. 1982. Human cytotoxic T cell structures associated with expression of cytolysis. I. Analysis at the clonal cell level of the cytolysis-inhibiting effect of 7 monoclonal antibodies. *Eur. J. Immunol.* 12:739.
 20. Hochstenbach, F., V. David, S. Watkins, and M. B. Brenner. 1992. Endoplasmic reticulum resident protein of 90 kilodaltons associates with the T- and B-cell antigen receptors and major histocompatibility complex antigens during their assembly. *Proc. Natl. Acad. Sci. U. S. A* 89:4734.
 21. Hargrave, P. A., G. Adamus, A. Arendt, J. H. McDowell, J. Wang, A. Szaby, D. Curtis, and R. W. Jackson. 1986. Rhodopsin's amino terminus is a principal antigenic site. *Exp. Eye Res.* 42:363.
 22. Horst, D., D. van Leeuwen, N. P. Croft, M. A. Garstka, A. D. Hislop, E. Kremmer, A. B. Rickinson, E. J. Wiertz, and M. E. Rensing. 2009. Specific targeting of the EBV lytic phase protein BNLF2a to the transporter associated with antigen processing results in impairment of HLA class I-restricted antigen presentation. *J. Immunol.* 182:2313.
 23. Koch, J., R. Guntrum, and R. Tampe. 2006. The first N-terminal transmembrane helix of each subunit of the antigenic peptide transporter TAP is essential for independent tapasin binding. *FEBS Lett.* 580:4091.
 24. van den Born, E., C. C. Posthuma, K. Knoops, and E. J. Snijder. 2007. An infectious recombinant equine arteritis virus expressing green fluorescent protein from its replicase gene. *J. Gen. Virol.* 88:1196.
 25. Vellinga, J., T. G. Uil, V. J. de, M. J. Rabelink, L. Lindholm, and R. C. Hoeben. 2006. A system for efficient generation of adenovirus protein IX-producing helper cell lines. *J. Gene Med.* 8:147.
 26. van Lith, M., M. van Ham, A. Griekspoor, E. Tjin, D. Verwoerd, J. Calafat, H. Janssen, E. Reits, L. Pastoors, and J. Neefjes. 2001. Regulation of MHC class II antigen presentation by sorting of recycling HLA-DM/DO and class II within the multivesicular body. *J. Immunol.* 167:884.
 27. Favaloro, V., M. Spasic, B. Schwappach, and B. Dobberstein. 2008. Distinct targeting pathways for the membrane insertion of tail-anchored (TA) proteins. *J. Cell Sci.* 121:1832.
 28. Kikkert, M., G. Hassink, M. Barel, C. Hirsch, F. J. van der Wal, and E. Wiertz. 2001. Ubiquitination is essential for human cytomegalovirus US11-mediated dislocation of MHC class I molecules from the endoplasmic reticulum to the cytosol. *Biochem. J.* 358:369.
 29. Favaloro, V., F. Vilardi, R. Schlecht, M. P. Mayer, and B. Dobberstein. 2010. Asna1/TRC40-mediated membrane insertion of tail-anchored proteins. *J. Cell Sci.* 123:1522.
 30. van Ham, S. M., E. P. Tjin, B. F. Lillemeier, U. Gruneberg, K. E. van Meijgaarden, L. Pastoors, D. Verwoerd, A. Tulp, B. Canas, D. Rahman, T. H. Ottenhoff, D. J. Pappin, J. Trowsdale, and J. Neefjes. 1997. HLA-DO is a negative modulator of HLA-DM-mediated MHC class II peptide loading. *Curr. Biol.* 7:950.
 31. Salter, R. D., D. N. Howell, and P. Cresswell. 1985. Genes regulating HLA class I antigen expression in T-B lymphoblast hybrids. *Immunogenetics* 21:235.
 32. Karttunen, J. T., P. J. Lehner, S. S. Gupta, E. W. Hewitt, and P. Cresswell. 2001. Distinct functions and cooperative interaction of the subunits of the transporter associated with antigen processing (TAP). *Proc. Natl. Acad. Sci. U. S. A* 98:7431.
 33. Carlotti, F., M. Bazuine, T. Kekarainen, J. Seppen, P. Pognonec, J. A. Maassen, and R. C. Hoeben. 2004. Lentiviral vectors efficiently transduce quiescent mature 3T3-L1 adipocytes. *Mol. Ther.* 9:209.
 34. Wiertz, E. J., T. R. Jones, L. Sun, M. Bogyo, H. J. Geuze, and H. L. Ploegh. 1996. The human cytomegalovirus US11 gene product dislocates MHC class I heavy chains from the endoplasmic reticulum to the cytosol. *Cell* 84:769.
 35. Wilson, R., A. J. Allen, J. Oliver, J. L. Brookman, S. High, and N. J. Bulleid. 1995. The translocation, folding, assembly and redox-dependent degradation of secretory and membrane proteins in semi-permeabilized mammalian cells. *Biochem. J.* 307 (Pt 3):679.
 36. Chen, C., and H. Okayama. 1987. High-efficiency transformation of mammalian cells by plasmid DNA. *Mol. Cell Biol.* 7:2745.

37. Zhang, Y. 2008. I-TASSER server for protein 3D structure prediction. *BMC. Bioinformatics.* 9:40.
38. Jo, S., T. Kim, and W. Im. 2007. Automated builder and database of protein/membrane complexes for molecular dynamics simulations. *PLoS. One.* 2:e880.
39. Kyte, J., and R. F. Doolittle. 1982. A simple method for displaying the hydropathic character of a protein. *J. Mol. Biol.* 157:105.
40. Borgese, N., S. Colombo, and E. Pedrazzini. 2003. The tale of tail-anchored proteins: coming from the cytosol and looking for a membrane. *J. Cell Biol.* 161:1013.
41. Wattenberg, B., and T. Lithgow. 2001. Targeting of C-terminal (tail)-anchored proteins: understanding how cytoplasmic activities are anchored to intracellular membranes. *Traffic.* 2:66.
42. Rabu, C., and S. High. 2007. Membrane protein chaperones: a new twist in the tail? *Curr. Biol.* 17:R472-R474.
43. Rabu, C., V. Schmid, B. Schwappach, and S. High. 2009. Biogenesis of tail-anchored proteins: the beginning for the end? *J. Cell Sci.* 122:3605.
44. Rabu, C., P. Wipf, J. L. Brodsky, and S. High. 2008. A precursor-specific role for Hsp40/Hsc70 during tail-anchored protein integration at the endoplasmic reticulum. *J. Biol. Chem.* 283:27504.
45. Hessa, T., N. M. Meindl-Beinker, A. Bernsel, H. Kim, Y. Sato, M. Lerch-Bader, I. Nilsson, S. H. White, and H. G. von. 2007. Molecular code for transmembrane-helix recognition by the Sec61 translocon. *Nature* 450:1026.
46. Stefanovic, S., and R. S. Hegde. 2007. Identification of a targeting factor for posttranslational membrane protein insertion into the ER. *Cell* 128:1147.
47. Sullivan, B. M., and L. Coscoy. 2010. The U24 protein from human herpesvirus 6 and 7 affects endocytic recycling. *J. Virol.* 84:1265.

Supplementary data

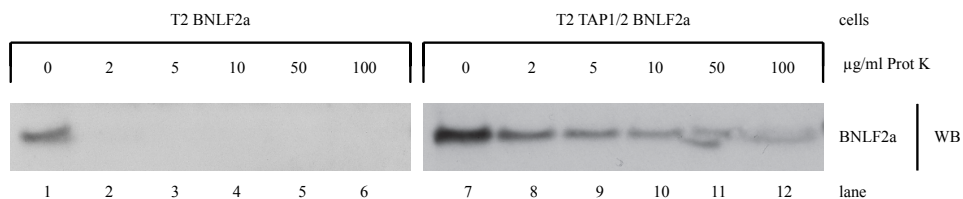


Figure S1. TAP protects BNLf2a from cleavage by proteinase K

T2 cells (lacking TAP) and T2 TAP1/2 cells (reconstituted with TAP1 and TAP2), both stably expressing BNLf2a, were permeabilized with digitonin and incubated with or without proteinase K. Protein samples were separated by SDS-PAGE and analysed by Western blotting for the presence of BNLf2a (mAb 8E2).

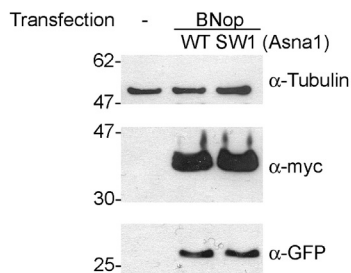


Figure S2. Protein expression levels in transiently transfected HeLa cells

HeLa cells were transiently transfected to express BNo and to co-express either Asna1-myc wild-type (Asna1 WT) or the dominant negative Asna1-myc SW1 mutant (Asna1 SW1) in a ratio of 3:1. Untransfected cells were taken along as a control. After 42 hours, cell lysates were prepared, separated by SDS-PAGE and analysed by Western blotting for protein expression using antibodies against the control protein tubulin (mAb DM1A), the c-Myc tag added to Asna1 (mAb 9E10) and GFP (anti-GFP rabbit serum). GFP is expressed from the same mRNA as BNLf2a using an internal ribosomal entry site (IRES), thereby correlating GFP protein levels with BNLf2a expression.

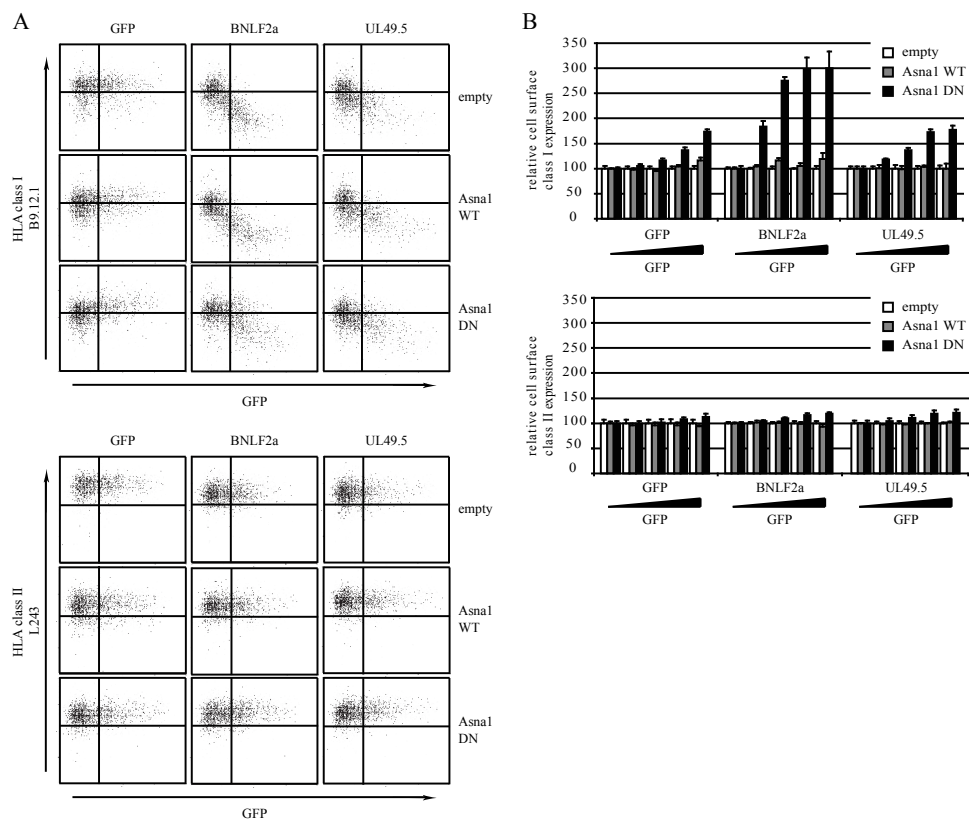


Figure S3. Asn1 is involved in BNLf2a-mediated HLA class I downregulation

A MJS cells were transiently transfected to co-express viral TAP inhibitors and either Asn1-myc wild-type (Asn1 WT) or the dominant negative Asn1-myc SW1 mutant (Asn1 DN) in a ratio of 1:3 to evaluate the effect of the TA protein insertion machinery on HLA class I immune evasion. The TAP inhibitors were: EBV BNLf2a (TA protein) and bovine herpesvirus-1 UL49.5 (type I membrane protein). The empty pcDNA3 vector and GFP were used as controls. After 48 hours, cells were stained for surface expression of HLA class I (mAb B9.12.1) and the control protein HLA class II (mAb L243) and analysed by flow cytometry. These results show that BNLf2a-mediated HLA class I downregulation is dependent on functional Asn1, whereas UL49.5-mediated HLA class I downregulation is unaffected by DN Asn1. B Quantification of A. To allow easier comparison of the data in A, we quantified the mean fluorescence intensities of HLA class I and HLA class II for the range of GFP expression. The latter reflects the expression of the viral TAP inhibitors. Samples were normalized for HLA expression on their GFP negative cells (set at 100%). At the same time, samples were normalized for HLA expression at the surface of the corresponding empty vector control samples (set at 100%). Data are represented as mean \pm SD.

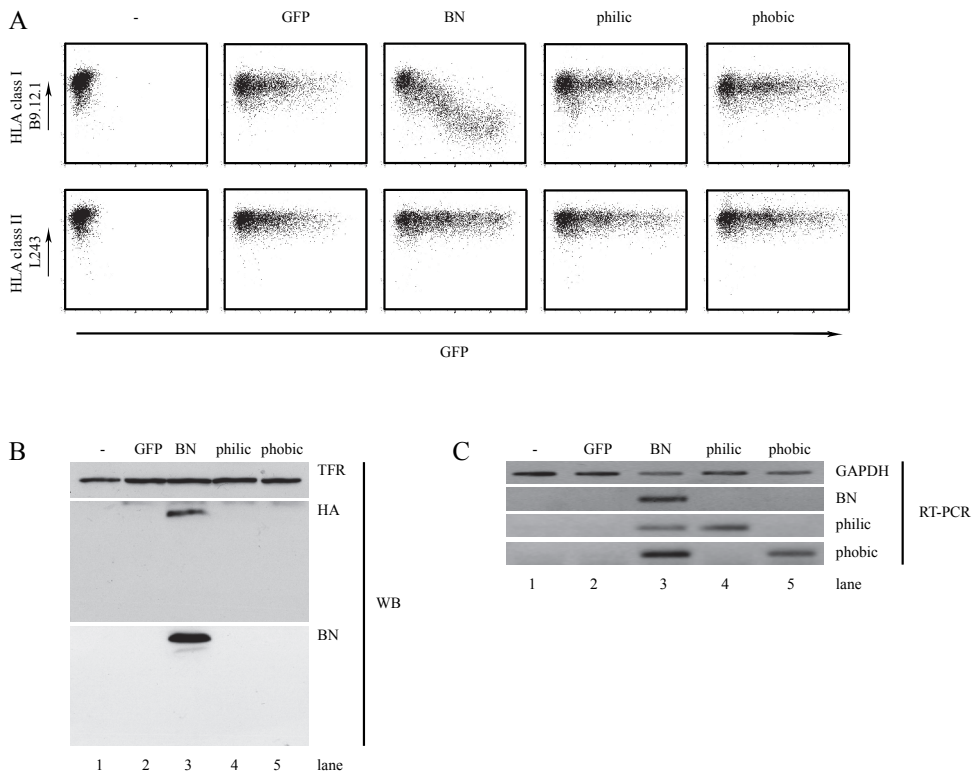


Figure S4. The hydrophilic and hydrophobic domains of BNLF2a are incapable of HLA class I downregulation when expressed individually

A MJS cells were transiently transfected to express GFP, BNLF2a (BN), the N-terminal hydrophilic domain of BNLF2a (philic) or the C-terminal hydrophobic domain of BNLF2a (phobic). After 48 hours, cells were stained for HLA class I (mAb B9.12.1) or HLA class II (mAb L243) and analysed by flow cytometry. Untransfected cells were taken along as a control. B Total protein lysates of the transiently transfected cells (see S2A) were separated by SDS-PAGE and analysed by Western blotting for the expression of transferrin receptor (TfR; mAb H68.4) and BNLF2a (mutants) using the mAbs 5B9, recognizing the N-terminus of BNLF2a, and 12CA5, recognizing the HA-tag added to the C-terminus of full length BNLF2a and the hydrophobic mutant. Untransfected cells were taken along as a control. C RNA of the transiently transfected MJS cells (see S2A) was isolated and used for the synthesis of cDNA. PCR reactions were performed to detect GAPDH as a control and either full length BNLF2a (BN) or the N-terminal hydrophilic (philic) and C-terminal hydrophobic (phobic) domains of BNLF2a. Untransfected cells were taken along as a control.

Chapter 5

Epstein-Barr virus isolates retain their capacity to evade T cell immunity through BNLF2a despite extensive sequence variation

D. Horst*, S.R. Burrows*, D. Gatherer, B. van Wilgenburg, M.J. Bell, I.G.J. Boer, M.E. Rensing** and E.J.H.J. Wiertz**.

Submitted

*** These authors contributed equally to this manuscript

Abstract

The Epstein-Barr virus (EBV)-encoded immune evasion protein BNLF2a inhibits the Transporter associated with Antigen Processing (TAP), thereby downregulating HLA class I expression at the cell surface. As a consequence, recognition of EBV-infected cells by cytotoxic T cells is impaired. Here, we show that sequence polymorphism of the BNLF2a protein is observed in natural EBV isolates, with evidence for positive selection. Despite these mutations, all BNLF2a variants efficiently reduce cell surface HLA class I levels. This conservation of BNLF2a function during evolution of EBV implies an important role of the viral TAP inhibitor in preventing T cell recognition during viral infection.

Name	Sequence	Frequency mutation (%)	Frequency IM
B95.8	MVHVLERALLEQQSSACGLPGSSSTETRP SHPCPEDPDVSRRLRLLLVVLVLCVLFGLLCLLLI	5/22 (22.7%)	2/5
A8T/R40K	MVHVLERTLLEQQSSACGLPGSSSTETRP SHPCPEDPDVSKLRLLLVVLCVLFGLLCLLLI	12/22 (54.5)	7/12
H3Q/A8T/R40K	MVQVLERLLEQQSSACGLPGSSSTETRP SHPCPEDPDVSKLRLLLVVLCVLFGLLCLLLI	2/22 (9.1%)	0/2
A8T/S39R/R40K	MVHVLERTLLEQQSSACGLPGSSSTETRP SHPCPEDPDVRLRLLLVVLVLCVLFGLLCLLLI	1/22 (4.5%)	0/1
A8T/V46A	MVHVLERTLLEQQSSACGLPGSSSTETRP SHPCPEDPDVSRRLRLLLVVLVLCVLFGLLCLLLI	1/22 (4.5%)	0/1
V46A	MVHVLERALLEQQSSACGLPGSSSTETRP SHPCPEDPDVSRRLRLLLVVLVLCVLFGLLCLLLI	1/22 (4.5%)	1/1

Cytosolic domain
Membrane domain

Table 1. BNLF2a protein sequences of EBV isolates (all EBV type 1)

Epstein-Barr virus (EBV) is a γ 1-herpesvirus carried by over 90% of the adult human population worldwide. Whereas primary EBV infection of young children usually occurs unnoticed, primary infection of adolescents results in the development of infectious mononucleosis in at least 25% of the cases (19). In either scenario, primary infection is controlled by EBV-specific immunity. Despite this, the virus persists for life in the infected host. Specific viral immune evasion strategies, eluding both innate and adaptive immunity, are thought to contribute to this (18, 20).

Cytotoxic T lymphocytes (CTLs) play an important role in controlling EBV infection. Virus-infected cells are recognized by CTLs through the detection of virus-derived peptides presented at the cell surface in the context of HLA class I (HLA I) molecules. These peptides, generated by proteasomal degradation of viral proteins in the cytosol, are transported into the ER via the Transporter associated with Antigen Processing (TAP) and subsequently are loaded onto newly synthesized HLA I molecules. To evade CTL recognition, the EBV lytic phase protein BNLF2a inhibits TAP by interfering with the binding of both ATP and peptide to the TAP transporter (10, 12). As a result of diminished TAP-mediated peptide transport into the ER, peptide loading onto HLA I molecules is impaired and surface display of HLA I/peptide complexes is reduced (10, 12).

In humans, two EBV types (1 and 2) are distinguished based on sequence variation in the EBV latent proteins EBNA2, 3A, 3B, and 3C (6, 21). Additionally, considerable polymorphism is found amongst different strains belonging to the same type (4). Such mutations have been found to profoundly affect the T-cell immunogenicity of EBV-encoded proteins. For instance, mutations in the HLA-A11-restricted immunodominant EBNA3B epitope allow escape from T cell recognition (7, 8). These mutant epitopes are more abundant in regions where HLA-A11 is highly prevalent compared to regions where HLA-A11 is found at low frequencies, suggesting that these variants are selected by immunological pressure (7, 8). Similarly, polymorphisms in CTL epitopes of EBNA1 (3) and EBNA3A (1) affect T cell recognition. Sequence polymorphism has not been detected within the BNLF2a gene of the three EBV strains that have

been fully sequenced, which are the type 1 strains B95.8 (infectious mononucleosis) and GD1 (Chinese nasopharyngeal carcinoma), and the type 2 strain AG876 (African Burkitt's lymphoma) (2, 9, 27).

In this study, we investigated the extent to which variation occurs for the immune evasion protein BNLF2a. The functional consequences of this variation were evaluated by measuring HLA I downregulation resulting from BNLF2a-mediated TAP inhibition.

Sequence variation among BNLF2a proteins of EBV isolates

To investigate the frequency of genotypic variation within the EBV-encoded TAP inhibitor, the BNLF2a gene from 22 EBV isolates from Australian Caucasians was sequenced. These viruses were isolated from lymphoblastoid cell lines raised "spontaneously" (without exogenous EBV addition) from either healthy individuals or from infectious mononucleosis patients (3). At the DNA level, multiple mutations were found; of these, two nucleotide substitutions found in the EBV isolates were silent, whereas all other mutations resulted in amino acid changes (Figure S1). The nucleotide polymorphisms observed in these 22 isolates resulted in six different BNLF2a protein sequences (Table 1). In five EBV isolates (23%), the BNLF2a amino acid sequence corresponded to that of the B95.8 reference strain (wt). More than half of the isolates encoded the same two amino acid substitutions, namely an alanine to threonine replacement at position 8 combined with an arginine to lysine mutation at position 40. Other mutations were found only once or twice in this cohort (Table 1). In this small cohort, we did not observe an association between occurrence of BNLF2a variants and frequency of infectious mononucleosis.

In an earlier study, 19 of these EBV isolates were also sequenced across the gene that encodes the EBNA1 protein and heterogeneity was also observed (3). Interestingly, the mutation patterns of BNLF2a and EBNA1 seem to frequently co-segregate (data not shown). For example, the two isolates with the H3Q/A8T/R40K BNLF2a sequence were the only two isolates with a histidine residue in place of the wt glutamine residue at position 471 of EBNA1 (3). In another example, 3 of the 5 donors with the

wt BNLF2a sequence had the wt EBNA1 residue (threonine) at position 524, while none of the other strains had threonine at this position in EBNA1. These SNPs are clearly inherited together as haplotypes, but since EBV sequences may undergo recombination, complete linkage cannot be assumed.

Positive selection of the EBV BNLF2a protein during viral evolution

The BNLF2a alignment was analysed to identify individual residue positions likely to be under positive selection and also overall ratios of the rates of non-synonymous to synonymous substitution (omega) using the codeml module from PAML 4.2b (26). Position 8 in the alignment, containing an alanine to threonine substitution (A8T) is the only residue identified as under positive selection at significance level $p < 0.01$. The other 4 variable positions are significant at $p < 0.1$ only (Table S1), so considerably more caution would have to be exercised in attributing positive selection at those sites. Collection of more clinical and other naturally occurring isolates would be necessary to improve the statistical confidence.

Conservation of BNLF2a function in different EBV isolates

To examine whether the immune evasive properties of BNLF2a are affected by the mutations as found in the EBV isolates, we transiently transfected Mel JuSo (MJS) (24) cells to express (mutant) BNLF2a using the Amara Nucleofector II. Two days after transfection, cells were analysed by flow cytometry. The different BNLF2a mutants were cloned into the pLV-CMV-IRES-eGFP vector (25). This vector contains an internal ribosomal entry site (IRES) immediately downstream of BNLF2a resulting in co-expression of eGFP together with the viral protein. Indeed, intracellular staining using a BNLF2a-specific antibody confirmed that expression levels of the BNLF2a protein correlated with GFP intensities (Fig. 1A). Therefore, in the experiments that follow, GFP protein levels are used as an indicator of the amounts of BNLF2a expressed.

Surface expression of HLA I molecules was downregulated upon transfection of wild-type BNLF2a in a dose-dependent fashion, i.e. correlating with GFP expression (Fig. 1B, second panel on the left). This effect was specific since surface HLA I display was not affected upon transfection of the control protein GFP (empty vector; Fig. 1B, upper panel on the left) and cellular HLA II levels remained unaltered in the presence of BNLF2a (Fig. 1B, right panel). Expression of the BNLF2a mutants did not cause major alterations in HLA I surface expression compared to wild-type BNLF2a, indicating that they retained their ability to reduce cell surface display of HLA I molecules (Fig. 1B, compare left panels).

To allow statistical analysis, the dot plot data were divided into small regions with comparable GFP

expression levels. For each of these regions, the mean fluorescence intensity of HLA class I staining is depicted in figure 1C and D. This analysis revealed subtle differences between wild-type BNLF2a and the mutants. Cell surface HLA I expression is lower in BNLF2a-A8T/R40K-expressing cells compared to wild-type BNLF2a-expressing cells; this difference is small but statistically significant (Fig. 1C). Also the other mutant proteins were more efficient in downregulating HLA I expression than wild-type BNLF2a (Fig. 1D). No differences in the efficiency of reducing HLA I cell surface expression were observed among the various mutants (Fig. 1D).

N-terminal amino acid residues influence immune evasive properties of BNLF2a

The A8T mutation occurs in conjugation with other substitutions only, so its contribution to BNLF2a function cannot be inferred from these naturally occurring variants. Therefore, an A8T only recombinant has been constructed and tested for TAP inhibition. Furthermore, we determined the effect of a double H3Q/A8T mutation in BNLF2a.

The BNLF2a-A8T and BNLF2a-H3Q/A8T mutants were slightly more efficient in downregulating cell surface HLA I expression compared to wild-type BNLF2a (Fig. 2A-C). No differences were found between the two mutants, indicating that the alanine to threonine substitution at position 8 alone is sufficient to improve BNLF2a's HLA I downregulating properties, whereas the histidine to glutamine substitution at position 3 has no additional effect. Furthermore, our data confirm the important role of the N-terminal domain of BNLF2a in inhibiting TAP-mediated peptide transport.

H3P mutation negatively affects BNLF2a-mediated HLA I downregulation

Previously, we have demonstrated that BNLF2a prevents peptide binding to TAP (10). This might be achieved by binding of the cytosolic N-terminus of BNLF2a, which is required for TAP inhibition (11), to the peptide-binding site of TAP, thereby directly competing with binding of peptides. For 7- to 11-mer peptide epitopes, a proline at position 1, 2, or 3 hampers interaction with TAP (16, 17, 22, 23). We hypothesized that were the N-terminus of BNLF2a to associate with the peptide-binding domain of TAP, a histidine to proline substitution at position 3 of the BNLF2a protein might interfere with its ability to inhibit TAP and, consequently, to downregulate cell surface HLA I display.

Compared to wild-type BNLF2a, BNLF2a-H3P is impaired in its ability to reduce HLA I cell surface levels (Fig. 3A-C). This observation indicates that the protein residue at position 3 critically interferes with BNLF2a function, possibly through perturbing the interaction between the N-terminus of BNLF2a and the peptide-binding domain of TAP.

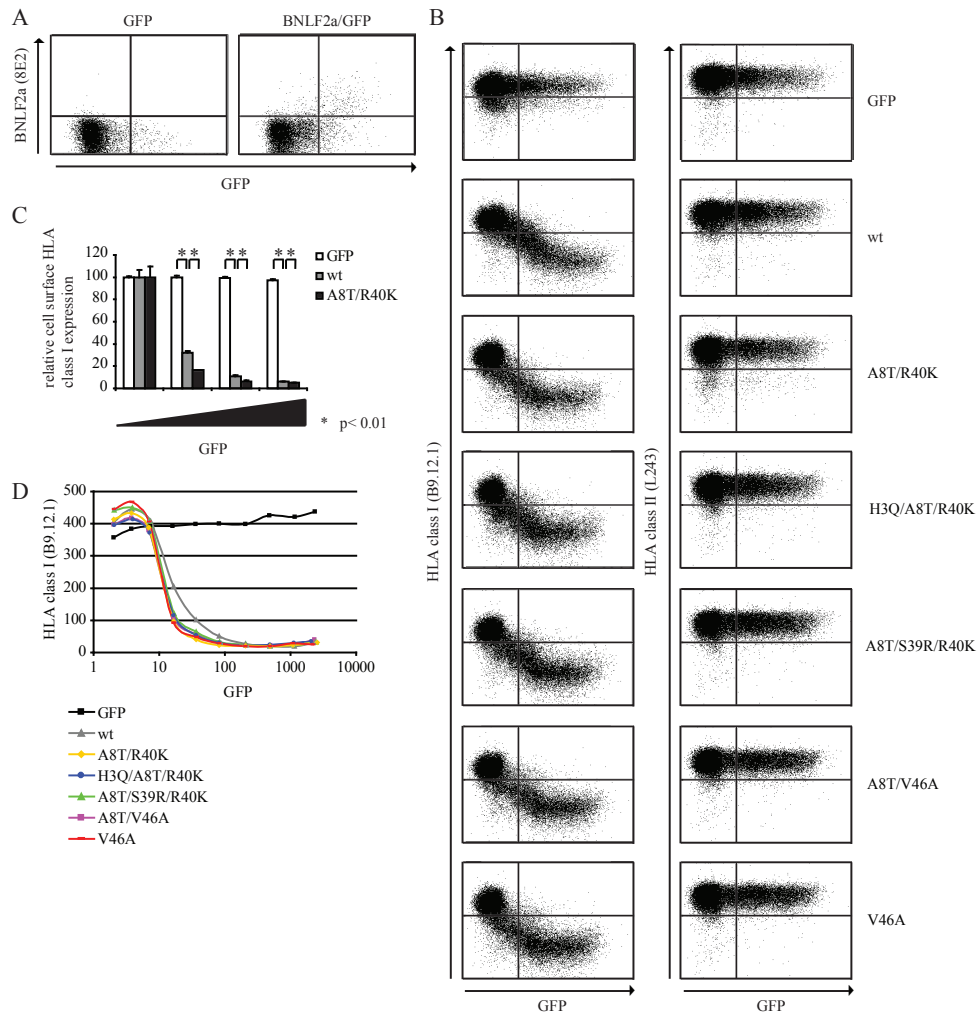


Figure 1. EBV isolates retain BNLF2a-mediated HLA I downregulation

(A) MJS cells were transiently transfected to express the control protein GFP or to coexpress wild-type BNLF2a and GFP. After 48 hours, cells were stained for intracellular expression of BNLF2a (mAb 8E2). Subsequently, the cells were analysed by flow cytometry using CellQuest Pro software (BD Biosciences). (B) MJS cells were transiently transfected to express the control protein GFP, wild-type BNLF2a (wt) or one of the BNLF2a mutants (A8T/R40K, H3Q/A8T/R40K, A8T/S39R/R40K, A8T/V46A and V46A). After 48 hours, cells were stained for cell surface expression of HLA I (mAb B9.12.1) and HLA II (mAb L243) and analysed by flow cytometry using CellQuest Pro software (BD Biosciences). (C) Quantification of flow cytometry data. Cell surface expression levels of HLA I were correlated with GFP expression for cells transfected to express the control protein GFP, wildtype (wt) BNLF2a or the BNLF2a mutant A8T/R40K. To this end, values were corrected for cell surface expression of HLA I in GFP negative cells. (* p < 0.01 as determined by a t-test). (D) Graphical display of B. The mean fluorescence index of HLA I expression is plotted against the mean fluorescence index of GFP expression.

In conclusion, the data presented in this study indicate that, whereas a single mutation within BNLF2a can impair its ability to reduce cell surface HLA I expression, the BNLF2a mutants as identified in the natural isolates all retained their HLA I downregulating properties despite the presence of multiple mutations in most cases. Furthermore, there is evidence for positive selection of the A8T substitution, which slightly

improves the TAP inhibiting capacities of the BNLF2a protein. These results suggest that BNLF2a has an important role in preventing antigen presentation to CTLs. In accordance, B-cell lines transformed with a BNLF2a-deletion mutant of EBV display increased susceptibility towards CTLs targeting (immediate) early EBV antigens, when compared to wild-type EBV-transformed cells (5).

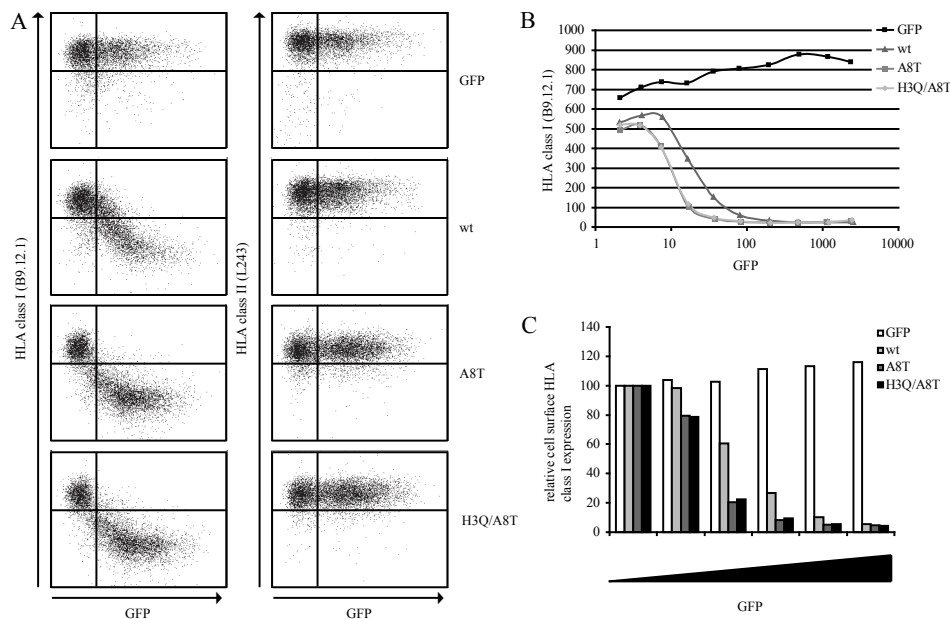


Figure 2. N-terminal amino acids of BNL2a affect its immune evasion function
 (A) MJS cells were transiently transfected to express the control protein GFP, wild-type BNL2a (wt), BNL2a-A8T (A8T) or BNL2a-H3Q/A8T (H3Q/A8T). After 48 hours, cells were stained for cell surface expression of HLA I (mAb B9.12.1) and HLA II (mAb L243) and analysed by flow cytometry using CellQuest Pro software (BD Biosciences). (B) Graphical display of A. The mean fluorescence index of HLA I expression is plotted against the mean fluorescence index of GFP expression. (C) Quantification of A. Cell surface expression levels of HLA I were correlated with GFP expression. To this end, values were corrected for cell surface expression of HLA I in GFP negative cells.

Besides for BNL2a, genetic variation is also observed for other EBV lytic proteins that influence host-pathogen interactions. Sequencing of EBV isolates revealed mutations within the viral IL-10 protein (14), a cytokine that has immunomodulating properties (13). Similarly, amino acid sequence variation was observed for the anti-apoptotic BHRF1 protein. These BHRF1 variants still confer protection against apoptosis, indicating conservation of the function of this viral protein (15).

Taken together, our current results demonstrate that the function of the TAP inhibitor BNL2a is conserved during evolution of EBV, pointing towards an important contribution of immune evasion during the viral life cycle. By interfering with T-cell recognition during productive EBV infection, BNL2a is anticipated to create a window for the generation of viral progeny in the face of memory T cell immunity.

Acknowledgements

We thank Drs A.J. Davison (University of Glasgow Centre for Virus Research, Glasgow, United Kingdom) and R.C. Hoeben and A. Mulder (Leiden University Medical Center, Leiden, The Netherlands) for helpful

advice and generously sharing reagents and constructs. This work was supported by the Dutch Cancer Foundation (grant RUL 2005-3259 to D.H., M.R. and E.W.), the Netherlands Scientific Organization (NWO Vidi 917.76.330 to M.R.), the National Health and Medical Research Council of Australia (to S.B.) and the UK Medical Research Council (to D.G.). The authors declare that they have no conflict of interest.

References

1. Apolloni, A., D. Moss, R. Stumm, S. Burrows, A. Suhrbier, I. Misko, C. Schmidt, and T. Sculley. 1992. Sequence variation of cytotoxic T cell epitopes in different isolates of Epstein-Barr virus. *Eur. J. Immunol.* 22:183-189.
2. Baer, R., A. T. Bankier, M. D. Biggin, P. L. Deininger, P. J. Farrell, T. J. Gibson, G. Hatfull, G. S. Hudson, S. C. Satchwell, C. Seguin, P. S. Tuffnell, and B. G. Barrell. 1984. DNA sequence and expression of the B95-8 Epstein-Barr virus genome. *Nature* 310:207-211.
3. Bell, M. J., R. Brennan, J. J. Miles, D. J. Moss, J. M. Burrows, and S. R. Burrows. 2008.

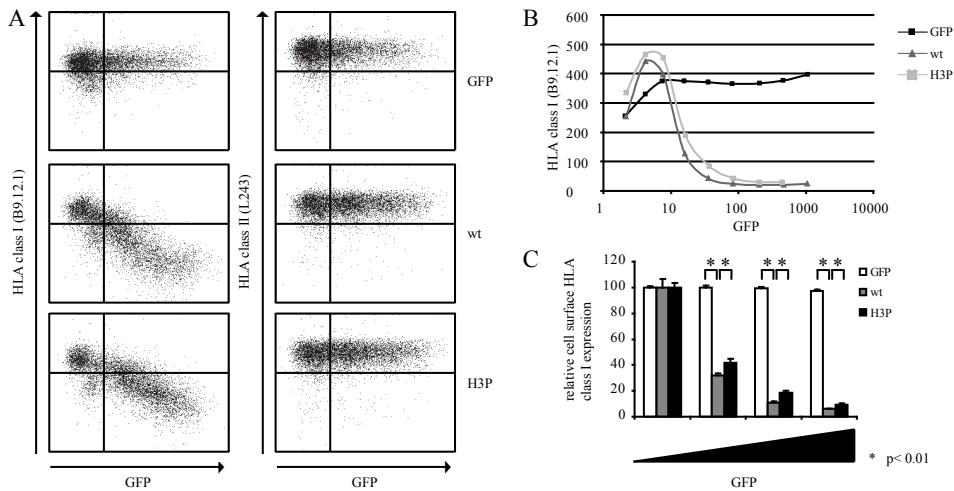


Figure 3. H3P mutation negatively affects functioning BNLF2a (A) MJS cells were transiently transfected to express the control protein GFP, wild-type BNLF2a (wt) or BNLF2a-H3P (H3P). After 48 hours, cells were stained for cell surface expression of HLA I (mAb B9.12.1) and HLA II (mAb L243) and analysed by flow cytometry using CellQuest Pro software (BD Biosciences). (B) Graphical display of A. The mean fluorescence index of HLA I expression is plotted against the mean fluorescence index of GFP expression. (C) Quantification of A. Cell surface expression levels of HLA I were correlated with GFP expression. To this end, values were corrected for cell surface expression of HLA I in GFP negative cells. (* $p < 0.01$ as determined by a t-test).

- Widespread sequence variation in Epstein-Barr virus nuclear antigen 1 influences the antiviral T cell response. *J. Infect. Dis.* 197:1594-1597.
- Chang, C. M., K. J. Yu, S. M. Mbulaiteye, A. Hildesheim, and K. Bhatia. 2009. The extent of genetic diversity of Epstein-Barr virus and its geographic and disease patterns: a need for reappraisal. *Virus Res.* 143:209-221.
 - Croft, N. P., C. Shannon-Lowe, A. I. Bell, D. Horst, E. Kremmer, M. E. Rensing, E. J. Wiertz, J. M. Middeldorp, M. Rowe, A. B. Rickinson, and A. D. Hislop. 2009. Stage-specific inhibition of MHC class I presentation by the Epstein-Barr virus BNLF2a protein during virus lytic cycle. *PLoS Pathog.* 5:e1000490.
 - Dambaugh, T., K. Hennessy, L. Chamnankit, and E. Kieff. 1984. U2 region of Epstein-Barr virus DNA may encode Epstein-Barr nuclear antigen 2. *Proc. Natl. Acad. Sci. U. S. A.* 81:7632-7636.
 - de Campos-Lima, P. O., R. Gavioli, Q. J. Zhang, L. E. Wallace, R. Dolcetti, M. Rowe, A. B. Rickinson, and M. G. Masucci. 1993. HLA-A11 epitope loss isolates of Epstein-Barr virus from a highly A11⁺ population. *Science* 260:98-100.
 - de Campos-Lima, P. O., V. Levitsky, J. Brooks, S. P. Lee, L. F. Hu, A. B. Rickinson, and M. G. Masucci. 1994. T cell responses and virus evolution: loss of HLA A11-restricted CTL epitopes in Epstein-Barr virus isolates from highly A11-positive populations by selective mutation of anchor residues. *J. Exp. Med.* 179:1297-1305.
 - Dolan, A., C. Addison, D. Gatherer, A. J. Davison, and D. J. McGeoch. 2006. The genome of Epstein-Barr virus type 2 strain AG876. *Virology* 350:164-170.
 - Hislop, A. D., M. E. Rensing, D. van Leeuwen, V. A. Pudney, D. Horst, D. Koppers-Lalic, N. P. Croft, J. J. Neefjes, A. B. Rickinson, and E. J. Wiertz. 2007. A CD8⁺ T cell immune evasion protein specific to Epstein-Barr virus and its close relatives in Old World primates. *J. Exp. Med.* 204:1863-1873.
 - Horst, D., V. Favalaro, F. Vilardi, H. C. van Leeuwen, M. A. Garstka, A. D. Hislop, C. Rabu, E. Kremmer, A. B. Rickinson, S. High, B. Dobberstein, M. E. Rensing, and E. J. Wiertz. 2011. EBV protein BNLF2a exploits host tail-anchored protein integration machinery to inhibit TAP. *J. Immunol.* 186:3594-3605.
 - Horst, D., D. van Leeuwen, N. P. Croft, M. A. Garstka, A. D. Hislop, E. Kremmer, A. B. Rickinson, E. J. Wiertz, and M. E. Rensing. 2009. Specific targeting of the EBV lytic phase protein BNLF2a to the transporter associated with antigen processing results in impairment of HLA class I-restricted antigen presentation. *J. Immunol.* 182:2313-2324.
 - Hsu, D. H., M. R. de Waal, D. F. Fiorentino, M. N. Dang, P. Vieira, J. de Vries, H. Spits, T. R. Mosmann, and K. W. Moore. 1990. Expression of interleukin-10 activity by Epstein-Barr virus protein BCRF1. *Science* 250:830-832.
 - Kanai, K., Y. Satoh, H. Yamanaka, A.

- Kawaguchi, K. Horie, K. Sugata, Y. Hoshikawa, T. Sata, and T. Sairenji. 2007. The vIL-10 gene of the Epstein-Barr virus (EBV) is conserved in a stable manner except for a few point mutations in various EBV isolates. *Virus Genes* 35:563-569.
15. Khanim, F., C. Dawson, C. A. Meseda, J. Dawson, M. Mackett, and L. S. Young. 1997. BHRF1, a viral homologue of the Bcl-2 oncogene, is conserved at both the sequence and functional level in different Epstein-Barr virus isolates. *J. Gen. Virol.* 78 (Pt 11):2987-2999.
 16. Momburg, F., J. Roelse, J. C. Howard, G. W. Butcher, G. J. Hammerling, and J. J. Neefjes. 1994. Selectivity of MHC-encoded peptide transporters from human, mouse and rat. *Nature* 367:648-651.
 17. Neefjes, J., E. Gottfried, J. Roelse, M. Gromme, R. Obst, G. J. Hammerling, and F. Momburg. 1995. Analysis of the fine specificity of rat, mouse and human TAP peptide transporters. *Eur. J. Immunol.* 25:1133-1136.
 18. Rensing, M. E., D. Horst, B. D. Griffin, J. Tellam, J. Zuo, R. Khanna, M. Rowe, and E. J. Wiertz. 2008. Epstein-Barr virus evasion of CD8(+) and CD4(+) T cell immunity via concerted actions of multiple gene products. *Semin. Cancer Biol.* 18:397-408.
 19. Rickinson, A. B. and E. Kieff. 2007. Epstein-Barr Virus, p. 2655-2700. In D. M. Knipe and P. M. Howley (eds.), *Fields's virology*, vol. 2. Lippincott Williams & Wilkins, a Wolters Kluwer Business, Philadelphia.
 20. Rowe, M. and J. Zuo. 2010. Immune responses to Epstein-Barr virus: molecular interactions in the virus evasion of CD8⁺ T cell immunity. *Microbes. Infect.* 12:173-181.
 21. Sample, J., L. Young, B. Martin, T. Chatman, E. Kieff, A. Rickinson, and E. Kieff. 1990. Epstein-Barr virus types 1 and 2 differ in their EBNA-3A, EBNA-3B, and EBNA-3C genes. *J. Virol.* 64:4084-4092.
 22. Uebel, S., W. Kraas, S. Kienle, K. H. Wiesmuller, G. Jung, and R. Tampe. 1997. Recognition principle of the TAP transporter disclosed by combinatorial peptide libraries. *Proc. Natl. Acad. Sci. U. S. A* 94:8976-8981.
 23. van Endert, P. M., D. Riganelli, G. Greco, K. Fleischhauer, J. Sidney, A. Sette, and J. F. Bach. 1995. The peptide-binding motif for the human transporter associated with antigen processing. *J. Exp. Med.* 182:1883-1895.
 24. van Ham, S. M., E. P. Tjin, B. F. Lillemeier, U. Gruneberg, K. E. van Meijgaarden, L. Pastoors, D. Verwoerd, A. Tulp, B. Canas, D. Rahman, T. H. Ottenhoff, D. J. Pappin, J. Trowsdale, and J. Neefjes. 1997. HLA-DO is a negative modulator of HLA-DM-mediated MHC class II peptide loading. *Curr. Biol.* 7:950-957.
 25. Vellinga, J., T. G. Uil, V. J. de, M. J. Rabelink, L. Lindholm, and R. C. Hoeben. 2006. A system for efficient generation of adenovirus protein IX-producing helper cell lines. *J. Gene Med.* 8:147-154.
 26. Yang, Z. 2007. PAML 4: phylogenetic analysis by maximum likelihood. *Mol. Biol. Evol.* 24:1586-1591.
 27. Zeng, M. S., D. J. Li, Q. L. Liu, L. B. Song, M. Z. Li, R. H. Zhang, X. J. Yu, H. M. Wang, I. Ernberg, and Y. X. Zeng. 2005. Genomic sequence analysis of Epstein-Barr virus strain GD1 from a nasopharyngeal carcinoma patient. *J. Virol.* 79:15323-15330.

Supplementary data

	1	ATG	GTA	CAC	GTC	CTG	GAG	CGT	GCT	TTG	CTA	GAG	CAG	CAG	TCC	TCT	GCC	TGC	GGC	CTG	CCC	GGC	TCT	TCT	ACG	GAG	ACC	AGG	CCT	AGC						
	M	V	H	V	L	E	R	A	A	L	L	E	Q	Q	S	S	A	C	G	L	P	G	S	S	T	E	T	R	P	S						
B95-8	-	-	-	-	-	-	-	-	-	-	-	-	-	-	-	-	-	-	-	-	-	-	-	-	-	-	-	-	-	-	-					
Donor 16	-	-	-	-	-	-	-	-	-	-	-	-	-	-	-	-	-	-	-	-	-	-	-	-	-	-	-	-	-	-	-	-				
Donor 48	-	-	-	-	-	-	-	-	-	-	-	-	-	-	-	-	-	-	-	-	-	-	-	-	-	-	-	-	-	-	-	-	-			
Donor 4	-	-	-	-	-	-	-	-	-	-	-	-	-	-	-	-	-	-	-	-	-	-	-	-	-	-	-	-	-	-	-	-	-	-		
Donor 6	-	-	-	-	-	-	-	-	-	-	-	-	-	-	-	-	-	-	-	-	-	-	-	-	-	-	-	-	-	-	-	-	-	-	-	
Donor 5	-	-	-	-	-	-	-	-	-	-	-	-	-	-	-	-	-	-	-	-	-	-	-	-	-	-	-	-	-	-	-	-	-	-	-	
Donor 30	-	-	-	-	-	-	-	-	-	-	-	-	-	-	-	-	-	-	-	-	-	-	-	-	-	-	-	-	-	-	-	-	-	-	-	
Donor 7	-	-	-	-	-	-	-	-	-	-	-	-	-	-	-	-	-	-	-	-	-	-	-	-	-	-	-	-	-	-	-	-	-	-	-	-
Donor 39	-	-	-	-	-	-	-	-	-	-	-	-	-	-	-	-	-	-	-	-	-	-	-	-	-	-	-	-	-	-	-	-	-	-	-	-
Donor 43	-	-	-	-	-	-	-	-	-	-	-	-	-	-	-	-	-	-	-	-	-	-	-	-	-	-	-	-	-	-	-	-	-	-	-	-
Donor 14	-	-	-	-	-	-	-	-	-	-	-	-	-	-	-	-	-	-	-	-	-	-	-	-	-	-	-	-	-	-	-	-	-	-	-	-
Donor 31	-	-	-	-	-	-	-	-	-	-	-	-	-	-	-	-	-	-	-	-	-	-	-	-	-	-	-	-	-	-	-	-	-	-	-	-
Donor 29	-	-	-	-	-	-	-	-	-	-	-	-	-	-	-	-	-	-	-	-	-	-	-	-	-	-	-	-	-	-	-	-	-	-	-	-
Donor 9	-	-	-	-	-	-	-	-	-	-	-	-	-	-	-	-	-	-	-	-	-	-	-	-	-	-	-	-	-	-	-	-	-	-	-	-
Donor 49	-	-	-	-	-	-	-	-	-	-	-	-	-	-	-	-	-	-	-	-	-	-	-	-	-	-	-	-	-	-	-	-	-	-	-	-
Donor 10	-	-	-	-	-	-	-	-	-	-	-	-	-	-	-	-	-	-	-	-	-	-	-	-	-	-	-	-	-	-	-	-	-	-	-	-
Donor 13	-	-	-	-	-	-	-	-	-	-	-	-	-	-	-	-	-	-	-	-	-	-	-	-	-	-	-	-	-	-	-	-	-	-	-	-
Donor 42	-	-	-	-	-	-	-	-	-	-	-	-	-	-	-	-	-	-	-	-	-	-	-	-	-	-	-	-	-	-	-	-	-	-	-	-
Donor 22	-	-	-	-	-	-	-	-	-	-	-	-	-	-	-	-	-	-	-	-	-	-	-	-	-	-	-	-	-	-	-	-	-	-	-	-
Donor 20	-	-	-	-	-	-	-	-	-	-	-	-	-	-	-	-	-	-	-	-	-	-	-	-	-	-	-	-	-	-	-	-	-	-	-	-
Donor 34	-	-	-	-	-	-	-	-	-	-	-	-	-	-	-	-	-	-	-	-	-	-	-	-	-	-	-	-	-	-	-	-	-	-	-	-
Donor 50	-	-	-	-	-	-	-	-	-	-	-	-	-	-	-	-	-	-	-	-	-	-	-	-	-	-	-	-	-	-	-	-	-	-	-	-
Donor 25	-	-	-	-	-	-	-	-	-	-	-	-	-	-	-	-	-	-	-	-	-	-	-	-	-	-	-	-	-	-	-	-	-	-	-	-

B95-8	59			
	CTC L	ATC I	TAA Stop	
Donor 16	-	-	-	-
Donor 48	-	-	-	-
Donor 4	-	-	-	-
Donor 6	-	-	-	-
Donor 5	-	-	-	-
Donor 30	-	-	-	-
Donor 7	-	-	-	-
Donor 39	-	-	-	-
Donor 43	-	-	-	-
Donor 14	-	-	-	-
Donor 31	-	-	-	-
Donor 29	-	-	-	-
Donor 9	-	-	-	-
Donor 49	-	-	-	-
Donor 10	-	-	-	-
Donor 13	-	-	-	-
Donor 42	-	-	-	-
Donor 22	-	-	-	-
Donor 20	-	-	-	-
Donor 34	-	-	-	-
Donor 50	-	-	-	-
Donor 25	-	-	-	-

Figure S1. BNLF2a nucleotide and amino acid sequences of EBV isolates

Residue	Pr($\omega > 1$)	post mean \pm SE for ω
H3	0.932	7.112 \pm 2.729
A8	0.991**	7.533 \pm 2.268
S39	0.925	7.054 \pm 2.777
R40	0.928	7.082 \pm 2.754
V46	0.927	7.072 \pm 2.762

Table S1. Statistical analysis of the BNLF2a alignment

Codeml (<http://abacus.gene.ucl.ac.uk/software/paml.html>) performs a statistical test between different models of selection. The following models were compared: M0 (single ω over entire alignment), M1 (2 categories: $\omega < 1$ and $\omega = 1$), M2 (3 categories: $\omega < 1$, $\omega = 1$ and $\omega > 1$), M3 (3 categories, no constraints), M7 (10 categories, beta distributed from $\omega = 0$ to $\omega = 1$), M8 (M7 plus an additional category: $\omega > 1$), M8a (M7 plus an additional category: $\omega = 1$). The following pairs were tested: M0 vs. M3 (test for uniform versus multiple categories of ω , i.e. variation in selective pressure along alignment), M1 vs. M2 (test of selection versus neutrality with discrete categories of ω), M7 vs. M8 (test of selection versus neutrality with beta distribution of ω), M8 vs. M8a (test for strong vs. weak selection). Amino acids refer to the B95.8 EBV sequence. Positively selected sites (*: $P > 95\%$; **: $P > 99\%$), SE = standard error of the mean

A probability of positive selection at $\text{Pr}(\omega > 1) > 90\%$ (corresponding to a statistical significance of $p < 0.1$) in model comparison M7 vs. M8 was detected at all mutant sites using the BEB model (1). If a conservative threshold of statistical significance is adopted at $\text{Pr}(\omega > 1) > 99\%$, evidence for positive selection at $p < 0.01$ is restricted to residue 8. The more general statistical tests for the presence of positive selection in the alignment, M1 vs. M2, M7 vs. M8 and M8 vs. M8a (see above) were significant at $p < 0.05$ in all cases.

Supplemental references

1. Yang, Z., W. S. Wong, and R. Nielsen. 2005. Bayes empirical bayes inference of amino acid sites under positive selection. *Mol. Biol. Evol.* 22:1107-1118.

Chapter 6

Stage-specific inhibition of MHC class I presentation by the Epstein-Barr virus BNLF2a protein during virus lytic cycle

N.P. Croft, C. Shannon-Lowe, A.I. Bell, D. Horst, E. Kremmer, M.E. Rensing, E.J.H.J. Wiertz, J.M. Middeldorp, M. Rowe, A.B. Rickinson and A.D. Hislop.

PLoS Pathogens 2009

Abstract

The gamma-herpesvirus Epstein-Barr virus (EBV) persists for life in infected individuals despite the presence of a strong immune response. During the lytic cycle of EBV many viral proteins are expressed, potentially allowing virally infected cells to be recognized and eliminated by CD8⁺ T cells. We have recently identified an immune evasion protein encoded by EBV, BNLF2a, which is expressed in early phase lytic replication and inhibits peptide- and ATP-binding functions of the transporter associated with antigen processing. Ectopic expression of BNLF2a causes decreased surface MHC class I expression and inhibits the presentation of indicator antigens to CD8⁺ T cells. Here we sought to examine the influence of BNLF2a when expressed naturally during EBV lytic replication. We generated a BNLF2a-deleted recombinant EBV (Δ BNLF2a) and compared the ability of Δ BNLF2a and wild-type EBV-transformed B cell lines to be recognized by CD8⁺ T cell clones specific for EBV-encoded immediate early, early and late lytic antigens. Epitopes derived from immediate early and early expressed proteins were better recognized when presented by Δ BNLF2a transformed cells compared to wild-type virus transformants. However, recognition of late antigens by CD8⁺ T cells remained equally poor when presented by both wild-type and Δ BNLF2a cell targets. Analysis of BNLF2a and target protein expression kinetics showed that although BNLF2a is expressed during early phase replication, it is expressed at a time when there is an upregulation of immediate early proteins and initiation of early protein synthesis. Interestingly, BNLF2a protein expression was found to be lost by late lytic cycle yet Δ BNLF2a-transformed cells in late stage replication downregulated surface MHC class I to a similar extent as wild-type EBV-transformed cells. These data show that BNLF2a-mediated expression is stage-specific, affecting presentation of immediate early and early proteins, and that other evasion mechanisms operate later in the lytic cycle.

Introduction

The detection and elimination of virally infected cells by the host immune system relies heavily upon CD8⁺ T cells recognizing peptides endogenously processed and presented by HLA class I molecules. Proteasomal degradation of endogenously synthesized proteins provides a source of peptides which are delivered into the endoplasmic reticulum by the transporter associated with antigen processing (TAP), where they are loaded onto nascent HLA-class I molecules. Peptide:HLA-class I complexes are then transported to the cell surface where CD8⁺ T cells examine these complexes with their T cell receptors. Recognition of these complexes leads to the killing of the infected cell by the CD8⁺ T cell (reviewed in [1],[2]).

As such, many viruses have developed strategies to evade CD8⁺ T cell recognition in order to aid their transmission and persistence within hosts. This is particularly true for the herpesviruses; large double-stranded DNA viruses characterized by their ability to enter a latent state within specialized cells in their respective hosts, with this itself a form of immune evasion due to the transcriptional silencing of most if not all genes. However, herpesviruses occasionally undergo reactivation into their lytic cycle, where a large number of viral genes are expressed. Here there is a sequential cascade of gene expression beginning with the immediate early genes, followed by the early genes and finally the late genes. Potentially then many targets for CD8⁺ T cell recognition are generated during lytic cycle replication. The finding of immune evasion mechanisms in members of each of the three α -, β - and γ -herpesvirus subfamilies highlights the strong immunological pressure these viruses are under. These evasion strategies often subvert cellular processes involved in the generation and presentation of epitopes to T cells (reviewed in [3],[4]). The importance of these processes is highlighted by the convergent evolution seen in herpesviruses, where members of the different subfamilies target the same points involved in the generation of CD8⁺ T cell epitopes but use unrelated proteins to do this.

Until recently, less evidence has been available on immune evasion by the lymphocryptoviruses (LCV, γ 1-herpesviruses) during lytic cycle. The prototypic virus of this genus, Epstein-Barr virus (EBV), infects epithelial cells and B lymphocytes, establishing latency in the latter cell type. Central to EBV's biology is its ability to expand the reservoir of latently infected B cells through growth-transforming gene expression, independent of lytic replication [5]. It was unclear then whether lytic immune evasion mechanisms would be required by EBV to amplify the viral reservoir within a host. However, during lytic cycle replication, presentation of EBV epitopes to cognate CD8⁺ T cells falls with the progression of the lytic cycle, while B cells replicating EBV have decreased levels of surface HLA-class I and decreased TAP

function [6]–[8]. These observations suggested that EBV interferes with antigen processing during lytic cycle replication. Targeted screening of EBV genes for immune evasion function led to the identification of the early expressed lytic cycle gene *BNLF2a* which functions as a TAP inhibitor [9]. This novel immune evasion gene encodes for a 60 amino acid protein that disrupts TAP function by preventing both peptide- and ATP-binding to this complex. Consequently, cells expressing *BNLF2a in vitro* show decreased surface HLA-class I levels and are refractory to CD8⁺ T cell killing when co-expressed with target antigens [9].

In the current study we analyze the influence *BNLF2a* has on presentation of EBV-specific epitopes during lytic cycle replication, to determine whether *BNLF2a* acts alone or whether other immune evasion mechanisms are present in EBV and how *BNLF2a* affects antigen presentation during the different phases of gene expression. The impact of *BNLF2a* was isolated through the construction of a recombinant EBV lacking the gene and this virus used to infect cells for antigen processing and presentation studies. Cells replicating this *BNLF2a*-deleted virus were found to be better recognized by immediate early and early antigen-specific CD8⁺ T cells but not late antigen-specific T cells. Consistent with this finding, surface class I HLA expression was restored to normal levels in cells expressing immediate early but not late expressed EBV proteins. Our results suggest that immune evasion mechanisms in addition to *BNLF2a* are operational during EBV lytic cycle replication.

Results

Construction of a Δ *BNLF2a* mutant virus

We initially disrupted the *BNLF2a* gene of the B95.8 strain of EBV contained within a BAC by insertional mutagenesis (Figure 1A). A targeting plasmid was created in which the majority of the *BNLF2a* gene was replaced with a tetracycline resistance cassette which in turn was flanked by FLP recombinase target (FRT) sites. This vector was recombined with the EBV BAC and recombinants selected. Such clones, designated Δ *BNLF2a*, had the tetracycline gene removed by FLP recombinase and were screened for deletion of the *BNLF2a* gene by restriction endonuclease analysis and sequencing (data not shown). Δ *BNLF2a* BACs were then stably transfected into 293 cells and virus replication induced by transfection of a plasmid encoding the EBV lytic switch protein BZLF1. Virus was also produced from cells transduced with the wild-type B95.8 EBV BAC and a B95.8 EBV BZLF1-deleted BAC (Δ BZLF1) [10], encoding a virus unable to undergo lytic cycle replication unless BZLF1 is supplied *in trans*.

The different recombinant EBVs derived from the 293 cells were used to transform primary B cells, to establish lymphoblastoid cell lines (LCLs). To

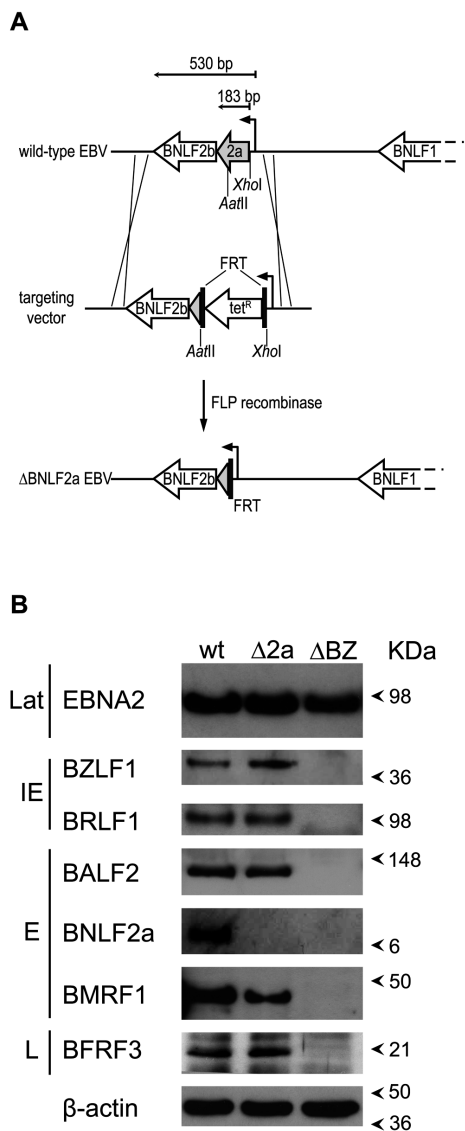


Figure 1. Generation of a mutant Epstein-Barr virus deleted for BNL2a (ΔBNL2a)

(A) Schematic drawing of the BNL2a-containing region of the EBV genome, before and after disruption of the BNL2a open reading frame. Removal of the tetracycline resistance cassette by flp recombinase leaves one flp recombinase target (FRT) site intact. (B) LCLs transformed with either the wild-type (wt), ΔBNL2a (Δ2a) or ΔBZLF1 (ΔBZ) viruses were analysed by Western blot for expression of BNL2a, several representative lytic cycle antigens, and the latent cycle expressed protein EBNA2. Antibodies specific for β-actin were used to ensure equal protein loading. Lat, latent; IE, immediate early; E, early; L, late.

determine if expression of other viral proteins was affected by the deletion of BNL2a, western blot analysis on lysates of LCLs generated from wild-type, ΔBNL2a and ΔBZLF1 viruses was performed. As a subset of cells in the LCL culture will spontaneously enter lytic cycle replication, blots were probed with antibodies specific for representative proteins expressed during lytic cycle as well as latent cycle expressed proteins. Figure 1B shows typical blots of lysates probed for the immediate early proteins BZLF1 and BRLF1, the early proteins BALF2, BNL2a and BMRF1, the late protein BFRF3 and the latent protein EBNA2. No difference in expression of these proteins was observed between the wild-type and ΔBNL2a virus transformed LCLs, with the exception of BNL2a protein which was not present as expected in ΔBNL2a LCLs. No lytic cycle protein expression could be detected in ΔBZLF1 LCLs.

Deletion of BNL2a confers an increase in immediate early and early antigen recognition by cognate CD8⁺ T cells, but has no effect on late antigen recognition

A panel of different donor derived LCLs transformed with wild-type, ΔBNL2a, and ΔBZLF1 viruses were employed to study lytic antigen recognition by EBV lytic phase-specific CD8⁺ T cells. Here we planned to incubate these LCLs with the different types of lytic antigen-specific CD8⁺ T cells and assay for T cell recognition by IFN-γ secretion. However, the percentage of LCLs that spontaneously enter lytic cycle is variable. Initially then we quantified the number of cells within the LCL cultures expressing the lytic cycle marker BZLF1 by flow cytometry. Figures 2A and 2B show representative flow plots of wild-type, ΔBNL2a and ΔBZLF1 LCLs stained for BZLF1 expression using LCLs derived from two donors. Typically we found between 0.5–3% of wild-type and ΔBNL2a LCLs expressed BZLF1 (upper and middle panels), whilst none was observed in ΔBZLF1 LCLs (lower panels).

To ensure we used equivalent numbers of the different types of lytic antigen positive cells in our T cell recognition experiments, we developed a system to equalize the number of lytic antigen positive cells in each assay. Here the proportion of BZLF1 expressing cells in each culture were equalized by making a dilution series of the LCL with the highest percentage of BZLF1 expressing cells with the antigen negative ΔBZLF1 LCL derived from that donor. T cell recognition of the different LCL transformants was then measured by incubating these LCLs with CD8⁺ T cells specific for epitopes derived from proteins expressed in immediate early, early and late phases of the EBV lytic cycle and measuring IFN_γ release by the T cells. We have previously shown that CD8⁺ T cells in these assays directly recognize lytically infected cells and not cells which have exogenously taken up antigen and re-presented it [6]. Figure 2C shows results of a T

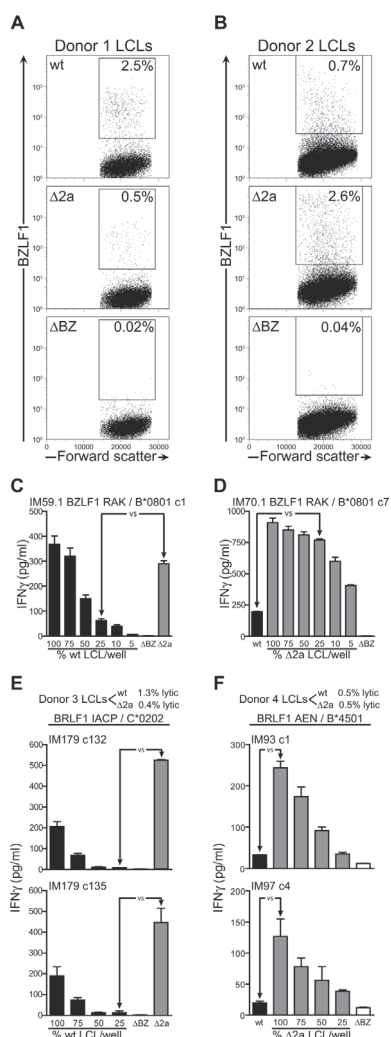


Figure 2. Estimation of Δ BNLF2a and wild-type LCLs expressing lytic antigens; recognition by immediate early antigen-specific CD8⁺ T cells

The proportion of LCLs spontaneously reactivating into lytic cycle was assessed by intracellular BZLF1 staining and analysis by flow cytometry, with representative examples shown for LCLs derived from two different donors: (A) donor 1 and (B) donor 2. Immediate early lytic cycle CD8⁺ T cell recognition of wild-type (wt), Δ BNLF2a (Δ 2a) and Δ BZLF1 (Δ BZ) LCLs using HLA-B*0801-restricted RAK (BZLF1) clones against appropriately HLA matched donor 1 and 2 LCLs (C and D respectively) was measured by IFN γ ELISA. Results using wild-type or Δ BNLF2a cells diluted with Δ BZLF1 cells as appropriate are shown, where arrows indicate equivalent numbers of lytic antigen expressing cells. Experiments were also conducted using HLA-C*0202-restricted IACP (BRLF1) clones against donor 3 LCLs (E), and HLA-B*4501-restricted AEN (BRLF1) clones against donor 4 LCLs (F). For donor 4, both the wild-type and Δ BNLF2a LCLs were diluted with Δ BZLF1 LCL (wild-type-LCL titration data not shown). Data are represented as mean \pm SEM.

cell recognition experiment using LCL targets derived from donor 1. In this case the more lytic wild-type LCL was diluted with the Δ BZLF1 LCL to give equivalent numbers of lytic targets in the assay. When CD8⁺ T cells specific for the immediate early HLA-B*0801 restricted BZLF1 RAK epitope were incubated with the different LCLs, a 6-fold increase in recognition of the Δ BNLF2a LCL was observed compared to the wild-type LCL as measured by secretion of IFN γ . Similar results were obtained using LCLs derived from donor 2 (Figure 2D). In this case the more lytic Δ BNLF2a LCL was diluted with the antigen-negative Δ BZLF1 LCL. When the cultures were equalized for BZLF1 expression a 3-fold increase in recognition of the Δ BNLF2a LCL was seen when compared to recognition of the wild-type LCL.

A similar trend was observed for recognition of epitopes derived from the other immediate early protein BRLF1. Here CD8⁺ T cells specific for the HLA-C*0202 restricted epitope IACP (Figure 2E) and the HLA-B*4501 restricted epitope AEN (Figure 2F) were used to probe antigen presentation by the LCL sets derived from donors 3 and 4 respectively. As shown in Figures 2E and 2F, the Δ BNLF2a LCLs from both donors were recognized more efficiently than the wild-type LCL using both T cell specificities. The IACP clones showed a 50-fold increase and the AEN clones showed a 4–5-fold increase in IFN γ secretion upon challenge with the LCLs.

We next measured recognition of the different LCL types using CD8⁺ T cells specific for two early antigens; the HLA-B*2705 restricted ARYA epitope from BALF2 and the HLA-A*0201 restricted TLD epitope from BMRF1. Here we tested multiple T cell clones derived from three donors against three different donor derived sets of LCLs. Figure 3 shows representative results using ARYA- and TLD-specific T cell clones against LCLs derived from donor 3. Similar to what was seen for the immediate early antigens, T cell recognition of the early antigens was increased upon challenge with the Δ BNLF2a LCL compared to the wild-type LCL, with the most potent increase in recognition observed using the BALF2-specific clones which showed a 20-fold increase in recognition (Figure 3A). The TLD epitope from BMRF1 was found to be recognized the poorest in these assays, never the less a two-fold increase in recognition of the Δ BNLF2a LCL compared to the wild-type was consistently observed using independently derived T cell clones and LCLs derived from different donors (Figure 3B). Multiple clones of a third early specificity, HLA-A*0201 BMLF1, also showed increased recognition of the Δ BNLF2a LCL (see below).

We next turned to study recognition of late-expressed antigens using T cells specific for the HLA-A*0201 restricted FLD epitope from BALF4 and the HLA-B*2705 restricted RRRK epitope from BILF2. We have found that these two epitopes are processed

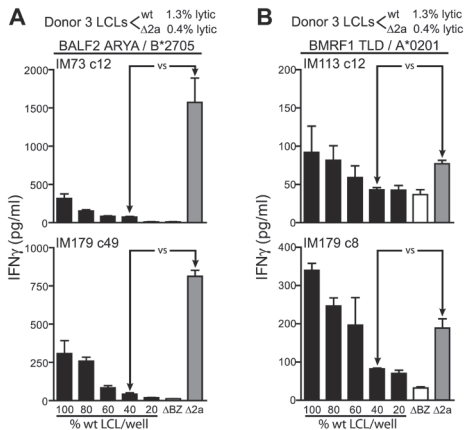


Figure 3. Recognition of Δ BNLF2a LCLs and wild-type LCLs by early antigen-specific CD8⁺ T cells

LCLs from donor 3 were measured for lytic antigen expression and the percentage positive indicated. The proportion of lytic antigen positive wild-type (wt) and Δ BNLF2a (Δ 2a) cells were equalised by dilution with Δ BZLF1 (Δ BZ) LCL and recognition assays performed as described in Figure 2. Recognition of early lytic antigen targets was assessed using CD8⁺ T cells specific for the HLA-B*2705-restricted ARYA (BALF2) epitope (A) and the HLA-A*0201-restricted TLD (BMRF1) epitope (B). Arrows indicate equivalent numbers of lytic antigen expressing cells. Data are represented as mean \pm SEM.

independently and dependently of the proteasome respectively, with the BALF4 epitope presented independently of TAP (data not shown). We would predict from our previous studies of TAP dependence of peptide-epitopes that the hydrophilic BILF2 peptide RRRK would be processed in a TAP dependent manner [11]. Figures 4A and 4B show representative results of experiments using two FLD-specific clones and one RRRK-specific clone assayed against two different donor derived LCLs. T cell recognition of late-expressing Δ BNLF2a and wild-type LCLs was found to be low but of an equivalent level. This pattern of recognition was seen using LCL sets derived from three other donors (data not shown).

To confirm the above results and minimize any variability between assays, we tested the recognition of the different LCL types in parallel by CD8⁺ T cell clones specific for epitopes that were presented by the same HLA molecule but produced at different phases in the replication cycle. Initially we compared recognition of the donor 1 set of LCLs by the HLA-A*0201 restricted CD8⁺ T cells specific for the YVL epitope from the immediate early protein BRLF1, the GLC epitope derived from the early expressed protein BMLF1 and the FLD epitope from the late expressed BALF4 protein. In LCLs made with the BNLF2a-deleted virus there was a clear increase in the ability of YVL- and GLC-specific CD8⁺ T cells to recognize these targets in comparison to the wild-

type LCLs, with these specificities showing a 20- and 6-fold increase in IFN- γ secretion respectively (Figure 5A left panels). We also checked recognition in parallel with the HLA-A*0201 restricted TLD-specific clones which showed an increase in recognition similar to what we observed above (data not shown). By contrast, no apparent difference in recognition was observed using the CD8⁺ T cells specific for the late-derived FLD epitope. In parallel we also estimated the functional avidity of these T cell clones by IFN γ secretion in response to Δ BZLF1 LCLs loaded with 10-fold dilutions of epitope peptide (Figure 5A right panels). The 50% optimal recognition of the late effector FLD c21 was similar to that of the immediate early effector YVL c10, both being in the 10^{-8} – 10^{-9} M range of peptide avidity, whilst the early effector GLC c10 was less avid with a 50% optimal recognition of 10^{-6} M.

In a second series of experiments we compared the ability of the donor 3 set of LCLs to be recognized by HLA-B*2705 restricted CD8⁺ T cells. Here we used clones specific for the ARYA epitope derived from the early protein BALF2 and the RRRK epitope derived from the late protein BILF2. Again we found that the LCLs made using the BNLF2a-deleted virus were well recognized by the early antigen-specific effector compared to the wild-type transformed LCLs with a 14-fold increase in recognition (Figure 5B left panels), but both LCL types were recognized at an equivalent low level by the late-specific cells. In peptide titration

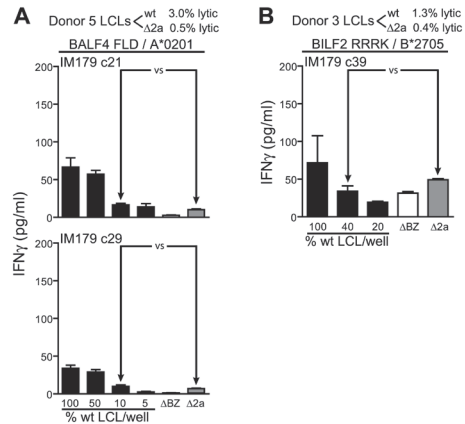


Figure 4. Recognition of Δ BNLF2a LCLs and wild-type LCLs by late antigen-specific CD8⁺ T cells

LCLs from donors 3 and 5 were measured for lytic antigen expression and the percentage positive indicated. The proportion of lytic antigen positive wild-type (wt) and Δ BNLF2a (Δ 2a) cells were equalised by dilution with Δ BZLF1 (Δ BZ) LCL and recognition assays performed as described in Figure 2. Recognition of late lytic antigen targets was assessed using CD8⁺ T cells specific for the HLA-A*0201-restricted FLD (BALF4) epitope (A) and the HLA-B*2705-restricted RRRK (BILF2) epitope (B). Arrows indicate equivalent numbers of lytic antigen expressing cells. Data are represented as mean \pm SEM.

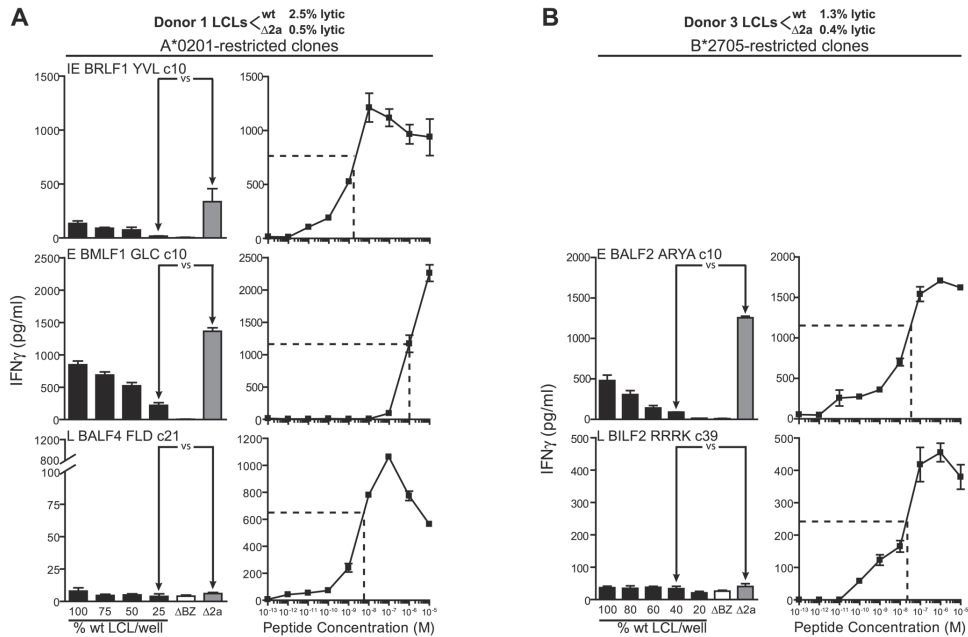


Figure 5. Comparative CD8⁺ T cell recognition of immediate early, early and late antigens expressed by Δ BNLF2a versus wild-type LCLs

(A) LCLs from donor 1 were measured for lytic antigen expression and the percentage positive indicated. The proportion of lytic antigen positive wild-type (wt) and Δ BNLF2a (Δ 2a) cells were equalised by dilution with Δ BZLF1 (Δ BZ) LCL and recognition assays performed as described in Figure 2. Recognition of immediate early (IE), early (E) and late (L) lytic antigen targets was assessed in parallel using representative CD8⁺ T cells specific for the HLA-A*0201 restricted epitopes YVL (BRLF1), GLC (BMLF1) and FLD (BALF4) (left panels). Simultaneously, the functional avidity of these clones was measured by challenging the CD8⁺ T cells with Δ BZLF1 LCLs sensitized with 10-fold dilutions of the peptide epitope and the dose of peptide giving 50% maximal recognition determined (dashed line, right panels). (B) LCLs from donor 3 were measured for lytic antigen expression and the percentage positive indicated. The proportion of lytic antigen positive cells were equalised by dilution with Δ BZLF1 LCL and recognition assays performed as described in Figure 2. Recognition of early and late lytic antigen targets was assessed in parallel using representative CD8⁺ T cells specific for the HLA-B*2705 restricted epitopes ARYA (BALF2), and RRRK (BILF2) (left panels). Functional avidity of these clones was measured simultaneously as in (A). Arrows indicate equivalent numbers of lytic antigen expressing cells. Data are represented as mean \pm SEM.

assays the 50% optimal CD8⁺ T cell recognition values for the ARYA and RRRK clones were similar, at 4×10^{-7} and 2×10^{-7} respectively (Figure 5B right panels).

To confirm that the increased recognition of the Δ BNLF2a LCLs by the immediate early and early T cells seen in these experiments was due to the absence of BNLF2a and not to a secondary mutation within the Δ BNLF2a virus, we re-expressed BNLF2a in the Δ BNLF2a LCLs and conducted recognition assays on these cells. Δ BNLF2a LCLs were transfected with a BNLF2a expression vector which co-expressed the truncated nerve growth factor receptor (NGFR) and cells expressing this receptor selected with magnetic beads. These BNLF2a expressing cells and were used as targets in standard recognition assays alongside NGFR negative BNLF2a negative cells from the transfection, wild-type LCLs, unmanipulated Δ BNLF2a LCLs and Δ BZLF1 LCLs. T cells specific for the immediate early epitope AEN and early epitope

ARYA were used as effectors in parallel assays. Figure S1 shows representative results of two independent transfection experiments. For both CD8⁺ T cell clones, re-expression of BNLF2a in the Δ BNLF2a LCLs decreased recognition of these LCLs to low levels relative to the unmanipulated Δ BNLF2a LCL, suggesting the increased recognition of the Δ BNLF2a LCLs observed in the previous experiments is due to the absence of BNLF2a.

EBV BNLF2a is expressed during lytic cycle concomitant with peak immediate early and early gene expression

An unexpected outcome of the recognition experiments was the increased detection of immediate early antigens in the Δ BNLF2a transformed LCLs by the cognate CD8⁺ T cells. Immediate early genes are expressed prior to when the early gene *BNLF2a* would be expected to be expressed and so epitopes derived from immediate early proteins would not likely be well

protected from presentation to CD8⁺ T cells. To clarify when *BNLF2a* is transcribed and expressed relative to the other genes of interest, we studied the transcription and protein expression kinetics of this gene and others that were used in our T cell recognition assays by qRT-PCR and western blot analysis during lytic replication. Here we used the EBV-infected AKBM cell line in which lytic EBV replication can be induced by cross-linking surface IgG receptors with anti-IgG antibodies [8] as a source of RNA and protein for analysis.

Following induction of EBV replication in the AKBM cells, RNA samples were harvested over 48 hours post-induction (pi). qRT-PCR analysis was conducted on the two immediate early genes (*BZLF1* and *BRLF1*), two representative early genes (*BMLF1* and *BNLF2a*) and two representative late genes (*BLLF1* (encoding gp350) and *BALF4* (encoding gp110)). Upon induction, immediate early gene expression (*BZLF1* and *BRLF1*) occurred very rapidly with an increase in transcripts observed 1 hr pi, followed by peak expression at 2–3 hours pi (Figure 6A, upper panel). Transcripts for these two immediate early genes did not disappear completely after their peak expression, however *BZLF1* decreased quickly to low levels consistent with previous findings [12]. There were still more than 40% of the maximal *BRLF1* transcripts present 24 hours pi compared to only 5% of the maximal *BZLF1* transcripts at the same time point. Early gene message was expressed rapidly after induction with both *BMLF1* and *BNLF2a* reaching their peak expression at 4 hours pi (Figure 6A, middle panel). However, *BMLF1* message decreased quickly over the next 8 hours almost to its final levels, while high relative levels of *BNLF2a* message were maintained over the next 20 hours from peak expression dropping to 40% of the maximal level by 48 hours pi. As expected, induction of the late gene *BALF4* and *BLLF1* transcripts was slower, with peak expression at 12 hours and 24 hours, respectively (Figure 6A, lower panel).

We next turned to examine the protein expression kinetics in lytically induced AKBM cells by western blot analysis, employing antibodies specific to proteins used in our recognition assays where available (Figure 6B). Protein from each of the genes that had been measured by qRT-PCR was detected shortly following the expression of the corresponding transcript. Thus *BZLF1*, *BRLF1* and *BMLF1* protein were clearly detected at 2 hours pi as was another early protein *BALF2*. *BNLF2a* protein was also weakly detected at this point and clearly detected at 3 hours pi. *BMRF1* showed delayed protein expression kinetics, being detected at 3–4 hours pi. Expression of the protein levels remained mostly stable for the duration of the time course, with the exception of *BNLF2a* which was lost from the cells at 12–48 hours pi. The late protein *BALF4* was expressed by 6 hours and increased with time, while a second representative late protein, *BFRF3*, showed much delayed expression kinetics.

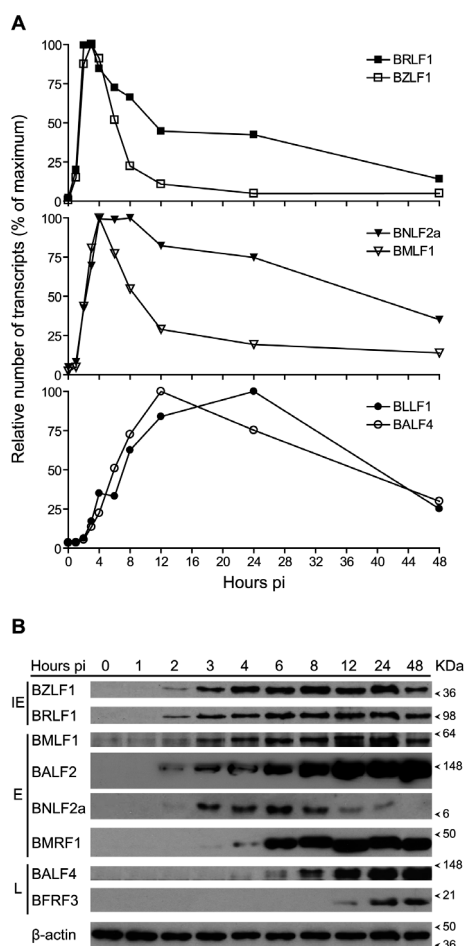


Figure 6. RNA and protein expression kinetics of *BNLF2a* relative to immediate early, early and late genes

AKBM cells containing latent virus were stimulated to induce lytic cycle replication, samples harvested at the indicated times and selected viral transcript and protein levels estimated. Samples were harvested from 0 to 48 hours post induction (pi), and RNA was harvested and subjected to qRT-PCR detection of *BZLF1*, *BRLF1*, *BMLF1*, *BNLF2a*, *BALF4* and *BLLF1* transcripts (A). Values shown are represented as expression relative to their maximum. Protein samples harvested from the same time points were subjected to western blot analysis, where samples were probed with antibodies to the indicated lytic cycle antigens (B).

Surface HLA class I levels remain unaltered in the immediate early/early phases of lytic cycle in Δ *BNLF2a* LCLs, yet are downmodulated during late lytic cycle

The results from our recognition experiments indicated that the deletion of *BNLF2a* did not lead to any increase in recognition of late antigens by their cognate CD8⁺ T cells. Interestingly these late proteins were expressed when protein levels of *BNLF2a* were

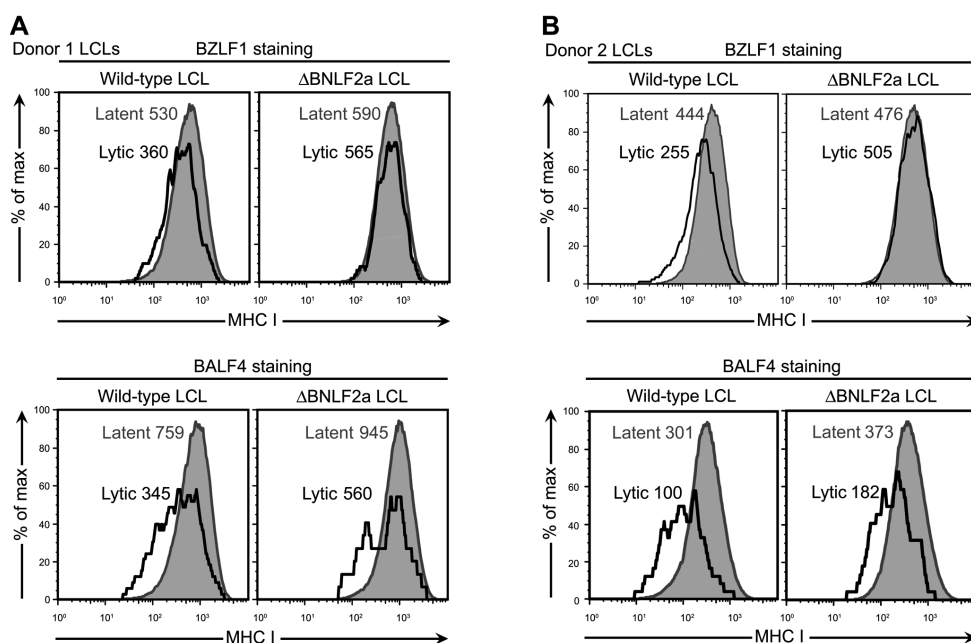


Figure 7. Surface HLA-class I expression in wild-type and Δ BNLF2a LCLs expressing immediate early or late antigens

Wild-type and Δ BNLF2a LCLs were stained for surface HLA-class I and expression levels measured by flow cytometry on cells co-stained for lytic antigens: either the immediate early antigen BZLF1 (upper panels), or the late antigen BALF4 (lower panels). The panels show histograms and MFI values of cell surface HLA-class I expression gated on cells with latent virus (lytic antigen negative, shaded histogram) or lytic virus (lytic antigen positive, open histogram). Staining data is presented from (A) Donor 1 LCLs and (B) Donor 2 LCLs.

declining to low levels. Potentially other immune evasion proteins may be active at these later time points, preventing efficient presentation of epitopes to CD8⁺ T cells. To explore this possibility we performed flow cytometric analysis of surface HLA class I levels on wild-type and Δ BNLF2a LCLs from different donors, which had been co-stained for viral proteins expressed at different phases of lytic cycle. Wild-type LCLs stained for BZLF1 expression showed a decrease in surface HLA class I levels by around 1/3 of the level in latent (lytic antigen negative) cells, yet BZLF1 expressing Δ BNLF2a LCLs showed little to no decrease in surface HLA class I levels (Figure 7A and B upper panels). However, when cells were stained for the late lytic cycle protein BALF4, surface HLA class I levels in both the wild-type and Δ BNLF2a LCLs were decreased by around half of the level of that seen in latent cells (Figure 7A and B lower panels).

Discussion

In this study we have shown that CD8⁺ T cell recognition of immediate early and early lytic cycle antigens is dramatically increased in LCLs transformed with a mutant EBV lacking the immune evasion gene BNLF2a compared to the recognition

of wild-type EBV transformed LCLs. This increase in recognition was conserved across different HLA-class I backgrounds and these effects were seen using multiple different CD8⁺ T cell specificities, reinforcing the role of BNLF2a in active immune evasion during EBV lytic cycle replication. No observable difference in recognition of late lytic cycle antigens was observed, and peptide titration analysis of the late-specific CD8⁺ T cell clones ruled out the possibility that these effectors were simply less avid than those specific for the immediate early and early phases.

The observed increase in recognition of immediate early antigens was not anticipated when considered in the light of BNLF2a's previously described expression kinetics, where BNLF2a transcripts were not found to peak until at least 4 hours after immediate early gene expression [13]. By performing detailed analysis of the transcription and protein expression kinetics of BNLF2a and the immediate early genes in an EBV-infected B cell line in which lytic replication could be induced, we found that although immediate early protein expression was initiated prior to that of BNLF2a, there was a substantial increase in the expression immediate early proteins coincident with the expression of BNLF2a at 3 hours post induction. Epitopes derived from the first wave of immediate early protein synthesis will have no protection from

being processed and presented to CD8⁺ T cells. However given that the major source of epitopes feeding the class I antigen processing pathway is now thought to be from *de novo* synthesized proteins in the form of short-lived defective ribosomal products (DRiPs) rather than long lived protein (reviewed in [14]), expression of BNLF2a during this second wave of expression of the immediate early proteins would restrict the supply of epitope peptides at this time.

Analysis of the sequence of early protein expression using the inducible lytic replication system showed that BNLF2a was expressed with the first wave of early proteins, BALF2 and BMLF1. Similar to what is seen with the immediate early proteins, BNLF2a's expression was upregulated coincident with the increasing expression of these early proteins, again at a time when epitope production from these proteins is likely to be maximal. T cell recognition experiments using effectors specific for these proteins showed that deletion of BNLF2a from the targets caused clear increases in recognition of epitopes derived from these proteins compared to those expressed in wild-type targets. This indicates that although BNLF2a is expressed coincidentally with these proteins, it can afford a substantial degree of protection from T cell recognition at this stage. Consistent with this finding was the observation that BNLF2a-deficient cells expressing BZLF1, and thus including those cells progressing through to early stages of the replicative cycle, showed an increase in class I MHC levels relative to wild type transformed cells, confirming BNLF2a's role in inhibiting antigen presentation at this time.

When different CD8⁺ T cell specificities were assayed for their ability to recognize their cognate antigen presented by the Δ BNLF2a LCLs as compared to the wild-type LCLs, variable levels of increased recognition were seen for the different T cell specificities. In some cases why this variability occurs is not clear. The abundance of the source protein does not appear to play a role as T cells specific for the three epitopes derived from BRLF1 namely AEN, YVL and IACP show quite different levels of increased recognition of the Δ BNLF2a LCL. The TAP dependence of the epitopes studied where determined does not appear to correlate with recognition. Furthermore as the hydrophobicity of peptides broadly correlates with the TAP independence [11], no clear correlation is seen between the hydrophobicity or likely TAP independence and the increase in recognition. The HLA C presented epitope IACP was consistently more greatly recognized when presented by the Δ BNLF2a LCL compared to other epitopes presented from these LCLs. Some immune evasion proteins have been described to have allele specificity, such as the cytomegalovirus encoded US3 protein [15], however whether BNLF2a shows allele-specificity requires further investigation.

When the expression profile of the early protein

BMRF1 was examined it showed a delayed pattern of expression relative to BNLF2a and the other early proteins studied. T cell recognition assays with clones specific to epitopes derived from BMRF1 consistently showed the lowest increase in recognition by T cells in BNLF2a-deficient targets, indicating that BNLF2a has some but perhaps a lesser effect on presentation of epitopes from this protein. This raises the possibility that other mechanisms are preventing effective antigen presentation during this later phase of early gene expression. More compelling evidence for other EBV-encoded class I evasion mechanisms comes from the study of the T cell recognition and expression kinetics of late phase protein targets. The expression of the best characterized late protein, BALF4, was seen to increase in the inducible cell line from 6 hours post induction, with heightened expression occurring at 8–12 hours. At this stage BNLF2a protein levels were decreasing in these cells, yet T cell recognition experiments using late-specific effectors to BALF4 and BILF2 show very poor recognition of wild-type LCL targets. Importantly however, when using the same late-specific effectors in recognition assays of BNLF2a-deleted targets, no increase in detection is seen compared to wild-type targets. Given that the target of BNLF2a is the TAP complex and we have shown previously that this complex is not degraded during EBV lytic cycle replication, at least at 24 hours post-induction of lytic cycle [8], this would suggest that EBV-encoded mechanisms other than BNLF2a are operating to block antigen presentation during the late phase of replication. Supporting this idea is the observation that BNLF2a-deficient LCLs expressing the late antigen BALF4 show decreased levels of surface class I MHC molecules similar to wild-type virus transformed cells.

Evasion of CD8⁺ T cell recognition is likely to be most efficient when multiple points of the antigen processing pathway are targeted, with BNLF2a being one of potentially several immune evasion proteins. Other proteins potentially involved in this process include the early-expressed gene *BGLF5* which functions as an alkaline exonuclease and a host protein synthesis inhibitor. BGLF5's inhibition of global protein synthesis, including that of class I MHC, can inhibit effective CD8⁺ T cell recognition of cognate targets [16],[17]. A second candidate recently identified in modulating surface class I levels is the early phase expressed gene *BILF1*, whose product acts to promote turnover of surface class I molecules [18]. Conceivably these proteins may act in a complementary manner to BNLF2a at early time points, initially by BILF1 clearing class I complexes containing immediate early epitopes from the surface of the cell that were produced before BNLF2a function was established and then BGLF5 acting to prevent effective class I synthesis.

As to BNLF2a's function *in vivo*, it is difficult to draw direct inferences from animal herpesvirus models in

which immune evasion genes have been disrupted since the viruses used, either the β -herpesvirus murine cytomegalovirus (MCMV) or the γ -2 herpesvirus MHV-68, have different *in vivo* infection biology compared to EBV. Nevertheless, recent work on the β -herpesvirus MCMV has indicated that deletion of viral regulators of antigen processing either has no effect on immunodominance hierarchies or virus loads [19],[20], or surprisingly, decreases the size of at least some CD8⁺ T cell reactivities [21]; perhaps as a consequence of increased antigen clearance. In the case of MHV-68 which has a similar cellular tropism to EBV, deletion of the immune evasion gene mK3, which is expressed during latency establishment and also during lytic replication, led to increased CD8⁺ T cell responses to lytic proteins yet had little effect on levels of virus undergoing lytic replication. It did however decrease latent viral loads, suggesting a role for mK3 in amplifying the latent virus reservoir [22]. By contrast, BNLF2a is not expressed during latency and EBV's mechanism of amplifying the latent viral load may come more from its growth transforming ability, by directly expanding latently infected B cells when first colonizing the B cell system. Ultimately, the impact BNLF2a has on immunodominance, viral loads and transmission may be best addressed using the closely related rhesus macaque lymphocryptovirus (Cercopithecine herpesvirus 15) model. This virus has a similar biology to EBV and the same repertoire of genes [23], including a BNLF2a homologue which has the ability to cause surface class I MHC downregulation when expressed in rhesus cell lines [9].

Overall, these results indicate that BNLF2a functions to protect the immediate early and early proteins from being efficiently processed and presented to CD8⁺ T cells. We would expect then that *in vivo* BNLF2a would function to shield virus reactivating from latency or initiating lytic cycle replication. Such stage-specific expression of immune evasion genes is a feature of several herpesviruses. Perhaps the clearest example comes from CMV where multiple proteins involved in disrupting CD8⁺ T cell recognition of infected cells have been described. During CMV replication the US3 gene, whose product retains class I complexes in the endoplasmic reticulum, is abundantly expressed during the immediate early phase [24]–[26], while the gene US11, whose product dislocates class I molecules from the endoplasmic reticulum into the cytosol, is expressed predominantly during early phase replication, and the TAP inhibitor US6 is transcribed in early and late phases [27]. The differential expression of these genes then may be in part why these viruses utilize multiple evasion mechanisms. In the case of EBV replication, as BNLF2a acts in a stage-specific manner we suggest that it will act in concert with other EBV encoded immune evasion genes to reduce efficient T-cell surveillance of reactivating or productively infected

host cells.

Materials and Methods

Ethics statement

All experiments were approved by the South Birmingham Local Research Ethics Committee (07/Q2702/24). All patients provided written informed consent for the collection of blood samples and subsequent analysis.

Recombinant EBV strains

Wild-type and Δ BZLF1 recombinant EBV BACs used have been previously described [10]. The generation of a recombinant EBV BAC deleted for *BNLF2a* was performed as follows: a targeting vector containing the *BNLF2a* region was used to delete *BNLF2a* from the wild-type B95.8 EBV BAC genome. The introduction of a tetracycline cassette, flanked by FLP recombinase target sites (FRT), between a unique XhoI site (–6 bp from the *BNLF2a* open reading frame ATG initiation codon) and AatII site (108 bp downstream of the BNLF2a initiation codon) allowed for the insertional mutagenesis of the *BNLF2a* ORF. This left a 66 bp 3' *BNLF2a* sequence fragment intact that was lacking an initiation codon. Homologous recombination of the target vector, via flanking sequences either side of the truncated *BNLF2a*, allowed for the introduction of the mutation into the wild-type EBV B95.8 BAC sequence. Successfully recombined clones were doubly selected on tetracycline and chloramphenicol (the latter resistance cassette present in the wild-type backbone sequence), followed by removal of the tetracycline cassette through transformation of an FLP recombinase. Bacterial clones that survived this selection process were screened with several restriction enzymes and also sequenced to confirm successful disruption of *BNLF2a* (data not shown). Wild-type, Δ BNLF2a and Δ BZLF1 recombinant virus preparations were generated by stably transfecting 293 cells with the corresponding EBV BAC genome and inducing lytic cycle replication, as previously described [10],[28].

Generation of target cell lines and T cell clones

B lymphoblastoid target cell lines (LCLs) were generated by transformation of laboratory donor B lymphocytes (isolated by positive CD19 Dynabead® (Invitrogen) selection, as per the manufacturer's instructions) with the following recombinant EBV viruses: wild-type, Δ BNLF2a and Δ BZLF1. LCLs were maintained in standard medium (RPMI-1640, 2 mM glutamine, and 10% [vol/vol] FCS). Effector CD8⁺ T cells were generated as previously described [6],[29]. CD8⁺ T cell clones used in this study were specific for the following epitopes derived from the respective EBV gene products: RAKFKQLL from BZLF1 presented by HLA-B*0801 [30], AENAGNDAC

from BRLF1 presented by HLA-B*4501 [6], IACPVMRYVLDHLI from BRLF1 presented by HLA-C*0202 [6], ARYAAYYLQF from BALF2 presented by HLA-B*2705 [6], TLDYKPLSV from BMRF1 presented by HLA-A*0201 [31], FLDKGTITL from BALF4 presented by HLA-A*0201 [6], RRRKGIWPL from BILF2 presented by HLA-B*2705 [6], YVLDHLIVV from BRLF1 presented by HLA-A*0201 [32], GLCTLVAML from BMLF1 presented by HLA-A*0201 [29],[33].

CD8⁺ T cell recognition experiments

The capacity of lytic-specific CD8⁺ T cell clones to recognize lytically replicating cells within LCLs of the relevant HLA type was measured by IFN γ ELISA (Endogen). Briefly, target LCLs (5×10^4 cells/well) were co-cultured in triplicate with effector CD8⁺ T cells (5×10^3 cells/well) in V-bottomed 96-well plates in a total of 200 μ l standard media/well and incubated overnight at 37°C with 5% CO₂. After 18 hours 50 μ l of culture supernatant from each well was used for IFN γ detection by ELISA

Reactivation of AKBM cells into EBV lytic cycle

AKBM cells and their use have been described previously [8]. Briefly, this EBV infected cell line contains a reporter GFP-rat CD2 construct under the control of an early EBV promoter to allow identification of cells in lytic cycle. Prior to induction, AKBM cells were sorted by FACS to exclude any GFP⁺ cells that had spontaneously entered lytic cycle. The GFP⁺ fraction was then induced into lytic cycle by crosslinking of surface IgG molecules as previously described [8]. Cells were then harvested at the indicated timepoints post induction for western blotting and qRT-PCR analysis.

Western blot assays

Total cell lysates were generated by denaturation in lysis buffer (final concentration: 8 M urea, 50 mM Tris/HCl pH 7.5, 150 mM sodium 2-mercaptoethanesulfonate) and sonicated. Protein concentration was determined using a Bradford protein assay (Bio-Rad), and 20 μ g of protein for each sample was separated by SDS-polyacrylamide gel electrophoresis (SDS-PAGE) using a Bio-Rad Mini Gel tank. Proteins were blotted onto nitrocellulose membranes and blocked by incubation for 1 hr in 5% skimmed-milk powder dissolved in PBS-Tween 20 detergent (0.05% [vol/vol]). Specific proteins were detected by incubation with primary antibodies for BZLF1 (murine monoclonal antibody (MAb) BZ.1, final concentration 0.5 μ g/ml, [34]), BRLF1 (murine MAb clone 8C12, final concentration 2.5 μ g/ml, Argene, cat. # 11-008), BMLF1 (rabbit serum to EBV BSLF2/BMLF1-encoded SM, clone EB-2, used at 1/6000 [35]), BMRF1 (murine MAb clone OT14-E, used at 1/2000 [36]), BALF2 (murine MAb clone

OT13B, used at 1/5000, [37]), BNLF2a (clone 5B9, used at 1/100, a rat hybridoma supernatant directed to the N-terminal region of BNLF2a generated by E. Kremmer through immunization of Lou/C rats with KLH-coupled BNLF2a peptides, followed by fusion of rat immune spleen cells with the myeloma cell line P3X63-Ag8.653), BALF4 (murine MAb clone L2, used at 1/100, [38]) BFRF3 (rat MAb clone OT15-E, used at 1/250, J. M. Middeldorp, [39]) and EBNA2 (murine MAb clone PE-2, used at 1/50, [40]) for 2 hrs at room temperature, followed by extensive washes with PBS-Tween. Detection of bound primary antibodies was by incubation for 1 hr with appropriate horseradish peroxidase (HRP)-conjugated secondary antibodies (goat anti-mouse IgG:HRP (Sigma, cat. #A4416), goat anti-rat IgG:HRP (Sigma, cat. #A9037), and goat anti-rabbit IgG:HRP (Sigma, cat. #A6154). Bound HRP was then detected by enhanced chemiluminescence (ECL, Amersham).

Quantitative real-time reverse transcription PCR

Total RNA was extracted from 0.5×10^6 cells using a NucleoSpin[®] RNA II kit (Machery-Nagel) followed by Turbo DNA-free[™] (Ambion/Applied Biosystems) treatment to remove any residual DNA contamination, as per the manufacturers' instructions. 500 ng of RNA was reverse transcribed into cDNA using a pool of primers specific for BZLF1, BRLF1, BMLF1, BNLF2a, BALF4 and BLLF1, with GAPDH included as an internal control, followed by subsequent quantitative-PCR (q-PCR). EBV lytic gene primers were as follows (primer sequences in parenthesis): BZLF1 (cDNA 5'GCA GCC ACC TCA CG3', F 5'ACG ACG CAC ACG GAA ACC3', R 5'CTT GGC CCG GCA TTT TCT3', probe 5'GCA TTC CTC CAG CGA TTC TGG CTG TT3'), BRLF1 (cDNA 5'CAG GAA TCA TCA CCC G3', F 5'TTG GGC CAT TCT CCG AAA C3', R 5'TAT AGG GCA CGC GAT GGA A3', probe 5'AGA CGG GCT GAG AAT GCC GGC3'), BMLF1 (cDNA 5'GAG GAT GAAATC TCT CCA T3', F 5'CCC GAA CTA GCA GCA TTT CCT3', R 5'GAC CGC TTC GAG TTC CAG AA3', probe 5'AAC GAG GAT CCC GCA GAG AGC CA3'), BNLF2a (cDNA 5'GTC TGC TGA CGT CTG G3', F 5'TGG AGC GTG CTT TGC TAG AG3', R 5'GGC CTG GTC TCC GTA GAA GAG3', probe 5'CCT CTG CCT GCG GCC TGC C3'), BALF4 (cDNA 5'CCA TCA ACA GGC CCT C3', F 5'CCA GCT TTC CTT TCC GAG TCT3', R 5'ACA CTG GAT GTC CGA GGA GAA3', probe 5'TCC AGC CAC GGC GAC CTG TTC3'), and BLLF1 (cDNA 5'ACT GCA GTA CTA GCA TGG3', F 5'AGA ATC TGG GCT GGG ACG TT3', R 5'ACA TGG AGC CCG GAC AAG T3', probe 5'AGC CCA CCA CAG ATT ACG GCG GT3'). cDNA and forward/reverse primers were synthesised by Alta Bioscience (University of Birmingham). Probes were synthesised by Eurogentec S.A and labelled with 5' FAM fluorophore and 3' TAMRA quencher. Data was normalised to GAPDH

expression, and expressed as relative to the maximal level of transcript for each gene.

Flow cytometry

LCLs were assayed for the percentage of cells spontaneously reactivating into lytic cycle by intracellular staining for BZLF1. Cells were first fixed using 100 μ l of Ebiosciences Intracellular (IC) Fixative (cat. # 00-8222-49) for 1 hr on ice, followed by permeabilisation through the addition of 100 μ l Triton X-100 (final concentration 0.2%) and a further 30 minute incubation on ice. After extensive washing with PBS, cells were incubated with 1 μ g/ml of either MAb BZ.1 (anti-BZLF1) or with an IgG₁ isotype control antibody for 1 hr at 37°C. Cells were washed twice in PBS and then incubated with 1:20-diluted R-phycoerythrin-conjugated goat anti-mouse IgG₁ antibody (AbD Serotec, cat. # STAR132PE) for 1 hr at 37°C. Following further washes cells were resuspended in IC fixative and analysed on a Dako Cyan flow cytometer (Dako, Denmark).

LCL surface HLA class I and intracellular lytic-cycle EBV antigens were detected simultaneously by first staining viable cells with 1:15-diluted allophycocyanin-conjugated-anti-human HLA-A,B,C (Biolegend, cat. # 311410) antibody for 30 minutes on ice. Cells were then washed extensively in PBS and fixed and permeabilised as above, followed by incubation for 1 hr at 37°C with 1 μ g/ml of either MAb BZ.1 (immediate early antigen BZLF1) or L2 (late antigen BALF4), or IgG₁ isotype control. After several washes in PBS cells were incubated for 1 hr with 1:20-diluted R-phycoerythrin-conjugated goat anti-mouse IgG₁ antibody as above. Cells were washed and fixed as above, followed by analysis on a Dako cytometer (Dako, Denmark). All flow data was analyzed using FlowJo software (Tree Star).

Acknowledgements

We thank Daphne van Leeuwen for excellent technical support.

This work was supported by a grant from the Medical Research Council (G9901249). ADH is funded by a Medical Research Council UK New Investigator Award (G0501074); ADH and MR are supported by the Wellcome Trust. Additional support for DH, MER and EJJW was from the Dutch Cancer Society (UL 2005-3259), the M.W. Beijerinck Virology Fund of the Royal Academy of Arts and Sciences, and the Netherlands Organisation for Scientific Research (Vidi 917.76.330). The funders had no role in study design, data collection and analysis, decision to publish, or preparation of the manuscript.

The authors have declared that no competing interests exist.

References

1. Stinchcombe JC, Griffiths GM. The role of the secretory immunological synapse in killing by CD8⁺ CTL. *Semin Immunol.* 2003;15:301–305.
2. Groothuis TA, Griekspoor AC, Neijssen JJ, Herberts CA, Neeffjes JJ. MHC class I alleles and their exploration of the antigen-processing machinery. *Immunol Rev.* 2005;207:60–76.
3. Vossen MT, Westerhout EM, Soderberg-Naucler C, Wiertz EJ. Viral immune evasion: a masterpiece of evolution. *Immunogenetics.* 2002;54:527–542.
4. Lilley BN, Ploegh HL. Viral modulation of antigen presentation: manipulation of cellular targets in the ER and beyond. *Immunol Rev.* 2005;207:126–144.
5. Rickinson A, Kieff E. Epstein-Barr virus. In: Knipe DM, Howley PM, editors. *Fields Virology* Philadelphia. Walters Kluwer/Lippincott, Williams & Wilkins; 2007. pp. 2655–2700.
6. Pudney VA, Leese AM, Rickinson AB, Hislop AD. CD8⁺ immunodominance among Epstein-Barr virus lytic cycle antigens directly reflects the efficiency of antigen presentation in lytically infected cells. *J Exp Med.* 2005;201:349–360.
7. Keating S, Prince S, Jones M, Rowe M. The lytic cycle of Epstein-Barr virus is associated with decreased expression of cell surface major histocompatibility complex class I and class II molecules. *J Virol.* 2002;76:8179–8188.
8. Rensing ME, Keating SE, van Leeuwen D, Koppers-Lalic D, Pappworth IY, *et al.* Impaired transporter associated with antigen processing-dependent peptide transport during productive EBV infection. *J Immunol.* 2005;174:6829–6838.
9. Hislop AD, Rensing ME, van Leeuwen D, Pudney VA, Horst D, *et al.* A CD8⁺ T cell immune evasion protein specific to Epstein-Barr virus and its close relatives in Old World primates. *J Exp Med.* 2007;204:1863–1873.
10. Feederle R, Kost M, Baumann M, Janz A, Drouet E, *et al.* The Epstein-Barr virus lytic program is controlled by the co-operative functions of two transactivators. *Embo J.* 2000;19:3080–3089.
11. Lautscham G, Mayrhofer S, Taylor G, Haigh T, Leese A, *et al.* Processing of a multiple membrane spanning Epstein-Barr virus protein for CD8(+) T cell recognition reveals a proteasome-dependent, transporter associated with antigen processing-independent pathway. *J Exp Med.* 2001;194:1053–1068.
12. Takada K, Ono Y. Synchronous and sequential activation of latently infected Epstein-Barr virus genomes. *J Virol.* 1989;63:445–449.
13. Yuan J, Cahir-McFarland E, Zhao B, Kieff E. Virus and cell RNAs expressed during Epstein-Barr virus replication. *J Virol.* 2006;80:2548–

- 2565.
14. Yewdell JW, Nicchitta CV. The DRiP hypothesis decennial: support, controversy, refinement and extension. *Trends Immunol.* 2006;27:368–373.
 15. Park B, Kim Y, Shin J, Lee S, Cho K, *et al.* Human cytomegalovirus inhibits tapasin-dependent peptide loading and optimization of the MHC class I peptide cargo for immune evasion. *Immunity.* 2004;20:71–85.
 16. Rowe M, Glaunsinger B, van Leeuwen D, Zuo J, Sweetman D, *et al.* Host shutoff during productive Epstein-Barr virus infection is mediated by BGLF5 and may contribute to immune evasion. *Proc Natl Acad Sci U S A.* 2007;104:3366–3371.
 17. Zuo J, Thomas W, van Leeuwen D, Middeldorp JM, Wiertz EJ, *et al.* The DNase of gammaherpesviruses impairs recognition by virus-specific CD8⁺ T cells through an additional host shutoff function. *J Virol.* 2008;82:2385–2393.
 18. Zuo J, Currin A, Griffin BD, Shannon-Lowe C, Thomas WA, *et al.* The Epstein-Barr virus g-protein-coupled receptor contributes to immune evasion by targeting MHC class I molecules for degradation. *PLoS Pathog.* 2009;5:e1000255. doi:10.1371/journal.ppat.1000255.
 19. Munks MW, Pinto AK, Doom CM, Hill AB. Viral interference with antigen presentation does not alter acute or chronic CD8 T cell immunodominance in murine cytomegalovirus infection. *J Immunol.* 2007;178:7235–7241.
 20. Gold MC, Munks MW, Wagner M, McMahon CW, Kelly A, *et al.* Murine cytomegalovirus interference with antigen presentation has little effect on the size or the effector memory phenotype of the CD8 T cell response. *J Immunol.* 2004;172:6944–6953.
 21. Bohm V, Simon CO, Podlech J, Seckert CK, Gendig D, *et al.* The immune evasion paradox: immunoevasins of murine cytomegalovirus enhance priming of CD8 T cells by preventing negative feedback regulation. *J Virol.* 2008;82:11637–11650.
 22. Stevenson PG, May JS, Smith XG, Marques S, Adler H, *et al.* K3-mediated evasion of CD8(+) T cells aids amplification of a latent gamma-herpesvirus. *Nat Immunol.* 2002;3:733–740.
 23. Rivaille P, Jiang H, Cho YG, Quink C, Wang F. Complete nucleotide sequence of the rhesus lymphocryptovirus: genetic validation for an Epstein-Barr virus animal model. *J Virol.* 2002;76:421–426.
 24. Biegelke BJ. Regulation of human cytomegalovirus US3 gene transcription by a cis-repressive sequence. *J Virol.* 1995;69:5362–5367.
 25. Tenney DJ, Colberg-Poley AM. Human cytomegalovirus UL36-38 and US3 immediate-early genes: temporally regulated expression of nuclear, cytoplasmic, and polysome-associated transcripts during infection. *J Virol.* 1991;65:6724–6734.
 26. Jones TR, Wiertz EJ, Sun L, Fish KN, Nelson JA, *et al.* Human cytomegalovirus US3 impairs transport and maturation of major histocompatibility complex class I heavy chains. *Proc Natl Acad Sci U S A.* 1996;93:11327–11333.
 27. Jones TR, Muzithras VP. Fine mapping of transcripts expressed from the US6 gene family of human cytomegalovirus strain AD169. *J Virol.* 1991;65:2024–2036.
 28. Delecluse HJ, Hilsendegen T, Pich D, Zeidler R, Hammerschmidt W. Propagation and recovery of intact, infectious Epstein-Barr virus from prokaryotic to human cells. *Proc Natl Acad Sci U S A.* 1998;95:8245–8250.
 29. Steven NM, Annels NE, Kumar A, Leese AM, Kurilla MG, *et al.* Immediate early and early lytic cycle proteins are frequent targets of the Epstein-Barr virus-induced cytotoxic T cell response. *J Exp Med.* 1997;185:1605–1617.
 30. Bogedain C, Wolf H, Modrow S, Stuber G, Jilg W. Specific cytotoxic T lymphocytes recognize the immediate-early transactivator Zta of Epstein-Barr virus. *J Virol.* 1995;69:4872–4879.
 31. Hislop AD, Annels NE, Gudgeon NH, Leese AM, Rickinson AB. Epitope-specific evolution of human CD8(+) T cell responses from primary to persistent phases of Epstein-Barr virus infection. *J Exp Med.* 2002;195:893–905.
 32. Saulquin X, Ibsch C, Peyrat MA, Scotet E, Hourmant M, *et al.* A global appraisal of immunodominant CD8 T cell responses to Epstein-Barr virus and cytomegalovirus by bulk screening. *Eur J Immunol.* 2000;30:2531–2539.
 33. Scotet E, David-Ameline J, Peyrat MA, Moreau-Aubry A, Pinczon D, *et al.* T cell response to Epstein-Barr virus transactivators in chronic rheumatoid arthritis. *J Exp Med.* 1996;184:1791–1800.
 34. Young LS, Lau R, Rowe M, Niedobitek G, Packham G, *et al.* Differentiation-associated expression of the Epstein-Barr virus BZLF1 transactivator protein in oral hairy leukoplakia. *J Virol.* 1991;65:2868–2874.
 35. Buisson M, Manet E, Trescol-Biemont MC, Gruffat H, Durand B, *et al.* The Epstein-Barr virus (EBV) early protein EB2 is a posttranscriptional activator expressed under the control of EBV transcription factors EB1 and R. *J Virol.* 1989;63:5276–5284.
 36. Zhang JX, Chen HL, Zong YS, Chan KH, Nicholls J, *et al.* Epstein-Barr virus expression within keratinizing nasopharyngeal carcinoma. *J Med Virol.* 1998;55:227–233.
 37. Zeng Y, Middeldorp J, Madjar JJ, Ooka T. A

- major DNA binding protein encoded by BALF2 open reading frame of Epstein-Barr virus (EBV) forms a complex with other EBV DNA-binding proteins: DNAase, EA-D, and DNA polymerase. *Virology*. 1997;239:285–295.
38. Kishishita M, Luka J, Vroman B, Poduslo JF, Pearson GR. Production of monoclonal antibody to a late intracellular Epstein-Barr virus-induced antigen. *Virology*. 1984;133:363–375.
 39. van Grunsven WM, van Heerde EC, de Haard HJ, Spaan WJ, Middeldorp JM. Gene mapping and expression of two immunodominant Epstein-Barr virus capsid proteins. *J Virol*. 1993;67:3908–3916.
 40. Young L, Alfieri C, Hennessy K, Evans H, O'Hara C, *et al*. Expression of Epstein-Barr virus transformation-associated genes in tissues of patients with EBV lymphoproliferative disease. *N Engl J Med*. 1989;321:1080–1085.

Supplementary data

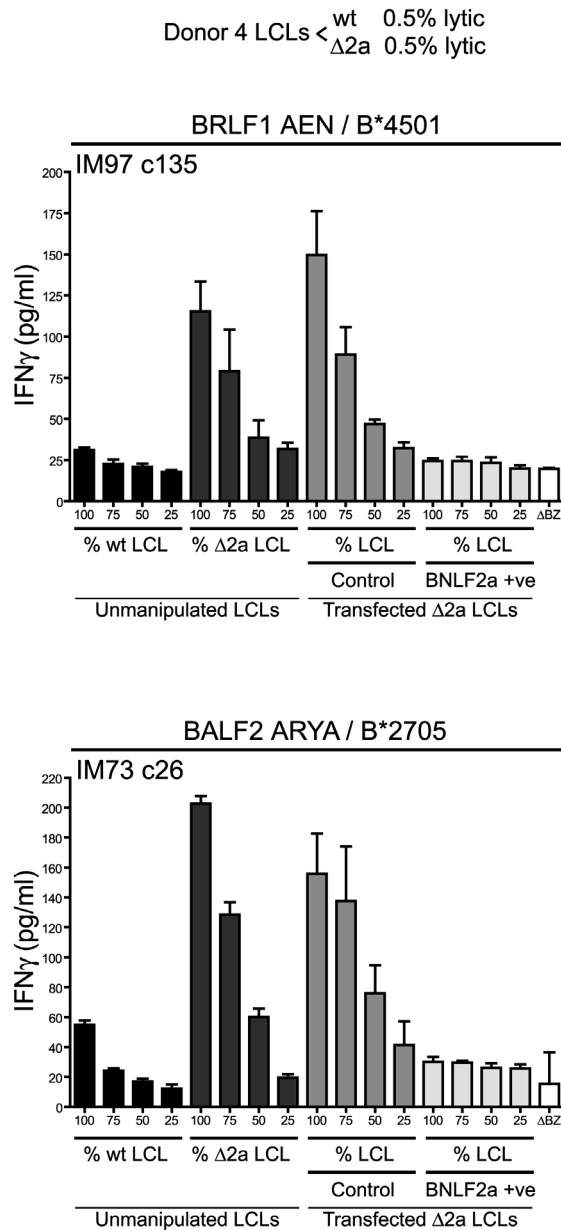


Figure S1. T cell recognition of Δ BNL f 2a LCLs when BNL f 2a is expressed in these cells

Δ BNL f 2a LCLs were transfected by electroporation with a plasmid which co-expressed BNL f 2a and the truncated nerve growth factor (NGFR) gene. After 48 hours, BNL f 2a expressing cells were purified by selecting NGFR expressing cells. These cells were used in standard T cell recognition assays in parallel with the NGFR-negative cells from the transfection, wild-type virus transformed LCLs, the unmanipulated Δ BNL f 2a LCL and the Δ BZLF1 knock out LCL. CD8 $^{+}$ T cells specific for the immediate early epitope AEN and early epitope ARYA were used as effectors in parallel assays. One representative assay of two transfection experiments is shown.

Chapter 7

Residues required for host shutoff activity are located in the “bridge” of the Epstein-Barr virus protein BGLF5

D. Horst, W.P. Burmeister, I.G.J. Boer, D. van Leeuwen, A.E. Gorbalenya, M. Buisson, E.J.H.J. Wiertz and M.E. Rensing

In preparation

Abstract

Replication of the human herpesvirus Epstein-Barr virus (EBV) drastically impairs cellular protein synthesis. This host shutoff phenotype results from mRNA degradation upon expression of the early lytic-phase protein BGLF5. Interestingly, BGLF5 is the viral DNase, or alkaline exonuclease, homologues of which are present throughout the herpesvirus family. During productive infection, this DNase is essential for processing and packaging of the viral genome. In contrast to the widely conserved DNase activity, host shutoff is only mediated by the alkaline exonucleases of the subfamily of gamma-herpesviruses.

Here, we show that BGLF5 degrades mRNAs of both cellular and viral origin, irrespective of poly-adenylation. Furthermore, host shutoff by BGLF5 induces nuclear relocalization of the cytosolic poly-A binding protein (PABPC). Guided by the recently resolved BGLF5 structure, mutants were generated and analysed for functional consequences on DNase and RNase activities. On the one hand, a point mutation destroying DNase activity also blocks RNase function, implying that both activities share a catalytic site. On the other hand, other mutations are more selective, having a more pronounced effect on either DNA degradation or shutoff. The latter results are indicative of an oligonucleotide binding site partially shared by DNA and RNA. Finally, the flexible “bridge” that crosses the active site canyon of BGLF5 appears to contribute to the interaction with RNA substrates.

These findings contribute to our understanding of the molecular basis for the additional host shutoff function that is shared by the alkaline exonucleases of gamma-herpesviruses, but that is absent from the homologues of alpha- and beta-herpesviruses.

Introduction

Herpesviruses are large DNA viruses that cause lifelong infections in their host. After primary infection, herpesviruses enter a stage of latency during which few (if any) viral proteins are expressed. However, for transmission to another host, a lytic infection is required, resulting in the generation of viral progeny. In cells productively infected with either alpha- or gamma-herpesviruses, an almost complete block in host protein synthesis is observed (18, 41, 43). This host shutoff activity contributes to immune evasion by inhibiting the synthesis of proteins involved in antigen presentation and pathogen recognition (41, 45, 46). Furthermore, blocking host protein synthesis could provide an advantage to viral replication as it is anticipated to devote the cellular ribosomes to the synthesis of viral proteins.

For alpha-herpesviruses, such as herpes simplex virus (HSV) types 1 and 2 and bovine herpesvirus type 1, host shutoff activity is mediated by the virion host shutoff protein (vhs) (20, 23, 28, 31, 32, 36, 39). In contrast, host shutoff upon productive infection with gamma-herpesviruses, including the two human viruses Epstein-Barr virus (EBV) and Kaposi's sarcoma-associated herpesvirus (KSHV), is mediated by the alkaline exonucleases BGLF5 (41) and SOX (18), respectively. These alkaline exonucleases (AEs), which were originally identified as viral DNases, are conserved throughout the herpesvirus family. However, host shutoff activity exerted by these AE proteins is only observed for gamma-herpesviruses. Possibly, the alkaline exonucleases of gamma-herpesviruses attained host shutoff activity relatively late during evolution, i.e. after separation of the gamma-herpesvirus subfamily from the alpha- and beta-herpesvirus subfamilies. Alternatively, host shutoff activity might have been lost by the AEs of alpha- and beta-herpesviruses.

Despite the host shutoff proteins encoded by alpha- and gamma-herpesviruses being completely unrelated, they all act through mRNA degradation. The alpha-herpesvirus HSV-encoded vhs protein, which was identified decades ago as mediator of host shutoff, has intrinsic RNase activity (10, 49) and associates with eIF4H and eIF4F (14, 15, 37). Interaction of vhs with these translation initiation factors is likely to account for the specific targeting of mRNAs for degradation. However, for the gamma-herpesviruses, the first light is just beginning to be shed on the mechanism(s) contributing to AE-mediated host shutoff. Interestingly, AE proteins of both EBV and KSHV have recently been shown to also exert RNase activity *in vitro* (2, 4). The SOX protein of KSHV additionally affects the cytosolic poly-A binding protein (PABPC). Under steady-state conditions, PABPC associates with both eIF4G and the poly-A tail of mRNAs in the cytoplasm, thereby inducing the circularization of mRNAs. This facilitates translation initiation and

hampers mRNA degradation (21). Furthermore, the interaction of PABPC with mRNAs retains PABPC in the cytoplasm (30). Upon expression of KSHV SOX and subsequent mRNA depletion from the cytoplasm, PABPC is relocalized to the nucleus (30, 33), where it induces hyperadenylation and nuclear retention of mRNAs (29, 33). So far, it is unknown whether this also occurs for EBV BGLF5.

Recently, the crystal structures of the EBV BGLF5 (4) and KSHV SOX (2, 8) proteins were solved. These structures reveal a high degree of similarity between the viral proteins and lambda exonuclease, all belonging to the D-(D/E)XK superfamily of nucleases. Previously, mutation of the aspartic acid 203 residue of BGLF5, which forms part of the catalytic site, was found to destroy both DNase (4, 34) and RNase (4) activity of the AE protein. So far, it is not clear to what extent the two activities share a common site and what mechanism underlies the host shutoff activity only exerted by gamma-herpesvirus AE proteins. To address this issue and to obtain more detailed insight into the molecular mechanism(s) of BGLF5 function, we examined mutants of this EBV protein for their DNase and host shutoff activities.

Results

Modelling and sequence alignments point to a role for the "bridge" in the host shutoff activity of EBV BGLF5

Based on the assumption that functional conservation of host shutoff activity among the gamma-herpesviruses would be based on amino acid sequence homology, we aligned, modelled, and compared the amino acid sequences of the EBV AE protein BGLF5 and its homologues encoded by 18 other gamma-herpesviruses (Figure 1). A complete amino acid sequence alignment of the AE proteins encoded by the different gamma-herpesviruses is shown in Figure S1. We observed that conserved residues map principally to the region involved in catalysis and to the surface involved in the contact with dsDNA, as well as to the "bridge" that crosses the active site (Figure 1A). To a lesser extent, residues on top of the nuclease domain are conserved (Figure 1A, top right of the structure). There is no significant residue conservation on the bottom of the protein (data not shown).

Next, the AE protein sequences of these gamma-herpesviruses were compared to those of 8 beta-herpesviruses and 23 alpha-herpesviruses, with the latter only exerting DNase and lacking host shutoff activity. The dual function of the gamma-herpesvirus exonucleases, having both DNase and RNase activity, is probably reflected by their higher degree of conservation (39% for gamma-herpesviruses versus 30% and 35% for beta-herpesviruses and alpha-herpesviruses, respectively). This conservation appears to be mostly lost in the bridge region of the

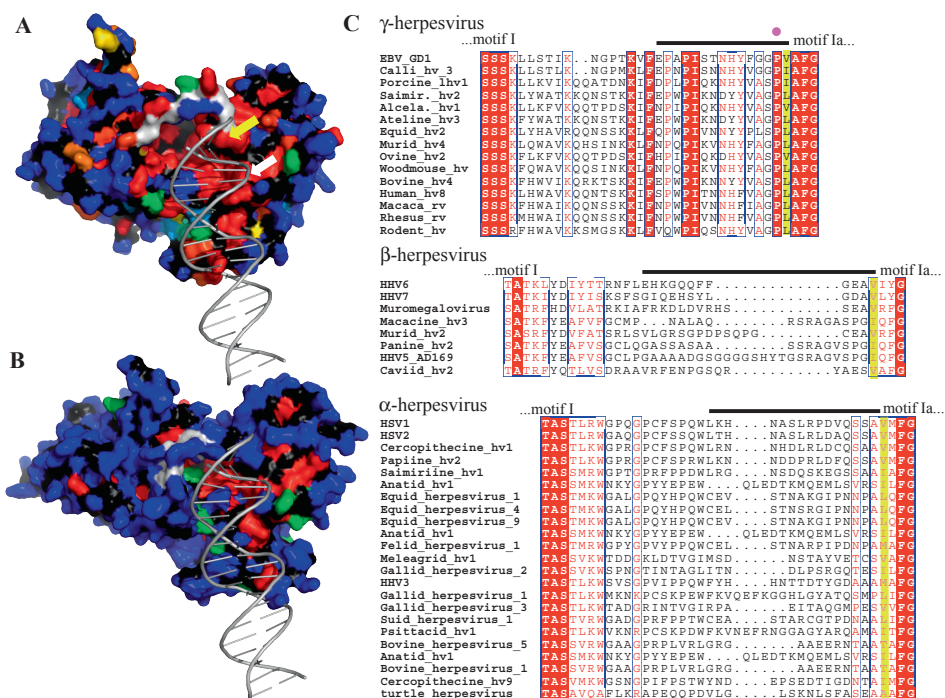


Figure 1. Structure and amino acid sequence comparisons for herpesvirus exonucleases

(A) Sequence conservation among 28 AE sequences of gamma-herpesviruses (See Table S1) mapped onto the surface of the EBV nuclease BGLF5. Conservation of the side chains decreases from red (strictly conserved) over orange, yellow and green to blue (variable residues). Main chain atoms are coloured in black, the ones of the bridge are coloured in white. The position of a dsDNA substrate is derived from the KSHV dsDNA-SOX complex (2). The position of lambda exonuclease (50), is indicated by a yellow arrow, the white arrow indicates the K231 residue mutated in this study. (B) Analysis of the sequence conservation within 8 beta-herpesvirus exonucleases (See Table S1) based on a theoretical model of their structure. Colours as in panel A. (C) Sequence conservation in the region of the bridge, which is indicated by a black line above the amino acid sequence alignments. A yellow background marks the residues corresponding to the amino acid essential for exonuclease activity in lambda exonuclease (50). The pink dot marks the position of EBV P158. (hv, herpesvirus; rv, rhadinovirus).

beta-herpesvirus AE proteins; the areas likely involved in the DNase function present the same pattern of sequence conservation as in the gamma-herpesvirus AE proteins (Figure 1B). Likewise, the residues corresponding to the bridge of alpha-herpesvirus AEs show virtually no conservation (Figure 1C).

In conclusion, amino acids of the bridge (Figure 1) show a high degree of conservation among the gamma-herpesvirus AE proteins, but not for alpha- and beta-herpesvirus AE proteins. This points towards a specific role for the bridge in the gamma-herpesvirus AE proteins for their additional host shutoff function.

Selective mutagenesis of BGLF5

To obtain more insight into the mechanism of host shutoff by the gamma-herpesvirus alkaline exonucleases, we integrated various assays to probe the different effector functions of EBV BGLF5 and mutants thereof. As a measure of DNase activity, we investigated the ability of *in vitro* synthesized (mutant) BGLF5 to degrade linearized DNA (51) (Figure

2). Shutoff activity was measured in transiently transfected cells by (i) downregulation of GFP reporter protein levels by (mutant) BGLF5 (51) (Figure 3) and (ii) nuclear relocalization of PABPC, used earlier to assess SOX shutoff activity (33) (Figure 4).

Using the above assays, we have studied the following mutants of BGLF5 (Figure S2). First, the catalytically inactive mutant D203S was included in our assays as a positive control, as this mutation is known to destroy both DNase and RNase activity (4).

Secondly, guided by the structural model of BGLF5 and the sequence alignments of the viral AE proteins (Figure 1), we mutated the proline residue at amino acid position 158 of BGLF5. This P158 residue is located at the C-terminal side of the bridge that crosses the active site of BGLF5 ((4) and Figure 1C, pink dot) and terminates the α -helix that contains motif Ia. This residue is conserved within the gamma-herpesvirus AE proteins, but not among the AE proteins encoded by alpha- and beta-herpesviruses (Figure 1C). The P158 residue of BGLF5 was substituted for an alanine,

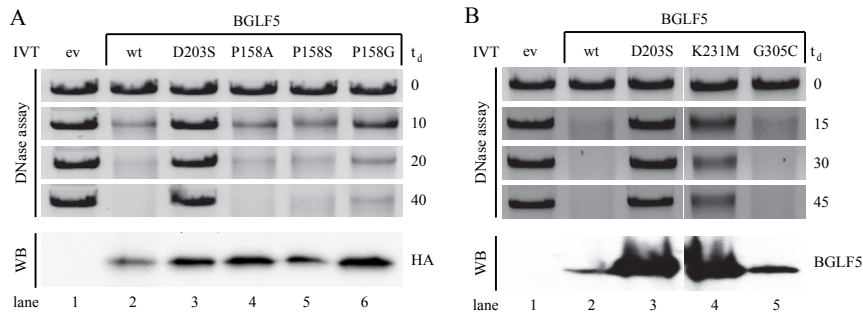


Figure 2. Point mutations within EBV BGLF5 differentially affect DNase activity

(A and B) Linearized pcDNA3 DNA was incubated with the indicated (mutant) BGLF5 proteins synthesized as *in vitro* translation products. Samples of pcDNA3 substrate taken before and at the indicated time points during the degradation reaction (t_d : time of degradation in minutes) were resolved by agarose gel electrophoresis and visualized by ethidium bromide staining. To visualize the AE proteins as added to the enzyme reaction mixtures, 5 μ l of the *in vitro* translation products were separated by SDS-PAGE and analyzed by Western blotting (WB) using either antibodies specific for (A) the HA-tag added to the C-terminus of BGLF5 (3F10) or (B) with a BGLF5-specific polyclonal rabbit serum (k120). (ev, empty vector; wt, wild-type).

serine, or glycine residue, amino acid substitutions that progressively affect the flexibility of the bridge or affect the termination of the α -helix. These residues naturally occur in the AE proteins encoded by alpha- and beta-herpesviruses (Figure 1C).

Thirdly, an earlier random mutagenesis screen yielded a BGLF5 mutant containing two amino acid substitutions, K231M and G305C, that appeared to have lost shutoff activity while retaining DNase activity (51). The individual K231M substitution was concluded to be responsible for this genetic separation. However, from the position of the K231 residue in the structure and sequence alignments, no obvious explanation for a selective block in shutoff or retention of DNase activity occurred to us, as it localizes to motif 3. Therefore, the individual K231M and G305C mutations were also included in our analysis.

Mutations affecting the conserved motifs of BGLF5 completely abolish DNase activity, whereas those in the bridge do not

The effects of the mutations within the BGLF5 protein on DNase activity were examined by incubation of linearized DNA plasmid with *in vitro* synthesized BGLF5 protein. Western blot analysis verified that all BGLF5 proteins were synthesized (Figure 2A and B, respectively). Subsequently, samples were taken at various time points during the DNase reaction and were resolved by agarose gel electrophoresis. In the presence of wild-type (wt) BGLF5, linear DNA is completely digested within 40 minutes (Figure 2A, lane 2). This DNase activity is comparable to that exerted by the AE protein of the alpha-herpesvirus HSV-1 (data not shown). On the contrary, no degradation was observed for samples incubated with the catalytic site mutant BGLF5 D203S (Figure 2A, lane 3 and 4)). Analysis of the P158 “bridge” mutants revealed that the capacity to degrade DNA was comparable for the alanine and serine mutants and the

wild-type protein at all times (Figure 2A, lanes 2, 4, and 5). Surprisingly, substitution of P158 by a glycine residue affected DNase activity, although not resulting in complete loss of DNase activity as observed for D203S (Figure 2A, lanes 2, 3 and 6).

We observed a drastically reduced ability of the BGLF5 K231M protein to digest linearized DNA plasmids when compared to wild-type BGLF5 (Figure 2B, lanes 2 and 4), as opposed to earlier data (51). However, unlike the complete inactivation of BGLF5 by the D203S mutation, the DNase activity is not entirely destroyed by the K231M mutation (Figure 2B, compare lanes 3 and 4) and could thus account for the discrepancy between this study and previous results (51). The BGLF5 G305C mutant degraded the linearized plasmid as efficiently as wild-type BGLF5 (Figure 2B, lane 2 and 5).

In summary, the proline 158 residue of EBV BGLF5 can be mutated into an alanine or serine residue without consequences for DNase activity. Surprisingly, replacement of Pro158 by a glycine residue retarded DNase activity. Mutation of the K231 residue into a methionine resulted in a substantial drop in DNase activity.

Host shutoff function of BGLF5 is affected both by mutations leading to loss of DNase activity and, more selectively, by “bridge” mutations

Host shutoff activity of the alkaline exonucleases was examined using two approaches, namely by flow cytometry- and immunofluorescence-based assays. First, 293T cells were cotransfected to express the reporter protein GFP and the alpha-herpesvirus HSV-1 AE protein, or the gamma-herpesvirus AE proteins KSHV SOX and EBV (mutant) BGLF5. Two days after transfection, host shutoff activity was measured by determining the reduction in GFP levels using flow cytometry.

In control cells cotransfected with GFP and an empty

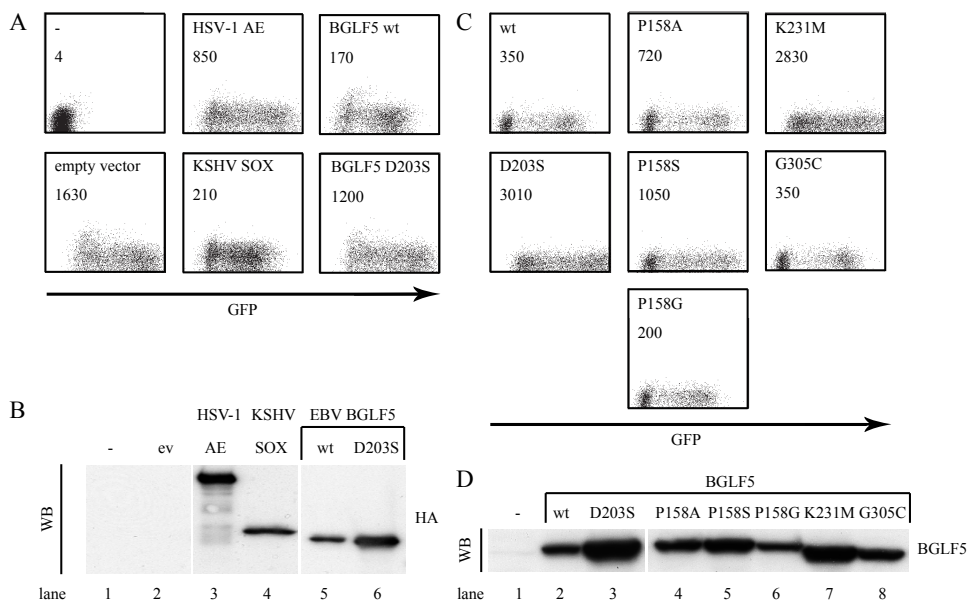


Figure 3. Point mutations within BGLF5 differentially affect shutoff activity

(A and C) 293T cells were cotransfected with the reporter plasmid pcDNA3-IRES-nlsGFP and a pcDEF vector encoding HSV-1 AE, KSHV SOX, wild-type BGLF5 (wt), or the indicated BGLF5 mutants (at a 1:4 ratio). At 48 h after transfection, GFP intensity was analyzed by flow cytometry as a measure of shutoff activity. The geometric mean fluorescence intensity for GFP is indicated in the left upper corner of the dotplots. (B and D) Cellular expression of the various AE proteins tested in A and C was assessed by Western blot analysis using antibodies specific for (B) the HA-tag (3F10) or (D) BGLF5 (k120).

vector, high levels of GFP were observed (Figure 3A, lower left panel). A vector encoding the HSV-1 AE protein, lacking host shutoff activity, was taken along as a negative control. Expression of HSV-1 AE did not result in a major reduction in the expression of GFP (Figure 3A, upper middle panel). In contrast, cells cotransfected with GFP and either wild-type SOX or BGLF5 had markedly reduced levels of GFP (Figure 3A, lower middle and upper right panel). The BGLF5 D203S mutant did not profoundly diminish GFP expression (Figure 3A, lower right panel), in support of this protein having lost its host shutoff activity. Thus, this flow cytometry-based assay reflects host shutoff activity exerted by AE proteins of the subfamily of gamma-herpesviruses.

In the next experiment, mutants of EBV BGLF5 were compared to the wild-type protein (Figure 3C). Expression of the three P158 “bridge” mutants caused a reduction in GFP levels, but the degree of host shutoff varied. The alanine and serine mutants were impaired in their host shutoff activity compared to the wild-type protein, albeit less so than the D203S mutant (Figure 3C, left and middle panels). Interestingly, substitution of the proline 158 residue by a glycine retained or even slightly enhanced host shutoff activity (Figure 3C, compare the lower middle and upper left panel). Similar to the catalytic site D203S mutation, the K231M “motif 3” mutation completely abrogated

the ability of BGLF5 to block GFP expression (Figure 3C, lower left and upper right panel). In contrast, host shutoff activity was not affected by the G305C mutation (Figure 3C, lower right panel).

Proper cellular expression of the constructs was visualized by Western blotting using antibodies specific for BGLF5 or for the HA-tag added to the herpesvirus alkaline exonucleases. All proteins were expressed properly (Figure 3 B and D). Interestingly, expression levels of the AE proteins were negatively correlated with their host shutoff activity. The highest protein band intensities were detected for HSV-1 AE and the catalytically inactive EBV BGLF5 D203S mutant (Figure 3B, lanes 3 and 6). In contrast, the AE proteins capable of RNA degradation, BGLF5 and SOX, (Figure 3B, lanes 4 and 5) appeared to also reduce their own protein expression. The flow cytometric data were in line with the Western blot results in that the BGLF5 mutants that had (partly) lost shutoff activity were expressed to the highest levels (Figure 3D, D203S, P158A & S and K231M, lanes 3, 4, 5, and 7, respectively). Conveniently, this strengthens the results regarding the shutoff-defective mutants: no reduction in GFP levels was observed, even though these proteins were expressed at higher levels.

Taken together, both amino acid residues important for DNase activity (D203S and K231M) as well as a

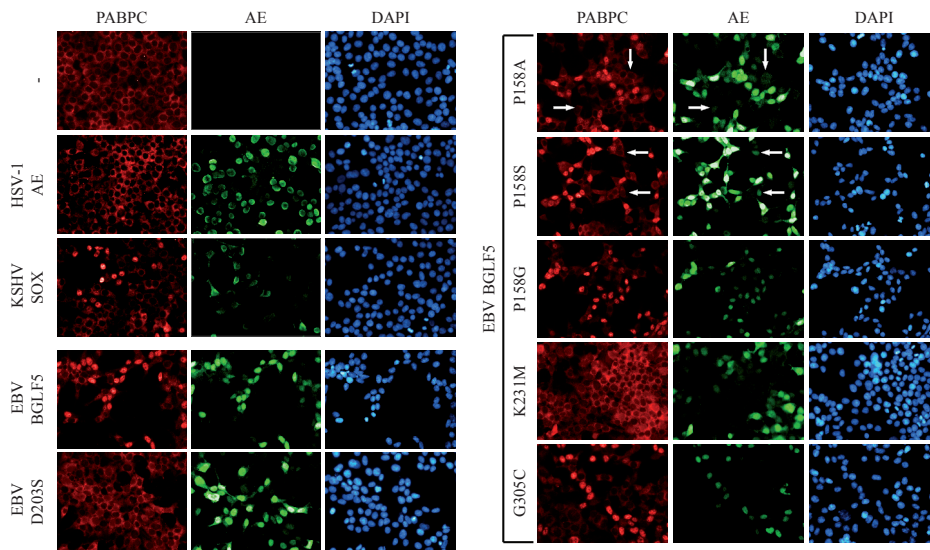


Figure 4. BGLF5 induces nuclear relocalization of PABPC, an activity that is correlated with host shutoff

293T cells were transfected with pcDEF plasmids encoding the individual herpesvirus AE proteins as in Figure 3A and C. After 24 h of transfection, cells were subjected to triple-label immunofluorescence analysis using PABPC-specific antibodies (mAb 10E10 and anti-mouse-Cy3; left panels); AE expression was visualized with HA-specific antibodies (mAb 3F10 and anti-rat Alexa 488; middle panels for negative control, HSV-1 AE and KSHV SOX samples) or with BGLF5-specific antibodies (k120 polyclonal antisera and anti-rabbit Alexa 488; middle panels for (mutant) BGLF5 samples). Cells were counterstained with DAPI to identify nuclei (right panels). The white arrows indicate cells with low levels of the P158A and P158S mutant proteins.

“bridge” amino acid (P158) are involved in BGLF5-mediated host shutoff. The host shutoff activity of the gamma-herpesvirus AE proteins hampers their protein expression.

Shutoff-competent EBV BGLF5 induces nuclear relocalization of PABPC

Our second approach to evaluate shutoff activity exerted by AE variants relied on the nuclear relocalization of PABPC. Previously, Lee *et al.* demonstrated that cellular SOX expression induced relocalization of PABPC to the nucleus and this correlated with host shutoff activity mediated by SOX (33). To assess whether BGLF5 has a similar effect on the distribution of PABPC, localization of endogenous PABPC was determined by immunofluorescence assays using 293T cells transfected to transiently express the shutoff-defective alpha-herpesvirus HSV-1 AE protein, or the shutoff-competent gamma-herpesvirus KSHV SOX and EBV BGLF5 proteins. Paraformaldehyde-fixed, detergent-permeabilized cells were stained using antibodies specific for PABPC and for the HA-tagged viral nucleases. DAPI staining visualized the nuclei.

In control cells, PABPC resided exclusively in the cytoplasm (Figure 4, first panel). Whereas PABPC was still restricted to the cytoplasm of HSV-1 AE-expressing cells, nuclear relocalization of PABPC clearly occurred in those cells that expressed KSHV SOX (Figure 4, compare panels 2 and 3), in agreement

with published results (33). We here show that also BGLF5 induced nuclear relocalization of PABPC (Figure 4, panel 4), further supporting that BGLF5 and SOX use the same strategy to effectuate host shutoff. The cytoplasmic localization of PABPC in cells expressing the catalytically inactive BGLF5 D203S protein (Figure 4, fifth panel) is in line with its loss of host shutoff activity.

Next, effects of the selected BGLF5 mutants on shutoff activity were evaluated using this immunofluorescence-based assay. At large, the P158 and G305C mutants induced nuclear relocalization of PABPC comparable to wild-type BGLF5, whereas the K231M mutant did not (Figure 4, right panels). Interestingly, PABPC relocalization was not observed in cells with low levels of the “bridge” mutant P158A and P158S proteins (Figure 4, panel 6 and 7, indicated by white arrow), suggesting that a certain threshold of BGLF5-mediated host shutoff activity is required to mediate PABPC relocalization.

Altogether, these results show that EBV BGLF5 induces the nuclear relocalization of PABPC, as has been reported for KSHV SOX (33). This ability of the mutant BGLF5 proteins to relocalize PABPC to the nucleus correlates with their ability to reduce GFP expression and, therefore, host shutoff (Table 1).

Specificity of the nuclease activities of BGLF5

Production of relatively large quantities of purified baculovirus-expressed recombinant BGLF5 allowed

BGLF5	Motif	<i>In vitro</i> DNase activity	Reduction GFP levels	Relocalization PABPC	<i>In vitro</i> RNase activity
Wild-type		++	++	++	+
D203S	Catalytic site/II	-	-	-	-
ΔN	-	-	-	-	nt
P158A	I	++	+	+	nt
P158S	I	++	+	+	nt
P158G	I	+	++	++	nt
K231M	III	+/-	-	-	nt
G305C	-	++	++	++	nt

Table 1: Summary of the activities of the BGLF5 protein and mutants thereof. (nt: not tested)

us to investigate the nuclease activities of the EBV protein *in vitro*. The specificity of the viral DNase activity was examined by incubation of linear and circular DNA with either recombinant wild-type or D203S mutant BGLF5. Both linear and circular DNA were digested by wild-type BGLF5, but linear DNA was degraded more efficiently (Figure 5A, lanes 2-5), indicating that the exonuclease activity of BGLF5 is more competent than its endonuclease activity. Recombinant BGLF5 protein with the catalytic site mutation (D203S) did not induce DNA degradation of linear DNA (Figure 5A, lanes 6-9). Surprisingly, incubation of circular DNA with increasing amounts of the D203S mutant resulted in elevated levels of nicked plasmid (Figure 5A, lanes 6-9), suggesting that some endonuclease activity is retained by BGLF5 D203S.

Recently, we demonstrated BGLF5 to have intrinsic RNase activity, resulting in degradation of mRNA, but not of tRNA (4). The specificity of this ribonuclease activity was further investigated by incubating various RNA substrates with recombinant BGLF5 proteins. Requirement of mRNA poly-adenylation for BGLF5-mediated degradation was analysed using *in vitro* transcription of a GFP-encoding plasmid linearized

before or after the poly-adenylation consensus sequence. These experiments showed that the presence of a poly-A tail was not essential for BGLF5-mediated RNA degradation (Figure 5B, lanes 2 and 5). No RNase activity was observed for the control protein BGLF5 D203S (Figure 5B, lanes 3 and 6).

To examine whether BGLF5 specifically digests host-derived mRNA, recombinant BGLF5 was incubated with RNA encoding proteins of exogenous (GFP), cellular (HLA-A2), or viral (EBV gp42) origin. These different RNA substrates were all completely digested by wild-type BGLF5, but not by the catalytically inactive D203S mutant (Figure 5C). Our results may thus imply that BGLF5 is incapable of discriminating host from viral RNAs.

In conclusion, BGLF5 has both endo- and exonuclease activities towards DNA substrates. Whereas the D203S mutation obstructs the exonuclease activity of BGLF5 towards DNA, some endonuclease activity is preserved. The RNase activity of BGLF5 is completely abolished by the D203S mutation. This intrinsic RNase activity does not appear to be influenced by poly-adenylation or the source of the transcripts.

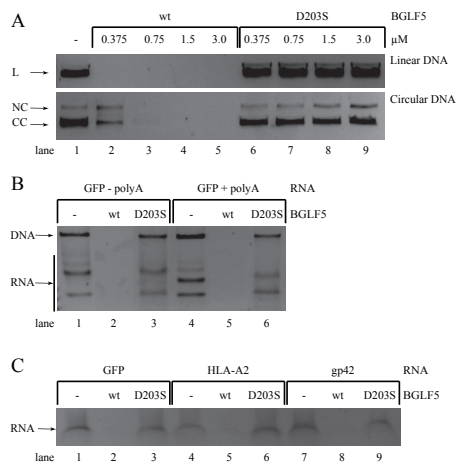


Figure 5. Specificities of EBV BGLF5-mediated DNA and RNA degradation

(A) Linear and circular pMaxGFP plasmids (0.05 pmol) were incubated with wt or D203S mutant EBV BGLF5 recombinant proteins in the presence of 5 mM Mg²⁺. After 2 h at 37 °C, samples were resolved by agarose gel electrophoresis and visualized by ethidium bromide staining. L, linear DNA; CC, closed circle; NC, nicked circle. (B and C) Specificity of RNase activity was studied by incubating wt or D203S mutant EBV BGLF5 recombinant proteins with *in vitro* transcribed RNA in the presence of 10 mM Mn²⁺. (B) GFP RNA was synthesized from a plasmid linearized before (-polyA) or after (+polyA) the poly-adenylation signal sequence. (C) RNAs for a foreign protein (GFP), a cellular protein (HLA-A2), or a viral protein (EBV gp42) were used. Following degradation periods of 30 minutes (B) or 6 h (C) at 37°C, samples were resolved by agarose gel electrophoresis and visualized by ethidium bromide staining. DNA and RNA bands have been identified according to their susceptibility to digestion with an RNase A/T1 mix (Ambion) (data not shown).

Discussion

In this study, we have acquired novel information on the DNase and shutoff functions of the EBV BGLF5 protein. Similar to the homologous KSHV SOX protein, BGLF5 directs PABPC to the nucleus. This nuclear relocalization of PABPC is associated with the shutoff activity of BGLF5. Whereas mutation of a catalytic site residue (D203S) blocked both DNase and host shutoff activities completely, other mutations (P158 and K231M) more specifically affected either DNA degradation or host shutoff (Table 1); however, complete separation of the two activities was never observed. Interestingly, the D203S mutation destroys the RNase and DNA exonuclease, but not the DNA endonuclease activity of BGLF5. Finally, BGLF5 degrades both cellular and viral transcripts, irrespective of poly-adenylation.

We were interested in the elements that confer the host shutoff activity to gamma-herpesvirus exonucleases, in addition to the widespread DNase function. Interestingly, gamma-herpesvirus exonucleases show a higher degree of sequence conservation compared to their counterparts of other herpesvirus subfamilies (39% for gamma-herpesvirus exonucleases versus 30% and 35% for beta-herpesvirus and alpha-herpesvirus exonucleases, respectively), which may be imposed by the additional constraint of a host shutoff activity. Sequence alignment of gamma-herpesvirus AE proteins does not point to prominent conserved surface areas outside the active site (Figure 1A), as would be expected if the activity were mediated through an interaction with co-factor(s). Most of the sequence conservation affects the region involved in the dsDNA binding; in particular, there is prominent conservation in the region of the bridge that crosses the active-site cleft, which is in contrast to the homologous proteins of the other herpesvirus subfamilies (Figure 1). Based on the similarity with the lambda-exonuclease–DNA complex structure, only one residue within the bridge with a direct participation in exonuclease processivity has very recently been identified ((50), indicated in yellow in Fig. 1C). Conservation among the gamma-herpesvirus subfamily of additional residues within the bridge suggests a role for their interaction with mRNA substrates. Indeed, we show that mutations of the conserved proline 158 residue located in the bridge of the BGLF5 protein differentially affect nuclease activity on dsDNA substrates and host-shutoff activity: substitution for an alanine or serine residue selectively hampers host shutoff, whereas replacement by a glycine residue slightly reduces DNase activity (Table 1). In line with this, mutagenesis of the corresponding amino acid of SOX (P176S) reduced shutoff activity and preserved DNase activity (16).

Mutation of the catalytic site residue aspartic acid 203 into serine (D203S) impaired both DNase and RNase activities, indicating that the two activities share their catalytic site. Interestingly, mutation of

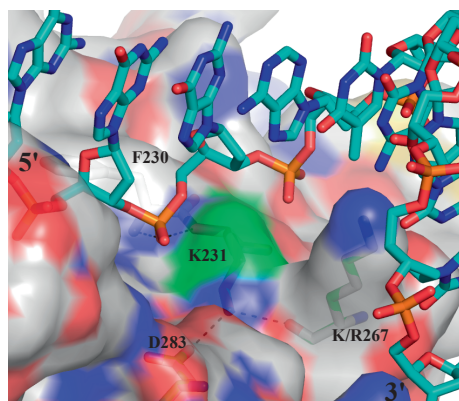


Figure 6. Role of the EBV BGLF5 residue K231

View of the KSHV SOX structure in complex with dsDNA (2). Only one of the DNA strands is shown (cyan carbon atoms). The protein (white carbon atoms) is represented with a semi-transparent surface with some key residues indicated. Residue K231 is shown with green carbon atoms. Residues are labeled with the numbers corresponding to EBV BGLF5. These residues are conserved between BGLF5 and SOX with the exception of an R/K substitution. Dotted lines show hydrogen bonds.

the D203 residue of the BGLF5 protein destroyed the exonuclease, but not the endonuclease activity towards DNA. In agreement with these results, mutation of the D340 residue of HSV AE, which is equivalent to D203 of BGLF5, destroyed its exo-, but not its endonuclease activity (19). These results suggest that the endonuclease activity of the viral alkaline exonucleases is mechanistically distinct from their exo(ribo)nuclease activities.

The structure of the KSHV SOX–DNA complex (2) reveals that the residue corresponding to EBV K231 is probably not directly involved in nucleic acid substrate binding via its amino group, but rather forms part of the binding surface for the DNA and structures part of the interacting surface (Figure 6) due to its hydrogen bonds with D283 and the amide of R267 (all residues are numbered according to the EBV sequence). The neighbouring amide nitrogen atoms of K231 and F230 form hydrogen bonds to a backbone phosphate of the dsDNA. The mutation of K231 to a methionine residue would lead to loss of the hydrogen bonds involving the amino group and in a different organisation of the structure around the mutated residue. The importance of the K231 residue for both DNase and host shutoff activities of BGLF5 suggests that the conformation of bound ssRNA is similar to one of the DNA strands, at least for the first 5 bases. As the interaction surface with a dsDNA substrate is larger than the interaction surface with a ssRNA substrate, the effect of a single point mutation affecting nucleic acid interaction is anticipated to be stronger on RNase activity than on DNase activity, and this is indeed observed (Table 1). Previously, the DNase and host shutoff activities

of BGLF5 and SOX were found to be genetically separable (16, 51). In this study, we have not found mutants of BGLF5 that had completely lost either the ability to degrade DNA or to inhibit host protein synthesis (Table 1). Although the P158 and K231M mutations affected the DNase and host shutoff activities to varying degrees, no absolute separation of the two activities was obtained, whereas previously, mutation of the K231 residue was found to obstruct host shutoff activity but not DNase activity (51). This discrepancy in K231M effects on DNase activity may be explained by differences in the ratio of plasmid/BGLF5 and the incubation time during the DNase assay.

Expression of the gamma-herpesvirus host shutoff proteins KSHV SOX (33) and EBV BGLF5 (this study) results in nuclear relocalization of cytosolic PABPC, a protein involved in the stabilization of mRNA. The ability of these viral proteins to relocalize PABPC likely correlates with their host shutoff activity. Interestingly, infection with members from all herpesvirus subfamilies affects PABPC expression. Infection with the alpha-herpesvirus HSV induces the accumulation of PABPC in the nucleus (9, 42). This is not induced by the AE protein, but rather by ICP27, which inhibits mRNA splicing and thus host protein synthesis, and the vhs protein (9, 29). Infection with the beta-herpesvirus human cytomegalovirus increases PABPC protein levels (38, 48). However, unlike the nuclear relocalization of PABPC induced by alpha- and gamma-herpesvirus infection, PABPC is accumulated in the cytosol of HCMV-infected cells (38). Together, these results suggest a strong association between the nuclear relocalization of PABPC and the capability of herpesviruses to shut off host protein synthesis. Recent data implicate that the nuclear accumulation of PABPC occurs as a result of the virus-induced mRNA depletion from the cytoplasm (30).

Recently, recombinant gamma-herpesvirus AE proteins were shown to exert RNase activity *in vitro* (2, 4). However, whether their intrinsic RNase activity is sufficient for virus-induced host shutoff remains to be answered. The alkaline exonuclease of HSV can also degrade RNA substrates *in vitro*, but has no host shutoff activity in cells (25, 27). In contrast to the BGLF5 and SOX proteins, which are present in both the nucleus and cytoplasm, HSV AE expression is strictly nuclear. This might restrict the ability of this protein to degrade cytoplasmic mRNAs and, consequently, to induce host shutoff. Still, a mutant HSV AE protein that is partially localized to the cytoplasm was incapable of inducing host shutoff (7), suggesting that an intrinsic RNase activity of alkaline exonucleases is insufficient for host shutoff. On the contrary, although we cannot exclude an interaction of BGLF5 and SOX with cellular co-factor(s) that might increase the RNA turnover activity of these gamma-herpesvirus proteins in cells, the absence of gamma-herpesvirus-specific conserved surface areas on the

exonuclease rather speaks against the involvement of co-factor(s).

In this study, we have demonstrated that the BGLF5 protein is capable of degrading both cellular and viral mRNAs *in vitro*. Although additional studies are required to determine the entire specificity of BGLF5-mediated mRNA degradation, several studies support our results implying broad activity of EBV-induced shutoff. Using deletion mutant EBV viruses, Feederle *et al.* showed that BGLF5 reduces mRNA and protein levels of several viral gene products in EBV-infected cells (12, 13). Furthermore, the HSV vhs protein not only degrades cellular mRNAs but also viral mRNAs, most likely to facilitate the transition between the different phases of infection, i.e. between immediate early, early, and late viral protein synthesis (31, 35, 36, 39). Some selectivity in RNA substrates is likely as, for example, a small subset of cellular transcripts escapes KSHV SOX-induced degradation. Among them is IL-6, which is frequently found upregulated in KSHV-associated malignancies (5, 6, 17).

On the basis of these combined results, we propose the following model for EBV BGLF5 function: BGLF5 degrades both linear DNA and RNA using the same catalytic site, albeit that the ion requirements and efficiencies differ for the two substrates. In contrast, the endonuclease activity of BGLF5 seems to be mediated via a somewhat different mechanism. Whereas DNA binding is conserved for the herpesvirus alkaline exonucleases, gamma-herpesvirus AEs, including BGLF5, probably have acquired the ability to also bind RNA during evolution. Recognition of RNA substrates most likely involves the flexible bridge sequence located between motifs I and Ia of the gamma-herpesvirus AE proteins (4). BGLF5-mediated mRNA degradation causes a block in *de novo* protein synthesis and relocalization of PABPC to the nucleus. Within the nucleus, PABPC causes hyperadenylation and retention of nuclear mRNA molecules, thereby augmenting the host shutoff phenotype initiated by BGLF5. Interestingly, protein expression levels of BGLF5 (mutants) are clearly anti-correlated with their host shutoff activity, indicating that BGLF5 degrades its own messenger.

Inhibition of host protein synthesis is probably helpful to herpesviruses in different ways. Firstly, in the absence of host protein synthesis, the cellular ribosomes will be committed to the synthesis of viral proteins. Secondly, by controlling the transition between immediate early, early, and late protein synthesis, the virus can progress efficiently between the different phases of productive infection. Finally, host shutoff contributes to immune evasion by preventing the synthesis of proteins involved in antiviral immunity. For example, EBV BGLF5 reduces expression of MHC molecules, thereby hampering antigen presentation to T cells (41, 51). Similarly, expression of KSHV SOX and of HSV vhs impairs T cell recognition (45, 51). Recently, BGLF5 was

demonstrated to also contribute to the downregulation of Toll-like receptor 9 (46), an important pattern-recognition receptor that detects viral dsDNA.

Overall, by orchestrating viral and cellular gene expression and thwarting both innate and adaptive immunity, BGLF5 contributes to the efficient synthesis of viral progeny in the absence of immune recognition, thereby facilitating the spread of EBV to new hosts.

Materials and Methods

Sequence analysis

The sequences of different gamma-herpesvirus BGLF5 homologues have been retrieved at NCBI using BLAST (1) and aligned with ClustalW (44). Sequence identities are above 39%. Sequence conservation (identities) has been mapped onto a full model of the EBV nuclease structure (4) using ESPrpt (22). Using the HHV6 sequence as reference, beta-herpesvirus sequences can be aligned with an overall sequence conservation of above 30%. A model of the beta-herpesvirus exonuclease based on the template KSHV exonuclease (8) (pdb entry 3fhf) and the sequence of HHV6 has been built using SWISS-MODEL (3) and has been used for the analysis of conserved residues. Alpha-herpesvirus exonuclease sequences were aligned with the one of HSV-1 as reference (sequence identities above 35%). Because of the longer sequence of HSV-1 AE compared to EBV BGLF5 or KSHV SOX, we avoided to model the HSV-1 AE structure and only used the sequence alignment for analysis. A list of the sequences used is given in table S1.

Constructs

The *EBV BGLF5* gene with a C-terminal HA-tag (BGLF5) was cloned into the pcDEF and pcDNA3-IRES-nlsGFP vectors as described (41). The pcDNA3 vector contains an internal ribosomal entry site (IRES) immediately downstream of the inserted gene-of-interest to allow co-expression of the marker gene *GFP* (47) (kindly provided by Dr. E. Reits, Academic Medical Center, Amsterdam, The Netherlands).

The BGLF5 mutants D203S, P158A, P158S, and P158G were constructed using a BGLF5-HA-encoding plasmid as template for site-directed mutagenesis. The following primers were used: GAT GGC ATT TTT GGG GTG TCT CTA AGC TTG TGC GTC AAT GTG GAG TCA CAG GG (sD203S), CCC TGT GAC TCC ACA TTG ACG CAC AAG CTT AGA GAC ACC CCA AAA ATG CCA TC (asD203S), AAT CAC TAC TTT GGG GGC GCC GTG GCC TTT GGC CTG CGG (sP158A), CCG CAG GCC AAA GGC CAC GGC CCC AAA GTA GTG ATT TG (asP158A), AAT CAC TAC TTT GGG GGA TCC GTG GCC TTT GGC CTG CGG (sP158S), CCG CAG GCC AAA GGC CAC GGA TCC CCC AAA GTA GTG ATT TG (asP158S), AAT CAC TAC TTT

GGG GGA GGT GTG GCC TTT GGC CTG CGG (sP158G) and CCG CAG GCC AAA GGC CAC ACC TCC CCC AAA GTA GTG ATT TG (asP158G). The resulting mutant BGLF5 genes were cloned into the pcDNA3-IRES-nlsGFP and pcDEF vectors.

The BGLF5 mutants K231M and G305C were generated and cloned into the pcDNA3-IRES-nlsGFP vector as described (51) (kindly provided by Drs. J. Zuo and M. Rowe, University of Birmingham, Birmingham, United Kingdom), and were additionally cloned into the pcDEF vector.

The pcDEF HSV HA-AE and pcDEF KSHV HA-SOX constructs were described before (16) (kindly provided by Dr. B. Glaunsinger, University of California, Berkeley, United States of America).

The pcDNA3-GFP (41), pcDNA3 HLA-A2.1 (26) and pcDNA3 EBV gp42-4Met (40) constructs were described before and pMaxGFP was obtained from Lonza.

Recombinant BGLF5 protein

Large quantities of recombinant proteins of wild-type (wt) and D203S mutant BGLF5 were produced using a baculovirus-based expression system, as described previously (4).

In vitro transcription and translation

As a source of small amounts of (mutant) BGLF5 protein and other AEs, pcDNA3-IRES-nlsGFP-derived vectors were linearized and used for *in vitro* transcription with T7 polymerase (Promega). Transcripts were translated at 30 °C for 90 minutes in rabbit reticulocyte lysate (Promega). To visualize the proteins produced, the *in vitro* translation products were separated by SDS-PAGE and detected by Western blotting (see below).

Cell lines and transient transfection

Human Embryonic Kidney 293T cells (293T cells) were maintained in complete culture medium consisting of DMEM (Lonza) supplemented with 10% FCS (PAA), 2 mM glutamine, 100 U/ml penicillin, and 100 µg/ml streptomycin.

Cells were transiently transfected with the above mentioned constructs using Lipofectamine 2000 (Invitrogen) according to the manufacturers' instructions.

DNase assay

In vitro translated AE protein products were incubated with linearized plasmids in IVT-Mg²⁺ buffer (5 mM MgCl₂, 50 mM Tris pH 8.8, 0.1 mg/ml BSA, and 1.6% beta-mercaptoethanol) at 37 °C to allow digestion of the DNA.

Alternatively, recombinant BGLF5 wild-type and D203S protein (see above) was incubated with linearized or circular plasmids in Mg²⁺ buffer (250 mM NaCl, 20 mM Tris pH 7.5, and 10 mM MgCl₂) at 37 °C. At the indicated time points, samples of the

degradation reaction were resolved by agarose gel electrophoresis and visualized by ethidium bromide staining.

Antibodies

The following antibodies were used: mouse monoclonal antibody 10E10, directed against PABPC (Santa Cruz Biotechnology); rat monoclonal antibody 3F10, recognizing an Influenza virus hemagglutinin (HA) epitope that is employed as a protein tag (Roche Diagnostics) and rabbit serum k120, specific for BGLF5 (11), kindly provided by Dr. J. Middeldorp, Free University Medical Center, Amsterdam, The Netherlands).

Western blot analysis

SDS-PAGE and immunoblotting were performed as reporter earlier (24). In brief, cell lysates were generated as follows: cells were lysed using 0.5% NP-40 buffer (0.5% NP-40, 50 mM Tris-HCl (pH 7.5), 5 mM MgCl₂, 10 μM leupeptin, and 1 mM 4-(2-aminoethyl)benzenesulfonyl fluoride (AEBSF)) and subsequently centrifuged to obtain post-nuclear lysates. For Western blot analysis, cell lysates or *in vitro* translation products (see above) were denatured in sample buffer (0.05 M Tris pH 8.0, 2% SDS, 10% glycerol, 5% β-mercaptoethanol, and 0.025% bromophenol blue), separated by SDS-PAGE, and transferred to polyvinylidene difluoride membranes (GE Healthcare). Proteins of interest were detected by incubating the membranes with specific antibodies (see above) followed by horseradish peroxidase-conjugated secondary antibodies (Jackson ImmunoResearch Laboratories). Antibody binding was visualized using ECL (GE Healthcare).

Flow cytometry

GFP levels of transfected 293T cells were analysed by flow cytometry. Data was obtained on a FACSCalibur flow cytometer using CellQuest Pro (BD Biosciences) and analysed using FlowJo (Tree Star) software.

Immunofluorescence

Transfected 293T cells were grown overnight on microscope slides (Lab-Tek™ II Chamber Slide™ System, Thermo Scientific) and fixed in 3% paraformaldehyde for 30 minutes at 37 °C. After permeabilization with perm buffer (1% Triton X-100 and 0.1% sodium citrate in PBS) for 5 minutes and blocking with 5% BSA in PBS for 60 minutes, cells were stained with primary antibodies for 60 minutes. Subsequently, cells were washed and stained with fluorescently labeled secondary antibodies (Jackson ImmunoResearch Laboratories) and DAPI to visualize nuclei for 60 minutes and embedded with Mowiol (Brunschwig Chemie). All incubation steps were performed at room temperature unless stated otherwise. Cells were visualized with a fluorescence microscope (EVOS fl, Advanced Microscopy Group).

RNase assay

As a source of RNA, pcDNA3-derived vectors were linearized before or after the poly-adenylation signal sequence and used for *in vitro* transcription with T7 polymerase (Promega). The *in vitro* transcripts were incubated with recombinant BGLF5 protein (see above) in Mn²⁺ buffer (250 mM NaCl, 20 mM Tris pH 7.5, and 10 mM MnCl₂) at 37 °C to allow digestion of the RNA. At the indicated time points, samples of the degradation reaction were resolved by agarose gel electrophoresis and visualized by ethidium bromide staining.

Acknowledgements

We gratefully acknowledge Drs. Jaap M. Middeldorp (Free University Medical Center, Amsterdam, The Netherlands), Britt A. Glaunsinger (University of California, Berkeley, United States of America), Hans C. van Leeuwen, Sjaak van Voorden (Leiden University Medical Center, Leiden, The Netherlands), Jianmin Zuo, Martin Rowe (University of Birmingham, Birmingham, United Kingdom), and Janneke G.C. Peeters (University Medical Center Utrecht, Utrecht, The Netherlands) for helpful advice, technical assistance, and for generously sharing reagents and constructs. We thank Dr. Tracey A. Barret (Birkbeck College, London, United Kingdom) for providing coordinates for the SOX-DNA complex.

This work was supported by the Dutch Cancer Foundation (grant RUL 2005-3259 to D.H., M.R. and E.W.), the Netherlands Scientific Organization (NWO Vidi 917.76.330 to M.R.), the ANR-MIME-2006 program of the French government, and the cluster 10 Infectiology of the Région Rhône-Alpes.

The authors declare that they have no conflict of interest.

References

1. Altschul, S. F., T. L. Madden, A. A. Schaffer, J. Zhang, Z. Zhang, W. Miller, and D. J. Lipman. 1997. Gapped BLAST and PSI-BLAST: a new generation of protein database search programs. *Nucleic Acids Res.* 25:3389-3402.
2. Bagneris, C., L. C. Briggs, R. Savva, B. Ebrahimi, and T. E. Barrett. 2011. Crystal structure of a KSHV-SOX-DNA complex: insights into the molecular mechanisms underlying DNase activity and host shutoff. *Nucleic Acids Res.*
3. Benkert, P., M. Biasini, and T. Schwede. 2011. Toward the estimation of the absolute quality of individual protein structure models. *Bioinformatics.* 27:343-350.
4. Buisson, M., T. Geoui, D. Flot, N. Tarbouriech, M. E. Rensing, E. J. Wiertz, and W. P. Burmeister. 2009. A bridge crosses the active-site canyon of

- the Epstein-Barr virus nuclease with DNase and RNase activities. *J. Mol. Biol.* 391:717-728.
5. Chandriani, S. and D. Ganem. 2007. Host transcript accumulation during lytic KSHV infection reveals several classes of host responses. *PLoS. One.* 2:e811.
 6. Clyde, K. and B. A. Glaunsinger. 2011. Deep sequencing reveals direct targets of gammaherpesvirus-induced mRNA decay and suggests that multiple mechanisms govern cellular transcript escape. *PLoS. One.* 6:e19655.
 7. Covarrubias, S., J. M. Richner, K. Clyde, Y. J. Lee, and B. A. Glaunsinger. 2009. Host shutoff is a conserved phenotype of gammaherpesvirus infection and is orchestrated exclusively from the cytoplasm. *J. Virol.* 83:9554-9566.
 8. Dahlroth, S. L., D. Gurmu, J. Haas, H. Erlandsen, and P. Nordlund. 2009. Crystal structure of the shutoff and exonuclease protein from the oncogenic Kaposi's sarcoma-associated herpesvirus. *FEBS J.* 276:6636-6645.
 9. Dobrikova, E., M. Shveygert, R. Walters, and M. Gromeier. 2010. Herpes simplex virus proteins ICP27 and UL47 associate with polyadenylate-binding protein and control its subcellular distribution. *J. Virol.* 84:270-279.
 10. Everly, D. N., Jr., P. Feng, I. S. Mian, and G. S. Read. 2002. mRNA degradation by the virion host shutoff (Vhs) protein of herpes simplex virus: genetic and biochemical evidence that Vhs is a nuclease. *J. Virol.* 76:8560-8571.
 11. Fachiroh, J., T. Schouten, B. Hariyianto, D. K. Paramita, A. Harijadi, S. M. Haryana, M. H. Ng, and J. M. Middeldorp. 2004. Molecular diversity of Epstein-Barr virus IgG and IgA antibody responses in nasopharyngeal carcinoma: a comparison of Indonesian, Chinese, and European subjects. *J. Infect. Dis.* 190:53-62.
 12. Feederle, R., H. Bannert, H. Lips, N. Muller-Lantzsch, and H. J. Delecluse. 2009. The Epstein-Barr virus alkaline exonuclease BGLF5 serves pleiotropic functions in virus replication. *J. Virol.* 83:4952-4962.
 13. Feederle, R., A. M. Mehl-Lautscham, H. Bannert, and H. J. Delecluse. 2009. The Epstein-Barr virus protein kinase BGLF4 and the exonuclease BGLF5 have opposite effects on the regulation of viral protein production. *J. Virol.* 83:10877-10891.
 14. Feng, P., D. N. Everly, Jr., and G. S. Read. 2001. mRNA decay during herpesvirus infections: interaction between a putative viral nuclease and a cellular translation factor. *J. Virol.* 75:10272-10280.
 15. Feng, P., D. N. Everly, Jr., and G. S. Read. 2005. mRNA decay during herpes simplex virus (HSV) infections: protein-protein interactions involving the HSV virion host shutoff protein and translation factors eIF4H and eIF4A. *J. Virol.* 79:9651-9664.
 16. Glaunsinger, B., L. Chavez, and D. Ganem. 2005. The exonuclease and host shutoff functions of the SOX protein of Kaposi's sarcoma-associated herpesvirus are genetically separable. *J. Virol.* 79:7396-7401.
 17. Glaunsinger, B. and D. Ganem. 2004. Highly selective escape from KSHV-mediated host mRNA shutoff and its implications for viral pathogenesis. *J. Exp. Med.* 200:391-398.
 18. Glaunsinger, B. and D. Ganem. 2004. Lytic KSHV infection inhibits host gene expression by accelerating global mRNA turnover. *Mol. Cell* 13:713-723.
 19. Goldstein, J. N. and S. K. Weller. 1998. The exonuclease activity of HSV-1 UL12 is required for *in vivo* function. *Virology* 244:442-457.
 20. Gopinath, R. S., A. P. Ambagala, S. Hinkley, and S. Srikumaran. 2002. Effects of virion host shutoff activity of bovine herpesvirus 1 on MHC class I expression. *Viral Immunol.* 15:595-608.
 21. Gorgoni, B. and N. K. Gray. 2004. The roles of cytoplasmic poly(A)-binding proteins in regulating gene expression: a developmental perspective. *Brief. Funct. Genomic. Proteomic.* 3:125-141.
 22. Gouet, P., E. Courcelle, D. I. Stuart, and F. Metz. 1999. ESPript: analysis of multiple sequence alignments in PostScript. *Bioinformatics.* 15:305-308.
 23. Hinkley, S., A. P. Ambagala, C. J. Jones, and S. Srikumaran. 2000. A vhs-like activity of bovine herpesvirus-1. *Arch. Virol.* 145:2027-2046.
 24. Horst, D., D. van Leeuwen, N. P. Croft, M. A. Garstka, A. D. Hislop, E. Kremmer, A. B. Rickinson, E. J. Wiertz, and M. E. Rensing. 2009. Specific targeting of the EBV lytic phase protein BNLF2a to the transporter associated with antigen processing results in impairment of HLA class I-restricted antigen presentation. *J. Immunol.* 182:2313-2324.
 25. Kehm, E., M. Goksu, S. Bayer, and C. W. Knopf. 1998. Herpes simplex virus type 1 DNase: functional analysis of the enzyme expressed by recombinant baculovirus. *Intervirology* 41:110-119.
 26. Kikkert, M., G. Hassink, M. Barel, C. Hirsch, F. J. van der Wal, and E. Wiertz. 2001. Ubiquitination is essential for human cytomegalovirus US11-mediated dislocation of MHC class I molecules from the endoplasmic reticulum to the cytosol. *Biochem. J.* 358:369-377.
 27. Knopf, C. W. and K. Weisshart. 1990. Comparison of exonucleolytic activities of herpes simplex virus type-1 DNA polymerase and DNase. *Eur. J. Biochem.* 191:263-273.
 28. Koppers-Lalic, D., F. A. Rijsewijk, S. B. Verschuren, van Gaans-Van den Brink JA, A. Neisig, M. E. Rensing, J. Neeffjes, and E. J.

- Wiertz. 2001. The UL41-encoded virion host shutoff (vhs) protein and vhs-independent mechanisms are responsible for down-regulation of MHC class I molecules by bovine herpesvirus 1. *J. Gen. Virol.* 82:2071-2081.
29. Kumar, G. R. and B. A. Glaunsinger. 2010. Nuclear import of cytoplasmic poly(A) binding protein restricts gene expression via hyperadenylation and nuclear retention of mRNA. *Mol. Cell Biol.* 30:4996-5008.
 30. Kumar, G. R., L. Shum, and B. A. Glaunsinger. 2011. Importin $\{\alpha\}$ -Mediated Nuclear Import of Cytoplasmic Poly(A) Binding Protein Occurs as a Direct Consequence of Cytoplasmic mRNA Depletion. *Mol. Cell Biol.* 31:3113-3125.
 31. Kwong, A. D. and N. Frenkel. 1987. Herpes simplex virus-infected cells contain a function(s) that destabilizes both host and viral mRNAs. *Proc. Natl. Acad. Sci. U. S. A* 84:1926-1930.
 32. Kwong, A. D., J. A. Kruper, and N. Frenkel. 1988. Herpes simplex virus virion host shutoff function. *J. Virol.* 62:912-921.
 33. Lee, Y. J. and B. A. Glaunsinger. 2009. Aberrant herpesvirus-induced polyadenylation correlates with cellular messenger RNA destruction. *PLoS Biol.* 7:e1000107.
 34. Liu, M. T., H. P. Hu, T. Y. Hsu, and J. Y. Chen. 2003. Site-directed mutagenesis in a conserved motif of Epstein-Barr virus DNase that is homologous to the catalytic centre of type II restriction endonucleases. *J. Gen. Virol.* 84:677-686.
 35. Oroskar, A. A. and G. S. Read. 1989. Control of mRNA stability by the virion host shutoff function of herpes simplex virus. *J. Virol.* 63:1897-1906.
 36. Oroskar, A. A. and G. S. Read. 1987. A mutant of herpes simplex virus type 1 exhibits increased stability of immediate-early (alpha) mRNAs. *J. Virol.* 61:604-606.
 37. Page, H. G. and G. S. Read. 2010. The virion host shutoff endonuclease (UL41) of herpes simplex virus interacts with the cellular cap-binding complex eIF4F. *J. Virol.* 84:6886-6890.
 38. Perez, C., C. McKinney, U. Chulunbaatar, and I. Mohr. 2011. Translational control of the abundance of cytoplasmic poly(A) binding protein in human cytomegalovirus-infected cells. *J. Virol.* 85:156-164.
 39. Read, G. S. and N. Frenkel. 1983. Herpes simplex virus mutants defective in the virion-associated shutoff of host polypeptide synthesis and exhibiting abnormal synthesis of alpha (immediate early) viral polypeptides. *J. Virol.* 46:498-512.
 40. Rensing, M. E., D. van Leeuwen, F. A. Verreck, S. Keating, R. Gomez, K. L. Franken, T. H. Ottenhoff, M. Spriggs, T. N. Schumacher, L. M. Hutt-Fletcher, M. Rowe, and E. J. Wiertz. 2005. Epstein-Barr virus gp42 is posttranslationally modified to produce soluble gp42 that mediates HLA class II immune evasion. *J. Virol.* 79:841-852.
 41. Rowe, M., B. Glaunsinger, D. van Leeuwen, J. Zuo, D. Sweetman, D. Ganem, J. Middeldorp, E. J. Wiertz, and M. E. Rensing. 2007. Host shutoff during productive Epstein-Barr virus infection is mediated by BGLF5 and may contribute to immune evasion. *Proc. Natl. Acad. Sci. U. S. A* 104:3366-3371.
 42. Salaun, C., A. I. MacDonald, O. Larralde, L. Howard, K. Lochtie, H. M. Burgess, M. Brook, P. Malik, N. K. Gray, and S. V. Graham. 2010. Poly(A)-binding protein 1 partially relocalizes to the nucleus during herpes simplex virus type 1 infection in an ICP27-independent manner and does not inhibit virus replication. *J. Virol.* 84:8539-8548.
 43. Smiley, J. R. 2004. Herpes simplex virus virion host shutoff protein: immune evasion mediated by a viral RNase? *J. Virol.* 78:1063-1068.
 44. Thompson, J. D., D. G. Higgins, and T. J. Gibson. 1994. CLUSTAL W: improving the sensitivity of progressive multiple sequence alignment through sequence weighting, position-specific gap penalties and weight matrix choice. *Nucleic Acids Res.* 22:4673-4680.
 45. Tigges, M. A., S. Leng, D. C. Johnson, and R. L. Burke. 1996. Human herpes simplex virus (HSV)-specific CD8⁺ CTL clones recognize HSV-2-infected fibroblasts after treatment with IFN-gamma or when virion host shutoff functions are disabled. *J. Immunol.* 156:3901-3910.
 46. van Gent M., B. D. Griffin, E. G. Berkhoff, L. D. van, I. G. Boer, M. Buisson, F. C. Hartgers, W. P. Burmeister, E. J. Wiertz, and M. E. Rensing. 2011. EBV lytic-phase protein BGLF5 contributes to TLR9 downregulation during productive infection. *J. Immunol.* 186:1694-1702.
 47. van Lith, M., M. van Ham, A. Griekspoor, E. Tjin, D. Verwoerd, J. Calafat, H. Janssen, E. Reits, L. Pastoors, and J. Neeffes. 2001. Regulation of MHC class II antigen presentation by sorting of recycling HLA-DM/DO and class II within the multivesicular body. *J. Immunol.* 167:884-892.
 48. Walsh, D., C. Perez, J. Notary, and I. Mohr. 2005. Regulation of the translation initiation factor eIF4F by multiple mechanisms in human cytomegalovirus-infected cells. *J. Virol.* 79:8057-8064.
 49. Zelus, B. D., R. S. Stewart, and J. Ross. 1996. The virion host shutoff protein of herpes simplex virus type 1: messenger ribonucleolytic activity *in vitro*. *J. Virol.* 70:2411-2419.
 50. Zhang, J., K. A. McCabe, and C. E. Bell. 2011. Crystal structures of $\{\lambda\}$ exonuclease

- in complex with DNA suggest an electrostatic ratchet mechanism for processivity. *Proc. Natl. Acad. Sci. U. S. A* 108:11872-11877.
51. Zuo, J., W. Thomas, D. van Leeuwen, J. M. Middeldorp, E. J. Wiertz, M. E. Rensing, and M. Rowe. 2008. The DNase of gammaherpesviruses impairs recognition by virus-specific CD8⁺ T cells through an additional host shutoff function. *J. Virol.* 82:2385-2393.

Supplementary data

γ -herpesvirus

gi 119691	Epstein-Barr virus strain B95-8
gi 82503243	Epstein-Barr virus strain B95-8/Raji
gi 123845633	Epstein-Barr virus strain GD1 derived from NPC
gi 139424516	Epstein-Barr virus strain AG876
gi 228537	Epstein-Barr virus strain P3HR1
gi 51518056	Macacine herpesvirus 4
gi 24943119	Callitrichine herpesvirus 3
gi 20453824	Porcine lymphotropic herpesvirus 1
gi 27452874	Porcine lymphotropic herpesvirus 2
gi 30348540	Saimiriine herpesvirus 2
gi 9625993	Saimiriine herpesvirus 2
gi 27452835	Porcine lymphotropic herpesvirus 3
gi 10140958	Alcelaphine herpesvirus 1
gi 9631229	Ateline herpesvirus 3
gi 9628040	Equid herpesvirus 2
gi 9629578	Murid herpesvirus 4
gi 83642873	Ovine herpesvirus 2
gi 78127870	Ovine herpesvirus 2
gi 262285082	Wood mouse herpesvirus
gi 134038663	Wood mouse herpesvirus
gi 13095614	Bovine herpesvirus 4
gi 2246484	Human herpesvirus 8
gi 1718290	Human herpesvirus 8 type M
gi 139472831	Human herpesvirus 8
gi 46519394	Macaca fuscata rhadinovirus
gi 18653844	Macacine herpesvirus 5
gi 7330027	Rhesus monkey rhadinovirus H26-95
gi 321496589	Rodent herpesvirus Peru

β -herpesvirus

gi 9633139	Human herpesvirus 6
gi 51874292	Human herpesvirus 7
gi 190887040	Muromegalovirus C4A
gi 51556591	Macacine herpesvirus 3
gi 9845385	Murid herpesvirus 2
gi 20026688	Panine herpesvirus 2
gi 259016230	Human herpesvirus 5 strain AD169
gi 213159230	Caviid herpesvirus 2

α -herpesvirus

gi 330077	Human herpesvirus 1
gi 9629281	Human herpesvirus 2
gi 28804647	Cercopithecine herpesvirus 1
gi 83722580	Papiine herpesvirus 2
gi 312162843	Saimiriine herpesvirus 1
gi 165911567	Anatid herpesvirus 1
gi 50313291	Equid herpesvirus 1
gi 9629778	Equid herpesvirus 4
gi 216905903	Equid herpesvirus 9
gi 255683203	Anatid herpesvirus 1
gi 270339487	Felid herpesvirus 1
gi 11095844	Meleagrid herpesvirus 1
gi 125745063	Gallid herpesvirus 2
gi 66866009	Human herpesvirus 3
gi 57790979	Gallid herpesvirus 1
gi 10834881	Gallid herpesvirus 3
gi 51557529	Suid herpesvirus 1
gi 38638245	Psittacid herpesvirus 1
gi 296316049	Bovine herpesvirus 5
gi 145685896	Anatid herpesvirus 1
gi 9629863	Bovine herpesvirus 1
gi 13242441	Cercopithecine herpesvirus 9
gi 52551080	Fibropapilloma-associated turtle herpesvirus

Table S1. Sequences used in the analysis of the sequence conservation of herpesvirus exonucleases
GI identifiers refer to the Protein database at NCBI.

Chapter 7 - Characteristics of host shutoff by EBV BGLF5

gi	119691	α1										α2										α3																										
		10	20	30	40	50	60	70	80	90	100	10	20	30	40	50	60	70	80	90	100	10	20	30	40	50	60	70	80	90	100																	
gi	119691	M	A	D	V	D	E	L	E	D	P	M	E	E	M	T	S	Y	F	F	A	R	F	L	R	S	P	E	T	E	A	F	V	R	N	L	D	R	P	P	M	A	R	F	V	L	Y	C
gi	82503243	M	A	D	V	D	E	L	E	D	P	M	E	E	M	T	S	Y	F	F	A	R	F	L	R	S	P	E	T	E	A	F	V	R	N	L	D	R	P	P	M	A	R	F	V	L	Y	C
gi	123845633	M	A	D	V	D	E	L	E	D	P	M	E	E	M	T	S	Y	F	F	A	R	F	L	R	S	P	E	T	E	A	F	V	R	N	L	D	R	P	P	M	A	R	F	V	L	Y	C
gi	139424516	M	A	D	V	D	E	L	E	D	P	M	E	E	M	T	S	Y	F	F	A	R	F	L	R	S	P	E	T	E	A	F	V	R	N	L	D	R	P	P	M	A	R	F	V	L	Y	C
gi	228537	M	A	D	V	D	E	L	E	D	P	M	E	E	M	T	S	Y	F	F	A	R	F	L	R	S	P	E	T	E	A	F	V	R	N	L	D	R	P	P	M	A	R	F	V	L	Y	C
gi	51518056	M	A	D	V	D	E	L	E	D	P	M	E	E	M	T	S	Y	F	F	A	R	F	L	R	S	P	E	T	E	A	F	V	R	N	L	D	R	P	P	M	A	R	F	V	L	Y	C
gi	24943119	M	A	D	V	D	E	L	E	D	P	M	E	E	M	T	S	Y	F	F	A	R	F	L	R	S	P	E	T	E	A	F	V	R	N	L	D	R	P	P	M	A	R	F	V	L	Y	C
gi	20453824	M	A	D	V	D	E	L	E	D	P	M	E	E	M	T	S	Y	F	F	A	R	F	L	R	S	P	E	T	E	A	F	V	R	N	L	D	R	P	P	M	A	R	F	V	L	Y	C
gi	27452874	M	A	D	V	D	E	L	E	D	P	M	E	E	M	T	S	Y	F	F	A	R	F	L	R	S	P	E	T	E	A	F	V	R	N	L	D	R	P	P	M	A	R	F	V	L	Y	C
gi	30348540	M	A	D	V	D	E	L	E	D	P	M	E	E	M	T	S	Y	F	F	A	R	F	L	R	S	P	E	T	E	A	F	V	R	N	L	D	R	P	P	M	A	R	F	V	L	Y	C
gi	9625993	M	A	D	V	D	E	L	E	D	P	M	E	E	M	T	S	Y	F	F	A	R	F	L	R	S	P	E	T	E	A	F	V	R	N	L	D	R	P	P	M	A	R	F	V	L	Y	C
gi	27452835	M	A	D	V	D	E	L	E	D	P	M	E	E	M	T	S	Y	F	F	A	R	F	L	R	S	P	E	T	E	A	F	V	R	N	L	D	R	P	P	M	A	R	F	V	L	Y	C
gi	10140958	M	A	D	V	D	E	L	E	D	P	M	E	E	M	T	S	Y	F	F	A	R	F	L	R	S	P	E	T	E	A	F	V	R	N	L	D	R	P	P	M	A	R	F	V	L	Y	C
gi	9631229	M	A	D	V	D	E	L	E	D	P	M	E	E	M	T	S	Y	F	F	A	R	F	L	R	S	P	E	T	E	A	F	V	R	N	L	D	R	P	P	M	A	R	F	V	L	Y	C
gi	9628040	M	A	D	V	D	E	L	E	D	P	M	E	E	M	T	S	Y	F	F	A	R	F	L	R	S	P	E	T	E	A	F	V	R	N	L	D	R	P	P	M	A	R	F	V	L	Y	C
gi	9629578	M	A	D	V	D	E	L	E	D	P	M	E	E	M	T	S	Y	F	F	A	R	F	L	R	S	P	E	T	E	A	F	V	R	N	L	D	R	P	P	M	A	R	F	V	L	Y	C
gi	83642873	M	A	D	V	D	E	L	E	D	P	M	E	E	M	T	S	Y	F	F	A	R	F	L	R	S	P	E	T	E	A	F	V	R	N	L	D	R	P	P	M	A	R	F	V	L	Y	C
gi	78127870	M	A	D	V	D	E	L	E	D	P	M	E	E	M	T	S	Y	F	F	A	R	F	L	R	S	P	E	T	E	A	F	V	R	N	L	D	R	P	P	M	A	R	F	V	L	Y	C
gi	262285082	M	A	D	V	D	E	L	E	D	P	M	E	E	M	T	S	Y	F	F	A	R	F	L	R	S	P	E	T	E	A	F	V	R	N	L	D	R	P	P	M	A	R	F	V	L	Y	C
gi	134038663	M	A	D	V	D	E	L	E	D	P	M	E	E	M	T	S	Y	F	F	A	R	F	L	R	S	P	E	T	E	A	F	V	R	N	L	D	R	P	P	M	A	R	F	V	L	Y	C
gi	13095614	M	A	D	V	D	E	L	E	D	P	M	E	E	M	T	S	Y	F	F	A	R	F	L	R	S	P	E	T	E	A	F	V	R	N	L	D	R	P	P	M	A	R	F	V	L	Y	C
gi	2246484	M	A	D	V	D	E	L	E	D	P	M	E	E	M	T	S	Y	F	F	A	R	F	L	R	S	P	E	T	E	A	F	V	R	N	L	D	R	P	P	M	A	R	F	V	L	Y	C
gi	1718290	M	A	D	V	D	E	L	E	D	P	M	E	E	M	T	S	Y	F	F	A	R	F	L	R	S	P	E	T	E	A	F	V	R	N	L	D	R	P	P	M	A	R	F	V	L	Y	C
gi	139472831	M	A	D	V	D	E	L	E	D	P	M	E	E	M	T	S	Y	F	F	A	R	F	L	R	S	P	E	T	E	A	F	V	R	N	L	D	R	P	P	M	A	R	F	V	L	Y	C
gi	46519394	M	A	D	V	D	E	L	E	D	P	M	E	E	M	T	S	Y	F	F	A	R	F	L	R	S	P	E	T	E	A	F	V	R	N	L	D	R	P	P	M	A	R	F	V	L	Y	C
gi	18653844	M	A	D	V	D	E	L	E	D	P	M	E	E	M	T	S	Y	F	F	A	R	F	L	R	S	P	E	T	E	A	F	V	R	N	L	D	R	P	P	M	A	R	F	V	L	Y	C
gi	7330027	M	A	D	V	D	E	L	E	D	P	M	E	E	M	T	S	Y	F	F	A	R	F	L	R	S	P	E	T	E	A	F	V	R	N	L	D	R	P	P	M	A	R	F	V	L	Y	C
gi	321496589	M	A	D	V	D	E	L	E	D	P	M	E	E	M	T	S	Y	F	F	A	R	F	L	R	S	P	E	T	E	A	F	V	R	N	L	D	R	P	P	M	A	R	F	V	L	Y	C

gi 119691 α9 β2 β3 β4 β5 β6

 170 180 190 200 210 220

```

gi 119691  FGRRCEDTVKDIIVCKLITCDASANRCFGFPMISPTIGFVGSLLDCVNVV.ESQGDFLFTDRRCIYIEIKC
gi 82503243  FGRRCEDTVKDIIVCKLITCDASANRCFGFPMISPTIGFVGSLLDCVNVV.ESQGDFLFTDRRCIYIEIKC
gi 123845633  FGRRCEDTVKDIIVCKLITCDASANRCFGFPMISPTIGFVGSLLDCVNVV.ESQGDFLFTDRRCIYIEIKC
gi 139424516  FGRRCEDTVKDIIVCKLITCDASANRCFGFPMISPTIGFVGSLLDCVNVV.ESQGDFLFTDRRCIYIEIKC
gi 228537     FGRRCEDTVKDIIVCKLITCDASANRCFGFPMISPTIGFVGSLLDCVNVV.ESQGDFLFTDRRCIYIEIKC
gi 51518056  FGRRCEDTVKDIIVCKLITCDAAANRCFGFPMISPTIGFVGSLLDCVNVV.ESRGDFLFTDRRCIYIEIKC
gi 24943119  FGRRCEDTVKDIICNLIQKVDSEQRQCFGPMISPTIGFVGSLLDCVNVV.KTEGDLVFTDRRCIYIEIKC
gi 20453824  FGVNRNNTVRLITLQLIAKESWNTTNFGFMLSPITIGFVGSLLMCLKASVDVHNKVMFSSLLTEYIEIKC
gi 27452874  FGVNRNNTVRLITLQLIAKESWNTTNFGFMLSPITIGFVGSLLMCLKASVDVHNKVMFSSLLTEYIEIKC
gi 30348540  FGRRCBEVVKTLVNLICTFKQASCFDCGFMSPBLGIFVGSLLDYCNVETNKDNLVFPDPTVEYIEIKS
gi 9625993   FGRRCBEVVKTLVNLICTFKQASCFDCGFMSPBLGIFVGSLLDYCNVETNKDNLVFPDPTVEYIEIKS
gi 27452835  FGVNRNNTVRLITLQLIAKESWNTTNFGFMLSPITIGFVGSLLMCLKASVDVHNKVMFSSLLTEYIEIKC
gi 10140958  FGVNRNNTVRLVSELVVEEGIGCVTFEGFMLSPITIGFVGSLLMCLKASVDVHNKVMFSSLLTEYIEIKC
gi 9631229   FGRRCBEVVKTLVNLICTSKQVCGCFDCGFMSPBLGIFVGSLLDYCNVETNKDNLVFPDPTVEYIEIKS
gi 9628040   FGRRCEDAVKTLIAEFPVCGRKEVMCDVGFLOSGKIGFVGSLLMCANVSVGRDNLVFPDADAEYIEIKC
gi 9629578   FGRRCEDTVKTLIAELIHPNLPRFHDGCFPLSAIIGFVGSLLDAPNVFTDSSGLVFPDPTVEYIEIKS
gi 83642873  FGVNRNNTVRLVSELVLEENVKCIDTFGFMSPITIGFVGSLLMCANACLTSDNVVFQBATHTYIEIKC
gi 78127870  FGRRCEDTVKTLVSELVLEENVKCIDTFGFMSPITIGFVGSLLMCANACLTSDNVVFQBATHTYIEIKC
gi 262285082  FGRRCEDTVKTLIAELIHPNLPRFHDGCFPLSAIIGFVGSLLDAPNVFTDSSGLVFPDPTVEYIEIKS
gi 134038663  FGRRCEDTVKTLIAELIHPNLPRFHDGCFPLSAIIGFVGSLLDAPNVFTDSSGLVFPDPTVEYIEIKS
gi 13095614  FGRRCBEVVKTLIAELIHPNLPRFHDGCFPLSAIIGFVGSLLDAPNVFTDSSGLVFPDPTVEYIEIKS
gi 2246484   FGRRCBEVVKTLIAELIHPNLPRFHDGCFPLSAIIGFVGSLLDAPNVFTDSSGLVFPDPTVEYIEIKS
gi 1718290   FGRRCBEVVKTLIAELIHPNLPRFHDGCFPLSAIIGFVGSLLDAPNVFTDSSGLVFPDPTVEYIEIKS
gi 139472831  FGRRCBEVVKTLIAELIHPNLPRFHDGCFPLSAIIGFVGSLLDAPNVFTDSSGLVFPDPTVEYIEIKS
gi 46519394  FGRRCBEVVKTLIAELIHPNLPRFHDGCFPLSAIIGFVGSLLDAPNVFTDSSGLVFPDPTVEYIEIKS
gi 18653844  FGRRCBEVVKTLIAELIHPNLPRFHDGCFPLSAIIGFVGSLLDAPNVFTDSSGLVFPDPTVEYIEIKS
gi 7330027   FGRRCBEVVKTLIAELIHPNLPRFHDGCFPLSAIIGFVGSLLDAPNVFTDSSGLVFPDPTVEYIEIKS
gi 321496589  FGRRCBEVVKTLIAELIHPNLPRFHDGCFPLSAIIGFVGSLLDAPNVFTDSSGLVFPDPTVEYIEIKS

```

gi 119691 α10 α11 β7 β8

 230 240 250 260 270 280 290

```

gi 119691  RFXKYLFSKSEFDPIYPSYATLYKRPCKRSFIRFNSIARTVEYVFDGRIPSEGDVLTQDEAWNLK.DV
gi 82503243  RFXKYLFSKSEFDPIYPSYATLYKRPCKRSFIRFNSIARTVEYVFDGRIPSEGDVLTQDEAWNLK.DV
gi 123845633  RFXKYLFSKSEFDPIYPSYATLYKRPCKRSFIRFNSIARTVEYVFDGRIPSEGDVLTQDEAWNLK.DV
gi 139424516  RFXKYLFSKSEFDPIYPSYATLYKRPCKRSFIRFNSIARTVEYVFDGRIPSEGDVLTQDEAWNLK.DV
gi 228537     RFXKYLFSKSEFDPIYPSYATLYKRPCKRSFIRFNSIARTVEYVFDGRIPSEGDVLTQDEAWNLK.DV
gi 51518056  RFXKYLFSKSEFDPIYPSYATLYKRPCKRSFIRFNSIARTVEYVFDGRIPSEGDVLTQDEAWNLK.DV
gi 24943119  RFXKYLFSKSEFDPIYPSYATLYKRPCKRSFIRFNSIARTVEYVFDGRIPSEGDVLTQDEAWNLK.EV
gi 20453824  RFXKYLFSKSEFDPIYKDYALYNNPKCATLVDFISSIPKPAVEHVPGRVPTQNDLSDPKMWNFPNQ
gi 27452874  RFXKYLFSKSEFDPIYKDYALYNNPKCATLVDFISSIPKPAVEHVPGRVPTQNDLSDPKMWNFPNQ
gi 30348540  RFXKYLFSKSECDTLYKDYALYNNPKCATLVDFISSIPKPAVEHVPGRVPTQNDLSDPKMWNFPNQ
gi 9625993   RFXKYLFSKSECDTLYKDYALYNNPKCATLVDFISSIPKPAVEHVPGRVPTQNDLSDPKMWNFPNQ
gi 27452835  RFXKYLFSKSEFDPIYKDYALYNNPKCATLVDFISSIPKPAVEHVPGRVPTQNDLSDPKMWNFPNQ
gi 10140958  RFXKYLFSKSEFDPIYKDYALYNNPKCATLVDFISSIPKPAVEHVPGRVPTQNDLSDPKMWNFPNQ
gi 9631229   RFXKYLFAKCDYDPIYNYLALYNNPKCATLVDFISSIPKPAVEHVPGRVPTQNDLSDPKMWNFPNQ
gi 9628040   RFXKYLFAKCDYDPIYNYLALYNNPKCATLVDFISSIPKPAVEHVPGRVPTQNDLSDPKMWNFPNQ
gi 9629578   RFXKYLFAKCDYDPIYNYLALYNNPKCATLVDFISSIPKPAVEHVPGRVPTQNDLSDPKMWNFPNQ
gi 83642873  RFXKYLFAKCDYDPIYNYLALYNNPKCATLVDFISSIPKPAVEHVPGRVPTQNDLSDPKMWNFPNQ
gi 78127870  RFXKYLFAKCDYDPIYNYLALYNNPKCATLVDFISSIPKPAVEHVPGRVPTQNDLSDPKMWNFPNQ
gi 262285082  RFXKYLFAKCDYDPIYNYLALYNNPKCATLVDFISSIPKPAVEHVPGRVPTQNDLSDPKMWNFPNQ
gi 134038663  RFXKYLFAKCDYDPIYNYLALYNNPKCATLVDFISSIPKPAVEHVPGRVPTQNDLSDPKMWNFPNQ
gi 13095614  RFXKYLFAKCDYDPIYNYLALYNNPKCATLVDFISSIPKPAVEHVPGRVPTQNDLSDPKMWNFPNQ
gi 2246484   RFXKYLFAKMECDPIYAAQRLYEAQPKLALKDFYYSISKPAVEYVGLGKIPSSDVLVAYDQEWAEAC.PR
gi 1718290   RFXKYLFAKMECDPIYAAQRLYEAQPKLALKDFYYSISKPAVEYVGLGKIPSSDVLVAYDQEWAEAC.PR
gi 139472831  RFXKYLFAKMECDPIYAAQRLYEAQPKLALKDFYYSISKPAVEYVGLGKIPSSDVLVAYDQEWAEAC.PR
gi 46519394  RFXKYLFAKMECDPIYAAQRLYEAQPKLALKDFYYSISKPAVEYVGLGKIPSSDVLVAYDQEWAEAC.PR
gi 18653844  RFXKYLFAKMECDPIYAAQRLYEAQPKLALKDFYYSISKPAVEYVGLGKIPSSDVLVAYDQEWAEAC.PR
gi 7330027   RFXKYLFAKMECDPIYAAQRLYEAQPKLALKDFYYSISKPAVEYVGLGKIPSSDVLVAYDQEWAEAC.PR
gi 321496589  RFXKYLFAKMECDPIYAAQRLYEAQPKLALKDFYYSISKPAVEYVGLGKIPSSDVLVAYDQEWAEAC.PR

```

gi 119691 α12 β9 β10 β11 β12 α13

 300 310 320 330 340 350 360

```

gi 119691  RRRKRLGPGHDLVADSLAANRGVBSMLYVMVTDPSENAGRICTKDRVPIIFINPRHNFYVQLQYKIVGD
gi 82503243  RRRKRLGPGHDLVADSLAANRGVBSMLYVMVTDPSENAGRICTKDRVPIIFINPRHNFYVQLQYKIVGD
gi 123845633  RRRKRLGPGHDLVADSLAANRGVBSMLYVMVTDPSENAGRICTKDRVPIIFINPRHNFYVQLQYKIVGD
gi 139424516  RRRKRLGPGHDLVADSLAANRGVBSMLYVMVTDPSENAGRICTKDRVPIIFINPRHNFYVQLQYKIVGD
gi 228537     RRRKRLGPGHDLVADSLAANRGVBSMLYVMVTDPSENAGRICTKDRVPIIFINPRHNFYVQLQYKIVGD
gi 51518056  RRRKRLGPGHDLVADSLAANRGVBSMLYVMVTDPSENAGRICTKDRVPIIFINPRHNFYVQLQYKIVGD
gi 24943119  RRRKRLGPGHDLVADSLAANRGVBSMLYVMVTDPSENAGRICTKDRVPIIFINPRHNFYVQLQYKIVGD
gi 20453824  RRRKRLGPGHDLVADSLAANRGVBSMLYVMVTDPSENAGRICTKDRVPIIFINPRHNFYVQLQYKIVGD
gi 27452874  RRRKRLGPGHDLVADSLAANRGVBSMLYVMVTDPSENAGRICTKDRVPIIFINPRHNFYVQLQYKIVGD
gi 30348540  RRRKRLGPGHDLVADSLAANRGVBSMLYVMVTDPSENAGRICTKDRVPIIFINPRHNFYVQLQYKIVGD
gi 9625993   RRRKRLGPGHDLVADSLAANRGVBSMLYVMVTDPSENAGRICTKDRVPIIFINPRHNFYVQLQYKIVGD
gi 27452835  RRRKRLGPGHDLVADSLAANRGVBSMLYVMVTDPSENAGRICTKDRVPIIFINPRHNFYVQLQYKIVGD
gi 10140958  RRRKRLGPGHDLVADSLAANRGVBSMLYVMVTDPSENAGRICTKDRVPIIFINPRHNFYVQLQYKIVGD
gi 9631229   RRRKRLGPGHDLVADSLAANRGVBSMLYVMVTDPSENAGRICTKDRVPIIFINPRHNFYVQLQYKIVGD
gi 9628040   RRRKRLGPGHDLVADSLAANRGVBSMLYVMVTDPSENAGRICTKDRVPIIFINPRHNFYVQLQYKIVGD
gi 9629578   RRRKRLGPGHDLVADSLAANRGVBSMLYVMVTDPSENAGRICTKDRVPIIFINPRHNFYVQLQYKIVGD
gi 83642873  RRRKRLGPGHDLVADSLAANRGVBSMLYVMVTDPSENAGRICTKDRVPIIFINPRHNFYVQLQYKIVGD
gi 78127870  RRRKRLGPGHDLVADSLAANRGVBSMLYVMVTDPSENAGRICTKDRVPIIFINPRHNFYVQLQYKIVGD
gi 262285082  RRRKRLGPGHDLVADSLAANRGVBSMLYVMVTDPSENAGRICTKDRVPIIFINPRHNFYVQLQYKIVGD
gi 134038663  RRRKRLGPGHDLVADSLAANRGVBSMLYVMVTDPSENAGRICTKDRVPIIFINPRHNFYVQLQYKIVGD
gi 13095614  RRRKRLGPGHDLVADSLAANRGVBSMLYVMVTDPSENAGRICTKDRVPIIFINPRHNFYVQLQYKIVGD
gi 2246484   RRRKRLGPGHDLVADSLAANRGVBSMLYVMVTDPSENAGRICTKDRVPIIFINPRHNFYVQLQYKIVGD
gi 1718290   RRRKRLGPGHDLVADSLAANRGVBSMLYVMVTDPSENAGRICTKDRVPIIFINPRHNFYVQLQYKIVGD
gi 139472831  RRRKRLGPGHDLVADSLAANRGVBSMLYVMVTDPSENAGRICTKDRVPIIFINPRHNFYVQLQYKIVGD
gi 46519394  RRRKRLGPGHDLVADSLAANRGVBSMLYVMVTDPSENAGRICTKDRVPIIFINPRHNFYVQLQYKIVGD
gi 18653844  RRRKRLGPGHDLVADSLAANRGVBSMLYVMVTDPSENAGRICTKDRVPIIFINPRHNFYVQLQYKIVGD
gi 7330027   RRRKRLGPGHDLVADSLAANRGVBSMLYVMVTDPSENAGRICTKDRVPIIFINPRHNFYVQLQYKIVGD
gi 321496589  RRRKRLGPGHDLVADSLAANRGVBSMLYVMVTDPSENAGRICTKDRVPIIFINPRHNFYVQLQYKIVGD

```

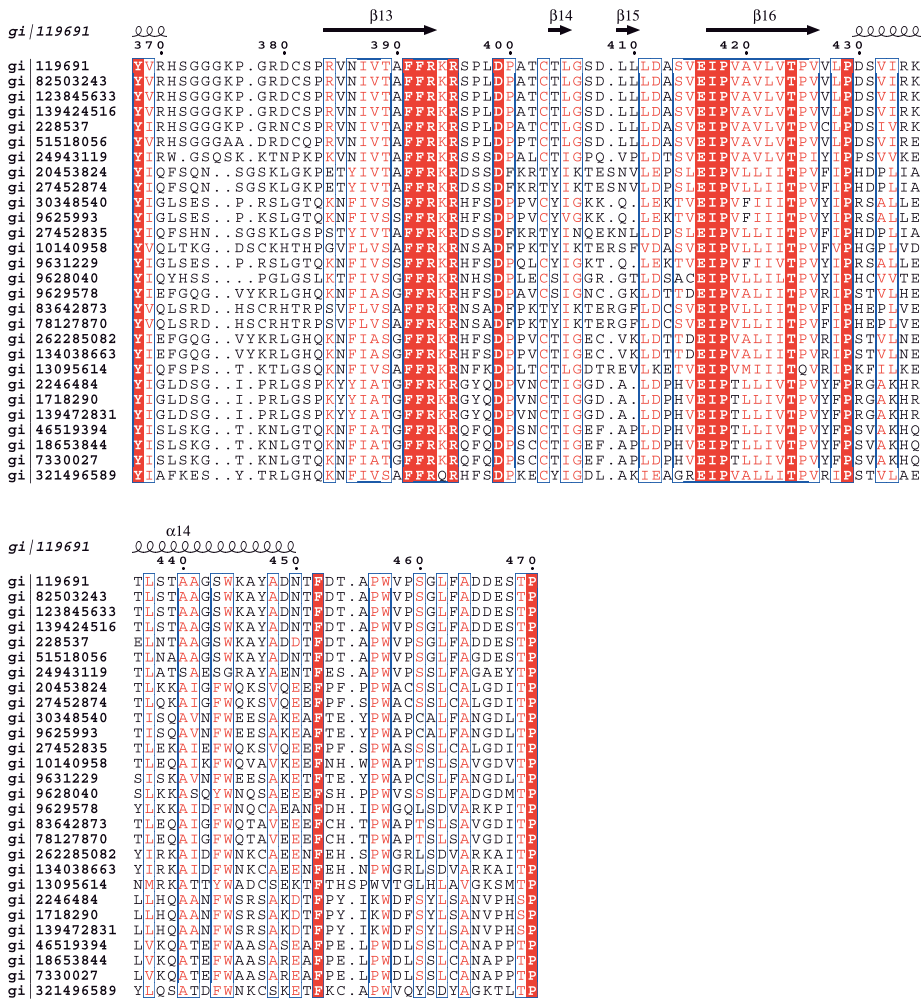



Figure S1. Alignment of gamma-herpesvirus exonuclease sequences

ESPrnt (1) was used to prepare this figure. Strictly conserved residues are printed on a red background, residues where some conservative substitutions occur are printed in red. The secondary structure elements are derived from the crystallographic structure of EBV BGLF5 (pdb entry 2W45).

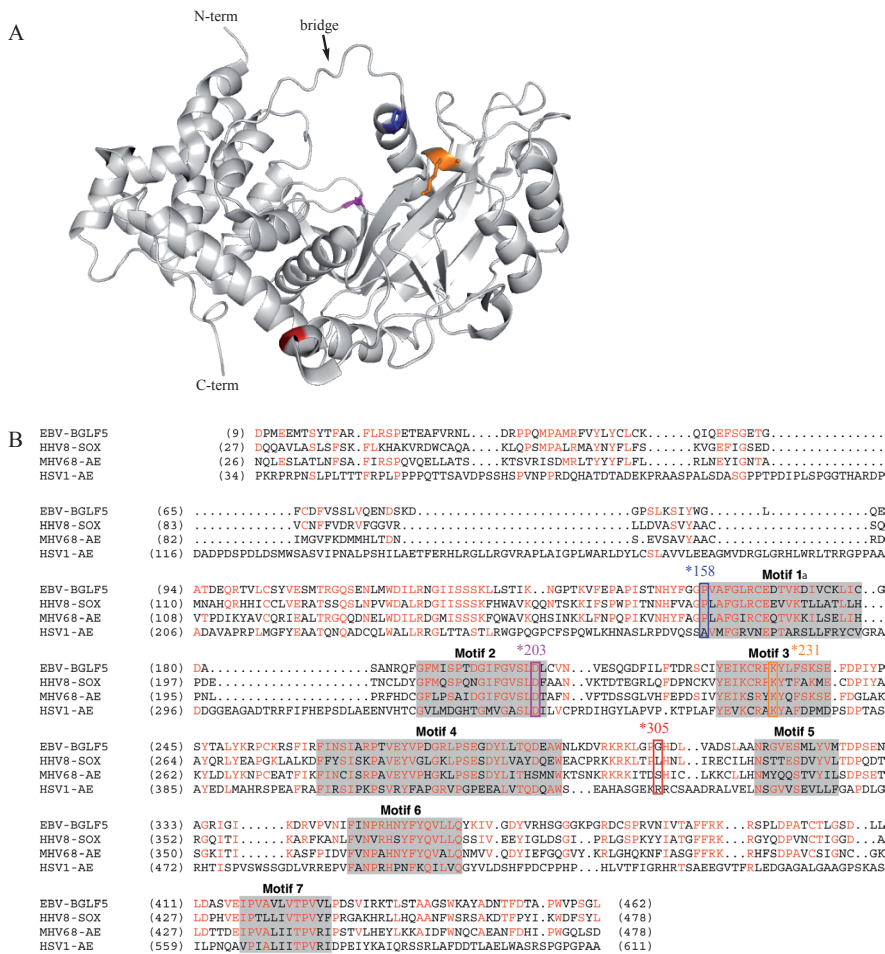


Figure S2. Structure and sequence comparisons for EBV BGLF5

(A) Architecture of the EBV nuclease: the flexible bridge is indicated with an arrow (adapted from (2)). The mutants under study are colored as follows: P158 mutants in dark blue, D203S mutant in purple, K231M mutant in yellow, and G305C mutant in red. (B) Sequence alignment of AE homologs of three gamma-herpesviruses that combine DNase and RNase function - EBV BGLF5 (amino acids 9-462), KSHV SOX (amino acids 27-478), MHV68 AE (amino acids 26-478) - and one alpha-herpesvirus with only DNase activity - HSV-1 AE (amino acids 34-611) (adapted from (3)). The alignments, which were made without the nonconserved amino terminus sequences, were selected from a seed alignment of 14 different AE genes reported on the Wellcome Trust Sanger Institute Pfam web site (<http://www.sanger.ac.uk/Software/Pfam/data/jml/seed/PF01771.shtml>). Residues identical to the BGLF5 sequence are colored red. The boxed regions represent the seven conserved motifs within herpesvirus AE homologs. The mutants under study are colored as in A.

Supplemental references

- Gouet, P., E. Courcelle, D. I. Stuart, and F. Metoz. 1999. ESPript: analysis of multiple sequence alignments in PostScript. *Bioinformatics*. 15:305-308.
- Buisson, M., T. Geoui, D. Flot, N. Tarbouriech, M. E. Rensing, E. J. Wiertz, and W. P. Burnmeister. 2009. A bridge crosses the active-site canyon of the Epstein-Barr virus nuclease with DNase and RNase activities. *J. Mol. Biol.* 391:717-728.
- Rowe, M., B. Glaunsinger, D. van Leeuwen, J. Zuo, D. Sweetman, D. Ganem, J. Middeldorp, E. J. Wiertz, and M. E. Rensing. 2007. Host shutoff during productive Epstein-Barr virus infection is mediated by BGLF5 and may contribute to immune evasion. *Proc. Natl. Acad. Sci. U. S. A* 104:3366-3371.

Chapter 8

General discussion

Partly published in:

Epstein-Barr virus evasion of CD8⁺ and CD4⁺ T cell immunity via concerted actions of multiple gene products

M.E. Ressing*, D. Horst*, B.D. Griffin*, J. Tellam, J. Zuo, R. Khanna, M. Rowe and E.J.H.J. Wiertz.

Seminars in Cancer Biology 2008

Viral evasion of T cell immunity: ancient mechanisms offering new applications

D. Horst*, M.C. Verweij*, A.J. Davison, M.E. Ressing and E.J.H.J. Wiertz.

Current Opinion in Immunology 2011

Exploiting human herpesvirus immune evasion for therapeutic gain: potential and pitfalls

D. Horst, M.E. Ressing and E.J.H.J. Wiertz.

Immunology and Cell Biology 2011

Viral inhibition of TAP: a striking example of convergent evolution

M.C. Verweij*, D. Horst*, B.D. Griffin, A.J. Davison, M.E. Ressing and E.J.H.J. Wiertz.

In preparation

* These authors contributed equally to this manuscript

General discussion – Part I

Immune evasion by herpesviruses

Herpesviruses stand out for their capacity to establish lifelong infections of immunocompetent hosts, generally without causing overt symptoms. Herpesviruses are equipped with sophisticated immune evasion strategies, allowing these viruses to persist for life despite the presence of a strong antiviral immune response. The MHC class I (MHC I) antigen processing and presentation pathway appears to be a prime target for viral evasion, illustrating the evolutionary pressure exerted by CD8⁺ cytotoxic T lymphocytes (CTLs) during co-evolution of these viruses with their hosts. In the preceding chapters of this thesis, I have focused on two Epstein-Barr virus (EBV)-encoded immune evasion proteins: the Transporter associated with Antigen Processing (TAP) inhibitor BNLF2a and the host shutoff protein BGLF5. In this part of the discussion, I will focus on the role of immune evasion in viral infection.

Thwarting antigen presentation by inhibition of TAP-mediated peptide transport

Members of all three subfamilies in the family *Herpesviridae* appear to exploit inhibition of TAP-mediated peptide transport as an immune evasion strategy to perturb recognition and elimination by MHC I-restricted T cells. A viral block to TAP function results in diminished supply of potentially antigenic peptides into the ER lumen and, consequently, reduced display of newly formed MHC I-peptide complexes at the surface of infected cells.

Various herpesviruses, and more recently also cowpox virus (CPXV), have been found to encode TAP inhibitors. These proteins exhibit substantial variation in structural characteristics as well as in mechanisms of action. Among the herpesvirus TAP inhibitors are cytosolic proteins (ICP47 (1-4)), type I transmembrane proteins (US6 (5-7) and UL49.5 (8, 9)), and a tail-anchored transmembrane protein (BNLF2a (10, 11)). The CPXV-encoded TAP inhibitor CPXV012 has the features of a type II membrane protein (12, 13). The mechanisms exploited by the various viral inhibitors to block TAP function include preventing association of peptide or ATP or both peptide and ATP to the cytosolic domains of TAP (ICP47, equid herpesvirus (EHV)-1 and -4 UL49.5, US6, and BNLF2a). The viral inhibitors may impose conformational restrictions on the TAP complex (UL49.5, US6 and possibly also BNLF2a). In addition, some TAP inhibitors cause degradation of the transporter's subunits (bovine herpesvirus (BoHV)-1 and -5, bubaline herpesvirus 1 and cervid herpesvirus 1 UL49.5). Finally, a viral immune evasion protein can be dedicated to this

particular function (ICP47, US6, BNLF2a, and CPXV012), or it may exert other functions unrelated to immune evasion (UL49.5). Despite their large diversity in structural and functional features, the viral TAP inhibitors have evolved to serve a common and compelling end: inhibition of peptide transport by TAP, with the ultimate aim to avoid elimination of the virus-producing cell by MHC I-restricted CTLs. The manner in which this has been achieved represents a striking example of functional convergent evolution.

The acquisition of TAP inhibitors by so many viruses testifies to the importance of CTLs in antiviral immunity and at the same time identifies TAP as an Achilles' heel of the immune system. In view of the fact that this bottleneck early in the antigen processing pathway is targeted by these viruses, it is not surprising that the timing of expression of the viral TAP inhibitors during natural infection appears rather similar. Appearance of the TAP-inhibiting proteins encoded by alpha-, beta-, and gammaherpesviruses starts in all cases at early times in the viral replication cycle (2, 6, 11, 14, 15). Expression of EBV BNLF2a seems to be reduced at later times in infection (16), when other EBV-encoded immune evasive molecules are effective. In contrast, BoHV-1 UL49.5 is expressed from 3 hours after infection onwards, and levels do not drop until 12 hours after infection (15). This prolonged expression may be explained by the dual role of the UL49.5 protein: at early times, in the absence of gM, UL49.5 acts as a TAP inhibitor only, while at later times of infection the protein also functions as a chaperone for the late, structural protein gM that facilitates cell-to-cell spread of virus (15). The early expression of herpesvirus-encoded TAP inhibitors ensures inhibition of transport of viral peptides into the ER for MHC association shortly after initiation of virus replication, before abundant viral protein synthesis starts. In line with this, T cell recognition of antigenic peptides expressed early after EBV reactivation is restored in cells infected with a BNLF2a-deleted recombinant EBV (16). These results substantiate the contribution of the virus-encoded TAP inhibitors to immune evasion during natural infection. While TAP inhibition permits rapid hiding from the immune system at the initial stages of infection, additional strategies are likely to contribute to immune evasion as infection progresses.

It is tempting to speculate that the capacity to inhibit TAP is particularly advantageous for herpesviruses because they cause a lifelong infection of their host, mostly in a latent state with limited viral gene expression. Occasionally, they reactivate from latency and express the complete catalogue of viral proteins in order to replicate and spread. During such episodes, virus-specific T memory cells are likely to be abundant, and compromising their effects at an early stage would be very beneficial to virus survival. However, this is unlikely to be the whole story. Like herpesviruses, poxviruses are large DNA viruses, but

they only cause transient infections. Nevertheless, they encode a panoply of immune evasion genes that is at least as impressive as that of herpesviruses, including several that interfere with MHC I-restricted T cell recognition (12, 13, 17, 18, 18, 19). Among the orthopoxviruses, CPXV encodes the broadest range of immune evasion molecules and, indeed, it has been proposed that CPXV best represents the ancestor of the modern orthopoxviruses, which include variola virus and vaccinia virus (20, 21). Vaccinia virus has been used successfully in a worldwide immunization campaign to eradicate smallpox caused by variola virus. The diminished virulence of vaccinia virus and its success as a vaccine against smallpox may be related to the fact that many of the immunomodulatory genes, including CPXV203 and CPXV012, are mutated or deleted in vaccinia virus (12, 13, 18, 18, 19, 22).

The presence of TAP-inhibiting proteins among members of all three herpesvirus subfamilies (Figure 1) and in CPXV underscores the importance of TAP-mediated peptide transport for effective antiviral immunity. Additionally, the fact that the various TAP inhibitors do not share any obvious similarity in structure, function or evolutionary origins suggests that a common strategy to specifically target TAP function has evolved independently at various times within the different herpesvirus subfamilies and also within the poxviruses. Even within an individual subfamily, viruses seem to use different strategies to block TAP – among the alphaherpesviruses, utilizing ICP47 in simplexviruses and UL49.5 in certain varicelloviruses.

In conclusion, five classes of TAP inhibitors have been identified so far. These classes appear to be unrelated and to have been acquired independently and probably relatively recently, during evolution. Blockage of TAP disturbs the recognition and elimination of virally infected cells by CTLs and maximizes the opportunity for viral replication and spread. The acquisition of unrelated proteins that block TAP function highlights the important role of TAP-mediated peptide transport in the generation of an effective immune response against these viruses.

Evading CTL recognition by shutting down protein synthesis

Infection with either alpha- or gamma-herpesviruses results in a global shutdown of host protein synthesis. The host shutoff proteins encoded by these two virus families are unrelated; the alpha-herpesviruses encode a virion host shutoff (vhs) protein, whereas gamma-herpesviruses mediate host shutoff via their alkaline exonuclease (AE). Although the AE protein is conserved across the herpesvirus family, its host shutoff activity has only been observed for the gamma-herpesvirus homologues of EBV and Kaposi's

sarcoma-associated herpesvirus (KSHV).

Both alpha- and gamma-herpesvirus host shutoff proteins induce the degradation of mRNA, thereby inhibiting translation. By reducing the synthesis of MHC I molecules and other proteins involved in antigen presentation, the host shutoff proteins might contribute to CTL evasion during viral infection. Indeed, the vhs proteins of the alpha-herpesviruses herpes simplexvirus (HSV) and BoHV-1 reduce MHC I expression during viral infection (23-25). Furthermore, HSV vhs was shown to thwart CTL recognition of virally infected cells (23). Similarly, expression of SOX and BGLF5, the host shutoff proteins of the gamma-herpesviruses KSHV and EBV, respectively, impairs T cell recognition (26).

In model experiments involving transient transfection of 293 epithelial cells or Mel JuSo melanoma cells, over 90% inhibition of recognition by EBV-specific T cells was observed following expression of BGLF5 (26). This is remarkably efficient considering that the levels of MHC I were reduced by less than 75% and the amount of EBV target protein was reduced by only 50%. However, the steady-state level of intact target protein may not be the critical factor determining the availability of antigenic peptides for presentation via MHC I. Rather, if one accepts the hypothesis that peptides presented by MHC I molecules arise mainly from proteasomal degradation of defective ribosomal products (27), then it is the rate of *de novo* synthesis that will predominantly determine the amount of target peptide available for binding to MHC I molecules. In the experimental model studied, *de novo* protein synthesis was inhibited by more than 95% (26, 28). It is also worth noting that the effect of BGLF5 on antigen presentation and T cell recognition is dose-dependent, and that the amount of BGLF5 expressed during lytic cycle in B cells may be sub-optimal. Nevertheless, during lytic cycle in B cells, protein synthesis is inhibited by more than 95%. Furthermore, BGLF5 does not work in isolation but instead it can cooperate with other immune evasion proteins to enhance the ability of EBV to escape T cell responses. Taken together, the host shutoff proteins of both alpha- and gamma-herpesviruses reduce MHC I expression and contribute to CTL evasion. In addition, these proteins might interfere with other functions of the immune system, e.g. recognition of MHC class II (MHC II) molecules by T helper cells and activation of pattern recognition receptors like Toll-like receptors.

Consequences of MHC I evasion

Herpesviruses are highly species specific, hampering the use of animal models in evaluating the role of the human herpesvirus-encoded immune evasion proteins *in vivo*. However, a role for MHC I evasion *in vivo* was demonstrated using animal models of murine and primate herpesvirus infection.

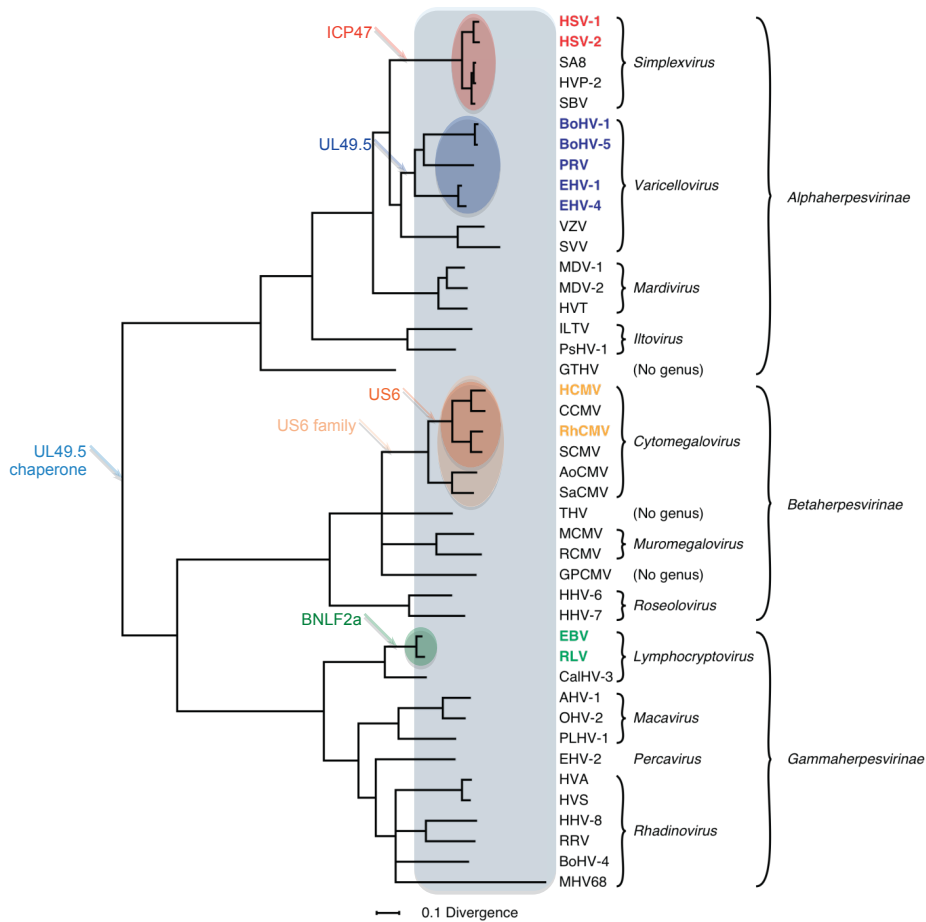


Figure 1. Phylogenetic tree for the family *Herpesviridae*

The Bayesian tree is based on amino acid sequence alignments for six large, well-conserved genes, namely the orthologues of HSV-1 genes UL15, UL19, UL27, UL28, UL29 and UL30, and is derived from McGeoch *et al.* (135). Assignments to genera and subfamilies are shown on the right. Red, blue, orange and green shading show viruses that have the ICP47, UL49.5, US6 or BNLF2a TAP inhibitor genes, and corresponding colouring of virus abbreviations show viruses in which these genes have been shown to be functional as TAP inhibitors. Light orange shading shows that all members of the genus *Cytomegalovirus* have members of the US6 gene family. Light blue shading shows that all members of the family *Herpesviridae* have a UL49.5 orthologue, which presumably preserves a more ancient function as a chaperone for gM.

Murine γ -herpesvirus-68 (MHV68) displays homology to KSHV. Similar to EBNA1 and LANA1, the MHV68 ORF73-encoded protein, which is required for episome maintenance, inhibits antigen presentation *in cis* (29). Another immune evasion protein encoded by MHV68, mK3, targets MHC I molecules for proteasomal degradation (30). Circumventing ORF73-inhibited antigen presentation (29) or deletion of mK3 (31) decreased latent viral loads in mice, indicating that MHC I-inhibiting proteins contribute to immune evasion *in vivo*.

HSV ICP47 efficiently blocks human TAP but has low affinity for murine TAP (3, 32), rendering murine infection models somewhat limited. Nonetheless, in an attempt better to understand the impact of MHC I immune evasion on HSV infection *in vivo*, recombinant HSVs expressing alternative immune evasion molecules (human cytomegalovirus (HCMV) US11 or murine cytomegalovirus (MCMV) m152) have been generated (33). Both recombinant viruses retained the ability to elicit CD8⁺ T cell responses in mice, but these were ineffective in controlling acute viral infection (33). In addition, the recombinant HSVs were more efficient at reactivating from latency, even in the presence of HSV-specific T cells (34). Apparently, efficient evasion of local T cell-mediated control facilitates HSV reactivation, identifying MHC I evasion as a virulence factor for HSV infection in mice. Viral TAP inhibitors might contribute to the viral life cycle in a similar fashion.

Although MHC I-inhibiting proteins prevent immune recognition of virus-infected cells, they appear to have a modest influence on the development of an antiviral immune response. The majority of the MCMV-specific CD8⁺ T cells has been proposed to be induced via cross-presentation (35), thereby limiting the role for MHC I-inhibiting proteins in shaping the immune response. Accordingly, the CD8⁺ T cell response observed after MCMV infection was not markedly affected by the absence of the virus-encoded MHC I-inhibiting proteins (36, 37). Similarly, the overall immune response induced by rhesus CMV (RhCMV) was not affected by deletion of the viral MHC I-inhibiting proteins (38). It remains to be established whether this also applies to other herpesviruses.

Herpesvirus infection of immune hosts

The vigorous virus-specific immune response elicited after primary herpesvirus infection is not only incapable of eradicating the virus, resulting in lifelong persistence, but appears also unable to prevent new infections with the same or a similar virus (superinfection). Members of the alpha- (39), beta- (40) and gammaherpesvirus (41) family have been suggested to superinfect immune individuals. Recently, a landmark study by Hansen *et al.* revealed the essential role immune evasion molecules play in

enabling superinfection. RhCMV, which contains functional homologues of HCMV US2, US3, US6 and US11 (42), can superinfect RhCMV⁺ rhesus macaques (38, 43). This superinfection requires either interference with MHC I antigen presentation mediated by the US2-11 homologues or depletion of CD8⁺ T cells. In contrast, the MHC I-inhibiting proteins are dispensable for a lifelong infection of RhCMV-naïve rhesus macaques. Thus, CTL evasion allows herpesviruses to infect their host in the presence of virus-specific immunity (38).

General discussion – Part II

Exploiting viral immune evasion proteins

Viral immune evasion proteins target virtually every step in the MHC I pathway and therefore constitute powerful tools for antigen processing and presentation research. The power of this approach has been demonstrated in studies in which TAP inhibitors have been used to uncover important, basic features of cross-presentation. Elucidation of the mechanisms underlying viral immune evasion strategies reveals essential, hitherto unknown cell biological and immunological processes that have been discovered by viruses as effective targets for immune evasion millions of years ago, as discussed in the remainder of this chapter. Furthermore, I will review and discuss recent efforts to exploit human herpesvirus MHC I evasion strategies for the rational design of novel strategies for vaccine development, cancer treatment, transplant protection and gene therapy.

HERPESVIRUS IMMUNE EVASION PROTEINS AS RESEARCH TOOLS

Valuable tools in antigen presentation studies

EBV EBNA1 and KSHV LANA carry large repeats of glycine-alanine and serine-proline residues, respectively, that hamper proteasomal degradation of these viral gene products (44, 45). When transferred to other proteins, the repeats effectively block degradation of these proteins *in cis*. Thus, they can be used to inhibit the first stage of the MHC I presentation pathway, namely the generation of antigenic peptides by proteasomes (45, 46). EBNA1 has also been instrumental in uncovering the role of autophagy in antigen presentation. Using EBNA1 as a model antigen, autophagy was found to allow MHC II-mediated presentation of peptides derived from a nuclear or cytosolic protein (47, 48).

Herpesvirus-encoded TAP inhibitors have been particularly useful in cross-presentation studies aiming

to unravel the routes by which exogenous antigens are loaded onto MHC I molecules. A 35-residue peptide encompassing the TAP inhibiting domain of HSV ICP47 has been shown to be endocytosed and to subsequently block TAP function (49). Since ICP47 interferes with the binding of peptides to cytosolic domains of TAP, this finding implies that extracellular proteins can reach the cytosol of cells, possibly via the Sec61 dislocation pathway (discussed below) (50, 51). The ICP47 peptide inhibits both direct and cross-presentation, implicating the involvement of TAP in cross-presentation.

HCMV US6 inhibits TAP by interacting with ER-luminal domains of TAP. Exposure of dendritic cells (DCs) to a soluble form of US6 completely abrogates cross-presentation, confirming the essential role for TAP in cross-presentation (52, 53). At the same time, these experiments show the existence of a connection between the extracellular milieu and TAP-containing compartments and illustrate the contribution of phagosomes and pinosomes to presentation of exogenous antigens by DCs. Selective deposition of US6 into early endosomes using a US6-transferrin fusion protein identified these endosomes as loading compartments for cross-presented peptides derived from soluble antigens (54).

The herpesvirus-encoded TAP inhibitors each act in a unique way, targeting different steps of the peptide transport process (summarized in Table 1). The viral TAP inhibitors can be used to block the peptide translocation cycle at different stages and therefore are valuable tools to study the molecular biophysics of peptide translocation by TAP. In addition, viral TAP inhibitors may be used to freeze TAP at intermediate stages of the translocation cycle, which may be informative when resolving the crystal structure of the peptide transporter (55, 56). Elucidation of the molecular mechanisms underlying viral TAP inhibition will facilitate the use of TAP inhibitors for selective immune suppression in the context of, for example, autoimmune diseases and tissue and organ transplantation. In addition, this knowledge may aid the development of substances blocking other ABC transporters, for example those responsible for multiple drug resistance in bacterial and cancer cells.

Virus	Inhibitor	Structural features	Mechanism of TAP inhibition	Refs.
HSV-1/2	ICP47	Cytosolic protein	Interference with peptide binding	(1, 136)
BoHV-1	UL49.5	Type I membrane protein	Conformational alterations and degradation of TAP1/2	(8, 9)
EHV-1/4	UL49.5	Type I membrane protein	Conformational alterations and interference with ATP binding	(8, 9)
PRV	UL49.5	Type I membrane protein	Conformational alterations	(8, 9)
HCMV	US6	Type I membrane protein	Conformational alterations and interference with ATP binding	(5, 6, 137)
EBV	BNLF2a	Tail-anchored protein	Interference with ATP and peptide binding	(10, 11)
CPXV	CPXV012	Type II membrane protein	unknown	(12, 13)

Table 1. Comparison of the mechanisms by which virus-encoded proteins specifically interfere with TAP-mediated peptide transport. Abbreviations not mentioned in the text are: PRV, Pseudorabies virus.

Lessons in immunology and cell biology

Research into the mechanisms underlying viral evasion strategies has led to the discovery of previously unknown cellular processes. This is illustrated by the HCMV proteins US2 and US11, which target MHC I molecules for proteasomal degradation (57, 58). The MHC I heavy chains (HC) are properly translocated into the ER, as inferred from their N-linked glycosylation, but subsequently are redirected to the cytosol, where they are degraded through the ubiquitin-proteasome pathway. The retrograde movement of the MHC I HC, termed 'dislocation' (as opposed to translocation), appears to occur via a constitutive pathway in the cell that plays a role in many important cellular processes, including protein quality control, the release of proteins from the ER in the context of the Unfolded Protein Response (UPR) (59), and also antigen (cross-)presentation (discussed above). The US2 and US11-mediated dislocation of MHC I HC serves as a paradigm of ER protein dislocation and degradation and has facilitated the characterization of many features of this process. These include the involvement of the translocon or Sec61 complex as a channel mediating transport of at least certain categories of dislocation substrates (58), the role of the proteasome-ubiquitin system, and the discovery of hitherto unknown constituents of this protein degradation pathway, among which the AAA ATPase p97, members of the derlin family, and ER-resident ubiquitin E3 ligases (59, 60).

Recent studies indicate that protein dislocation plays a role in antigen presentation as well, allowing proteins to migrate from intracellular compartments, such as phagosomes, and the secretory pathway back to the cytosol, where they are degraded into peptides by the proteasome (49, 50, 54, 61). The peptides derived from dislocated ER proteins are re-imported into the ER by TAP for MHC I-restricted presentation. Additionally, TAP complexes are present in phagosomal compartments, facilitating translocation of peptides into those compartments for (cross-) presentation by MHC I molecules (49, 50, 53). In a number of studies, dislocation of proteins was found to involve the Sec61 complex, analogous to HCMV US2 and US11-mediated retrotranslocation of MHC I HC (49, 50, 61).

The role of the dislocation pathway in antigen processing is further illustrated by tyrosinase, a melanocyte differentiation protein that is a target for melanoma-reactive T cells (62). Glycoproteins that are dislocated from the ER back to the cytosol lose their N-linked glycans in a reaction that is catalyzed by a cytoplasmic N-glycanase. This deglycosylation involves the deamidation of asparagines, changing these amino acids into aspartic acid. The presence of an aspartic acid residue within a T cell epitope of tyrosinase at a position where the native protein carries an asparagine residue witnesses the involvement of

the cytosolic N-glycanase, and thus ER-to-cytosol dislocation, as an essential step in the processing of this particular epitope (63). Deamidation has been found for several other T cell epitopes, including epitopes derived from HIV-1 env, hepatitis C virus E1, and lymphocytic choriomeningitis virus (LCMV) GP1 (63), suggesting a wide role for protein dislocation in antigen presentation.

Another important cellular process that is manipulated by viruses in many ways is the ubiquitin system. Herpesviruses code for E3 ubiquitin ligases, such as HSV ICP0, KSHV K3 and K5, and MHV68 mK3, but also for numerous de-ubiquitinating enzymes. The intriguing interplay between viruses and the ubiquitin system has been reviewed by Isaacson and Ploegh (64). An example of an interesting, novel phenomenon discovered in the context of herpesvirus immune evasion pertains to ubiquitin conjugation by the E3 ligases mK3 and K3/K5 of MHV68 and KSHV, respectively. These proteins catalyze the ubiquitination of cytoplasmic domains of MHC I HC, resulting in the proteasomal degradation (in case of MHV68) or endocytosis (in case of KSHV) of MHC I molecules (65). When the amino acid residues that are ubiquitinated were identified within the MHC I HC, it was found that in addition to the common ubiquitin acceptor lysine, also cysteine, serine and threonine residues were ubiquitinated (66-68). These findings implicate a novel chemical mechanism of substrate ubiquitination via ester linkages. Most likely, cysteine, serine and threonine ubiquitination is used more widely by the cell. The functional implications of this particular type of conjugation are yet to be determined.

HERPESVIRUS IMMUNE EVASION AND VACCINATION

Herpesvirus vaccines

The finding that herpesviruses can superinfect immune hosts may have far-reaching consequences when attempting to develop herpesvirus vaccines. It may be very difficult, if not impossible, to prevent infection by wild-type viruses. On the other hand, although herpesvirus vaccination might not be able to prevent primary infection, vaccination may reduce pathogenicity. For instance, a phase II clinical trial demonstrated that a recombinant EBV capsid protein gp350 vaccine was incapable of preventing EBV infection, but was efficacious in preventing the development of EBV-induced infectious mononucleosis (69). On the other hand, the ability of herpesviruses to superinfect immune individuals enables the exploitation of these viruses as vaccine vectors or oncolytic agents in a population that is for the majority infected by the same herpesvirus.

Whereas much research is focussing on the

development of vaccines against human herpesviruses, so far, only vaccines against varicella-zoster virus (VZV) are available. These vaccines protect either against disease associated with primary infection (varicella) or viral reactivation (zoster) (70, 71). A live attenuated zoster vaccine is given to elderly to boost their cellular and humoral immune responses against VZV, as waning of VZV-specific immunity in elderly predisposes them to the development of zoster (70). A profound understanding of the interplay between herpesviruses and the host immune system is essential for rational design of innovative vaccination strategies. Below, examples are discussed of how new vaccines against herpesviruses may be developed and how herpesviruses may be used as effective vaccine vectors.

Immune evasion and herpesvirus vaccine development

Several studies investigated whether deletion of the HSV UL41 gene, which encodes the vhs protein, could improve the safety and immunogenicity of a HSV vaccine strain. This protein not only limits host and viral protein expression (72-74), but also inhibits the activation of HSV-infected DCs (75). Deletion of the vhs protein is expected to increase the amount of viral antigens expressed and to enhance MHC I surface levels, thereby improving the immunogenicity of this HSV strain.

Although the vhs protein is not required for viral replication nor for establishment of latency, HSV-1 and HSV-2 mutant strains that lack the vhs protein appeared highly attenuated in mice (76, 77). In addition, deletion of the UL41 gene increased the immunogenicity of HSV-1 and HSV-2 strains and improved protection induced by these vaccine strains against the development of disease in murine models of HSV infection (78, 79). However, in a guinea pig model of HSV-2 infection, no significant effects on the immunogenicity and protective capacity of the vaccine were observed by deletion of the UL41 gene, although this deletion improved the vaccine slightly (80). As the host shutoff activity of HSV-2 vhs is about 40 times more potent compared to that of HSV-1 vhs (81), a murine model was used to compare the efficacy of HSV-2 vaccines deleted for vhs or expressing the vhs protein of either HSV-1 or HSV-2. Whereas all three viruses protected against disease induced by HSV-2 infection, immunization with the vhs-deleted strain resulted in the largest reduction of virus shedding (82). In summary, deletion of the UL41 gene from a HSV vaccine can improve both immunogenicity and efficacy of this vaccine, most likely by increasing the levels of MHC I and viral antigens. However, the positive effects of this deletion seem to depend on the infection model used to test the vaccine.

Using herpesviruses as vectors for heterologues vaccination

The ability of herpesviruses to superinfect their host can be exploited for heterologues vaccination. As herpesviruses cause a lifelong infection of their host, herpesvirus-derived vaccine vectors can provide sustained levels of antigen expression, resulting in the generation of strong, long-lived immune responses. Indeed, after vaccination of rhesus macaques with a RhCMV or HSV vector encoding simian immunodeficiency virus (SIV) proteins, the animals developed long-lived, SIV-specific immune responses (43, 83, 84). After intrarectal challenge with SIV, all non-vaccinated control macaques were progressively infected, whereas around one third of the vaccinated rhesus macaques were protected from progressive SIV infection. (43, 83). However, after intravenous challenge with SIV, all vaccinated animals were progressively infected, although, at early times of infection, viral loads were lower in vaccinated macaques compared to non-vaccinated macaques (84). Kaur *et al.* generated a vaccine strain based on the d106 HSV-1 vector, which is severely attenuated by the deletion of the genes encoding for ICP4 and ICP27. These two proteins are required for efficient synthesis of early and late viral proteins and contribute to host shutoff by inhibiting the transcription of host genes. In addition, this vector lacks expression of the immediate early proteins ICP22 and ICP47, which are involved in the transcription of late viral genes and immune evasion by blocking TAP-mediated peptide transport, respectively (85). Vaccination using this d106 HSV-1 vector resulted in a more potent immune response compared to that elicited by a vector deleted for ICP27 only (83, 84). SIV protein levels were higher in cells infected with a d106-derived vector compared to a ICP27-deleted vector (86), suggesting that the improved immunogenicity is caused by elevated protein levels of the transgene. In an attempt to enhance the immunogenicity of a d106 vector expressing HIV gag, the UL41 gene encoding the vhs protein was deleted. Surprisingly, this deletion resulted in reduced expression levels of the gag transgene and negatively affected the induction of both a gag-specific antibody and CTL response (87). Overall, these results indicate that the immunogenicity of a protein is mostly determined by its expression level and that a host shutoff-mediated reduction in protein expression hampers the induction of an effective immune response.

APPLICATION OF HERPESVIRUSES IN THE FIGHT AGAINST CANCER

Using herpesviruses for oncolytic therapy

Herpesvirus vectors may also be exploited for

oncolytic therapy, which relies on the lytic replication of viruses in tumor cells. A safe oncolytic vector can be generated by deleting genes that are essential for viral replication in normal cells, but dispensable in tumor cells. Neurovirulence of HSV is determined by the viral ICP34.5 protein (88), which counteracts cellular antiviral responses. Upon viral infection, double-stranded RNA-dependent protein kinase R (PKR) is activated, resulting in phosphorylation of eIF-2 α and a subsequent shut down of protein synthesis. In HSV-infected cells, ICP34.5 interacts with protein phosphatase 1 α , resulting in dephosphorylation of eIF-2 α and continuation of viral protein synthesis (89). However, in the absence of ICP34.5, eIF-2 α remains phosphorylated and protein synthesis is inhibited, thereby severely impairing viral growth (90). This absence might not be problematic for viral replication in tumor cells, as the expression and activation of PKR and eIF-2 α is often altered in malignant cells (reviewed in (91, 92)). Virulence of HSV is also determined by ICP6, the large subunit of ribonucleotide reductase (93). This protein is involved in viral DNA synthesis and is required for efficient viral replication in non-dividing cells, but is dispensable in dividing cells (94, 95).

The HSV-1 vector G207, which is deleted for both ICP34.5 and ICP6, is attenuated for neurovirulence in mice and non-human primates (96) and can be safely administered to humans (97, 98). Because of these gene deletions, replication of the recombinant virus will be compromised in normal cells, but this virus will be capable of establishing a lytic infection in malignant cells, thereby eliminating these cells preferentially. Intraneoplastic inoculation of G207 indeed reduced the growth of human tumors in immunocompromised mice and improved their survival (96). Phase I clinical trials suggest that this vector has antitumor activity in humans as well (97, 98).

However, not all malignant cells support viral replication of HSV in the absence of ICP34.5. Repetitive infection with ICP34.5-deleted HSV of cells not supporting lytic replication generated several isolates that were selected for restored viral growth (99). In these isolates, the open reading frame of the TAP inhibitor ICP47 is disrupted, placing HSV US11 under control of the ICP47 promoter. As a consequence, US11 is expressed at immediate early instead of late times (99, 100), resulting in inhibition of eIF-2 α phosphorylation and sustained protein synthesis (100-102). Similarly, the G207-derived vector G47 Δ was deleted for ICP47 and expresses US11 as an immediate early protein (103). While these ICP47/US11^{IE} mutants had enhanced oncolytic activity in murine tumor models (103-105), this virus was still severely attenuated for neurovirulence (106). Whereas deletion of the TAP inhibitor ICP47 is expected to enhance the immunogenicity of infected cells and therefore the oncolytic activity of HSV, this has not been proven *in vivo* yet. Unfortunately,

ICP47 does not block murine TAP (1, 3). Thus, the role of this viral TAP inhibitor can not be investigated using murine tumor models. However, there are some indications that removal of ICP47 might be beneficial. Inoculation of a tumor with an oncolytic HSV vector not only caused a direct cytotoxic effect due to viral replication in the infected malignant cells, but also induced a tumor-specific immune response *in vivo* (107-109). This immune response is likely initiated by the virus-mediated destruction of tumor cells, thereby releasing tumor antigens that are taken up and presented by antigen presenting cells. Deletion of ICP47 increased MHC I expression on HSV-infected human tumor cells and enhanced recognition by tumor-specific T cells *in vitro* (103, 107). Taking these findings into consideration, it will be interesting to investigate whether deletion of ICP47 promotes the oncolytic activity of HSV vectors using *in vivo* primate tumor models.

Priming TEIPP-specific T cells

Antigen presentation defects are not only observed for virus-infected cells, as also tumors escape from immune recognition. Impairment of proteasome, TAP or tapasin function obstructs antigen presentation via MHC I molecules, allowing malignant cells to elude tumor-specific CTLs (110). Nevertheless, these antigen processing-deficient tumor cells may be targeted by another category of CTLs, which specifically recognize MHC I molecules presenting T cells epitopes associated with impaired peptide processing (TEIPPs). TEIPP-specific CTLs were induced by immunization of mice with TAP-deficient tumor cells and selected by repeated *in vitro* restimulation. Adoptive transfer of the TEIPP-specific CTLs resulted in selective targeting of TAP-deficient tumor cells in mice (111). Alternatively, immunization of mice with TAP-negative cells induced TEIPP-specific CTLs and protected these mice against the outgrowth of TAP-deficient tumors (112, 113).

Although TEIPPs are derived from common endogenous proteins, presentation of these epitopes is restricted to cells that have antigen processing defects (114). Normal cells can be induced to present TEIPPs by expression of UL49.5 (112, 115), a viral TAP inhibitor encoded by BoHV-1 (8). In contrast to ICP47 (1, 3) and BNLF2a (32), UL49.5 and also US6 efficiently block mouse TAP in addition to human TAP (8, 32, 115), making them an excellent tool to study TEIPP presentation *in vivo* using mouse models. Viral TAP inhibitors can also be used to expand TEIPP-specific CTLs from cancer patients, thus providing a novel means for immunotherapy.

EXPLOITING HERPESVIRUS STEALTH TECHNOLOGY

Improving gene therapy using herpesvirus immune evasion molecules

Gene therapy increasingly becomes an important approach to treat inherited genetic disorders. However, transgene products frequently represent antigens that are foreign to the host and therefore induce an immune response. In addition, depending on the virus used as a gene therapy vector, an immune response may be directed against the vector as well. These immune responses prevent long-term expression of the transgene and hamper the effectiveness of the therapy (116, 117). In this context, implementing viral immune evasion strategies might be beneficial.

Simultaneous expression of the MHC I evasion proteins HSV ICP47 and HCMV US11 prevented the presentation of transgene-specific antigens to CTLs *in vitro* (118). Likewise, expression of ICP47 by adenoviral vectors diminished the development of an adenovirus-specific CTL response in rhesus macaques (119). However, expression of these MHC I-inhibiting proteins sensitized the cells for NK-cell mediated lysis (118, 119), hampering the suitability of these immune evasion proteins.

Instead of impairing MHC I antigen presentation *in trans* by proteins like ICP47 and US11, viral immune evasion strategies can be exploited more specifically to restrict antigen presentation at the level of the transgene product *in cis*. Fusion of the Gly-Ala repeat of EBNA1 to a transgenic protein impaired presentation of peptides derived from this protein to CTLs (46, 120) and prolonged expression of the transgene *in vivo* (46, 121). Overall, exploiting virus stealth technology seems a promising strategy to reduce the immunogenicity of transgenic proteins, thereby improving the efficacy of gene therapy.

Avoiding transplant rejection through viral evasion mechanisms

The immune system not only eliminates virus-infected and malignant cells, but also discerns transplants as foreign. In many instances, suppression of the immune system of the recipient is required to prevent graft rejection. However, systemic immunosuppression frequently results in the occurrence of opportunistic infections, which may cause considerable morbidity and mortality. In contrast, selective expression of MHC I-inhibiting proteins in the transplant thwarts recognition by CTLs in the absence of systemic effects.

To our knowledge, human herpesvirus immune evasion proteins have not been used to prevent graft rejection *in vivo* yet. However, several studies have demonstrated that adenovirus immune evasion molecules represent

a powerful tool to reduce graft rejection in mice. The adenovirus E3 region contains, among others, the gp19K protein that interferes with MHC I-restricted antigen presentation (122-125) and three proteins that inhibit apoptosis (reviewed in (126-128)). Expression of the E3-encoded MHC I- and apoptosis-inhibiting proteins or the entire E3 region by β -cells protected them from allogeneic rejection after transplantation in mice (129, 130). Further experiments are needed to evaluate whether this protection is due to CTL evasion or inhibition of apoptosis.

Several *in vitro* experiments related to transplant rejection were performed using herpesvirus-encoded MHC I-inhibiting proteins; recognition of human antigen-presenting cells by both minor and major histocompatibility antigen-specific CTLs was impaired by expression of viral TAP inhibitors (131) and MHC I levels on human stem cells were lowered by the HCMV-encoded immune evasion proteins US2, US3, US6 and US11 (132, 133). Similarly, ICP47 expression by porcine cells downregulated surface MHC I and reduced recognition of these cells by human CTLs (134). In summary, these studies suggest that exploitation of virus stealth technology is a feasible approach to diminish rejection of both allo- and xenografts.

CONCLUDING REMARKS

New insights into viral immune evasion mechanisms not only enhance our understanding of virus-host interactions but also of immunological and cellular processes. Furthermore, this knowledge can be translated into clinical applications, opening new avenues for vaccination and immune modulation. Although the application of viral immune evasion mechanisms is still in its infancy, this chapter shows numerous applications of these sophisticated molecules that have been optimised and refined during millions of years of co-evolution of herpesviruses and their hosts.

References

1. Fruh, K., K. Ahn, H. Djaballah, P. Sempe, P. M. van Endert, R. Tampe, P. A. Peterson, and Y. Yang. 1995. A viral inhibitor of peptide transporters for antigen presentation. *Nature* 375:415-418.
2. York, I. A., C. Roop, D. W. Andrews, S. R. Riddell, F. L. Graham, and D. C. Johnson. 1994. A cytosolic herpes simplex virus protein inhibits antigen presentation to CD8⁺ T lymphocytes. *Cell* 77:525-535.
3. Ahn, K., T. H. Meyer, S. Uebel, P. Sempe, H. Djaballah, Y. Yang, P. A. Peterson, K. Fruh, and R. Tampe. 1996. Molecular mechanism and

- species specificity of TAP inhibition by herpes simplex virus ICP47. *EMBO J* 15:3247-3255.
4. Tomazin, R., A. B. Hill, P. Jugovic, I. York, P. van Endert, H. L. Ploegh, D. W. Andrews, and D. C. Johnson. 1996. Stable binding of the herpes simplex virus ICP47 protein to the peptide binding site of TAP. *EMBO J*. 15:3256-3266.
 5. Ahn, K., A. Gruhler, B. Galocha, T. R. Jones, E. J. Wiertz, H. L. Ploegh, P. A. Peterson, Y. Yang, and K. Fruh. 1997. The ER-luminal domain of the HCMV glycoprotein US6 inhibits peptide translocation by TAP. *Immunity* 6:613-621.
 6. Hengel, H., J. O. Koopmann, T. Flohr, W. Muranyi, E. Goulmy, G. J. Hammerling, U. H. Koszinowski, and F. Momburg. 1997. A viral ER-resident glycoprotein inactivates the MHC-encoded peptide transporter. *Immunity* 6:623-632.
 7. Hewitt, E. W., S. S. Gupta, and P. J. Lehner. 2001. The human cytomegalovirus gene product US6 inhibits ATP binding by TAP. *EMBO J*. 20:387-396.
 8. Koppers-Lalic, D., E. A. Reits, M. E. Rensing, A. D. Lipinska, R. Abele, J. Koch, R. M. Marcondes, P. Admiraal, D. van Leeuwen, K. Bienkowska-Szewczyk, T. C. Mettenleiter, F. A. Rijsewijk, R. Tampe, J. Neeffjes, and E. J. Wiertz. 2005. Varicelloviruses avoid T cell recognition by UL49.5-mediated inactivation of the transporter associated with antigen processing. *Proc. Natl. Acad. Sci. U. S. A* 102:5144-5149.
 9. Koppers-Lalic, D., M. C. Verweij, A. D. Lipinska, Y. Wang, E. Quinten, E. A. Reits, J. Koch, S. Loch, M. M. Rezende, F. Daus, K. Bienkowska-Szewczyk, N. Osterrieder, T. C. Mettenleiter, M. H. Heemskerk, R. Tampe, J. J. Neeffjes, S. I. Chowdhury, M. E. Rensing, F. A. Rijsewijk, and E. J. Wiertz. 2008. Varicellovirus UL 49.5 proteins differentially affect the function of the transporter associated with antigen processing, TAP. *PLoS. Pathog.* 4:e1000080.
 10. Hislop, A. D., M. E. Rensing, D. van Leeuwen, V. A. Pudney, D. Horst, D. Koppers-Lalic, N. P. Croft, J. J. Neeffjes, A. B. Rickinson, and E. J. Wiertz. 2007. A CD8⁺ T cell immune evasion protein specific to Epstein-Barr virus and its close relatives in Old World primates. *J. Exp. Med.* 204:1863-1873.
 11. Horst, D., D. van Leeuwen, N. P. Croft, M. A. Garstka, A. D. Hislop, E. Kremmer, A. B. Rickinson, E. J. Wiertz, and M. E. Rensing. 2009. Specific targeting of the EBV lytic phase protein BNLF2a to the transporter associated with antigen processing results in impairment of HLA class I-restricted antigen presentation. *J. Immunol.* 182:2313-2324.
 12. Alzhanova, D., D. M. Edwards, E. Hammarlund, I. G. Scholz, D. Horst, M. J. Wagner, C. Upton, E. J. Wiertz, M. K. Slifka, and K. Fruh. 2009. Cowpox virus inhibits the transporter associated with antigen processing to evade T cell recognition. *Cell Host. Microbe* 6:433-445.
 13. Byun, M., M. C. Verweij, D. J. Pickup, E. J. Wiertz, T. H. Hansen, and W. M. Yokoyama. 2009. Two mechanistically distinct immune evasion proteins of cowpox virus combine to avoid antiviral CD8 T cells. *Cell Host. Microbe* 6:422-432.
 14. Yuan, J., E. Cahir-McFarland, B. Zhao, and E. Kieff. 2006. Virus and cell RNAs expressed during Epstein-Barr virus replication. *J. Virol.* 80:2548-2565.
 15. Lipinska, A. D., D. Koppers-Lalic, M. Rychlowski, P. Admiraal, F. A. Rijsewijk, K. Bienkowska-Szewczyk, and E. J. Wiertz. 2006. Bovine herpesvirus 1 UL49.5 protein inhibits the transporter associated with antigen processing despite complex formation with glycoprotein M. *J. Virol.* 80:5822-5832.
 16. Croft, N. P., C. Shannon-Lowe, A. I. Bell, D. Horst, E. Kremmer, M. E. Rensing, E. J. Wiertz, J. M. Middeldorp, M. Rowe, A. B. Rickinson, and A. D. Hislop. 2009. Stage-specific inhibition of MHC class I presentation by the Epstein-Barr virus BNLF2a protein during virus lytic cycle. *PLoS. Pathog.* 5:e1000490.
 17. Seet, B. T., J. B. Johnston, C. R. Brunetti, J. W. Barrett, H. Everett, C. Cameron, J. Sypula, S. H. Nazarian, A. Lucas, and G. McFadden. 2003. Poxviruses and immune evasion. *Annu. Rev. Immunol.* 21:377-423.
 18. Dasgupta, A., E. Hammarlund, M. K. Slifka, and K. Fruh. 2007. Cowpox virus evades CTL recognition and inhibits the intracellular transport of MHC class I molecules. *J. Immunol.* 178:1654-1661.
 19. Byun, M., X. Wang, M. Pak, T. H. Hansen, and W. M. Yokoyama. 2007. Cowpox virus exploits the endoplasmic reticulum retention pathway to inhibit MHC class I transport to the cell surface. *Cell Host. Microbe* 2:306-315.
 20. Meyer, H., H. Neubauer, and M. Pfeffer. 2002. Amplification of 'variola virus-specific' sequences in German cowpox virus isolates. *J. Vet. Med. B Infect. Dis. Vet. Public Health* 49:17-19.
 21. Shchelkunov, S., A. Totmenin, and I. Kolosova. 2002. Species-specific differences in organization of orthopoxvirus kelch-like proteins. *Virus Genes* 24:157-162.
 22. Shchelkunov, S. N., P. F. Safronov, A. V. Totmenin, N. A. Petrov, O. I. Ryazankina, V. V. Gutorov, and G. J. Kotwal. 1998. The genomic sequence analysis of the left and right species-specific terminal region of a cowpox virus strain reveals unique sequences and a cluster of intact ORFs for immunomodulatory and host range proteins. *Virology* 243:432-460.

23. Tigges, M. A., S. Leng, D. C. Johnson, and R. L. Burke. 1996. Human herpes simplex virus (HSV)-specific CD8⁺ CTL clones recognize HSV-2-infected fibroblasts after treatment with IFN-gamma or when virion host shutoff functions are disabled. *J. Immunol.* 156:3901-3910.
24. Koppers-Lalic, D., F. A. Rijsewijk, S. B. Verschuren, van Gaans-Van den Brink JA, A. Neisig, M. E. Rensing, J. Neefjes, and E. J. Wiertz. 2001. The UL41-encoded virion host shutoff (vhs) protein and vhs-independent mechanisms are responsible for down-regulation of MHC class I molecules by bovine herpesvirus 1. *J. Gen. Virol.* 82:2071-2081.
25. Gopinath, R. S., A. P. Ambagala, S. Hinkley, and S. Srikumaran. 2002. Effects of virion host shut-off activity of bovine herpesvirus 1 on MHC class I expression. *Viral Immunol.* 15:595-608.
26. Zuo, J., W. Thomas, D. van Leeuwen, J. M. Middeldorp, E. J. Wiertz, M. E. Rensing, and M. Rowe. 2008. The DNase of gammaherpesviruses impairs recognition by virus-specific CD8⁺ T cells through an additional host shutoff function. *J. Virol.* 82:2385-2393.
27. Qian, S. B., E. Reits, J. Neefjes, J. M. Deslich, J. R. Bennink, and J. W. Yewdell. 2006. Tight linkage between translation and MHC class I peptide ligand generation implies specialized antigen processing for defective ribosomal products. *J. Immunol.* 177:227-233.
28. Rowe, M., B. Glaunsinger, D. van Leeuwen, J. Zuo, D. Sweetman, D. Ganem, J. Middeldorp, E. J. Wiertz, and M. E. Rensing. 2007. Host shutoff during productive Epstein-Barr virus infection is mediated by BGLF5 and may contribute to immune evasion. *Proc. Natl. Acad. Sci. U. S. A.* 104:3366-3371.
29. Bennett, N. J., J. S. May, and P. G. Stevenson. 2005. Gamma-herpesvirus latency requires T cell evasion during episome maintenance. *PLoS Biol.* 3:e120.
30. Boname, J. M. and P. G. Stevenson. 2001. MHC class I ubiquitination by a viral PHD/LAP finger protein. *Immunity.* 15:627-636.
31. Stevenson, P. G., J. S. May, X. G. Smith, S. Marques, H. Adler, U. H. Koszinowski, J. P. Simas, and S. Efsthathiou. 2002. K3-mediated evasion of CD8(+) T cells aids amplification of a latent gamma-herpesvirus. *Nat. Immunol.* 3:733-740.
32. Verweij, M. C., M. E. Rensing, W. Knetsch, E. Quinten, A. Halenius, B. N. van, H. Hengel, J. W. Drijfhout, H. T. van, and E. J. Wiertz. 2011. Inhibition of mouse TAP by immune evasion molecules encoded by non-murine herpesviruses. *Mol. Immunol.* 48:835-845.
33. Orr, M. T., K. H. Edelmann, J. Vieira, L. Corey, D. H. Raulet, and C. B. Wilson. 2005. Inhibition of MHC class I is a virulence factor in herpes simplex virus infection of mice. *PLoS Pathog.* 1:e7.
34. Orr, M. T., M. A. Mathis, M. Lagunoff, J. A. Sacks, and C. B. Wilson. 2007. CD8 T cell control of HSV reactivation from latency is abrogated by viral inhibition of MHC class I. *Cell Host. Microbe* 2:172-180.
35. Snyder, C. M., J. E. Allan, E. L. Bonnett, C. M. Doom, and A. B. Hill. 2010. Cross-presentation of a spread-defective MCMV is sufficient to prime the majority of virus-specific CD8⁺ T cells. *PLoS. One.* 5:e9681.
36. Gold, M. C., M. W. Munks, M. Wagner, C. W. McMahon, A. Kelly, D. G. Kavanagh, M. K. Slifka, U. H. Koszinowski, D. H. Raulet, and A. B. Hill. 2004. Murine cytomegalovirus interference with antigen presentation has little effect on the size or the effector memory phenotype of the CD8 T cell response. *J. Immunol.* 172:6944-6953.
37. Munks, M. W., A. K. Pinto, C. M. Doom, and A. B. Hill. 2007. Viral interference with antigen presentation does not alter acute or chronic CD8 T cell immunodominance in murine cytomegalovirus infection. *J. Immunol.* 178:7235-7241.
38. Hansen, S. G., C. J. Powers, R. Richards, A. B. Ventura, J. C. Ford, D. Siess, M. K. Axthelm, J. A. Nelson, M. A. Jarvis, L. J. Picker, and K. Fruh. 2010. Evasion of CD8⁺ T cells is critical for superinfection by cytomegalovirus. *Science* 328:102-106.
39. Remeijer, L., J. Maertzdorf, J. Buitenwerf, A. D. Osterhaus, and G. M. Verjans. 2002. Corneal herpes simplex virus type 1 superinfection in patients with recrudescence herpetic keratitis. *Invest Ophthalmol. Vis. Sci.* 43:358-363.
40. Meyer-Konig, U., K. Ebert, B. Schrage, S. Pollak, and F. T. Hufert. 1998. Simultaneous infection of healthy people with multiple human cytomegalovirus strains. *Lancet* 352:1280-1281.
41. Srivastava, G., K. Y. Wong, A. K. Chiang, K. Y. Lam, and Q. Tao. 2000. Coinfection of multiple strains of Epstein-Barr virus in immunocompetent normal individuals: reassessment of the viral carrier state. *Blood* 95:2443-2445.
42. Pande, N. T., C. Powers, K. Ahn, and K. Fruh. 2005. Rhesus cytomegalovirus contains functional homologues of US2, US3, US6, and US11. *J. Virol.* 79:5786-5798.
43. Hansen, S. G., C. Vieville, N. Whizin, L. Coyne-Johnson, D. C. Siess, D. D. Drummond, A. W. Legasse, M. K. Axthelm, K. Oswald, C. M. Trubey, M. Piatak, Jr., J. D. Lifson, J. A. Nelson, M. A. Jarvis, and L. J. Picker. 2009. Effector memory T cell responses are associated with protection of rhesus monkeys from mucosal simian immunodeficiency virus challenge. *Nat.*

- Med. 15:293-299.
44. Zaldumbide, A., M. Ossevoort, E. J. Wiertz, and R. C. Hoeben. 2007. *In cis* inhibition of antigen processing by the latency-associated nuclear antigen 1 of Kaposi sarcoma herpes virus. *Mol. Immunol.* 44:1352-1360.
 45. Levitskaya, J., M. Coram, V. Levitsky, S. Imreh, P. M. Steigerwald-Mullen, G. Klein, M. G. Kurilla, and M. G. Masucci. 1995. Inhibition of antigen processing by the internal repeat region of the Epstein-Barr virus nuclear antigen-1. *Nature* 375:685-688.
 46. Ossevoort, M., B. M. Visser, D. J. van den Wollenberg, d. van, V. R. Offringa, C. J. Melief, R. E. Toes, and R. C. Hoeben. 2003. Creation of immune 'stealth' genes for gene therapy through fusion with the Gly-Ala repeat of EBNA-1. *Gene Ther.* 10:2020-2028.
 47. Paludan, C., D. Schmid, M. Landthaler, M. Vockerodt, D. Kube, T. Tuschl, and C. Munz. 2005. Endogenous MHC class II processing of a viral nuclear antigen after autophagy. *Science* 307:593-596.
 48. Leung, C. S., T. A. Haigh, L. K. Mackay, A. B. Rickinson, and G. S. Taylor. 2010. Nuclear location of an endogenously expressed antigen, EBNA1, restricts access to macroautophagy and the range of CD4 epitope display. *Proc. Natl. Acad. Sci. U. S. A* 107:2165-2170.
 49. Ackerman, A. L., A. Giodini, and P. Cresswell. 2006. A role for the endoplasmic reticulum protein retrotranslocation machinery during cross-presentation by dendritic cells. *Immunity*. 25:607-617.
 50. Ackerman, A. L. and P. Cresswell. 2004. Cellular mechanisms governing cross-presentation of exogenous antigens. *Nat. Immunol.* 5:678-684.
 51. Cresswell, P., A. L. Ackerman, A. Giodini, D. R. Peaper, and P. A. Wearsch. 2005. Mechanisms of MHC class I-restricted antigen processing and cross-presentation. *Immunol. Rev.* 207:145-157.
 52. Ackerman, A. L., C. Kyritsis, R. Tampe, and P. Cresswell. 2005. Access of soluble antigens to the endoplasmic reticulum can explain cross-presentation by dendritic cells. *Nat. Immunol.* 6:107-113.
 53. Ackerman, A. L., C. Kyritsis, R. Tampe, and P. Cresswell. 2003. Early phagosomes in dendritic cells form a cellular compartment sufficient for cross presentation of exogenous antigens. *Proc. Natl. Acad. Sci. U. S. A* 100:12889-12894.
 54. Burgdorf, S., C. Scholz, A. Kautz, R. Tampe, and C. Kurts. 2008. Spatial and mechanistic separation of cross-presentation and endogenous antigen presentation. *Nat. Immunol.* 9:558-566.
 55. Procko, E., M. L. O'Mara, W. F. Bennett, D. P. Tieleman, and R. Gaudet. 2009. The mechanism of ABC transporters: general lessons from structural and functional studies of an antigenic peptide transporter. *FASEB J.* 23:1287-1302.
 56. Parcej, D. and R. Tampe. 2010. ABC proteins in antigen translocation and viral inhibition. *Nat. Chem. Biol.* 6:572-580.
 57. Wiertz, E. J., T. R. Jones, L. Sun, M. Bogyo, H. J. Geuze, and H. L. Ploegh. 1996. The human cytomegalovirus US11 gene product dislocates MHC class I heavy chains from the endoplasmic reticulum to the cytosol. *Cell* 84:769-779.
 58. Wiertz, E. J. H. J., D. Tortorella, M. Bogyo, J. Yu, W. Mothes, T. R. Jones, T. A. Rapoport, and H. L. Ploegh. 1996. Sec61-mediated transfer of a membrane protein from the endoplasmic reticulum to the proteasome for destruction. *Nature* 384:432-438.
 59. Hegde, R. S. and H. L. Ploegh. 2010. Quality and quantity control at the endoplasmic reticulum. *Curr. Opin. Cell Biol.* 22:437-446.
 60. Stagg, H. R., M. Thomas, B. D. van den, E. J. Wiertz, H. A. Drabkin, R. M. Gemmill, and P. J. Lehner. 2009. The TRC8 E3 ligase ubiquitinates MHC class I molecules before dislocation from the ER. *J. Cell Biol.* 186:685-692.
 61. Giodini, A., C. Rahner, and P. Cresswell. 2009. Receptor-mediated phagocytosis elicits cross-presentation in nonprofessional antigen-presenting cells. *Proc. Natl. Acad. Sci. U. S. A* 106:3324-3329.
 62. Ostankovitch, M., M. trich-Vanlith, V. Robila, and V. H. Engelhard. 2009. N-glycosylation enhances presentation of a MHC class I-restricted epitope from tyrosinase. *J. Immunol.* 182:4830-4835.
 63. Engelhard, V. H., M. trich-Vanlith, M. Ostankovitch, and A. L. Zarlring. 2006. Post-translational modifications of naturally processed MHC-binding epitopes. *Curr. Opin. Immunol.* 18:92-97.
 64. Isaacson, M. K. and H. L. Ploegh. 2009. Ubiquitination, ubiquitin-like modifiers, and deubiquitination in viral infection. *Cell Host. Microbe* 5:559-570.
 65. Hansen, T. H. and M. Bouvier. 2009. MHC class I antigen presentation: learning from viral evasion strategies. *Nat. Rev. Immunol.* 9:503-513.
 66. Cadwell, K. and L. Coscoy. 2005. Ubiquitination on nonlysine residues by a viral E3 ubiquitin ligase. *Science* 309:127-130.
 67. Wang, X., R. A. Herr, W. J. Chua, L. Lybarger, E. J. Wiertz, and T. H. Hansen. 2007. Ubiquitination of serine, threonine, or lysine residues on the cytoplasmic tail can induce ERAD of MHC-I by viral E3 ligase mK3. *J. Cell Biol.* 177:613-624.
 68. Wang, X., R. A. Herr, M. Rabelink, R. C. Hoeben, E. J. Wiertz, and T. H. Hansen. 2009. Ube2j2 ubiquitinates hydroxylated amino acids on ER-associated degradation substrates. *J. Cell Biol.* 187:655-668.

69. Sokal, E. M., K. Hoppenbrouwers, C. Vandermeulen, M. Moutschen, P. Leonard, A. Moreels, M. Haumont, A. Bollen, F. Smets, and M. Denis. 2007. Recombinant gp350 vaccine for infectious mononucleosis: a phase 2, randomized, double-blind, placebo-controlled trial to evaluate the safety, immunogenicity, and efficacy of an Epstein-Barr virus vaccine in healthy young adults. *J. Infect. Dis.* 196:1749-1753.
70. Sanford, M. and G. M. Keating. 2010. Zoster vaccine (Zostavax): a review of its use in preventing herpes zoster and postherpetic neuralgia in older adults. *Drugs Aging* 27:159-176.
71. Arvin, A. M. and A. A. Gershon. 1996. Live attenuated varicella vaccine. *Annu. Rev. Microbiol.* 50:59-100.
72. Read, G. S. and N. Frenkel. 1983. Herpes simplex virus mutants defective in the virion-associated shutoff of host polypeptide synthesis and exhibiting abnormal synthesis of alpha (immediate early) viral polypeptides. *J. Virol.* 46:498-512.
73. Kwong, A. D. and N. Frenkel. 1987. Herpes simplex virus-infected cells contain a function(s) that destabilizes both host and viral mRNAs. *Proc. Natl. Acad. Sci. U. S. A* 84:1926-1930.
74. Oroskar, A. A. and G. S. Read. 1989. Control of mRNA stability by the virion host shutoff function of herpes simplex virus. *J. Virol.* 63:1897-1906.
75. Samady, L., E. Costigliola, L. MacCormac, Y. McGrath, S. Cleverley, C. E. Lilley, J. Smith, D. S. Latchman, B. Chain, and R. S. Coffin. 2003. Deletion of the virion host shutoff protein (vhs) from herpes simplex virus (HSV) relieves the viral block to dendritic cell activation: potential of vhs- HSV vectors for dendritic cell-mediated immunotherapy. *J. Virol.* 77:3768-3776.
76. Smith, T. J., L. A. Morrison, and D. A. Leib. 2002. Pathogenesis of herpes simplex virus type 2 virion host shutoff (vhs) mutants. *J. Virol.* 76:2054-2061.
77. Strelow, L. I. and D. A. Leib. 1995. Role of the virion host shutoff (vhs) of herpes simplex virus type 1 in latency and pathogenesis. *J. Virol.* 69:6779-6786.
78. Dudek, T., L. C. Mathews, and D. M. Knipe. 2008. Disruption of the U(L)41 gene in the herpes simplex virus 2 dl5-29 mutant increases its immunogenicity and protective capacity in a murine model of genital herpes. *Virology* 372:165-175.
79. Geiss, B. J., T. J. Smith, D. A. Leib, and L. A. Morrison. 2000. Disruption of virion host shutoff activity improves the immunogenicity and protective capacity of a replication-incompetent herpes simplex virus type 1 vaccine strain. *J. Virol.* 74:11137-11144.
80. Hoshino, Y., L. Pesnicak, K. C. Dowdell, J. Lacayo, T. Dudek, D. M. Knipe, S. E. Straus, and J. I. Cohen. 2008. Comparison of immunogenicity and protective efficacy of genital herpes vaccine candidates herpes simplex virus 2 dl5-29 and dl5-29-41L in mice and guinea pigs. *Vaccine* 26:4034-4040.
81. Everly, D. N., Jr. and G. S. Read. 1997. Mutational analysis of the virion host shutoff gene (UL41) of herpes simplex virus (HSV): characterization of HSV type 1 (HSV-1)/HSV-2 chimeras. *J. Virol.* 71:7157-7166.
82. Reszka, N. J., T. Dudek, and D. M. Knipe. 2010. Construction and properties of a herpes simplex virus 2 dl5-29 vaccine candidate strain encoding an HSV-1 virion host shutoff protein. *Vaccine* 28:2754-2762.
83. Murphy, C. G., W. T. Lucas, R. E. Means, S. Czajak, C. L. Hale, J. D. Lifson, A. Kaur, R. P. Johnson, D. M. Knipe, and R. C. Desrosiers. 2000. Vaccine protection against simian immunodeficiency virus by recombinant strains of herpes simplex virus. *J. Virol.* 74:7745-7754.
84. Kaur, A., H. B. Sanford, D. Garry, S. Lang, S. A. Klumpp, D. Watanabe, R. T. Bronson, J. D. Lifson, M. Rosati, G. N. Pavlakis, B. K. Felber, D. M. Knipe, and R. C. Desrosiers. 2007. Ability of herpes simplex virus vectors to boost immune responses to DNA vectors and to protect against challenge by simian immunodeficiency virus. *Virology* 357:199-214.
85. Samaniego, L. A., L. Neiderhiser, and N. A. Deluca. 1998. Persistence and expression of the herpes simplex virus genome in the absence of immediate-early proteins. *J. Virol.* 72:3307-3320.
86. Watanabe, D., M. A. Brockman, T. Ndung'u, L. Mathews, W. T. Lucas, C. G. Murphy, B. K. Felber, G. N. Pavlakis, N. A. Deluca, and D. M. Knipe. 2007. Properties of a herpes simplex virus multiple immediate-early gene-deleted recombinant as a vaccine vector. *Virology* 357:186-198.
87. Liu, X., E. Broberg, D. Watanabe, T. Dudek, N. Deluca, and D. M. Knipe. 2009. Genetic engineering of a modified herpes simplex virus 1 vaccine vector. *Vaccine* 27:2760-2767.
88. Chou, J., E. R. Kern, R. J. Whitley, and B. Roizman. 1990. Mapping of herpes simplex virus-1 neurovirulence to gamma 134.5, a gene nonessential for growth in culture. *Science* 250:1262-1266.
89. He, B., M. Gross, and B. Roizman. 1997. The gamma(1)34.5 protein of herpes simplex virus 1 complexes with protein phosphatase 1alpha to dephosphorylate the alpha subunit of the eukaryotic translation initiation factor 2 and preclude the shutoff of protein synthesis by double-stranded RNA-activated protein kinase.

- Proc. Natl. Acad. Sci. U. S. A 94:843-848.
90. Chou, J., J. J. Chen, M. Gross, and B. Roizman. 1995. Association of a M(r) 90,000 phosphoprotein with protein kinase PKR in cells exhibiting enhanced phosphorylation of translation initiation factor eIF-2 alpha and premature shutoff of protein synthesis after infection with gamma 134.5- mutants of herpes simplex virus 1. *Proc. Natl. Acad. Sci. U. S. A* 92:10516-10520.
 91. Jagus, R., B. Joshi, and G. N. Barber. 1999. PKR, apoptosis and cancer. *Int. J. Biochem. Cell Biol.* 31:123-138.
 92. Rosenwald, I. B. 2004. The role of translation in neoplastic transformation from a pathologist's point of view. *Oncogene* 23:3230-3247.
 93. Jacobson, J. G., D. A. Leib, D. J. Goldstein, C. L. Bogard, P. A. Schaffer, S. K. Weller, and D. M. Coen. 1989. A herpes simplex virus ribonucleotide reductase deletion mutant is defective for productive acute and reactivatable latent infections of mice and for replication in mouse cells. *Virology* 173:276-283.
 94. Goldstein, D. J. and S. K. Weller. 1988. Herpes simplex virus type 1-induced ribonucleotide reductase activity is dispensable for virus growth and DNA synthesis: isolation and characterization of an ICP6 lacZ insertion mutant. *J. Virol.* 62:196-205.
 95. Goldstein, D. J. and S. K. Weller. 1988. Factor(s) present in herpes simplex virus type 1-infected cells can compensate for the loss of the large subunit of the viral ribonucleotide reductase: characterization of an ICP6 deletion mutant. *Virology* 166:41-51.
 96. Mineta, T., S. D. Rabkin, T. Yazaki, W. D. Hunter, and R. L. Martuza. 1995. Attenuated multi-mutated herpes simplex virus-1 for the treatment of malignant gliomas. *Nat. Med.* 1:938-943.
 97. Markert, J. M., M. D. Medlock, S. D. Rabkin, G. Y. Gillespie, T. Todo, W. D. Hunter, C. A. Palmer, F. Feigenbaum, C. Tornatore, F. Tufaro, and R. L. Martuza. 2000. Conditionally replicating herpes simplex virus mutant, G207 for the treatment of malignant glioma: results of a phase I trial. *Gene Ther.* 7:867-874.
 98. Markert, J. M., P. G. Liechty, W. Wang, S. Gaston, E. Braz, M. Karrasch, L. B. Nabors, M. Markiewicz, A. D. Lakeman, C. A. Palmer, J. N. Parker, R. J. Whitley, and G. Y. Gillespie. 2009. Phase Ib trial of mutant herpes simplex virus G207 inoculated pre- and post-tumor resection for recurrent GBM. *Mol. Ther.* 17:199-207.
 99. Mohr, I. and Y. Gluzman. 1996. A herpesvirus genetic element which affects translation in the absence of the viral GADD34 function. *EMBO J.* 15:4759-4766.
 100. He, B., J. Chou, R. Brandimarti, I. Mohr, Y. Gluzman, and B. Roizman. 1997. Suppression of the phenotype of gamma(1)34.5- herpes simplex virus 1: failure of activated RNA-dependent protein kinase to shut off protein synthesis is associated with a deletion in the domain of the alpha47 gene. *J. Virol.* 71:6049-6054.
 101. Cassady, K. A., M. Gross, and B. Roizman. 1998. The second-site mutation in the herpes simplex virus recombinants lacking the gamma134.5 genes precludes shutoff of protein synthesis by blocking the phosphorylation of eIF-2alpha. *J. Virol.* 72:7005-7011.
 102. Cassady, K. A., M. Gross, and B. Roizman. 1998. The herpes simplex virus US11 protein effectively compensates for the gamma1(34.5) gene if present before activation of protein kinase R by precluding its phosphorylation and that of the alpha subunit of eukaryotic translation initiation factor 2. *J. Virol.* 72:8620-8626.
 103. Todo, T., R. L. Martuza, S. D. Rabkin, and P. A. Johnson. 2001. Oncolytic herpes simplex virus vector with enhanced MHC class I presentation and tumor cell killing. *Proc. Natl. Acad. Sci. U. S. A* 98:6396-6401.
 104. Fukuhara, H., R. L. Martuza, S. D. Rabkin, Y. Ito, and T. Todo. 2005. Oncolytic herpes simplex virus vector g47delta in combination with androgen ablation for the treatment of human prostate adenocarcinoma. *Clin. Cancer Res.* 11:7886-7890.
 105. Taneja, S., J. MacGregor, S. Markus, S. Ha, and I. Mohr. 2001. Enhanced antitumor efficacy of a herpes simplex virus mutant isolated by genetic selection in cancer cells. *Proc. Natl. Acad. Sci. U. S. A* 98:8804-8808.
 106. Mohr, I., D. Sternberg, S. Ward, D. Leib, M. Mulvey, and Y. Gluzman. 2001. A herpes simplex virus type 1 gamma34.5 second-site suppressor mutant that exhibits enhanced growth in cultured glioblastoma cells is severely attenuated in animals. *J. Virol.* 75:5189-5196.
 107. Liu, B. L., M. Robinson, Z. Q. Han, R. H. Branston, C. English, P. Reay, Y. McGrath, S. K. Thomas, M. Thornton, P. Bullock, C. A. Love, and R. S. Coffin. 2003. ICP34.5 deleted herpes simplex virus with enhanced oncolytic, immune stimulating, and anti-tumour properties. *Gene Ther.* 10:292-303.
 108. Toda, M., S. D. Rabkin, H. Kojima, and R. L. Martuza. 1999. Herpes simplex virus as an in situ cancer vaccine for the induction of specific anti-tumor immunity. *Hum. Gene Ther.* 10:385-393.
 109. Todo, T., S. D. Rabkin, P. Sundaesan, A. Wu, K. R. Meehan, H. B. Herscovitz, and R. L. Martuza. 1999. Systemic antitumor immunity in experimental brain tumor therapy using a multimitated, replication-competent herpes simplex virus. *Hum. Gene Ther.* 10:2741-2755.
 110. Garcia-Lora, A., I. Algarra, and F. Garrido. 2003. MHC class I antigens, immune surveillance, and

- tumor immune escape. *J. Cell Physiol* 195:346-355.
111. van Hall T., E. Z. Wolpert, V. P. van, S. Laban, d. van, V. M. Roseboom, S. Bres, P. Grufman, R. A. de, H. Meiring, J. A. de, K. Franken, A. Teixeira, R. Valentijn, J. W. Drijfhout, F. Koning, M. Camps, F. Ossendorp, K. Karre, H. G. Ljunggren, C. J. Melief, and R. Offringa. 2006. Selective cytotoxic T-lymphocyte targeting of tumor immune escape variants. *Nat. Med.* 12:417-424.
 112. Chambers, B., P. Grufman, V. Fredriksson, K. Andersson, M. Roseboom, S. Laban, M. Camps, E. Z. Wolpert, E. J. Wiertz, R. Offringa, H. G. Ljunggren, and H. T. van. 2007. Induction of protective CTL immunity against peptide transporter TAP-deficient tumors through dendritic cell vaccination. *Cancer Res.* 67:8450-8455.
 113. Wolpert, E. Z., M. Petersson, B. J. Chambers, J. K. Sandberg, R. Kiessling, H. G. Ljunggren, and K. Karre. 1997. Generation of CD8⁺ T cells specific for transporter associated with antigen processing deficient cells. *Proc. Natl. Acad. Sci. U. S. A* 94:11496-11501.
 114. Oliveira, C. C., P. A. van Veelen, B. Querido, R. A. de, M. Sluijter, S. Laban, J. W. Drijfhout, S. H. van der Burg, R. Offringa, and H. T. van. 2010. The nonpolymorphic MHC Qa-1b mediates CD8⁺ T cell surveillance of antigen-processing defects. *J. Exp. Med.* 207:207-221.
 115. van Hall T., S. Laban, D. Koppers-Lalic, J. Koch, C. Precup, P. Asmawidjaja, R. Offringa, and E. J. Wiertz. 2007. The varicellovirus-encoded TAP inhibitor UL49.5 regulates the presentation of CTL epitopes by Qa-1b1. *J. Immunol.* 178:657-662.
 116. Schagen, F. H., M. Ossevoort, R. E. Toes, and R. C. Hoeben. 2004. Immune responses against adenoviral vectors and their transgene products: a review of strategies for evasion. *Crit Rev. Oncol. Hematol.* 50:51-70.
 117. Zaldumbide, A. and R. C. Hoeben. 2008. How not to be seen: immune-evasion strategies in gene therapy. *Gene Ther.* 15:239-246.
 118. Berger, C., S. Xuereb, D. C. Johnson, K. S. Watanabe, H. P. Kiem, P. D. Greenberg, and S. R. Riddell. 2000. Expression of herpes simplex virus ICP47 and human cytomegalovirus US11 prevents recognition of transgene products by CD8(+) cytotoxic T lymphocytes. *J. Virol.* 74:4465-4473.
 119. Scaria, A., J. A. Sullivan, J. A. St George, J. M. Kaplan, M. J. Lukason, J. E. Morris, M. Plog, C. Nicolette, R. J. Gregory, and S. C. Wadsworth. 2000. Adenoviral vector expressing ICP47 inhibits adenovirus-specific cytotoxic T lymphocytes in nonhuman primates. *Mol. Ther.* 2:505-514.
 120. Ossevoort, M., A. Zaldumbide, S. J. Cramer, E. I. van der Voort, R. E. Toes, and R. C. Hoeben. 2006. Characterization of an immuno 'stealth' derivative of the herpes simplex virus thymidine-kinase gene. *Cancer Gene Ther.* 13:584-591.
 121. Hendriks, W. T., R. Eggers, T. P. Carlstedt, A. Zaldumbide, M. R. Tannemaat, F. J. Fallaux, R. C. Hoeben, G. J. Boer, and J. Verhaagen. 2007. Lentiviral vector-mediated reporter gene expression in avulsed spinal ventral root is short-term, but is prolonged using an immune "stealth" transgene. *Restor. Neurol. Neurosci.* 25:585-599.
 122. Burgert, H. G. and S. Kvist. 1985. An adenovirus type 2 glycoprotein blocks cell surface expression of human histocompatibility class I antigens. *Cell* 41:987-997.
 123. Andersson, M., S. Paabo, T. Nilsson, and P. A. Peterson. 1985. Impaired intracellular transport of class I MHC antigens as a possible means for adenoviruses to evade immune surveillance. *Cell* 43:215-222.
 124. Bennett, E. M., J. R. Bennink, J. W. Yewdell, and F. M. Brodsky. 1999. Cutting edge: adenovirus E19 has two mechanisms for affecting class I MHC expression. *J. Immunol.* 162:5049-5052.
 125. Sester, M., K. Koebernick, D. Owen, M. Ao, Y. Bromberg, E. May, E. Stock, L. Andrews, V. Groh, T. Spies, A. Steinle, B. Menz, and H. G. Burgert. 2010. Conserved amino acids within the adenovirus 2 E3/19K protein differentially affect downregulation of MHC class I and MICA/B proteins. *J. Immunol.* 184:255-267.
 126. Horwitz, M. S. 2004. Function of adenovirus E3 proteins and their interactions with immunoregulatory cell proteins. *J. Gene Med.* 6 Suppl 1:S172-S183.
 127. Windheim, M., A. Hilgendorf, and H. G. Burgert. 2004. Immune evasion by adenovirus E3 proteins: exploitation of intracellular trafficking pathways. *Curr. Top. Microbiol. Immunol.* 273:29-85.
 128. Burgert, H. G., Z. Ruzsics, S. Obermeier, A. Hilgendorf, M. Windheim, and A. Elsing. 2002. Subversion of host defense mechanisms by adenoviruses. *Curr. Top. Microbiol. Immunol.* 269:273-318.
 129. Kojaoghlanian, T., A. Joseph, A. Follenzi, J. H. Zheng, M. Leiser, N. Fleischer, M. S. Horwitz, T. P. DiLorenzo, and H. Goldstein. 2009. Lentivectors encoding immunosuppressive proteins genetically engineer pancreatic beta-cells to correct diabetes in allogeneic mice. *Gene Ther.* 16:340-348.
 130. Efrat, S., G. Fejer, M. Brownlee, and M. S. Horwitz. 1995. Prolonged survival of pancreatic islet allografts mediated by adenovirus immunoregulatory transgenes. *Proc. Natl. Acad. Sci. U. S. A* 92:6947-6951.
 131. Oosten, L. E., D. Koppers-Lalic, E. Blokland,

- A. Mulder, M. E. Rensing, T. Mutis, A. G. van Halteren, E. J. Wiertz, and E. Goulmy. 2007. TAP-inhibiting proteins US6, ICP47 and UL49.5 differentially affect minor and major histocompatibility antigen-specific recognition by cytotoxic T lymphocytes. *Int. Immunol.* 19:1115-1122.
132. Lee, E. M., J. Y. Kim, B. R. Cho, W. K. Chung, B. W. Yoon, S. U. Kim, B. C. Lee, W. S. Hwang, S. Y. Moon, J. S. Lee, and C. Ahn. 2005. Down-regulation of MHC class I expression in human neuronal stem cells using viral stealth mechanism. *Biochem. Biophys. Res. Commun.* 326:825-835.
133. Kim, J. Y., D. Kim, I. Choi, J. S. Yang, D. S. Lee, J. R. Lee, K. Kang, S. Kim, W. S. Hwang, J. S. Lee, and C. Ahn. 2005. MHC expression in a human adult stem cell line and its down-regulation by hCMV US gene transfection. *Int. J. Biochem. Cell Biol.* 37:69-78.
134. Crew, M. D. and B. Phanavanh. 2003. Exploiting virus stealth technology for xenotransplantation: reduced human T cell responses to porcine cells expressing herpes simplex virus ICP47. *Xenotransplantation.* 10:50-59.
135. McGeoch, D. J. and A. J. Davison. 1999. The molecular evolutionary history of the herpesviruses, p. 441-465. In E. Domingo, R. Webster, and J. Holland (eds.), *In Origin and Evolution of Viruses.* Academic Press, London.
136. Hill, A., P. Jugovic, I. York, G. Russ, J. Bennink, J. Yewdell, H. Ploegh, and D. Johnson. 1995. Herpes simplex virus turns off the TAP to evade host immunity. *Nature* 375:411-415.
137. Lehner, P. J., J. T. Karttunen, G. W. Wilkinson, and P. Cresswell. 1997. The human cytomegalovirus US6 glycoprotein inhibits transporter associated with antigen processing-dependent peptide translocation. *Proc Natl Acad Sci USA* 94:6904-6909.

Nederlandse samenvatting

List of publications

Curriculum vitae

Nederlandse samenvatting

Vrijwel de gehele wereldbevolking is geïnfecteerd met een of meerdere herpesvirussen. Over het algemeen heeft de gastheer geen tot weinig last van deze infecties. Toch zijn herpesvirussen verantwoordelijk voor verschillende ziektebeelden. Deze kunnen relatief mild zijn, zoals de koortslip (herpes simplex virus type 1) en waterpokken (varicella zoster virus), maar ook heftiger, zoals gordelroos (varicella zoster virus) en de ziekte van Pfeiffer (Epstein-Barr virus, EBV). Bovendien zijn het Epstein-Barr virus en het verwante Kaposi's sarcoma-geassocieerde herpesvirus betrokken bij het ontstaan van bepaalde kwaadaardige tumoren.

Eén van de karakteristieke eigenschappen van herpesvirussen is het vermogen om een persistente infectie te veroorzaken: na primaire infectie blijft het virus voor altijd in de gastheer aanwezig. Het merendeel van de tijd bevindt deze infectie zich in de latente fase. Gedurende deze fase is het virus in een soort slaaptoestand en worden er geen nieuwe virusdeeltjes gemaakt. Zo is het virus onzichtbaar voor het immuunsysteem van de gastheer. Voor verspreiding naar nieuwe, niet-geïnfecteerde personen moeten nieuwe virusdeeltjes gemaakt worden, dit gebeurt tijdens de lytische ofwel productieve fase van de virale levenscyclus. De overgang van de latente naar de lytische fase wordt ook wel reactivatie genoemd. Tijdens deze reactivatie worden, afhankelijk van het type virus, 70 tot meer dan 200 virale eiwitten gesynthetiseerd. Door deze massale productie van virale eiwitten loopt het virus een groot risico om ontdekt te worden door het immuunsysteem van de gastheer. Zo gaat het ook in de praktijk: zodra een herpesvirus reactiveert komen de afweercellen in actie en wordt de infectie weer onder controle gebracht. Reactivatie van herpesvirussen wordt dan ook veelvuldig gezien in een gastheer bij wie het immuunsysteem verzwakt is door bijvoorbeeld ziekte, stress of toediening van afweer-onderdrukkende medicijnen.

Het immuunsysteem van de gastheer is opgebouwd uit de aangeboren respons en de aangeleerde respons. De aangeboren respons is in staat heel snel te reageren, maar heeft als nadeel dat deze vrij specifiek is. De aangeleerde respons moet eerst geactiveerd worden, en hierdoor duurt het één tot twee weken voordat deze respons werkzaam is. Het grote voordeel van de aangeleerde respons is dat deze specifiek is voor de ziekteverwekker die de afweerreactie veroorzaakt heeft. Bovendien heeft het aangeleerde deel van het immuunsysteem een "geheugen", waardoor het in staat is om snel en specifiek te reageren bij re-infectie of reactivatie van dezelfde ziekteverwekker. De aangeleerde respons kan worden onderverdeeld in twee componenten: de humorale respons (antilichamen) en de cellulaire respons (T-cellen). Antilichamen zijn vooral effectief doordat zij virusdeeltjes die zijn vrijgekomen uit de cel kunnen neutraliseren, terwijl T-cellen juist de virus-geïnfecteerde cellen kunnen herkennen en doden.

Voor het onder controle houden van herpesvirusinfecties is een belangrijke rol weggelegd voor cytotoxische T-cellen. Deze herkennen virus-geïnfecteerde cellen door middel van hun T-celreceptor, die bindt aan HLA klasse I moleculen. Deze HLA klasse I moleculen presenteren kleine stukjes eiwit, peptiden genaamd, aan het celoppervlak. De peptiden ontstaan als gevolg van afbraak van zowel cellulaire als virale eiwitten in het cytoplasma van de cel. Deze peptiden worden getransporteerd naar een gespecialiseerd compartiment in de cel, het endoplasmatisch reticulum (ER), met behulp van de Transporter geassocieerd met Antigeen-Processing (TAP). In het ER binden de peptiden aan de HLA klasse I moleculen. Vervolgens reizen de HLA klasse I-peptide complexen naar het celoppervlak, waar cytotoxische T-cellen deze HLA klasse I-peptide complexen kunnen herkennen. Indien deze peptiden van lichaamsvreemde eiwitten afkomstig zijn, zoals virale eiwitten, zullen de cytotoxische T-cellen overgaan tot het doden van de herkende cel.

Om te voorkomen dat geïnfecteerde cellen herkend worden door het immuunsysteem van de gastheer, hebben herpesvirussen "immuunevasiestrategieën" ontwikkeld. Allereerst hebben deze virussen natuurlijk de mogelijkheid om de latente fase in te gaan, waarbij er (bijna) geen virale eiwitten worden gesynthetiseerd. Op deze manier blijven de geïnfecteerde cellen onzichtbaar voor het immuunsysteem. Bovendien brengen herpesvirussen specifieke eiwitten tot expressie die tot doel hebben het immuunsysteem te saboteren, de zogeheten immuunevasie-eiwitten. Veel van deze virale eiwitten zijn erop gericht om HLA klasse I antigeenpresentatie aan cytotoxische T-cellen te voorkomen gedurende de lytische fase van infectie. Dit proefschrift is gewijd aan twee immuunevasie-eiwitten die tot expressie worden gebracht door EBV.

In het eerste deel van hoofdstuk 1 wordt een algemene introductie gegeven over herpesvirussen, HLA klasse I antigeenpresentatie en immuunevasie. In het tweede deel van hoofdstuk 1 wordt specifiek aandacht besteed aan EBV en de immuunevasiestrategieën van dit virus.

Hoofdstuk 2 beschrijft de ontdekking en karakterisatie van het EBV-eiwit BNLF2a als immuunevasie-eiwit. BNLF2a blokkeert TAP, waardoor het transport van peptiden naar het ER platgelegd wordt. Op deze wijze zorgt BNLF2a ervoor dat de oppervlakte-expressie van klasse I moleculen omlaag gaat. Uiteindelijk heeft dit tot gevolg dat cellen die BNLF2a tot expressie brengen, minder goed herkend worden door cytotoxische T-cellen. Bovendien zijn ook de BNLF2a-eiwitten van aan EBV-gerelateerde virussen in staat om de oppervlakte-expressie van HLA klasse I moleculen te reduceren.

In de hoofdstukken 3 en 4 wordt in meer detail ingegaan op de structurele en functionele eigenschappen van het BNLF2a-eiwit. BNLF2a is een klein eiwit van 60 aminozuurresiduen en komt tot expressie gedurende de lytische

fase van een EBV-infectie. BNLF2a bindt aan TAP, dit kan zowel gezien worden voor cellen die het BNLF2a-eiwit alleen tot expressie brengen, als voor cellen waarbij de EBV-infectie zich in de lytische fase bevindt en die dus (bijna) alle EBV-eiwitten tot expressie brengen. De interactie van BNLF2a met TAP is noodzakelijk voor de stabiliteit van BNLF2a: in afwezigheid van TAP is het BNLF2a-eiwit bijna niet detecteerbaar. Het BNLF2a-eiwit bestaat uit twee gedeelten, een hydrofiele N-terminus en een hydrofobe C-terminus. De N-terminus, die zich in het cytoplasma blijkt te bevinden, is nodig voor het blokkeren van het peptide transport via TAP. De C-terminus zorgt ervoor dat het BNLF2a-eiwit aan de membraan van het ER gekoppeld wordt.

Hoofdstuk 5 is gewijd aan de natuurlijke variatie van het BNLF2a-eiwit. Door de sequentie van het BNLF2a-gen van verschillende EBV-isolaten te bepalen, is er inzicht verkregen in de variatie van dit immuuevasie-eiwit in de EBV-populatie. In deze studie zijn vijf verschillende BNLF2a-varianten beschreven, waarbij de sequentie van iedere variant één tot maximaal drie aminozuurresiduen afwijkt van de referentiestam. Al deze BNLF2a-varianten verminderen de oppervlakte-expressie van HLA klasse I moleculen minstens zo effectief. Dat de functie van het BNLF2a-eiwit geconserveerd is gebleven gedurende de evolutie van EBV impliceert dat het van groot belang is voor het virus om T-celherkenning van productief geïnfecteerde cellen te voorkomen.

In hoofdstuk 6 wordt verder ingegaan op de rol van het BNLF2a-eiwit in de lytische fase van de EBV-infectie. Hiervoor is gebruik gemaakt van een BNLF2a-deletievirus. Een vergelijking tussen het natuurlijk voorkomende (wildtype) virus en het BNLF2a-deletievirus laat zien dat in afwezigheid van het BNLF2a-eiwit de oppervlakte-expressie van HLA klasse I moleculen hoger is. Geheel in overeenstemming hiermee worden productief geïnfecteerde cellen beter herkend door cytotoxische T-cellen. Dit geldt echter alleen gedurende de vroege fase van de productieve EBV-infectie; in de late fase heeft de afwezigheid van het BNLF2a-eiwit geen waarneembaar effect. In deze late fase is de herkenning van productief geïnfecteerde cellen door cytotoxische T-cellen sowieso geremd, ook al is BNLF2a afwezig. Dit suggereert dat het BNLF2a-eiwit vooral een belangrijke rol speelt in het verhinderen van T-celherkenning gedurende de vroege fase van een productieve EBV-infectie en dat andere immuuevasie-eiwitten het in de late fase overnemen.

In hoofdstuk 7 is een van de andere immuuevasie-eiwitten van EBV bestudeerd, namelijk BGLF5. Het BGLF5-eiwit heeft (ribo)nuclease activiteit; het breekt zowel DNA als mRNA af. Gedurende de productieve EBV-infectie heeft het BGLF5-eiwit twee functies: het speelt een rol in de replicatie van het EBV-genoom en legt de eiwitsynthese van de gastheercel stil. Dit laatste heeft tot gevolg dat er onder andere geen nieuwe HLA klasse I moleculen meer gemaakt worden. Zodoende zorgt het BGLF5-eiwit voor een belemmering van de T-celherkenning. Om meer inzicht te krijgen in het werkingsmechanisme van BGLF5 hebben wij verschillende BGLF5 mutanten bestudeerd met betrekking tot hun vermogen om DNA af te breken en de eiwitsynthese stil te leggen.

In hoofdstuk 8 wordt ingegaan op het belang van (onderzoek naar) immuuevasie. Het eerste deel belicht het doel van immuuevasie vanuit het oogpunt van het virus. In het tweede deel wordt aandacht besteed aan het belang van de kennis over immuuevasie-eiwitten voor de wetenschap. Onderzoek naar de verschillende immuuevasiestrategieën draagt bij aan zowel een beter inzicht in de relatie tussen het virus en zijn gastheer, als aan het vergroten van de kennis van algemene cellulaire en immunologische processen. Tevens beschrijven wij de mogelijkheden voor het gebruik van (kennis over) immuuevasie-eiwitten voor vaccinontwikkeling en verscheidene klinische toepassingen, waaronder de behandeling van kanker, het beschermen van transplantaten en genterapie.

List of publications

Cdc37p is required for stress-induced high-osmolarity glycerol and protein kinase C mitogen-activated protein kinase pathway functionality by interaction with Hog1p and Slf2p (Mpk1p)

P. Hawle, **D. Horst**, J.P. Bebelman, X.X. Yang, M. Siderius and S.M. van der Vies.
Eukaryot. Cell 2007, 6:521-532

A CD8⁺ T cell immune evasion protein specific to Epstein-Barr virus and its close relatives in Old World primates
A.D. Hislop*, M.E. Rensing*, D. van Leeuwen, V.A. Pudney, **D. Horst**, D. Koppers-Lalic, N.P. Croft, J.J. Neefjes, A.B. Rickinson and E.J.H.J. Wiertz.

J. Exp. Med. 2007, 204:1863-1873

Epstein-Barr virus evasion of CD8⁺ and CD4⁺ T cell immunity via concerted actions of multiple gene products

M.E. Rensing*, **D. Horst***, B.D. Griffin*, J. Tellam, J. Zuo, R. Khanna, M. Rowe and E.J.H.J. Wiertz.
Semin. Cancer Biol. 2008, 18:397-408

Synthesis and biological evaluation of a chitobiose-based peptide N-glycanase inhibitor library

M.D. Witte, **D. Horst**, E.J.H.J. Wiertz, G.A. van der Marel and H.S. Overkleef.
J. Org. Chem. 2009, 74:605-616

Specific targeting of the EBV lytic phase protein BNLF2a to the transporter associated with antigen processing results in impairment of HLA class I-restricted antigen presentation

D. Horst, D. van Leeuwen, N.P. Croft, M.A. Garstka, A.D. Hislop, E. Kremmer, A.B. Rickinson, E.J.H.J. Wiertz and M.E. Rensing.

J. Immunol. 2009, 182:2313-2324

Reduced human leukocyte antigen expression in advanced-stage Ewing sarcoma: implications for immune recognition

D. Berghuis*, A.S.K. de Hooge*, S.J. Santos, **D. Horst**, E.J.H.J. Wiertz, M.C. van Eggermond, P.J. van den Elsen, A.H.M. Taminiou, L. Ottaviano, K.L. Schaefer, U. Dirksen, E. Hooijberg, A. Mulder, C.J.M. Melief, R.M. Egeler, M.W. Schilham, E.S. Jordanova, P.C.W. Hogendoorn, and A.C. Lankester.

J. Pathol. 2009, 218:222-231

Stage-specific inhibition of MHC class I presentation by the Epstein-Barr virus BNLF2a protein during virus lytic cycle

N.P. Croft, C. Shannon-Lowe, A.I. Bell, **D. Horst**, E. Kremmer, M.E. Rensing, E.J.H.J. Wiertz, J.M. Middeldorp, M. Rowe, A.B. Rickinson and A.D. Hislop.

PLoS. Pathog. 2009, 5:e1000490

Cowpox virus inhibits the transporter associated with antigen processing to evade T cell recognition

D. Alzhanova*, D.M. Edwards*, E. Hammarlund, I.G. Scholz, **D. Horst**, M.J. Wagner, C. Upton, E.J.H.J. Wiertz, M.K. Slifka and K. Fruh.

Cell Host. Microbe 2009, 6:433-445

Viral evasion of T cell immunity: ancient mechanisms offering new applications

D. Horst*, M.C. Verweij*, A.J. Davison, M.E. Rensing and E.J.H.J. Wiertz.

Curr. Opin. Immunol. 2011, 23:96-103

EBV protein BNLF2a exploits host tail-anchored protein integration machinery to inhibit TAP

D. Horst, V. Favalaro*, F. Vilardi*, H.C. van Leeuwen, M.A. Garstka, A.D. Hislop, C. Rabu, E. Kremmer, A.B. Rickinson, S. High, B. Dobberstein, M.E. Rensing** and E.J.H.J. Wiertz**.

J. Immunol. 2011, 186:3594-3605

Exploiting human herpesvirus immune evasion for therapeutic gain: potential and pitfalls

D. Horst, M.E. Rensing and E.J.H.J. Wiertz.

Immunol. Cell Biol. 2011, 89:359-366

Epstein-Barr virus isolates retain their capacity to evade T cell immunity through BNLF2a despite extensive sequence variation

D. Horst*, S.R. Burrows*, D. Gatherer, B. van Wilgenburg, M.J. Bell, I.G.J. Boer, M.E. Rensing** and E.J.H.J. Wiertz**.

Submitted

Residues required for host shutoff activity are located in the “bridge” of the Epstein-Barr virus protein BGLF5

D. Horst, W.P. Burmeister, I.G.J. Boer, D. van Leeuwen, A.E. Gorbalenya, M. Buisson, E.J.H.J. Wiertz and M.E. Rensing.

In preparation

Epstein-Barr virus proteins gH, gL, and gp42 co-operate to mediate potent HLA class II-restricted T cell evasion

S.J. Piersma*, A.H. de Wilde*, A.N. Kremer, M. Makuch, **D. Horst**, D. van Leeuwen, L. Hutt-Fletcher, M.S. van Ham, M. Griffioen, E.J.H.J. Wiertz and M.E. Rensing.

In preparation

Viral inhibition of the Transporter associated with Antigen Processing (TAP): a striking example of convergent evolution

M.C. Verweij*, **D. Horst***, B.D. Griffin, A.J. Davison, M.E. Rensing and E.J.H.J. Wiertz.

In preparation

** These authors contributed equally to this manuscript

Curriculum Vitae

Daniëlle Horst was born on July 14, 1982 in Zaanstad, The Netherlands. She obtained her VWO (“gymnasium”) diploma at “het Zaanlands Lyceum” in Zaandam in 2000. From 2000 to 2005, she studied at the Free University in Amsterdam. In 2003, she obtained two bachelor’s degrees, in Pharmaceutical Sciences and Chemistry. Thereafter, she continued with a master in Chemistry, specializing on Biochemistry and Biomolecular Sciences. As part of this master, she did an internship at the Free University in Amsterdam under supervision of Dr. M.H. Siderius, focusing on the phosphorylation of Cdc37p by CK2 and its importance for osmoadaptation in *Saccharomyces cerevisiae*. Her second internship was performed at the Netherlands Organization for Applied Scientific Research (TNO) in Leiden under supervision of Dr. R. Kleemann, studying the role of pro-inflammatory cytokines in atherosclerosis and type II diabetes. In September 2005, she obtained her master’s degree in Chemistry (*cum laude*). Subsequently, she started her PhD studies (financed by the Dutch Cancer Society) in August 2005 at the department of Medical Microbiology of the Leiden University Medical Center under supervision of Dr. M.E. Rensing and Prof. E.J.H.J. Wiertz. In April 2009, the research group moved to the department of Medical Microbiology of the University Medical Center Utrecht, where Daniëlle finished her PhD training. The results of her PhD research are described in this thesis. Currently, Danielle continues her work in the group of Dr. Maaïke Rensing and Prof. Emmanuel Wiertz, focusing on novel aspects of evasion of the innate and adaptive immune system by Epstein-Barr virus.

